Studies on Utilization of Algal Biomass for Food Packaging

Thesis submitted in partial fulfillment of the requirements for the degree

of

DOCTOR OF PHILOSOPHY

Submitted by

KONA MONDAL

Department of Chemical Engineering

Indian Institute of Technology Guwahati

Assam, Guwahati – 781 039

May 2023

This Thesis is Dedicated to

My Beloved Parents

for their

Endless Love, Inspiration, and Support

Department of Chemical Engineering

Indian Institute of Technology Guwahati

CERTIFICATE

This is to certify that the research work in the thesis entitled "**Studies on Utilization of Algal Biomass for Food Packaging**", is carried out by me at the Department of Chemical Engineering, Indian Institute of Technology Guwahati, as partial fulfillment for the award of Doctor of Philosophy under the supervision of Dr. Vimal Katiyar, and Dr. Vaibhav V. Goud Professor at Department of Chemical Engineering, Indian Institute of Technology Guwahati, Assam, India. The research outcomes documented in this thesis are accomplished by me and have not been submitted to any other Institute or University for the award of any degree or diploma.

Kona Mondal

Roll No: 176107003

Department of Chemical Engineering

Indian Institute of Technology Guwahati

Guwahati - 781039, India.

Department of Chemical Engineering

Indian Institute of Technology Guwahati

CERTIFICATE

This is to certify that the thesis entitled "**Studies on Utilization of Algal Biomass for Food Packaging**", is being submitted by **Kona Mondal** for the award of Ph.D. The degree has been carried out by her at the Chemical Engineering Department, Indian Institute of Technology Guwahati, under our guidance and supervision. The work documented in this thesis has not been submitted to any other University or Institute for the award of any degree or diploma.

Prof. Vimal Katiyar

Professor

Department of Chemical Engineering

Indian Institute of Technology Guwahati

Guwahati - 781039, India.

Prof. Vaibhav V. Goud

Professor

Department of Chemical Engineering

Indian Institute of Technology Guwahati

Guwahati - 781039, India.

Thesis Acknowledgment

I am grateful and indebted to many people who have supported and helped me in the work of this thesis directly and indirectly. Foremost, I would like to express my deep sense of respect and gratitude to my supervisors **Prof. Vimal Katiyar** and **Prof. Vaibhav V. Goud** for their continuous support during my Ph.D. study and research, along with their patience, motivation, enthusiasm, and immense knowledge. Their guidance has helped me be confident in doing my work scientifically and precisely during my Ph.D. duration to complete my work within the stipulated time. It was a great privilege to work under them and a special thanks to **Prof. Katiyar** for his constant motivation and ideology to work hard and more during my Ph.D. study.

Besides my supervisor, I would also like to thank the rest of my doctoral committee members; **Dr. Amit Kumar** (Department of Chemical Engineering), **Prof. Chandan Das** (Department of Chemical Engineering), and **Prof. Lingaraj Sahoo** (Department of Biosciences & Bioengineering), for their insightful comments, brilliant suggestions, questions and encouragement during the Ph.D. course. I further owe a debt of gratitude to **Prof. Shinichi Sakurai** at the Department of Biobased Materials Science, Kyoto Institute of Technology, Kyoto, Japan for his research guidance and support during my part of the Ph.D. work at Kyoto.

I am also extending my heartful gratitude to the **Center of Excellence for Sustainable Polymers (CoE-SuSPol), Centre for Sustainable Polymers (CSP)**, Department of Chemical Engineering, Analytical Lab, and **Central Instruments Facility (CIF)**, Center for the Environment (CE), **IIT Guwahati**, for the availability of all the facilities of the sophisticated instruments. I would like to thank KIT Global Human Resource Department, **KIT Japan** for providing me scholarship during my stay in Japan to carry out part of my research work. Even, I would also like to thank the head and all the authorities for letting

me utilize all the required facilities during my research work. I am extremely thankful to the technical staff of the chemical engineering department, particularly Mr. Harsaraj Biswanath, Mr. Pankaj Kumar, Mr. Debojit, Ms. Ritumoni Kalita, Mr. Jayanta Kumar, Mr. Lukumoni, Mr. Prasun, Mr. Ariful and non-technical staff like Mr. Shoilen, Mr. Deepjyoti and Mr. Bhagya for their kind cooperation during the Ph.D. course. I would also like to thank a few CIF operators particularly, Mr. Bhaskar, and Mr. Kaustav from CE for their immense help in analyzing all the morphological analyses. I am also fortunate to have friends in the lab as well as in the hostel. I am very much thankful to my colleagues, and seniors Dr. Narendren, Dr. Siddhartha, Dr. Purabi, Dr. Gourhari, Dr. Surendra, Dr. Neha, Dr. Tabli, Sayan, Chethana, Pankaj, Dr. Riddhi, and Dr. Prasannavenkadesan for technical help and discussions, which helped me in my research work a lot. I am also thankful to all my co-research fellows, friends, and lab colleagues Dr. Naba, Dr. Modu, Dr. Doli, Munmi, Abhishekh, Bhanupriya, Durlov, Dr. Balendu, Mandavi, Parul, Vikash, Kshitij, Manoj, Arnab, and Lakhiya for all kinds of help and moral support made available to me in the lab and making my stay at IIT Guwahati cheerful and memorable.

The selflessness and countless sacrifices made by my wonderful parents and family members made it possible for me to reach this stage in my life. Finally, I would like to thank the almighty God, for letting me overcome all the difficulties to move forward and fulfil my wish.

Abstract

The increasing demands for safe and healthier food products have led to the development of novel packaging technologies that protect the globe from hazards arising from fossil-based non-biodegradable food packaging material. Several studies have reported the non-biodegradable nature of conventional food packaging materials and their negative impact on the environment. In this regard, renewable bio-based and biodegradable plastics produced by economically viable industrial processes can be considered and utilized as sustainable plastic food packaging material. Besides, the whole world is combating the crucial problem of post-harvest losses of fresh produces, wherein India is facing a 30-40% loss due to post-harvest. In this context, novel packaging technologies in the form of edible film and coating as a preservation technique can provide an alternative solution to protect post-harvest fresh produce. In the present work, the development of sustainable primary food packaging material in the form of edible films and coating is studied and characterized for various physicochemical, biochemical, and microbial properties. Also, the developed edible coating formulation is applied to real food systems (green chili, tomato, onion, and potato) to check the effectiveness of the coating. The storage study of the coated fresh produce has been conducted at room temperature to determine the effectiveness of coating on the quality and shelf-life extension of the produce and to draw a comparison against the uncoated. Among the variety of edible biopolymers, chitosan, and guar gum have been utilized in this work. These two biopolymers are mostly consumed in the food industry where, chitosan is used as an antimicrobial agent, and film-forming material whereas, guar gum is acted as a stabilizer and thickener. Further, targeting to develop active edible packaging and tuning the inherent properties of these edible biopolymers for obtaining better effectiveness, natural food additives such as green algae extract, and essential oil is added. Algae is an emerging biomaterial, predominantly used for biodiesel production by

utilizing its oil. It is used in the pharmaceuticals and food industry. However, the residue of algae biomass after oil extraction is treated as waste either used as cattle and aqua feed or dumped as waste. Interestingly, this industrial bio-based waste can be utilized as a whole or by extracting its bioactive compounds and can be incorporated into the biopolymer to obtain effective properties. The green algae biomass residue has been utilized and the extract is added to the edible packaging formulation for enhancement of barrier, physicochemical, antioxidant, antimicrobial, and other characteristics properties which are necessary for food packaging. The essential oil has been added to the edible packaging formulation along with the algae extract to obtain a synergistic effect, superior hydrophobicity, antimicrobial, and biochemical properties. Besides, sustainable bio-composites have been fabricated with the incorporation of nanostructured biomaterials extracted from algae biomass residue for the development of secondary packaging material. In this context, Poly(lactic acid) (PLA), and Poly(ε-caprolactone) (PCL) have been utilized in order develop secondary packaging, which are one of the most widely studied sustainable polymers that possess several properties that are comparable to conventional polymers. The developed biodegradable bio-composites are studied in detail for crystalline behavior and migration properties. Active agent curcumin is deliberately added to the bio-composites to study the effect of nanostructured material on the migration behavior of active compounds. The active secondary food packaging material is further applied to real food systems to understand the effect of packaging material. Further, a cytotoxicity test has been performed on all the developed packaging materials for understanding the non-toxicity and biocompatible nature. Since algae biomass contains various bioactive compounds and nutraceuticals, in this work the residue of algae biomass which is the leftover part after extraction of oil, has been subjected to ultrasound-assisted green extraction using a food-grade solvent to obtain crude algae ethanolic extract (CAEE) which is rich in antioxidant

activity (~40%) and adequate amount of total phenolic and flavonoid content. The optimization of ultrasound-assisted extraction of CAEE has been performed using response surface methodology. The CAEE-incorporated chitosan-based edible films have exhibited a reduction in film transparency, water vapor permeability (~60%), and improvement in crystallinity, tensile strength, antioxidant activity (~27%), and UV-Vis blocking properties as compared to the control film. Besides, the shelf-life of fresh produce such as tomatoes, chilies, potatoes, and onions has been extended effectively at room temperature storage by applying the developed CAEE-incorporated chitosan-based edible coating using a dipping technique. The CAEE and turmeric essential oil incorporated guar gum-based edible film and coating solutions have been developed and the films have shown superior antioxidant (~79%) and antimicrobial activity (~95%). This formulated coating has acted as an anti-browning agent on cut potato cubes and extended the shelf-life at room temperature storage. The cellulose nanocrystals (CNC) with high crystallinity index (~89%) have been isolated from waste algae biomass powder. The inclusion of CNC into the PLA and PCL matrix enhanced crystallinity in the developed bio-composite film. Further, the overall migration study has revealed that migration of PLA/CNC and PCL/CNC bio-nanocomposite films are under the specified standard limit (10 mg dm^{-2}). Active secondary packaging material has been developed with the inclusion of curcumin. Specific migration studies have been conducted to visualize the nanoparticle effect on curcumin migration. A higher rate of curcumin migration has been noticed in presence of CNC from PLA bio-nanocomposite at 40 °C storage conditions. Moreover, this study has tried to provide possible ways for utilization of waste (de-oiled) green algae biomass (*Dunaliella tertiolecta*) to minimize environmental hazard. This work imparts novel edible coating formulation incorporated with non-toxic algae biomass extract which is rich in β-carotene has prolonged the shelf-life of fresh produce such as green chilli, tomato, potato, and onion at room temperature

storage. The algae extract as a bio-filler contributes significant reduction in water vapor barrier properties, improved crystallinity, UV-Vis light blocking properties, antioxidant and antimicrobial properties to chitosan based primary packaging material. This extract is also compatible with other bio-fillers such as turmeric essential oil and provided synergistic effect to the packaging material. The guar gum-based formulation incorporated with algae extract and turmeric essential oil exhibited superior antioxidant, and antimicrobial activity and surface hydrophobicity and anti-browning activity. The obtained light blocking property would be beneficial for extending the product life of light sensitive foods. The algal extract has shown compatibility when incorporated into different biopolymer matrix. Therefore, this study provides successful development of algae extract incorporated primary active packaging material. Besides, successful extraction of cellulose nanocrystals as nanostructured material has been done from algae residue with adequate yield of around 30%. The cellulose nanocrystals acted as superior nucleating agent in both PLA and PCL-based secondary packaging material. Incorporation of CNC has shown impact on migration rate of active compounds such as curcumin from the packaging material to food simulant and presence of algal CNC in the packaging material did not hinder the functional activity of curcumin. Inclusion of curcumin has imparted effective UV-light blocking property, reduction in film transparency, antioxidant and antimicrobial activity against food pathogen. Overall, in this thesis, an alternative pathway for extending the shelf-life of perishables using edible coating technology has been reported and it has also demonstrated the capability of utilizing algae biomass waste for the fabrication of primary and secondary food packaging material. Also, this thesis work provides first step on utilization of algae biomass for development of primary active packaging material.

Keywords: Algae biomass, Edible films, Edible coating, Active packaging, Crystallization, Migration, Shelf-life.

Table of Contents

Thesis Acknowledgement..... *v*
Abstract..... *vii*
Contents..... *xi*
List of Figures..... *xviii*
List of Tables..... *xxiv*
Abbreviations..... *xxv*
Notations..... *xxvi*

CHAPTER 1

INTRODUCTION AND LITERATURE REVIEW..... 1
1.1 Introduction..... 2
1.2 Sustainable/Biodegradable Polymers..... 4
1.2.1 Need for Sustainable Polymers..... 5
1.3 Food Packaging..... 6
1.3.1 Classification of Food Packaging..... 7
1.3.2 Concerns Associated with Food and Packaging..... 8
1.3.2.1 Post-harvest Loss..... 9
1.3.3 Edible and Active Packaging..... 10
1.4 Edible Biopolymers for Food Packaging..... 12
1.4.1 Polysaccharide-based Edible Polymers..... 12
1.4.1.1 Chitosan..... 13
1.4.1.2 Guar gum..... 15
1.5 Non-edible Biopolymers for Secondary Food Packaging..... 18
1.5.1 Poly(lactic acid)..... 18
1.5.2 Poly(ε-caprolactone)..... 19
1.6 Algae Biomass..... 20
1.6.1 Algae as a Rich Source of Food and Medicine..... 21
1.6.2 Concerns Associated with Algae Biomass..... 22
1.6.3 Algae Biomass-based Composites..... 22
1.7 Bionanomaterials..... 25
1.7.1 Cellulose Nanocrystals..... 25
1.8 Migration of Food Packaging Material..... 27
1.9 Literature Review..... 28
1.10 Research Gap..... 30
1.11 Proposed Thesis Objectives..... 31
1.12 Organization of Thesis..... 32

CHAPTER 2

MATERIALS AND METHODS..... 37
2.1 Materials..... 37
2.2 Experimental Methods..... 38
2.2.1 Preparation of Algae Extract..... 38
2.2.1.1 Optimization of De-oiled Algal Biomass Ultrasound-Assisted Extraction Procedure Using Response Surface Methodology (RSM)..... 38
2.2.1.2 Extraction of Optimized De-oiled Crude Algae Ethanolic Extract. 40
2.2.2 Development of Biopolymer-based Edible Films as Primary Packaging Material..... 40
2.2.2.1 Fabrication of Chitosan-based Bio-composites Active Edible Films..... 40
2.2.2.2 Fabrication of Guar Gum-based Bio-composites Active Edible Films..... 41
2.2.3 Development of Biopolymer-based Edible Coating Formulation and Coating on Fresh Produce..... 43
2.2.3.1 Development of Chitosan-based Edible Coating Formulation..... 43
2.2.3.2 Coating of Chitosan-based Formulation on Fresh Produce..... 43
2.2.3.3 Optimization of Guar gum-based Edible Coating Formulation for Shelf-life Extension of Cut Potato..... 44
2.2.3.4 Guar Gum-based Edible Coating on Cut Potatoes..... 46
2.2.4 Isolation of Cellulose Nanocrystals (CNC) from Algae Biomass Residue. 46
2.2.5 Development of Biopolymer-based Secondary Packaging Material..... 48
2.2.5.1 Fabrication of PLA/algae and PLA/CNC Bio-composites..... 48
2.2.5.2 Fabrication of PCL/algae and PCL/CNC Bio-composites..... 49
2.2.5.3 Fabrication of Curcumin Loaded CNC Incorporated PLA Bio-composite Films..... 49
2.2.5.4 Fabrication of Curcumin Loaded CNC Incorporated PCL Bio-composite Films..... 50
2.3 Migration Study of Secondary Packaging..... 51
2.3.1 Migration Testing on PLA/CNC and PLA/CNC/CUR Bio-composites.... 51
2.3.1.1 Overall Migration Testing for PLA/CNC Films..... 51
2.3.1.2 Specific Migration Test for Curcumin Loaded PLA Films..... 52
2.3.2 Migration Testing on PCL/CNC and PCL/CNC/CUR Bio-composites.... 53
2.3.2.1 Overall Migration Testing for PCL/CNC Films..... 53
2.3.2.2 Specific Migration Test for Curcumin-loaded PCL Films..... 53
2.3.3 Migration Kinetics of Specific Migrant Curcumin..... 53
2.3.3.1 Zero-order Model..... 53
2.3.3.2 First-order Model..... 53
2.3.3.3 Higuchi Model..... 54
2.3.3.4 Korsemeyer-Peppas Model..... 54
2.4 Characterization of Bio-fillers and Developed Bio-composite Films..... 54

2.4.1 Compositional Analysis of ABR…… 54
2.4.1.1 Inductively Coupled Plasma Mass Spectroscopy (ICPMS)…… 55
2.4.2 Biochemical and Structural Characterization of Algae Extract (CAEE) and Developed Films…… 55
2.4.2.1 Determination of the Chlorophyll Content of CAEE……. 55
2.4.2.2 Nuclear Magnetic Resonance (NMR) Analysis of CAEE…….. 56
2.4.2.3 Matrix-Assisted Laser Desorption/Ionization Time of Flight (MALDI TOF) Mass Spectroscopy Analysis of CAEE…….. 56
2.4.2.4 Determination of β-Carotene in CAEE……... 57
2.4.2.5 Determination of Antioxidant capacity of CAEE and Films…….. 57
2.4.2.6 Determination of Total Phenolic Content of CAEE and Films…… 58
2.4.2.7 Color Parameters of CAEE and Films……. 58
2.4.2.8 Transparency of Developed Films…….. 58
2.4.3 Physicochemical Characterization of Developed Films…….. 59
2.4.3.1 Field Emission Scanning Electron Microscope (FESEM)…….. 59
2.4.3.2 Atomic Force Mass Spectroscopy (AFM)……. 59
2.4.3.3 Thermogravimetric Analysis (TGA)…….. 59
2.4.3.4 Fourier Transform Infrared Spectroscopy (FTIR)……... 59
2.4.3.5 X-ray diffraction (XRD)…… 60
2.4.3.6 Wettability Analysis…….. 60
2.4.3.7 Water Vapor Permeability (WVP)……. 60
2.4.3.8 Mechanical Properties……... 61
2.4.4 Rheological Properties of Edible Filmogenic Solution…… 61
2.4.4.1 Steady Shear Measurements……... 61
2.4.4.2 Strain Sweep Measurements……... 62
2.4.4.3 Frequency Sweep Measurements…… 62
2.4.5 Crystallization study…… 62
2.4.5.1 Differential Scanning Calorimetry (DSC)……... 62
2.4.5.2 Kinetics Study by Melt Crystallization using Avrami Model…… 63
2.4.5.3 Polarized Optical Microscopy (POM)……..... 64
2.4.5.4 Small-angle X-ray scattering (SAXS)……..... 64
2.4.6 Antimicrobial and Biocompatibility Study of Filmogenic Solution and Films……..... 65
2.4.6.1 Antimicrobial Activity…… 65
2.4.6.2 Cytotoxicity Study…….. 66
2.4.7 Shelf-life Study…… 67
2.4.7.1 Surface Morphology of Fruits…… 67
2.4.7.2 Color and Gloss Properties of Fruits……... 67
2.4.7.3 Weight Loss (%)…… 68
2.4.7.4 Determination of Total Soluble Solid Content and pH…… 68
2.4.7.5 Determination of Titratable Acidity…… 68

2.4.7.6 Determination of Reducing Sugar..... 69
2.4.7.7 Determination of Antioxidant Activity..... 69
2.4.7.8 Determination of Lycopene Content..... 69
2.4.7.9 Determination of Ascorbic acid..... 70
2.4.7.10 Determination of Firmness..... 70
2.4.7.11 Determination of Respiration Rate..... 70
2.4.7.12 Microbiological Analysis..... 71
2.4.7.13 Sensory Evaluation..... 71
2.4.8 Statistical Analysis..... 72

CHAPTER 3

EXTRACTION AND CHARACTERIZATION OF ALGAE AND ITS EXTRACT INCORPORATED CHITOSAN-BASED CAST FILM FOR EDIBLE ACTIVE PACKAGING..... 73
Graphical Abstract..... 74
3.1 Introduction..... 75
3.2 Results and Discussion..... 77
3.2.1 Compositional and Elemental Analysis of the ABR..... 77
3.2.2 Optimization of CAEE Extraction..... 77
3.2.2.1 Response Surface Analysis and Model Fitting..... 77
3.2.2.2 Analysis of Response Surfaces and DPPH Antioxidant Activity..... 79
3.2.2.3 Optimization, Prediction, and Validation of Parameters..... 80
3.2.3 Biochemical Analysis of Bio-filler CAEE..... 81
3.2.4 MALDI TOF MS Analysis of CAEE..... 82
3.2.5 NMR Study of CAEE..... 83
3.2.5.1 ^{1}*H NMR*..... 83
3.2.5.2 ^{13}*C NMR*..... 85
3.2.6 Chitosan-based Edible Films Characterization..... 85
3.2.6.1 Visual Aspect and Color Parameters..... 85
3.2.6.2 Transparency of the Films..... 86
3.2.6.3 Thermal Stability of Films..... 87
3.2.6.4 FTIR Analysis..... 89
3.2.6.5 Possible Mechanism of Developed CS/CAEE Films..... 90
3.2.6.6 Surface Morphology of Films..... 92
3.2.6.7 XRD Analysis of Developed Films..... 93
3.2.6.8 Water Vapor Permeability of Developed Films..... 93
3.2.6.9 Mechanical Properties of Developed Films..... 94
3.2.6.10 Rheological Behavior of Filmogenic Solutions..... 96
3.2.6.11 Antioxidant Activity and Total Phenolic Content of the Developed Films..... 101
3.2.6.12 Antimicrobial Activity of Formulated Active Edible Filmogenic Solution..... 102

3.2.6.13 Biocompatibility of Formulated Active Filmogenic Solutions….. 103
3.3 Summary..... 104

CHAPTER 4

SHELF-LIFE STUDY OF TOMATO, CHILI, ONION, AND POTATO USING CHITOSAN AND ALGAE EXTRACT INCORPORATED (CS/CAEE) EDIBLE PACKAGING..... 105
Graphical Abstract..... 106
4.1 Introduction..... 107
4.2 Results and Discussion..... 109
4.2.1 Effect of Coating Efficiency on Physicochemical Parameters of Tomatoes During Storage..... 109
4.2.1.1 Surface Morphology..... 109
4.2.1.2 Color Parameters and Gloss Value..... 111
4.2.1.3 Weight Loss..... 114
4.2.1.4 Total Soluble Solid..... 115
4.2.1.5 Measurement of pH..... 116
4.2.1.6 Titratable Acidity..... 117
4.2.1.7 Determination of Reducing Sugar..... 118
4.2.1.8 Firmness..... 120
4.2.1.9 Respiration Rate..... 120
4.2.2 Coating Effect on the Antioxidant Properties of Tomatoes During Storage..... 122
4.2.2.1 Antioxidant Activity..... 122
4.2.2.2 Lycopene Content..... 123
4.2.2.3 Ascorbic Acid Content..... 125
4.2.3 Coating Effect on Microbial and Sensory Properties of Tomatoes During Storage..... 126
4.2.3.1 Microbiological Analysis..... 126
4.2.3.2 Sensory Evaluation..... 127
4.2.4 Coating Efficiency on Physiological Characteristics of Green Chili…… 129
4.2.5 Coating Efficiency on Physiological Characteristics of Potato and Onion 132
4.3 Summary..... 135

CHAPTER 5

DEVELOPMENT OF GUAR GUM-BASED ANTIMICROBIAL AND ANTI-BROWNING FILMS USING ALGAE EXTRACT AND TURMERIC ESSENTIAL OIL..... 137
Graphical Abstract..... 138
5.1 Introduction..... 139
5.2 Results and Discussion..... 141
5.2.1 Surface Morphology..... 141
5.2.2 FTIR Analysis..... 143
5.2.3 Optical Properties..... 144

5.2.4 Water Vapor Transmission Rate…….. 146
5.2.5 Water Contact Angle..... 148
5.2.6 Mechanical Properties..... 149
5.2.7 Thermal Properties..... 151
5.2.8 Rheological Behavior of Filmogenic Solution..... 152
5.2.9 Antioxidant Activity..... 156
5.2.10 Antimicrobial Activity..... 157
5.3 Summary..... 159

CHAPTER 6

OPTIMIZATION OF GUAR GUM-BASED ANTI-BROWNING COATING FOR SHELF-LIFE EXTENSION OF THE CUT POTATO……... 161
Graphical Abstract..... 162
6.1 Introduction..... 163
6.2 Results and Discussion..... 164
6.2.1 Oxygen transmission rate (OTR)..... 164
6.2.2 Carbon dioxide transmission rate (CTR)..... 169
6.2.3 Water Vapor Transmission Rate (WVTR)..... 171
6.2.4 Color Properties..... 173
6.2.5 Visible Mold Appearance..... 175
6.2.6 Overall Acceptability..... 176
6.2.7 Optimization..... 178
6.3 Summary..... 179

CHAPTER 7

DEVELOPMENT OF CELLULOSE NANOCRYSTALS (CNC) AND ALGAE BIOMASS INCORPORATED PLA AND PCL BIO-COMPOSITES FOR SECONDARY PACKAGING..... 181
Graphical Abstract..... 182
7.1 Introduction..... 183
7.2 Results and Discussion..... 184
7.2.1 Extraction of Cellulose and Fabrication of CNCs..... 184
7.2.2 Morphological Properties..... 185
7.2.3 Thermal Properties of the Bio-fillers..... 186
7.2.4 FTIR and XRD Analysis..... 188
7.2.5 Crystallization Behavior of the PLA Bio-composites..... 190
7.2.5.1 DSC Analysis…… 190
7.2.5.2 POM Analysis……... 195
7.2.5.3 SAXS Analysis…….. 196
7.2.6 Crystallization Behavior of the PCL Bio-composites…… 198
7.2.6.1 DSC Analysis…… 198
7.2.6.2 POM Analysis……... 204
7.2.6.3 SAXS Analysis…….. 205

7.3 Summary..... 207

CHAPTER 8

STUDIES ON MIGRATION PROPERTIES OF ALGAL CNC AND CURCUMIN INCORPORATED PLA AND PCL BIO-COMPOSITES..... 209
Graphical Abstract..... 210
8.1 Introduction..... 211
8.2 Results and Discussion..... 213
8.2.1 Thermal Properties..... 213
8.2.2 FTIR Analysis..... 214
8.2.3 Surface Color..... 216
8.2.4 Transparency..... 217
8.2.5 Water Vapor Transmission Rate Analysis..... 218
8.2.6 Water Contact Angle Analysis..... 220
8.2.7 XRD Analysis..... 221
8.2.8 Migration Study..... 222
8.2.8.1 Overall Migration..... 222
8.2.8.2 Specific Migration Kinetics..... 225
8.2.9 Antioxidant Activity..... 234
8.2.10 Antimicrobial Activity..... 236
8.2.11 Biocompatibility Study..... 238
8.2.12 Application of Developed Bio-composite Films on Potato cubes as Secondary Packaging Material..... 239
8.3 Summary..... 241

CHAPTER 9

CONCLUSION & FUTURE PERSPECTIVES..... 243
9.1 Conclusions..... 243
9.2 Future Perspectives..... 248
APPENDIX..... 249
RESEARCH OUTCOME..... 263
Research Articles Published/Under Preparation..... 263
REFERENCES..... 267

List of Figures

Figure No.	Topic	Page No.
Figure 1.1:	Classification of different types of biodegradable polymers.	4
Figure 1.2:	Sustainable goals for socioeconomic benefits.	5
Figure 1.3:	(a) Concept of food packaging, and (b) global plastic packaging market.	6
Figure 1.4:	Basic and advanced classification of food packaging.	7
Figure 1.5:	(a) Pictorial view of edible coating and film, and (b) mechanism of active packaging.	10
Figure 1.6:	Functions of edible active packaging.	11
Figure 1.7:	Chemical structure of chitosan and its conversion from chitin along with the crystalline nature of native chitin.	13
Figure 1.8:	Chemical structure of guar gum.	15
Figure 1.9:	Chemical structure of poly(lactic acid).	18
Figure 1.10:	Chemical structure of poly(ε-caprolactone).	19
Figure 1.11:	Schematic of microalgae production and its use.	20
Figure 2.1:	Schematic of steps of extraction of algae extract from algae biomass residue.	38
Figure 2.2:	Flowsheet of preparation of the chitosan-based edible active film.	39
Figure 2.3:	Flowsheet of preparation of the guar gum-based edible active film.	40
Figure 2.4:	Schematic on the preparation of edible coating solution and coating on fresh produce.	42
Figure 2.5:	Schematic of isolation of cellulose nanocrystals from algae biomass residue.	45
Figure 3.1:	Response surface plots for the effects of (a) ethanol concentration and solvent to solid ratio, (b) ethanol concentration and time, (c) solvent to solid ratio to extraction time, and (d) ultrasonic frequency and time on antioxidant activity of CAEE.	79
Figure 3.2:	MALDI TOF MS spectra of crude algae ethanolic extract (CAEE).	82
Figure 3.3:	(a) ^{1}H NMR spectra of CAEE in $CDCl_3$ solvent (b) ^{13}C NMR spectra of CAEE in $CDCl_3$ solvent.	84

Figure 3.4:	Color coordinate values of (a) L*, b*, & c* (b) a*, and (c) UV-Vis light transparency of CAEE incorporated edible active films (bio-composites) along with control film.	86
Figure 3.5:	(a) Thermogravimetric, and (b) derivative thermogram of CAEE incorporated edible active films (bio-composites) along with control film, (c) FTIR spectrum of de-oil algae residue powder and CAEE, and (d) FTIR spectrum of developed bio-composite films with control.	88
Figure 3.6:	(a) Probable mechanism of CS/CAEE bio-composite film formation, and (b-e) surface morphology of developed bio-composite films with control.	90
Figure 3.7:	(a) XRD pattern, (b) water vapor permeability, (c) stress-strain curve, and (d) maximum tensile stress and elongation at break of developed bio-composite films with control.	93
Figure 3.8:	(a) Strain sweep parameters of G′ and G″ modulus at f = 1 Hz, (b) emphasizing of LVR, (c) frequency sweep parameter of G′ and G″ modulus, and (d) flow curve of developed bio-composite films with control.	95
Figure 3.9:	(a) Antioxidant activity, (b) total phenolic content, (c) antimicrobial activity, and (d) biocompatibility (MTT assay) of developed bio-composite films with control.	102
Figure 4.1:	Visual observation of (a) control, (b) nCS (c) CS/CAEE 2%, (d) CS/CAEE 4%, and FESEM images of the same fruits (e to h) at specific storage days, respectively.	109
Figure. 4.2:	(a) The ratio of red and yellow color intensity (a*/ b*) as a color index, and (b) glossiness at a higher angle (85°) of control and coated tomatoes during storage at 27-30 °C for 30 days. Each value is the average mean of three replicates, and vertical bars represent the standard deviation. The letters ‘a-g’ indicates significant differences ($p<0.05$).	111
Figure. 4.3:	(a) Weight loss, and (b) total soluble solid content of control and coated tomatoes during storage at 27-30 °C for 30 days. Each value is the average mean of three replicates, and vertical bars represent the standard deviation. The letters ‘a-g’ indicates significant differences ($p<0.05$).	113
Figure. 4.4:	(a) pH value, and (b) titratable acidity of control and coated tomatoes during storage at 27-30 °C for 30 days. Each value is the average mean of three replicates, and vertical bars represent the standard deviation.	115
Figure. 4.5:	(a) Reducing sugar content, (b) firmness, and (c) respiration rate of control and coated tomatoes during storage at 27-30 °C for 30 days. Each value is the average mean of three replicates, and vertical bars represent the standard deviation.	118

Figure. 4.6:	(a) DPPH free radical scavenging activity, (b) lycopene content, and (c) ascorbic acid content of control and coated tomatoes during storage at 27-30 °C for 30 days. Each value is the average mean of three replicates, and vertical bars represent the standard deviation.	123
Figure. 4.7:	An organoleptic score of tomato stored under ambient conditions (27-30 °C, 60-70% RH). Error bars represent the standard deviation.	127
Figure. 4.8:	(a) Weight loss, (b) visual observation, (c) polarized optical microscopic observation, and (d) firmness of coated and control green chili during ambient storage.	129
Figure 4.9:	(a) Visual observation, and surface morphology under FESEM of (b) uncoated, and (c) CS/CAEE coated potato during storage at room temperature.	131
Figure 4.10:	(a) Visual observation, and surface morphology under FESEM of (b) uncoated, and (c) CS/CAEE coated potato during storage at room temperature.	132
Figure 4.11:	(a) Visual observation, (b) weight loss (c) glossiness, and (d) texture of stored onion.	133
Figure 5.1:	(a) FESEM images, and (b) AFM images of developed GG-based edible films.	140
Figure 5.2:	FTIR spectra of guar gum powder, turmeric essential oil, and developed edible films.	141
Figure 5.3:	Total color difference (ΔE), and yellow index (YI) of developed edible films.	142
Figure 5.4:	Transparency of developed guar gum-based edible films.	144
Figure 5.5:	Water vapor transmission rate of developed guar gum-based edible films.	145
Figure 5.6:	(a) Contact angle value, and (b) recorded image of developed guar gum-based edible films after 10 sec time intervals.	146
Figure 5.7:	(a) TGA, (b) DTG thermograms of guar gum powder and turmeric essential oil, (c) TGA, and (d) DTG thermograms of developed edible films.	147
Figure 5.8:	(a) Strain sweep parameters of the G′ and G″ moduli at f =1 Hz, (b) emphasizing the LVR, (c) frequency sweep parameters of the G′ and G″ moduli, and (d) flow curves of the developed bio-composite films together with the control.	151
Figure 5.9:	(a) DPPH Antioxidant activity of developed film, and (b) Radical scavenging activity of developed edible films with time.	154

Figure 5.10:	Antimicrobial activity of *E. coli* (a, b), and *S. aureus* (c, d) in developed edible films.	155
Figure 6.1:	The effect of (a) algae extract and guar gum concentration, (b) turmeric essential oil and guar gum, and (c) algae extract and turmeric essential oil in the coating formulation on the oxygen transmission rate of cut potatoes after seven days of storage at room temperature.	163
Figure 6.2:	The effect of (a) algae extract and guar gum concentration, (b) turmeric essential oil and guar gum, and (c) algae extract and turmeric essential oil in the coating formulation on the carbon dioxide transmission rate of cut potatoes after seven days of storage at room temperature.	167
Figure 6.3:	The effect of (a) algae extract and guar gum concentration, (b) turmeric essential oil and guar gum, and (c) algae extract and turmeric essential oil in the coating formulation on the water vapor transmission rate of cut potatoes after seven days of storage at room temperature.	169
Figure 6.4:	The effect of (a) algae extract and guar gum concentration, (b) turmeric essential oil and guar gum, and (c) algae extract and turmeric essential oil in the coating formulation on the total color difference of cut potatoes after seven days of storage at room temperature.	170
Figure 6.5:	The effect of (a) algae extract and guar gum concentration, (b) turmeric essential oil and guar gum, and (c) algae extract and turmeric essential oil in the coating formulation on the visible mold of cut potatoes after seven days of storage at room temperature.	172
Figure 6.6:	The effect of (a) algae extract and guar gum concentration, (b) turmeric essential oil and guar gum, and (c) algae extract and turmeric essential oil in the coating formulation on the overall acceptability of cut potatoes after seven days of storage at room temperature.	173
Figure 7.1:	(a) Photographs of ABR, cellulose, and CNC suspension. FESEM micrographs of (b) ABR, (c) WABR, and (d) *Dunaliella* CNCs.	182
Figure 7.2:	Thermogravimetric curves of ABR, WABR, cellulose, and CNCs from *Dunaliella tertiolecta*.	183
Figure 7.3:	FTIR spectra of ABR, WABR, and CNCs obtained from *Dunaliella tertiolecta*.	184
Figure 7.4:	XRD diffraction patterns of WABR and CNCs obtained from *Dunaliella tertiolecta*.	185
Figure 7.5:	DSC non-isothermal thermograms of: (a) PLA/WABR bio-composites, (b) PLA/CNC bio-nanocomposites.	187

Figure 7.6:	DSC time curves of the isothermally crystallized: (a) PLA/WABR, (b) PLA/CNC films, and (c) comparison of the degree of crystallinity among the bio-composites.	188
Figure 7.7:	Avrami double log plot of (a) PLA/WABR bio-composites, and (b) PLA/CNC bio-nanocomposites.	190
Figure 7.8:	POM images of: (a) PLA/WABR bio-composites, (b) PLA/CNC bio-nanocomposites.	191
Figure 7.9:	(a) SAXS profile of the developed bio-composites, and (b) Comparison of lamellar thickness among PLA bio-composites.	192
Figure 7.10:	DSC non-isothermal thermogram of (a) first cooling scan, and (b) second heating scan of PCL bio-composites.	195
Figure 7.11:	Isothermal crystallization exotherms of (a) PCL/CNC/2 bio-nanocomposites, (b) PCL/WABR/2 bio-composites, and (c) Neat PCL with different crystallization temperatures; (d) PCL/WABR bio-composites, and (e) PCL/CNC bio-nanocomposites at 45 °C with various bio-filler content; (f) Comparison of degree of crystallinity among all bio-composites at 45 °C.	196
Figure 7.12:	Avrami double log plot of isothermal crystallization at 45 °C (a) PCL/WABR bio-composites and, (b) PCL/CNC bio-nanocomposites.	199
Figure 7.13:	POM images of (a) PCL/WABR bio-composites, and (b) PCL/CNC bio-nanocomposites at the isothermal temperature of 45 °C with different time intervals (0, 40, 80, and 120 s).	200
Figure 7.14:	Lorentz-corrected SAXS profile of PCL/WABR and PCL/CNC bio-composites.	202
Figure 8.1:	(a) TGA, (b) DTG curve of PLA bio-composite, (c) TGA, and (d) DTG curve of PCL bio-composite.	210
Figure 8.2:	FTIR spectra of (a) curcumin, PLA, and (b) PCL bio-composite films.	212
Figure 8.3:	Color properties of (a) neat PLA, PLA/CNC, and PLA/CUR/CNC bio-composites, and (b) neat PCL, PCL/CNC, and PCL/CUR/CNC bio-composites.	213
Figure 8.4:	Transparency of (a) neat PLA, PLA/CNC, and PLA/CUR/CNC bio-composites, and (b) neat PCL, PCL/CNC, and PCL/CUR/CNC bio-composites.	214
Figure 8.5:	Water vapor transmission rate of (a) neat PLA, PLA/CNC, and PLA/CUR/CNC bio-composites, and (b) neat PCL, PCL/CNC, and PCL/CUR/CNC bio-composite films.	216

Figure 8.6:	The water contact angle of (a) neat PLA, PLA/CNC, and PLA/CUR/CNC bio-composites, and (b) neat PCL, PCL/CNC, and PCL/CUR/CNC bio-composite films.	217
Figure 8.7:	XRD analysis of (a) neat PLA, PLA/CNC, and PLA/CUR/CNC bio-composites, and (b) neat PCL, PCL/CNC, and PCL/CUR/CNC bio-composite films.	218
Figure 8.8:	Overall migration of (a) PLA, and (b) PCL bio-composite films in three types of food simulant.	220
Figure 8.9:	Zero-order migration profile of curcumin molecules from PLA bio-composite films.	223
Figure 8.10:	First-order migration profile of curcumin molecules from PLA bio-composite films.	226
Figure 8.11:	Higuchi model of migration profile of curcumin molecules from PLA bio-composite films.	227
Figure 8.12:	Korsemeyer-Peppas model of migration profile of curcumin molecules from PLA bio-composite films.	228
Figure 8.13:	(a) Zero-order, and (b) First-order migration profile of curcumin molecules from PCL bio-composite films.	229
Figure 8.14:	(a) Higuchi, and (b) Korsemeyer-Peppas migration profile of curcumin molecules from PCL bio-composite films.	230
Figure 8.15:	Antioxidant activity of (a) neat PLA, PLA/CNC, and PLA/CUR/CNC bio-composites, and (b) neat PCL, PCL/CNC, and PCL/CUR/CNC bio-composite films.	231
Figure 8.16:	Antimicrobial activity of *E. coli* (a, b), and *S. aureus* (c, d) in developed PLA bio-composite films.	232
Figure 8.17:	Antimicrobial activity of *E. coli* (a, b), and *S. aureus* (c, d) in developed PCL bio-composite films.	233
Figure 8.18:	Effect of CNC and CUR on the biocompatibility of (a) PLA, and (b) PCL-based bio-composite films on BHK-21 fibroblast cells exposed for 72 h. The media along with the cell without the presence of any film sample was considered the control.	234
Figure 8.19:	(a) Weight loss, (b) firmness of stored potato cubes after seven days, and (c) visual appearance of the packet along with food during storage and after completion of the storage period.	236

List of Tables

Table 1.1:	Application of chitosan and guar gum as edible films and coatings material to prolong the shelf-life of perishables.	16
Table 1.2:	Utilization of algae biomass for the development of bio-composites.	23
Table 2.1:	Independent variables with their coded and actual values.	37
Table 2.2:	Composition of Guar gum-based edible films.	40
Table 2.3:	Independent variables of guar gum-based coating with their coded and uncoded values.	44
Table 2.4:	Composition of the developed PLA-based bio-composites.	46
Table 2.5:	Composition of the developed PCL-based bio-composites.	47
Table 2.6:	Composition of the developed PLA-based CNC and curcumin incorporated bio-composites.	49
Table 3.1:	Elemental analysis of the algae biomass residue by the ICPMS analysis.	77
Table 3.2:	Analysis of variance of the regression parameters.	78
Table 3.3:	Optimized condition of antioxidant activity with the predicted and experimental value.	80
Table 3.4:	Strain sweep parameters measured at room temperature with f = 1 Hz: Critical strain (γL), G′ modulus at the LVR limit (G'_{LVR}), G″modulus at the LVR limit (G″LVR), loss factor value (tanδ) and the difference between G'' and G' moduli at 1% strain.	96
Table 3.5:	Frequency sweep parameters were measured at room temperature for angular frequency ($\omega_{crossover}$) and storage modulus ($G'_{crossover}$) at the crossover point.	98
Table 4.1	Microbial analysis of coated and control fruits during storage days.	126
Table 5.1:	Mechanical properties of developed edible films.	148
Table 5.2	Frequency sweep parameters measured at room temperature for angular frequency ($\omega_{crossover}$) and storage modulus ($G'_{crossover}$) at the crossover point and flow behavior index of developed guar gum-based filmogenic solutions	153
Table 6.1:	Response data of experimental table of guar gum formulation.	161
Table 6.2:	The coefficient of regression equations to predict the gas transmission rates, respiration rates, physical properties, and subjective quality scores of cut potatoes coated with different concentrations of guar gum, algae extract and turmeric essential oil.	165
Table 6.3:	The experimental and predicted rate of response parameters of cut potatoes coated with the optimized coating formulation (0.9 g/100 mL GG, 0.9 mL/100 mL CAEE, and 0.5 mL/100 mL TEO) after	175

seven days of storage at 27±3 °C (room temperature) and 70-80% RH.

Table 8.1: Migration co-efficient of curcumin from developed active films to food simulant using four different mathematical model 225

Abbreviations

ABR	Algae Biomass Residue
WABR	Washed Algae Biomass Residue
DAB	De-oiled Algae Biomass
CS	Chitosan
GG	Guar gum
PLA	Poly(lactic)acid
PCL	Poly(ε-caprolactone)
CAEE	Crude Algae Ethanolic Extract
GRAS	Generally Recognized as Safe
CNC	Cellulose Nanocrystals
CUR	Curcumin
EF	Edible Films
TEO	Turmeric Essential Oil
EO	Essential Oil
DSC	Differential Scanning Calorimetry
TGA	Thermogravimetric Analysis
FTIR	Fourier Transform Infrared Spectroscopy
XRD	X-Ray Powder Diffraction
NMR	Nuclear Magnetic Resonance
MALDI TOF MS	Matrix-Assisted Laser Desorption Ionization-Time of Flight Mass Spectrometry
FESEM	Field Emission Scanning Electron Microscope
AFM	Atomic Force Mass Spectroscopy
HPLC	High-Pressure Liquid Chromatography
WCA	Water Contact Angle
POM	Polarized Optical Microscope
UV	Ultraviolet
SAXS	Small Angle X-Ray Scattering
ICPMS	Inductively Coupled Plasma Mass Spectrometry
WVTR	Water Vapor Transmission Rate
WL	Weight Loss
TSS	Total Soluble Solid
OTR	Oxygen Transfer Rate

CTR	Carbon dioxide Transfer Rate
ANOVA	Analysis of Variance
RSM	Response Surface Methodology
LVER	Linear Viscoelastic Region
RCCD	Rotatable Central Composite Design

Notations

ΔH_m	Enthalpy of Melting
ΔH_m^0	Enthalpy of Fusion
ΔH_{cc}	Enthalpy of Cold Crystallization
T_g	Glass Transition Temperature
T_{cc}	Cold Crystallization Temperature
T_c	Crystallization Temperature
T_m	Melting Point Temperature
$\phi(t)$	Degree of Crystallinity
n	Avrami exponent
k	Crystallization Rate Constant
$t_{0.5}$	Half Time of Crystallization
I_{Cr}	Percentage of Crystallinity Index
M	Overall Migration
G′	Storage Modulus
G″	Loss Modulus
q	Scattering Vector
R^2	Regression Coefficient
YI	Yellow Index
ΔE	Total Color Difference

CHAPTER 1

INTRODUCTION AND LITERATURE REVIEW

This chapter focuses on the need for environment-friendly sustainable packaging, which gained the scientific community's attention and interest in developing active sustainable food packaging materials. Researchers have begun to introduce sustainable active primary packaging including edible coating and films and secondary packaging material. The necessity of making sustainable packaging material active by tuning the inherent properties of sustainable polymers with the addition of active compounds is to obtain various functional properties such as antioxidant, antimicrobial, anti-browning, UV-Vis light blocking, color, and glossiness, textural, barrier, thermal and mechanical, and most importantly prolonging the shelf-life of fresh produce which are comparable with the conventional packaging material. The existing food packaging material is petroleum-based and responsible for raising environmental hazards and destroying carbon footprint. Therefore, the current chapter aims at providing insights into the utilization of biodegradable polymers in sustainable food packaging. However, the biodegradable polymer alone cannot fulfill the required functional properties. Thereby, this chapter includes an introduction to the preferable and desirable addition of new materials, and approaches like the utilization of renewable waste "algae biomass". Besides, the migration property of the packaging material has been discussed to understand the effect of algae. Moreover, the utilization of algal residue for the fabrication of primary and secondary sustainable material is also concerned with food safety, which will be extremely useful for academics and industries as a new concept.

Outcome: Mondal, K., Ghosh, T., Bhagabati, P., & Katiyar, V. (2019). Sustainable Nanostructured Materials in Food Packaging,' In *Dynamics of Advanced Sustainable Nanomaterials and Their Related Nanocomposites at the Bio-Nano Interface*. (pp. 171-213). Elsevier.

Mondal, K., Ghosh, T., & Katiyar, V. (2021). Edible Food Packaging in Targeted Food Preservation In *Nanotechnology in Edible Food Packaging: Food Preservation Practices for a Sustainable Future.* (pp. 371-409). Springer, Singapore.

1.1 Introduction

Packaging plays an important role in food preservation as it acts as a barrier against physical impacts, prevents contamination, increases shelf-life, and contains important information about packaged food [1]. In addition, the food packaging sector is one of the largest plastic consumers in the world. Conventional plastics or non-biodegradable polymers have been used as packaging material for many years because of their economic and technological feasibility. These synthetic polymers are hydrophobic in nature, cannot be degraded by microorganisms, and take many years to decompose. Thus, petroleum-based polymer is responsible for raising serious environmental hazards by generating a wide volume of solid waste [2]. To maintain the ecological balance, the need for the replacement of conventional plastics with biodegradable polymers is required. The use of plastic in packaging both rigid and flexible forms has increased and is a matter of concern as, many times, the packaging is not effectively collected, ending up in landfills and drains in the cities [3]. Owing to solve such serious environmental problems, researchers have started developing biodegradable food packaging materials. In General, food packaging materials are categorized traditionally as primary and secondary packaging wherein the former refers to the immediate container or material that comes into direct contact with the product and secondary one refers to the outer packaging material that is used to group, protect, or transport multiple units of the primary packaged products [1]. Besides, the concept of advanced packaging has gained more attention as it offers various benefits and address specific challenges in the packaging industry. In this context, active packaging which is a type of advanced packaging, refers to packaging materials that have active functionalities to interact with the product or the environment to enhance product quality, safety, or shelf-life. However, non-active packaging refers to packaging materials that do not have specific active functionalities but primarily serve as a passive barrier to protect the product. Further,

the active packaging may also act as edible packaging material, which refers to packaging materials that are safe for human consumption and can be ingested along with the packaged food or beverage. These materials are designed to provide a protective barrier for the product while also being edible and digestible.

In this regard, edible and active packaging as a primary packaging material is an emerging concept aimed to deliver quality and safe food along with prolonged shelf-life while at the same time mitigating environmental hazards caused by non-biodegradable food packaging waste. Besides, acting as a barrier, this innovative packaging also acts as one of the preservation methods and minimizes post-harvest losses of fresh produce. Post-harvest loss is one of the biggest concerns that the globe is facing throughout the century. The concerns associated with fruits and vegetables are consumption of contaminated perishables causes foodborne outbreaks and the lowering of economic values due to massive post-harvest loss, generated by improper storage and transportation capacity. Further, the increasing population and modern lifestyle also demand food with quality and safety. Therefore, providing sufficient food is also necessary to meet the hunger of everyone. In recent times, a mass scientific community has focused their research predominantly on the development of biodegradable active edible films and coating as primary packaging by utilizing natural bio-resources as a functional preservative with the due concern of food safety and security [4]. On the other hand, the demand for green consumerism with fewer added artificial additives, improved nutritional quality, and assurance of food safety with an extended shelf-life of fresh fruits and vegetables has drawn the attention of food industries, agronomists, and scientists to investigate and develop advanced technology for fulfilling the need. To resolve the hindrance associated with post-harvest loss of fresh fruits and vegetables, the application of the edible coating is one of the emerging packaging strategies and a preservation technique for prolonging the shelf-life of

perishables. Generally, edible coating polymers are extracted from natural resources which are environmentally benign and improves the quality and nutritional value of fresh produces [5]. Further, the coating material can provide various physicochemical properties including thermal, mechanical, sensory, microbiological, and quality attributes along with extended shelf-life to fruits and vegetables by creating a modified environment around the surface of fruits and vegetables by controlling the oxygen, carbon dioxide transmission rate and moisture evaporation rate.

Apart from edible primary packaging, the fabrication of secondary biodegradable packaging material is another way to make the globe free from non-biodegradable plastics. Several countries have already banned the use of conventional plastics; therefore, the fabrication of sustainable food packaging material is of the utmost need. In this context, improving the functionality of sustainable polymer is necessary for obtaining an effective tuned property by the incorporation of active natural substances, which are not available in conventional packaging [6]. The active packaging system generally consists of antimicrobial agents, antioxidants, and several other beneficial bioactive compounds [7]. The non-toxic renewable bio-fillers and other bioactive compounds are added to the packaging material for obtaining active sustainable food packaging material.

1.2 Sustainable/Biodegradable Polymers

Sustainable polymers are principally bio-based or bio-derived polymers that are generally synthesized from renewable sources [8]. These polymers are also recognized as green polymers having properties of biodegradability, biocompatibility, and non-toxicity. This class of polymers is obtaining significant attention for usage in food packaging, tissue engineering, and others. Additionally, renewable biological resources are one of the main advantageous factors of consideration for these biopolymers. These polymers can also be

broadly categorized depending on their different reproducible origin and process of manufacturing, as shown in **Figure 1.1**.

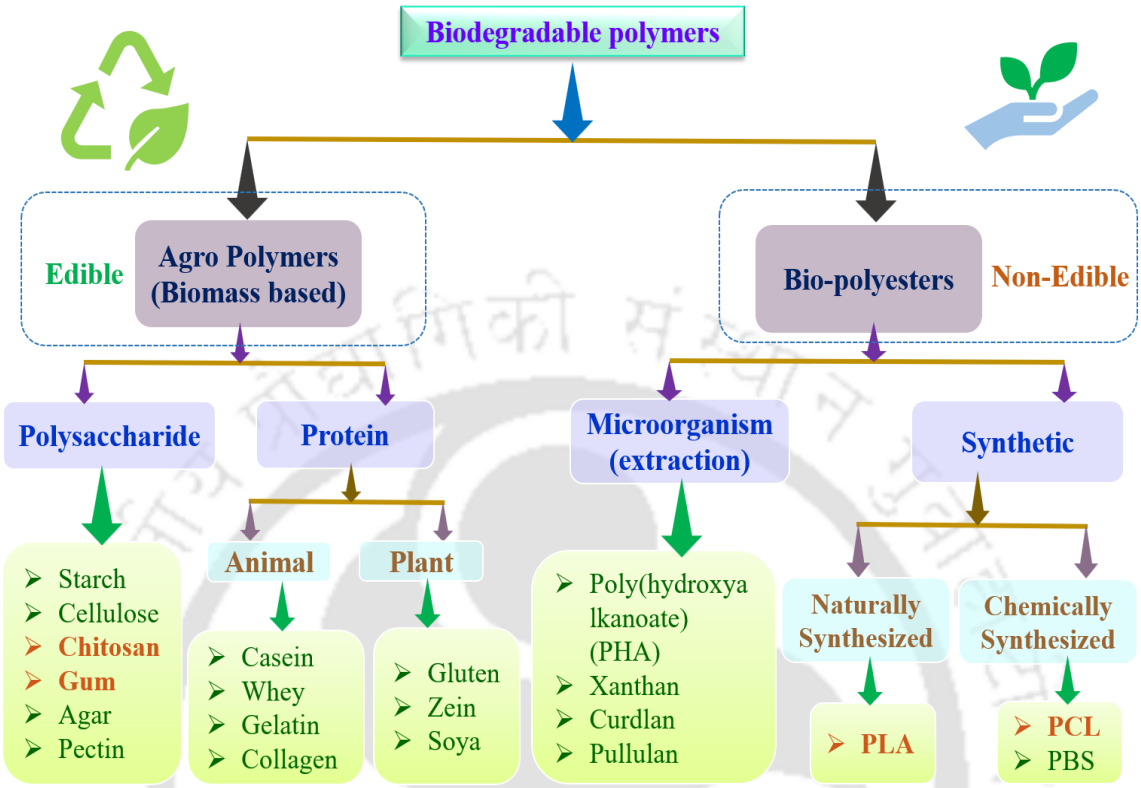

Figure 1.1: Classification of different types of biodegradable polymers.

1.2.1 Need for Sustainable Polymers

One of the most significant inventions in the twentieth century is the discovery and development of sustainable polymers to improve quality of life. So-called 'Plastic' which is the polymer has a wide interpretation in everyday life and society at large. From developing small plastic bottles to setting up modern space centers, it reflects the increase in demand for polymer use daily. Polymeric materials are widely used substances due to their various properties such as durability, lightweight, processability, physicochemical properties, etc. The few most widespread applications in industrial sectors are packaging, construction, transportation, aerospace, biomedical, energy, and military [8]. Nowadays the use of sustainable polymers has been gaining more attention due to the obstacle of using conventional polymers. Conventional polymers are largely associated with non-renewable

sources such as fossil feedstock, natural gas, and petroleum. The use of conventional polymers is related to environmental problems including the generation of solid waste that accrues in landfills and oceans, allowing the production of pollution, and related environmental issues due to increasing population and economic development in most countries.

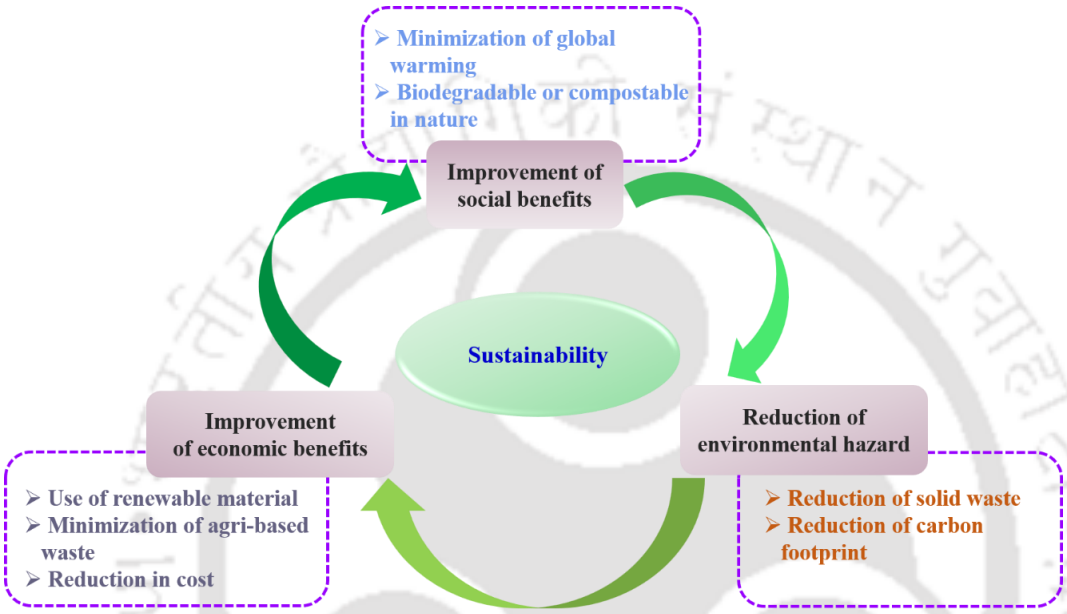

Figure 1.2: Sustainable goals for socioeconomic benefits.

In this context, people from different parts of the globe are recognizing the necessity of reducing the amount of disposable and waste plastics. Further, people are trying to recycle these wasted materials through new initiatives that will connect the practicality, feasibility, and economic condition of the globe. Thus, sustainability is the success of resolving the problems that will be benefitted by aiming towards the planet, enriching people, and will help to create social and economic benefits as depicted in **Figure 1.2**. Moreover, it is also an integrated way of philosophical thoughts on a product's entire lifecycle.

1.3 Food Packaging

In recent years packaging has developed well beyond its original function as merely a means of product protection and now plays a key marketing role in developing on-shelf

appeal, providing product information, and establishing brand image and awareness (**Figure 1.3a**). The principal function of food packaging is to protect food from environmental contamination and other influences (such as odors, shocks, dust, temperature, physical damage, light, microorganisms, and humidity), and it is key to ensuring the quality and safety of food, while at the same time extending shelf-life and minimizing food losses and wastage during the post-harvest stages [9-11].

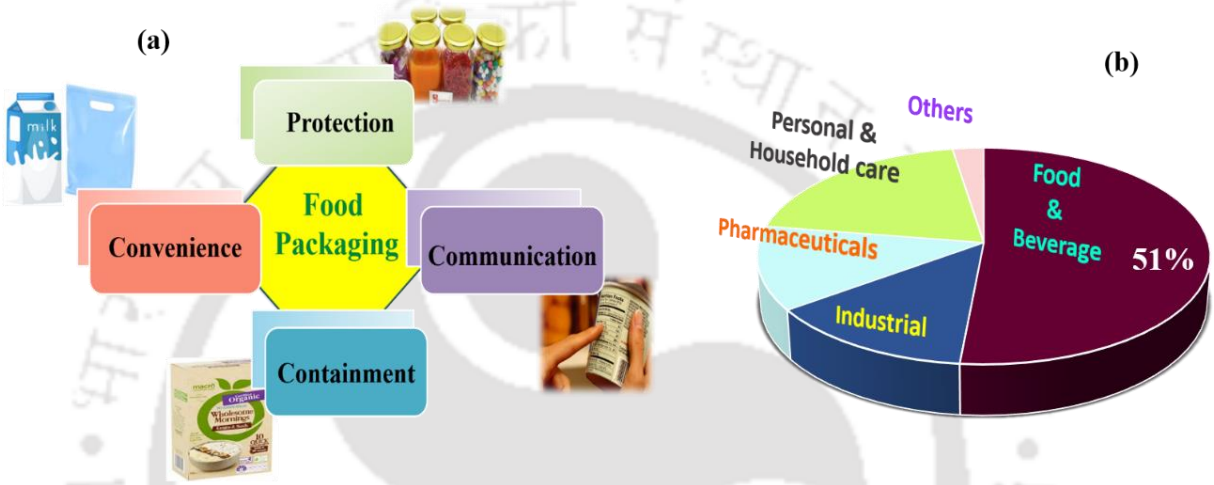

Figure 1.3: (a) Concept of food packaging, and (b) global plastic packaging market.

The continued quest for innovation in food and beverage packaging is mostly driven by consumer needs and demands influenced by changing global trends, such as increased life expectancy, fewer organizations investing in food production and distribution, and regionally abundant and diverse food supply. The use of food packaging is a socioeconomic indicator of the increased spending ability of the population or the gross domestic product, as well as regional food availability. In addition, food packaging is one of the global largest plastic-consuming sectors where almost half of the total consumed plastic is utilized (**Figure 1.3b**).

1.3.1 Classification of Food Packaging

Generally, food packaging is classified into three basic categories i.e., primary packaging, secondary packaging, and tertiary packaging as depicted in **Figure 1.4** [12]. Primary

packaging remains in contact with products, which can directly be purchased by the consumers for consumption purposes; secondary packages are used to carry the primary packages such as boxes, and cartons; tertiary food packaging contains many goods for transportation purposes and carries the secondary packages too.

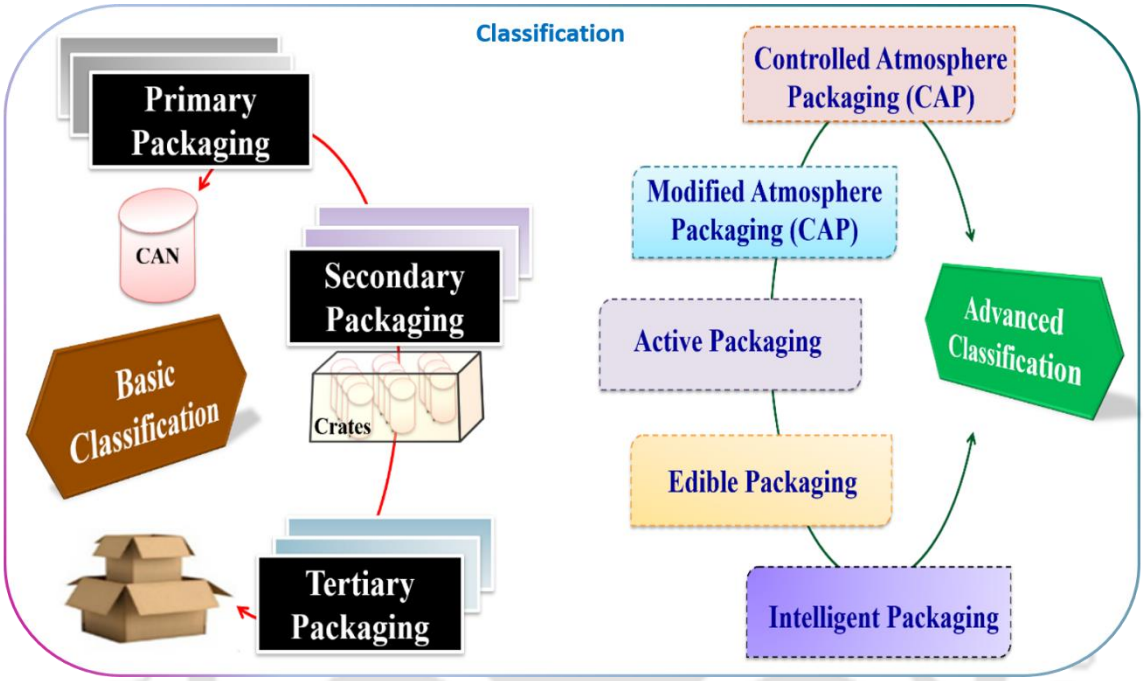

Figure 1.4: Basic and advanced classification of food packaging.

Under all the classes, secondary and tertiary food packaging are mostly found as packaging waste. However, nowadays it can be recycled and reused, but primary food packages get contaminated, which makes them unacceptable for reuse and recycling. In this regard, aiming to overcome the existing drawbacks and extend the shelf-life of food, advanced categories of packaging have been made as described in **Figure 1.4**.

1.3.2 Concerns Associated with Food and Packaging

Food packaging is one of the effective preservation techniques. However, the existing conventional packaging is responsible for the generation of food packaging waste. These wastes are non-biodegradable and raise environmental hazards. In India, 80% of total plastic consumption is discarded as waste and the country generates 25,940 tons of plastic

waste daily according to official statistics and at least 40% of which is still uncollected [13]. In addition, increasing population and economic growth throughout the globe have resulted in large waste production. Besides packaging, another biggest concern associated with food is post-harvest loss which arose due to poor storage facilities, transportation, packaging, and unawareness of proper handling. The prime reason for hurdles associated with food and packaging are as follows:

- Use of non-biodegradable packaging material
- Use of non-renewable resources
- Use of non-recyclable plastics
- Oversize packaging material
- Environmental hazard due to food packaging waste
- Post-harvest loss

These are the reasons that have turned to the use of sustainable polymers as food packaging material instead of petroleum-based traditional plastics.

1.3.2.1 Post-harvest Loss

Post-harvest loss can define as the loss at harvesting to the consumption resulting from qualitative, quantitative, and food loss altogether, which is one of the biggest concerns that the globe is facing throughout the century. Further, the increasing population and modern lifestyle also demand food with quality and safety. Therefore, providing enough food is also necessary to meet the hunger of everyone. According to the estimates in 2022, India administered around 30-40% post-harvest loss due to fresh produce such as fruits and vegetables [14]. Among these, fruits contribute 16% and vegetables contribute 13% loss. In addition, around 33% of post-harvest losses occurred during harvest, and 56% is due to storage. Fresh produce is perishable in nature therefore, the chances to get spoiled are high. Several factors affect post-harvest loss including physical damage, microbial

contamination, environmental factors, inadequate harvesting, handling, storage facilities, and field handling. Besides, transportation and distribution of fresh produce are the most important areas of post-harvest loss. Poor transportation causes mechanical and physical injury due to uncontrolled conditions such as temperature and humidity. Moreover, this loss provides a negative impact on the economic status of any country. In this regard, aiming to resolve this hindrance, sustainable packaging such as edible coating is one of the emerging packaging strategies and a preservation technique for prolonging the shelf-life of perishables.

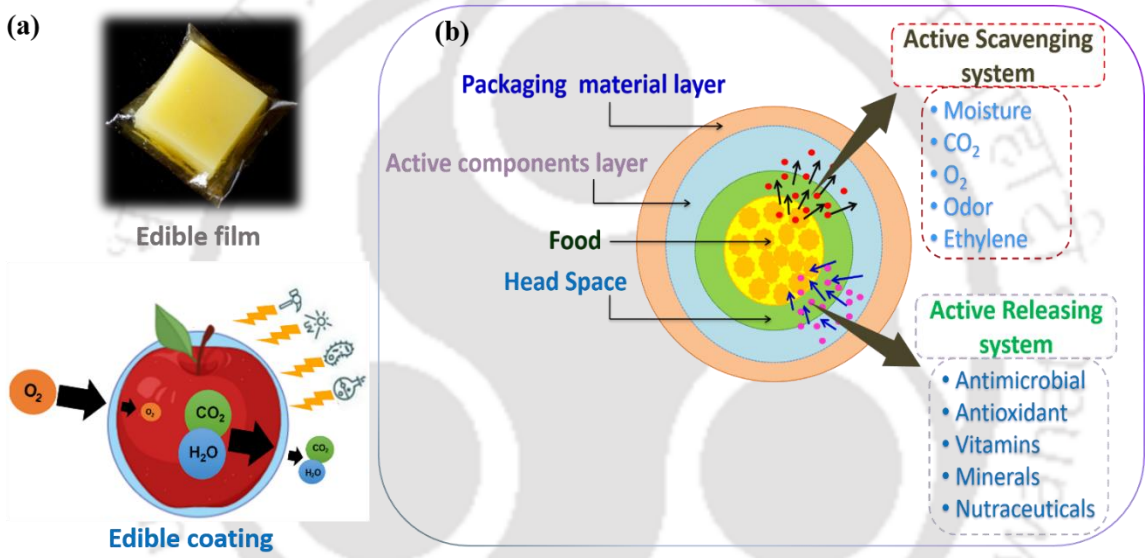

Figure 1.5: (a) Pictorial view of edible coating and film, and (b) mechanism of active packaging.

1.3.3 Edible and Active Packaging

Edible packaging consists of edible films and coating, defined as a thin continuous layer of edible material formed on, placed on, or between the foods or food components, which helps maintain the quality and increase the shelf-life of the products (**Figure 1.5a**). Besides, active packaging materials are designed to actively maintain or improve the condition of the food either by eliminating unwanted components from the package headspace and/or from the food itself or by releasing active components into the food or its surroundings

(**Figure 1.5b**). Edible packaging can act as active, either by incorporating active compounds which are edible in nature or by tuning the inherent properties of the edible polymer. In addition, some of the edible polymers are naturally active. The outcome of this packaging results in an extension of shelf-life, improved safety and sensory attributes, and the maintenance of product quality [15]. Unlike traditional packaging, edible active packaging plays a dynamic role in food preservation (**Figure 1.6**). The main applications have mostly focused on delaying oxidation and controlling moisture migration, gaseous exchange, microbial growth, respiration rates, volatile flavors, and aromas by creating a semipermeable layer over the food surface. Various edible coating techniques are available to coat the food such as dipping, brushing/or enrobing, spraying, electrostatic spraying, fluidized-bed coating, and panning. Among these dipping, brushing, and spraying are household techniques that farmers can easily avail whereas, the rest of the techniques are industry-friendly.

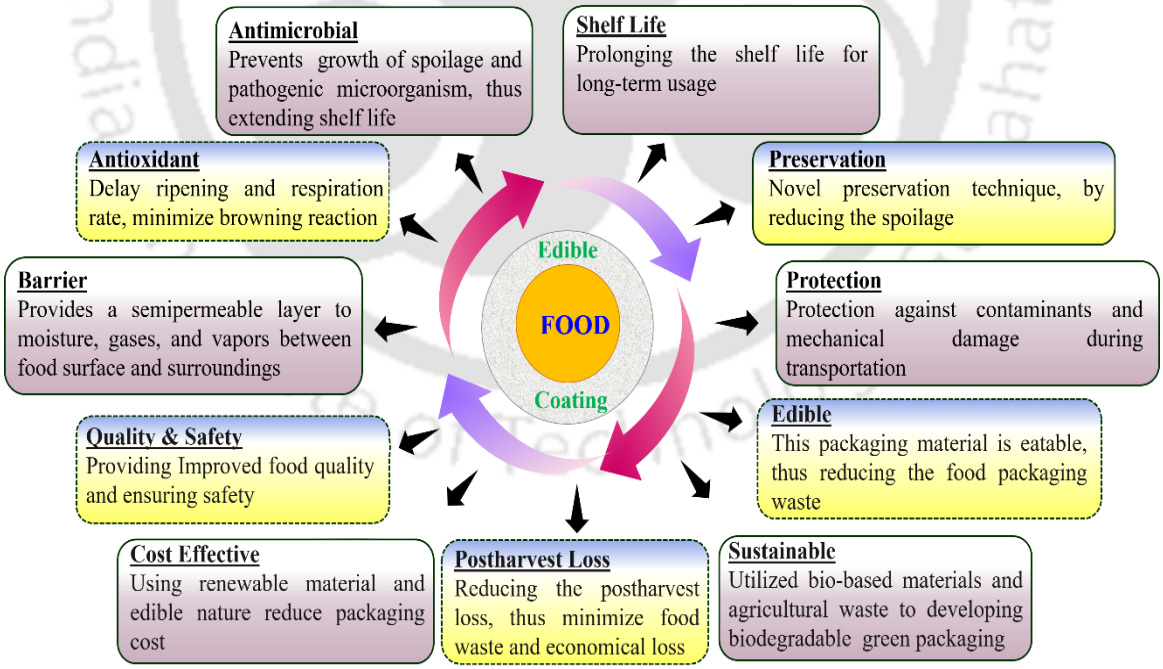

Figure 1.6: Functions of edible active packaging.

1.4 Edible Biopolymers for Food Packaging

The edible polymers are mostly extracted from renewable sources such as agri-biomass, plants, and animals as discussed in section 1.2. Extracted edible polymers are polysaccharides and proteins in nature (**Figure 1.1**). In addition, polysaccharide-based edible polymers are commonly used as packaging matrix material.

1.4.1 Polysaccharide-based Edible Polymers

Polysaccharides are complex carbohydrate molecules consisting of several long-chain monomeric units of glucose and linked together by glycosidic linkage. This class of polymers is principally obtained from plants and microbes as natural resources. Most often utilized polysaccharides in food packaging are considered cellulose, starch, chitosan, guar gum, agar, and its derivative. Various researchers have already investigated and established the broad application of polysaccharides from various natural sources for making different types of packaging materials either edible or non-edible with different properties. Researchers have found a positive and promising indication of using polysaccharides or carbohydrates as packaging material for food. These polymers are capable to form blown and cast films, and this property has compelled more to gain the attention of researchers to investigate and traverse them into food packaging applications. Several well-defined types of research have been executed on the various applications of polysaccharide films and coatings over a variety of fruits, vegetables, seafood, meats, and confectionery products. Also, the quality and shelf-life extension have been preserved by restricting a few natural phenomena like oxidation, dehydration, rancidity, surface browning, and oil diffusion.

Further, these polymers aid to enhance the physicochemical, nutritional, and sensorial properties of the products to restore quality attributes. Despite that, the main drawbacks associated with these polysaccharides-based films are inflexibility and strong hydrophilic nature in comparison to synthetic polymer-based films [16]. To overcome these

shortcomings, more focused research needs to be carried out to determine the best possible way the improvement of packaging films property. The good thing about polysaccharides is they can be easily modified to other forms to improve their physicochemical properties [17].

1.4.1.1 Chitosan

One of the most abundant and generally recognized as safe (GRAS) substances approved by US-FDA (United States Food and Drug Administration) natural edible polysaccharides is chitosan (CS) which is derived from chitin [18]. Chitin, a principal origin of chitosan is widely distributed in the animal and plant kingdom. The prime resources of chitin are fungi (mushrooms), algae, mollusks, annelids (segmented worms), cnidaria (jellyfish), aschelminthes (roundworms), arthropods, etc. Besides, the shells of shrimps, crabs, crustaceans, prawns, lobsters, etc. which are considered biowaste, contain a high amount of chitin. Thus, CS is also a waste utilized natural biopolymer, which is responsible for the minimization of environmental hazard issues. Seafood contains around 40-50% shell which contains a higher amount of chitin compared to other sources like insects such as silkworms, bees, cockroaches, etc. CS, a linear copolymer comprising of D-glucosamine and N-acetyl-D-glucosamine (NADG) associated by β-(1-4) glycosidic bond and is derived from chitin by a single-step process called deacetylation (**Figure 1.7**). Chitin has three different polymorphic solid-state forms namely α, β, and γ. These individual forms are non-identical by their degree of hydration, size of the unit cell, and the number of chitin chains per unit cell. α-chitin is composed of antiparallel sheets of chitin chains which are arranged in a tightly compacted manner of the crystalline structure whereas β-chitin is more mobile in nature and has parallel sheets and γ-chitin is the combination of both (**Figure 1.7**). The composition of CS may vary depending on the source, preparation technique, and physiological condition (reaction time, temperature, etc.). The structure of CS is

predominantly based on the degree of deacetylation (DD%), where the percentage removal of an acetyl group from the chitin molecule is occurred (**Figure 1.7**) [19].

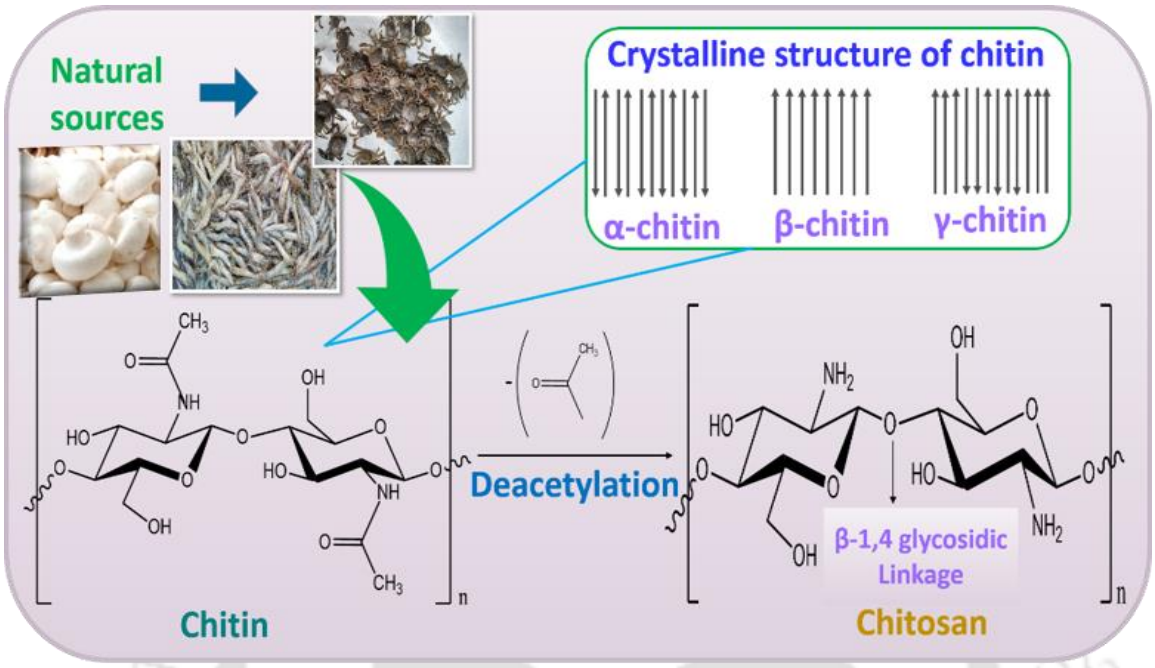

Figure 1.7: Chemical structure of chitosan and its conversion from chitin along with the crystalline nature of native chitin.

In general, chitin is a water-insoluble polymer with lesser chemical reactivity. However, CS becomes water-soluble in acidic pH at 50% degree of deacetylation, and the protonation of $–NH_2$ groups occurs resulting in solubilization, which makes pseudo-natural cationic biopolymer due to the positive surface charges on D-glucosamine repeat unit. The presence of an amine functional group at the carbon-carbon linkage of the monomeric unit differentiates chitin from chitosan, which thereby enhances the solubility and reactivity of CS in comparison to chitin. CS has been considered a versatile biopolymer as it can be converted into gels, films, nano, and micro-particles, beads, etc. along with its spreadable applications in food engineering, biomedical and cosmetic sciences [20]. In addition, the most unique characteristics of CS are good film-forming and gas barrier properties, antimicrobial activity, biocompatibility, biodegradability, and low toxicity. It is noteworthy to mention, the inherent antimicrobial property of CS makes it in high demand for various

applications. The property of antimicrobial activity mainly depends on the polycationic structure and positive charge which is related to DD. Kong et al., 2008 reported that for native CS, higher DD is responsible for more positive charge density which is responsible for strong electrostatic interaction and has shown higher antimicrobial activity [21]. Furthermore, CS and its derivatives can also be utilized as a food preservative and an additive as thickeners, stabilizers, gelling, and emulsifying agents. Also, it has a wide application in the edible coating as primary packaging [22]. CS is also blended with a non-biodegradable polymer for food packaging applications due to two reasons, i.e., increasing the bio-based content in non-bio-based material like polyethylene (PE), and polypropylene (PP) and obtaining antimicrobial packaging material [23].

Besides, these advantageous properties, some constraint of CS renders its application as commercial food packaging material. The main constraint is its hydrophilicity and brittleness. Therefore, modification is necessary to improve these properties and to expand the application possibilities by adding salt and plasticizers, use of a suitable solvent, cross-linking polysaccharides, chemical modification of hydroxyl groups, changing pH, blending with other polymers, and addition of bio-fillers/or additives. Because of its inherent flexibility and the presence of hydroxyl and amino groups at the backbones, the modification of chitosan has become facile.

1.4.1.2 Guar Gum

Guar gum (GG) is another polysaccharide and a good candidate for edible packaging material such as edible coating and films due to its long polymeric chain and high molecular weight as compared to other gums [24, 25]. However, this biopolymer does not impart antioxidant and antimicrobial activity because of its chemical structure. It is composed of two sugars namely mannose and galactose where mannose units are linked with the β-D-1,4-mannopyranose backbone and branched side chain of galactose and mannose linked

with α-D-1,6-glycosidic linkage as depicted in **Figure 1.8**. GG is extracted from the endosperm of legume plant guar beans [26]. This polysaccharide is a GRAS substance approved by the US FDA (United States Food and Drug Administration) organization and considered an edible polymer. In addition, GG is used as one of the most important and desired food additives and has an E-number (E 412) when added to food products.

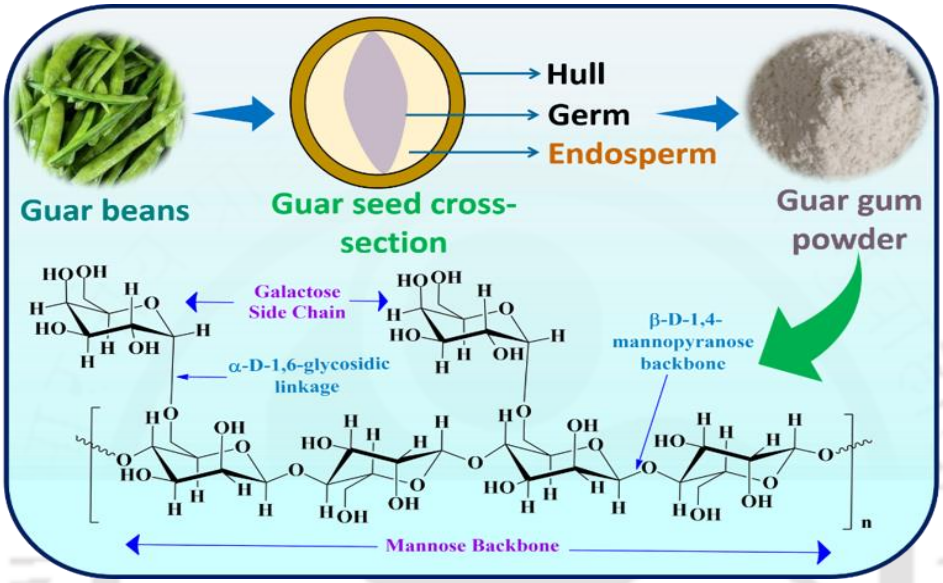

Figure 1.8: Chemical structure of guar gum.

GG has wide applications in various fields, predominantly in the food industry and textile, paper, pharmaceutical, and cosmetic industries. In the food industry, GG is used in baked goods (pastry), dairy products (milk, yogurt, ice cream), meat products, condiments (salad dressing, ketchup), frozen foods, dry soup, and others. Besides, GG has been applied as an edible coating material on fruits and vegetables for extending the shelf-life of perishables. However, commercial usage of GG is restricted to edible coating due to its inadequate mechanical, thermal, and barrier (moisture and gas) properties as compared with the polymers used in edible packaging [26,39-40]. Therefore, modification or tuning the native property of GG is required to obtain optimum functionalized characteristics for food packaging.

Table 1.1: Application of chitosan and guar gum as edible films and coatings material to prolong the shelf-life of perishables.

Matrix material	Active agent	Application	Effective property	Reference
Chitosan	Blueberry & blackberry pomace extracts	Edible smart film	Dry pH indicator film & Antioxidant activity	[27]
Chitosan	Clove essential oil & nisin	Edible active film	Antimicrobial & extended pork meat shelf-life	[28]
Chitosan	Fresh *Spirulina* extract	Edible active film	Antimicrobial, Barrier, mechanical property	[29]
Chitosan	Pomegranate peel extract	Edible active film	Improved barrier & Phenolic content	[30]
Chitosan	Plant extract	Edible coating on strawberry	Extended shelf-life & Phytochemical properties (low temperature)	[31]
Chitosan	Grapefruit seed extract	Edible coating on tomato	Extended shelf-life & Antimicrobial activity (low temperature)	[32]
Chitosan	Procyanidins extracted from grape seeds	Edible coating on fresh blueberry	Extended shelf-life for 14 days of storage at 4 °C.	[33]
Guar gum	Orange oil & curcumin	Edible films	Antimicrobial activity, Hydrophobicity, & Shelf-life of strawberry	[34]
Guar gum	Orange peel oil & halloysite nanotubes	Edible films	Antimicrobial activity, Hydrophobicity, Strength, & Water vapor barrier	[35]
Guar gum	Ag-Cu nanoparticle	Active food packaging	UV-light, Gas Barrier, & Antimicrobial property	[36]
Guar gum	Grape pomace extract	The edible coating on pomegranate arils	Extended shelf-life for 6 days at 10 °C	[37]
Guar gum	Glycerol	The edible coating on Roma tomato	Extended shelf-life for 20 days at 22 °C	[38]

In this regard, modification of GG and incorporation of bio-filler can help to resolve the requirement. On the other hand, this native polymer is widely used in food industries as a water binder, emulsifier, moisturizer, thickener, and stabilizer, and can suspend various liquid-solid systems [41]. In this thesis work, the two most advantageous polysaccharide-based edible polymers chitosan and guar gum has been focused on. In addition, the applications of the polymers the edible films, and coatings are provided in **Table 1.1.**

1.5 Non-edible Biopolymers for Secondary Food Packaging

There are polymers extracted either from renewable or through chemical modification of petroleum sources that are completely biodegradable within the stipulated time of 90 days, and these are non-edible in nature. Among them, Poly(lactic acid) (PLA) and Poly(ε-caprolactone) (PCL) are the most commonly available biodegradable polymers.

1.5.1 Poly(lactic acid)

Maximum scientific and industrial research has been carried out on PLA biopolymer in comparison to other biopolymers due to its lower cost of production, non-toxicity, and biodegradability, relative to other biopolymers and its high potential for commodity applications like food packaging. PLA is a thermoplastic polyester (**Figure 1.9**) and semi-crystalline polymer that is derived from various renewable sources including corn, sugar cane, and starch-based substances such as sweet potato and others, by fermentation. Moreover, PLA is biodegradable and compostable but under standard conditions [42]. The major drawback of PLA is its low barrier property, biochemical properties, and brittleness which lets it down as a competitive candidate in prospective food packaging applications, where both the mentioned properties hold great importance. Bio-nanocomposites and blends of PLA with a variety of bionanomaterials and other biopolymers enhance its physical properties like oxygen gas and moisture barrier properties, crystalline, mechanical, and other properties. [43,44].

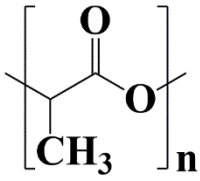

Figure 1.9: Chemical structure of poly(lactic acid).

1.5.2 Poly(ε-caprolactone)

Among others, Poly(ε-caprolactone) (PCL) is another important biodegradable polymer that has good physical properties and is commercially available, but at a slightly higher cost. It is also a thermoplastic polyester (**Figure 1.10**) that is semi-crystalline in nature. PCL exhibit relatively low melting (60 °C) and low glass transition (-60 °C) temperature and this is the reason why it is mostly blended with several other polymers with higher melting temperature. The high flexibility and elongation at the break value of PCL make it one of the most preferable choices for blending with another polymer. The incorporation of active compounds such as lemon extract, thymol, lysozyme, and others effectively enhances an antimicrobial property of PCL-based packaging films due to a low processing temperature (~63 °C), which causes no to little change in an antimicrobial property of these nature-derived chemical compound [45]. Further, various bio-fillers such as nanomaterials and others have been used to develop PCL-based biocomposites for improving the property and reducing the cost of the material for packaging applications [46]. Therefore, the incorporation of fillers, additives, and reinforcing agents is required to tune the inherent properties of biopolymers for wide applications.

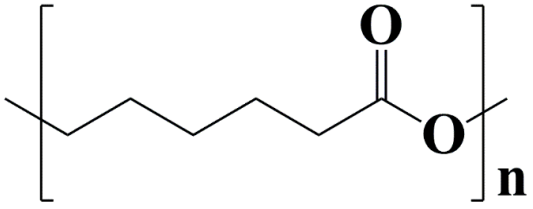

Figure 1.10: Chemical structure of poly(ε-caprolactone).

1.6 Algae Biomass

Algae are photosynthetic organisms that grow in a range of aquatic habitats, including lakes, ponds, rivers, oceans, and even wastewater. They can tolerate a wide range of temperatures, salinities, pH values, different light intensities, and conditions in reservoirs or deserts and grow alone or with other organisms [47]. It is a highly nutritious and rich source of polysaccharides, lipids, pigments, proteins, vitamins, bioactive compounds, and antioxidants [48] (**Figure 1.11**). In addition, algae are broadly classified as Rhodophyta (red algae), Phaeophyta (brown algae), and Chlorophyta (green algae) and classified by size as macroalgae or microalgae. Macroalgae (seaweed) are multicellular, large-size algae, visible with the naked eye, while microalgae are microscopic single cells and may be prokaryotic, like cyanobacteria (Chloroxybacteria), or eukaryotic, like green algae (Chlorophyta). In recent years, microalgae have gained enough attention as a possible solution to some imminently critical issues, including the role of an alternative fuel source, and as a potential source of many bioactive compounds intended for human consumption. Extensive research has been focused on renewable energy to reduce greenhouse gas emissions and ensure energy security [49]. It is a rich source of carbon compounds, which can be utilized in biofuels, health supplements, food, pharmaceuticals, and cosmetics [50]. However, these compositions are completely dependent on the variety of strains. Currently, a global algal biomass production stands at 38 million litres [50]. Primarily, two types of microalgal cultivation systems have been the subject of interest of academia and industry: photobioreactors (PBRs) and open raceway ponds (ORPs). The advantages of using microalgae as an oil source for biodiesel production are carbon dioxide capture, less land use, high biomass and oil yield, and no competition with terrestrial crops. In addition, the total cost of cultivating microalgae may range from $2–$15/kg using ORPs, compared with $32/kg employing PBRs [50]. Presently, the species of microalgae selected for oil

production in the industry include various strains of *Chlorella*, *Dunaliella*, *Nannochloropsis*, *Scenedesmus*, and *Schizochytrium* [51]. Besides these uses, the current market demand for algae-based food products is increasing as a healthy and nutritious supplement [52].

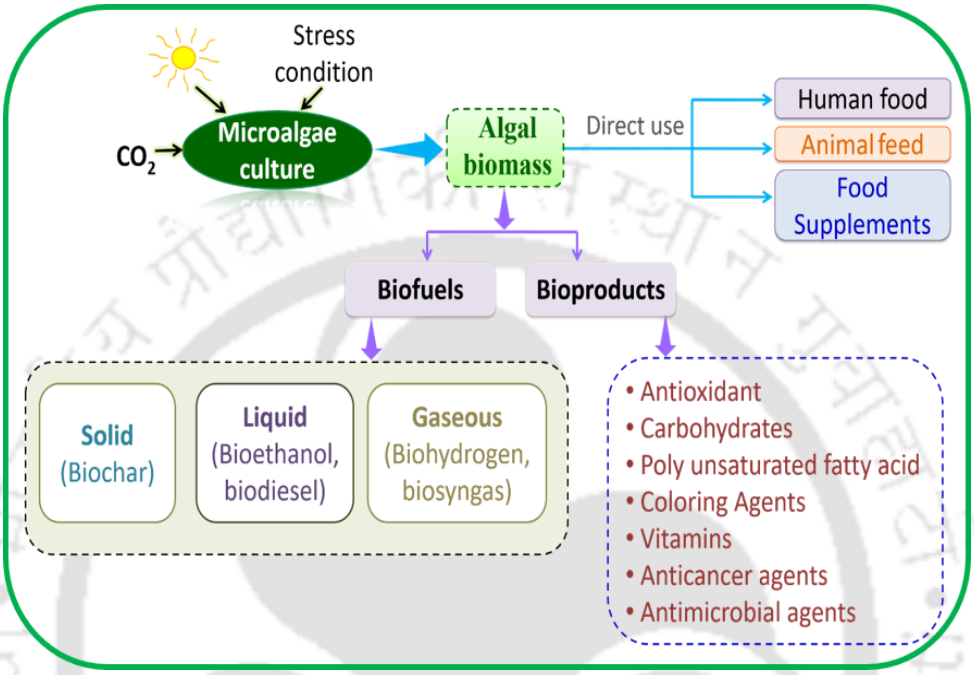

Figure 1.11: Schematic of microalgae production and its use.

1.6.1 Algae as a Rich Source of Food and Medicine

In most developed countries, people consume high-caloric food items due to the modern lifestyle, which leads to health problems, such as obesity, heart disease, and diabetes. A balanced nutritional diet that must contain vitamins, minerals, polyunsaturated fatty acids (PUFAs), etc., is needed for health. In this regard, microalgae are considered a remarkable but poorly explored natural source for a healthy diet. Several species of microalgae are identified as rich in carbohydrates, proteins, lipids, and nutritionally valuable components. Becker (2013) reported that microalgae are an abundant source of vitamins and minerals, such as vitamins A, B1, B2, C, and E, nicotinate, biotin, folic acid, pantothenic acid, niacin, iodine, potassium, iron, magnesium, and calcium [53]. The Chinese first consumed microalgae (*Nostoc sp*.) (over 2000 years ago) as food and, later, the commercial forms of

microalgae (*Chlorella sp*. and *Spirulina sp*.) have been used as healthy foods in Japan, Taiwan, and Mexico [54].

Currently, most of the commercialized products of microalgae are available in markets as a health food, in the forms of tablets, capsules, and liquids [55], and their products are mixed with pastes, snacks, candy, gums, noodles, wine, beverages, and breakfast cereals [56]. In addition, *Chlorella* sp., *Dunaliella sp*., and *Spirulina sp*. are some of the microalgae species widely used as human food sources because they are rich in protein content and have high nutritive value [57]. Moreover, microalgae have been incorporated into baked goods such as bread, cookies, crackers, and pastries, beverages, and milk products to increase protein content, bioactive compounds and extend the shelf-life [58]. Among these microalgae, *Spirulina* and *Chlorella* are currently dominating the microalgal market in food products.

1.6.2 Concern associated with Algae Biomass

Despite the high content of nutritious compounds found in algae, few concerns are associated with it. Predominantly, the microalgae fuel industry is facing technical challenges that after the cultivation of algae biomass and extraction of algal oil, the leftover algae biomass is treated as waste or residue. These generated wastes are either used as cattle feed or dumped on the coastal region which pollutes the environment. However, this waste or residue contains an adequate number of bioactive compounds. Therefore, it is essential to find out a possible way to utilize the waste algae biomass to minimize air pollution and restore the bioactive compounds.

1.6.3 Algae Biomass-based Composites

Currently, researchers have started utilizing algae and its residue for the fabrication of biocomposites for food packaging applications. Besides, the incorporation of algae residue helps to tune the primitive properties of biopolymers and enhance biodegradation. The

algae biomass residue (ABR) has been incorporated into various biopolymers such as poly (butylene adipate-co-terephthalate (PBAT), poly(butylene succinate (PBS), poly(vinyl alcohol) (PVA), PLA, starch, chitosan and others for obtaining improved property for packaging applications [5,59-63] as depicted in **Table 1.2**. Furthermore, *Botryococcus braunii, Nannochloropsis salina, Gelidium Elegance, Heterochlorella luteoviridis, Spirulina,* and *Dunaliella tertiolecta* are the algal species have been utilized for the development of bio-composites [64]. The bio-composites have been fabricated using various techniques such as blow molding, solution casting, and injection molding [5,65]. The addition of biomass has increased films' solubility, biodegradability, thermal stability, elongation, and rupture, and reduced the tensile strength and Young's modulus [66]. All films with microalgae showed higher antioxidant activity and other biochemical properties. The literature is supported that algae fiber can be used as an excellent reinforcement in bio-composites and this marine-based natural fiber, may be an alternative to plant-based fibers resulting in effectively improving the properties of bio-composite as “green-composite” or “eco-composite.”

Table 1.2: Utilization of algae biomass for the development of bio-composites.

Matrix material	Nature of algae	Filler material	Application	Effective property	Reference
Poly(vinyl alcohol) (PVA)	Residue	Lipid-extracted algal biomass (LEA)	3D printing material	Thermal stability, reduced tensile strength & elongation, &s mechanical property	[61]
Poly(butylene adipate-co-terephthalate)	Residue	Residual microlalgal biomass (RMB)	Agricultural film	Poor Tensile Strength& Low thermal stability	[59]
Poly(butylene succinate (PBS)	Residue	Residual microlalgal biomass (RMB)	-	Improved rigidity and reduction in cost	[60]
Polycaprolactone (PCL)	Fresh	Sea algae fiber (SAF)	Battery	Higher elastic modulus and improved mechanical property	[64]
Plasticized Polylactic acid (PLA)	Residue	Biomass extract & encapsulated with electrospun PVA nanofibers	Food Packaging	Improved barrier properties, mechanical resistance, thermal degradation & film crystallinity	[62]
Thermoplastic Corn starch (TPCS)	Fresh	Dried algae	Food packaging	Improved barrier properties	[63]
Cassava starch (CS)	Fresh	Biomass	Food packaging	Increased biodegradability, elongation, & antioxidant activity, reduced TS & barrier properties	[66]
Chitosan	Residue	De-oiled algae	Food packaging	Improved water vapor barrier and mechanical properties, reduced light transmission	[5]
Poly(lactic) acid (PLA)	Residue	Biomass	Packaging	Increased mechanical strength, crystallinity & reduced thermal stability	[67]

1.7 Bionanomaterials

The growing and emerging trends of developing and utilizing nanostructured material in several aspects of life offer a new approach to research, innovation, and governance. Further, bio-based, novel, renewable nanomaterials have gained much interest to reduce environmental hazards and value addition to the biowaste as these materials are extracted from lignocellulosic, and agri-based residue. Meanwhile, the synthesis and functionalization of nanomaterials with their well-defined structure and modifications have attracted increasing attention due to their various potential applications in the field of nanoscience and nanotechnology. The advancement of these nanomaterials has led to the development of functionalized nanoparticles that have broadened their area of application in research as well as in industrial sectors, such as in medicine, electronics, packaging, composites, biomaterials, and energy production [68]. However, due to the growing concerns of global warming and sustainable development, the need of substituting conventional or petroleum-based resources as raw materials with renewable bio-based is essential [69]. Furthermore, the ability to transform cheap and abundant material to yield high-value-added products will aid significant benefits. Recently, these nanomaterials have largely been used in the context of developing new composite materials with enhanced properties and functionalities derived from the nanomaterials and the structures they form. Cellulose nanocrystals (CNCs) are one of them, recently developed, biodegradable, environment-friendly, nontoxic green bio-nanomaterials.

1.7.1 Cellulose Nanocrystals

Cellulose is a standout amongst the richest crude materials found on the surface of the earth. It is a boundless biopolymer that has broad use because of its reasonable properties. Cellulose can be derived from various renewable sources like plants, microbial, algal, and aquatic animals, and their residue or byproducts [70]. Cellulose is a fibrous and water-

insoluble polymer that has various advantages like biodegradability, renewability, and biocompatibility. Previously, cellulose had its use limited to the clothes, paper and pulp, and construction industry, since CNC have unique properties, cellulose is converted to CNC for develop new applications.

CNCs are highly crystalline because of the linear and homogeneous nature of the cellulose polymer and the intermolecular hydrogen bonding between the cellulose chains that are adjacent to each other. The source of the cellulose and the isolation process determine the crystal's size and degree of crystallinity. For example, the degree of crystallinity in bacterial cellulose is 50% - 60%, 80% in tunicates, and 90% in some algae. Acid hydrolysis is generally employed to isolate crystalline cellulosic structures in the form of CNCs. This idea of acid hydrolysis to isolate CNCs, and form disarranged inter-crystalline areas of cellulose chain networks was developed by Nickerson et al., [71]. It was later confirmed by Ranby [72] after formation of colloidal suspensions of cellulose crystals. CNC has a different type of morphology with crystalline allomorphs of cellulose which are connected by poly(1- 4)-β-D-glucan units of cellulose biopolymer [73]. It is a nanostructured material that is used as a nanofillers in food packaging applications due to its superior barrier and mechanical properties [74]. They also act as a good reinforcement agent in the polymeric system and lead to significant improvement in mechanical properties. The improvement in significant water vapor and oxygen barrier properties of bio-nanocomposite has occurred due to the formation of the dense structure by intercalating into the polymer matrix while adding CNC. Therefore, the incorporation of CNCs in biopolymers will help to improve the inadequate property of biopolymers for packaging applications.

1.8 Migration of Food Packaging Material

In recent years, research on packaging systems has focused on active sustainable packaging. Such a packaging system contains compounds like antioxidants and antimicrobial agents that are migrated from packaging material to food to improve food quality and shelf-life. In this context, migration is an important property of any packaging material that must be determined to know the nature of the release of active compounds and other migrating compounds.

Migration is a process that refers to the release of a substance from one medium to another. Following Fick's law of diffusion, the substance will migrate due to a concentration gradient between both mediums [75]. The substance that is migrating is known as 'migrant.' Factors that affect migration include temperature, time, concentration gradient, material properties, migrant position in the material, and the interaction between the migrant and material. Migration itself does not stand for a health problem but is mainly a legal problem in most countries with legislation on acceptable materials, limits on substances, and restrictions for certain applications. In addition, two methods have been stated for carrying out migration studies, Overall migration (OM) and specific migration (SM). The OM is referred to the sum of all mobile substances of packaging released per unit area of the package under the influence of specific predetermined conditions. On the other hand, SM is only related to a specific, known substance [76]. An OM is more convenient than an SM, when the compound is shown to degrade in the food simulant or if the OM is of such a number that even if 100% of the compound migrates into the food, it would still be too low to become hazardous to public health. The overall migration limit has been introduced to control the total amount of substances migrating from packaging material into food, irrespective of the toxicological significance of these substances, and to reduce the number of SM determinations carried out to ensure that the packaging material

is suitable for use in contact with food. Particularly Directive 90/128/EEC sets an overall migration limit of 10 mg/dm^2 (60 mg/kg foodstuff) for the chemical migration of plastics and lists the monomers and other materials approved for use in the manufacture of plastics for food contact applications [77]. Generally, using food simulants is common in almost all migration studies. A major benefit of using food simulants is that they cover a wide range of food types and allow optimum migration due to exposure to a wide surface area [78].

1.9 Literature Review

A mass of the scientific community has reported about prolonging the shelf-life of fruits and vegetables by edible coating techniques with improved quality and unaltered freshness [79]. Among several polysaccharide-based edible packaging materials, CS-based primary sustainable packaging materials such as edible films and coating incorporated with various bio-fillers have exhibited effective characteristic properties to protect and extend the storage life of fresh produce. Various active agents like blueberry, blackberry, grape pomace, leaf, and pomegranate peel extract, essential oil, nisin, and others have been added to CS-based film for obtaining active edible packaging [80]. The addition of active compounds has contributed to antioxidant and antimicrobial activity, pH indicator, improved thermomechanical properties, and surface hydrophobicity reduced water vapor permeability, transparency, and extended shelf-life of fresh produce [27-28,30,81]. Among all, one researcher has reported on the incorporation of fresh *Spirulina* extract into the CS-matrix for the development of CS-based active edible film to improve antimicrobial, barrier, and mechanical properties [29]. CS-based edible coating incorporated with various plant and seed extracts enhanced the shelf-life of strawberries, tomatoes, blueberries, and others and has extended significant shelf-life during storage at low temperatures [31,33,82]. Besides, CS polymer, GG-based edible films, and coating incorporated with orange oil, curcumin, carvacrol, citral oil, whey protein isolates, nanomaterials, and others have

improved various physicochemical and biochemical properties same to CS-based edible packaging [34,83]. The GG-based edible coating has extended the shelf of various fresh produce like mango, mushroom, sweet cherry, pomegranate arils, tomato, and others at low temperatures mostly [84-87]. The existing literature indicates lesser exposure of algae as a bio-filler or active agent in the formulation of edible coating.

In addition, algae have been utilized as the source of microfibrils other than lignocellulosic materials. Due to high carbohydrate content such as cellulose and agar, red algae *Gelidium* has various applications [88]. Since red algae are readily available and abundant, it is widely used in the production of cellulose nanomaterials. Other cellulose-producing algae species are *Spirulina, Siphonocladales, Dunaliella,* and *Cladophorales* [89]. Cellulose microfibril structures are different for varying algae species because of the biosynthesis process. For example, cellulose obtained from *Cladophoraor Valonia* have a high degree of crystallinity that may reach up to 95% [90]. Moreover, not only fresh algae, but researchers have also reported the isolation of CNCs from green algae residue with acicular shape, 95% crystallinity, and diameter and length of 4.9±1.3, and 180±28 nm, respectively [91].

The incorporation of algae biomass or their residue into the polymeric matrix (PBAT) for the development of secondary packaging has exhibited improved mechanical properties, as reported by Torres et al., who also suggested 20% of ABR incorporated exhibited optimum properties [59]. Toro et al., (2013) have observed that ABR can be used as potential fillers material for the development of bio-composite with PBS polymeric matrix [60]. This study has reported improved rigidity obtained in fabricated bio-composites. Similarly, researchers have reported few studies on ABR incorporation into PVA, starch, PLA, and PCL matrix for the development of bio-composites as secondary packaging material [61,62,64]. Incorporation of ABR into the PCL matrix has shown higher

elastic modulus and improved mechanical property, whereas, in the case of PLA, improved barrier properties, mechanical resistance, thermal degradation & film crystallinity are obtained [64]. According to Carissimi et al., (2018), addition of biomass or biomass extract of microalgae *Heterochlorella luteoviridis* into the starch matrix has increased biodegradability, elongation, rupture, and reduced the tensile strength and Young's modulus [66]. Conversely, the addition of microalgae extracts caused the inverse effect on these properties. All films with microalgae showed higher antioxidant activity, evaluated by peroxide index, compared to the control ones. The film containing 2.0% of *H. luteoviridis* extract presented the lowest water vapor permeability and good mechanical characteristics and was applied in salmon packaging.

1.10 Research Gap

In the former section, a brief overview of food packaging on the shelf-life extension of fresh produce and concern related to post-harvest loss has been discussed. The usage of biodegradable polymers is getting attracted as a food packaging material due to the aim of minimizing waste raised from conventional packaging material. Besides, edible packaging as an emerging and novel preservation technique has gained huge acceptance. However, these biodegradable edible and non-edible biopolymers are restricted to use commercially due to their few inherent characteristics and high cost. Therefore, researchers have incorporated various bio-fillers, and food additives from agricultural and lignocellulosic sources to improve the characteristics property and reduced the cost. In this context, there is a lack of utilization of green algae biomass waste in the fabrication of biodegradable primary and secondary food packaging material. Therefore, aiming to improve the inherent properties of biodegradable polymers and broaden the application area, and to utilize the bio-waste, algal biomass residue can be utilized for the isolation of bioactive compounds and nanostructured material and used as a bio-filler or reinforcing agent since algae biomass

waste is a rich source of various bioactive molecules. Nevertheless, no proper investigations and standardizing methods are available to govern the usage of algae biomass for the development of secondary and primary edible active food packaging material, as it may be a safety issue for food and food consumers when biomass-derived component comes in contact with food. Besides, in reported literature, most of the edible coated perishables such as fruits and vegetables are stored in low-temperature conditions for extending the shelf-life which again consumes electrical energy and rises costs which could be a problem for agronomists. Therefore, in this thesis work following objectives would partially address the above knowledge gaps.

1.11 Proposed Thesis Objectives

As discussed previously, the following six objectives have been formulated to address the research gap obtained from the literature review. The proposed objectives are as follows:

1. To characterize the algae biomass residue (ABR) and its extract and development of algae extract incorporated chitosan-based cast film for edible active packaging
2. To study the shelf-life of tomato, green chilli, potato, and onion using chitosan and algae extract incorporated (CS/CAEE) edible packaging
3. To develop and characterize the algae extract and turmeric essential oil incorporated guar gum-based edible active packaging
4. To optimize the edible gum-based coating for shelf-life extension of the cut potato
5. To isolate and characterize the cellulose nanocrystals (CNC) from residual green algae biomass and its use in development of PLA and PCL bio-composites for food packaging
6. To study the migration properties and characterization of algal CNC and curcumin incorporated PLA and PCL bio-composites

1.12 Organization of Thesis

This Ph.D. research work is comprised of a total of nine chapters and the noteworthy outcomes of research activities carried out are compiled in this thesis as six chapters (chapters 3-8). The organization of the thesis and the content of each chapter are discussed briefly below excluding the present one:

Chapter 2, delivers a detailed description of the experimental protocol, materials, and methodologies for crude algae ethanolic extraction from waste algae biomass powder and the development of algae extract incorporated edible films and coating solution and application of edible coating solution on fresh produce. Besides, the isolation of cellulose nanocrystals from algae biomass residue and the development of polymeric bio-nanocomposite films as secondary food packaging material. The analytical instrumentation, optimization studies, and mathematical models carried out in this thesis have been discussed in detail.

Chapter 3, describes the detailed characterization and composition of biowaste de-oiled green algae biomass powder (*Dunaliella tertiolecta*) and the utilization of green extraction technology to obtain algae extract (CAEE) from waste powder. The optimization study of the extraction process has been performed based on optimum antioxidant activity using response surface methodology. Characterization is conducted on optimized algal extract and the CAEE-incorporated chitosan (CS) based edible film is developed by solvent casting. The developed film is undergone various physicochemical, Biochemical, antimicrobial, and biocompatibility studies. The rheological study has been performed for developed filmogenic solutions. The cell-toxicity study has been performed for algae extract (CAEE) and developed a filmogenic solution against the BHK-21 cell line.

Chapter 4, elaborates formulation and application of CS-based edible coating with varying CAEE concentrations. The developed coating has been applied on fresh produce

such as tomato, potato, onion, and green chili using the dipping method and stored at room temperature for 30, 60, and 10 days, respectively. The storage study of coated samples along with uncoated or control samples is carried out for the physicochemical, biochemical, and microbial characteristics to observe the best coating effect on the shelf-life extension of fresh produce. A detailed and comprehensive study has been done on tomatoes during storage.

Chapter 5, details the development of CAEE and turmeric essential oil (TEO) incorporated guar gum (GG)-based solvent-casted edible active films. The varying concentration of TEO has been mixed with a fixed amount of CAEE and GG to develop a variety of edible films and to find the best characteristic properties and synergistic effects of CAEE and TEO on film property. The properties of developed bio-composite films are compared among each other and against a neat GG film. All the films have been subjected to surface morphology, wettability, barrier, thermal, mechanical, biochemical, and microbial studies. The filmogenic solution is subjected to rheological studies to understand the nature of the solution after the inclusion of CAEE and TEO.

Chapter 6, deals with the optimization of GG-based CAEE and TEO-incorporated edible coating formulations on cut potato cubes to extend the shelf-life and minimization of browning on cut potatoes. The optimization study has been performed using a rotatable central composite design (RCCD) model by response surface methodology. The potato cubes have been stored for 7 days and the effectiveness of coating has been determined based on the response parameters such as oxygen transmission rate (OTR), carbon dioxide transmission rate (CTR), water vapor transmission rate (WVTR), color properties, visible mold appearance, and overall acceptability. The optimized coating formulation has shown effective anti-browning properties.

Chapter 7, depicts the isolation of cellulose nanocrystals (CNC) from algae biomass residue using the sulfuric acid hydrolysis method. Two types of bio-fillers i.e., Washed ABR (WABR) and CNC have been used separately for the comparison of physicochemical properties between fabricated PLA and PCL bio-composite films. The solution casting method has been followed to develop the bio-composite films. This chapter mainly focuses on the crystallization behavior of nanomaterial i.e., CNC, and algae powder i.e., WABR into biopolymer matrixes. The nucleating and crystallization behavior of the bio-composite films has been analyzed using DSC, SAXS, and POM analysis which indicated better effectiveness of CNCs. Isothermal crystallization kinetics have been performed using the Avrami model for both PLA and PCL bio-composite films.

Chapter 8, details the overall and specific migration properties of PLA and PCL-based bio-nanocomposite secondary packaging material. The active secondary packaging materials have been developed by the inclusion of curcumin (CUR) into PLA/CNC and PCL/CNC matrix. In the bio-composites, the CNC concentration has been varied whereas CUR is used at constant amounts to understand the effect of nanomaterials (CNC) on the migration behavior of specific agents i.e, curcumin. Specific migration kinetics have been performed using various mathematical models to determine the actual mechanism of CUR as a migrant during the migration period when placed in a side food simulant. Besides, other physicochemical, biochemical, antimicrobial, and cytotoxicity studies have been performed to characterize the developed active biodegradable secondary packaging materials. Further, small pouches or packets have been made using the developed films and real foods i.e. cut potatoes are stored inside the packet for 7 days at room temperature to obtain the effectiveness of packaging material on the shelf-life extension of food.

Chapter 9, summarizes the conclusion of all the chapters and highlights the fundamental issues along with the future scope of the current work. The effect of algae extracts (CAEE)

on the properties of developed edible active bio-composite films are compared and discussed. The inclusion of turmeric essential oil (TEO) along with CAEE and their synergistic effect on the characteristic properties of the edible film are also emphasized. Besides, the effect of developed edible coating formulations on the shelf-life extension of fresh produce such as tomato, chili, potato, and onion are also highlighted and discussed. The ease of the coating formulation and use of farmer-friendly coating techniques and their application in the reduction of post-harvest losses are highlighted. The characteristics of isolated algae waste-derived CNC and its incorporation and effect on inherent properties of biopolymer matrix are compared with algae biomass residue powder incorporated polymer matrix and discussed. The overall migration properties of CNC-incorporated bio-nanocomposite films are mentioned. The effect of algal CNC on the specific migration properties of curcumin has been discussed and the improved properties of developed films after the incorporation of curcumin are also highlighted. The effectiveness of active compound migration into a food system is mentioned. The biocompatibility of algae extracts and all the developed primary and secondary bio-composite films are emphasized. Based on the general conclusions of the work presented in the thesis, some suggestions for future prospective research work are made for the utilization of biowaste algae biomass in advanced food packaging applications.

Moreover, very specific prior art related to chapters are also been highlighted inside specific chapters.

CHAPTER 2

MATERIALS AND METHODS

This chapter provides details of the materials, chemical reagents, and protocols followed for executing various experiments. The green extraction technique and process optimization using RSM of waste algae biomass powder have been discussed. The fabrication of different types of edible active films and their detailed characterization are also mentioned. The formulation of edible coating solutions and optimization has also been focused on. The application technique of edible coating on fresh produce is discussed and the shelf-life study of fresh produce has been emphasized. Isolation of CNC from waste algae biomass powder is also described and the development of solvent-casting CNC and WABR-incorporated bio-composite films are also reported. The detailed crystallization study of CNC and WABR-incorporated bio-composite films has been discussed. Fabrication of curcumin-incorporated active packaging material using a customized solvent casting machine has been described. The overall and specific migration study of developed CNC-incorporated film is discussed. The specific migration kinetics study of CUR-incorporated active secondary packaging films is reported. The procedure of cell cytotoxicity study and antimicrobial study of developed films are reported. The analytical instrumentation used and the experimental procedure followed for the characterization of bio-fillers and developed bio-composites have also been discussed in this chapter.

2.1 Materials

The ABR of *Dunaliella tertiolecta* harvested in marine water, which was generated after algal oil extraction, was provided by the Energy and Resource Institute (TERI), India. Further, chitosan (medium molecular weight), dextrose, DPPH (2,2-diphenyl-

picrylhydrazyl), and β-carotene were procured from Sigma, Aldrich, USA. The acetic acid and ethanol (99% pure) were supplied by Finar, India. Sodium hydroxide, phenolphthalein, L-ascorbic acid, butylated hydroxyl toluene (BHT), 2,6-dichlorophenolindophenol (DCPIP), curcumin, glycerol, calcium chloride anhydrous, sulfuric acid (H_2SO_4 > 99%, pure), nitric acid (HNO_3, 69% pure), sodium hypochlorite, peptone, plate count agar, potato dextrose agar, and Luria-Bertani agar were supplied by Himedia, India. Guar gum was provided by Hindustan gums, India, and turmeric essential oil by Allin exporters, India. Chloroform, acetic acid, hydrogen peroxide, and sodium chlorite were procured from, Nacalai Tesque, Japan. PLA granules of 4032D and 2003D grade were from Nature Works® LLC, USA. The lab-synthesized PCL with a number average molecular weight (M_n) of 53,882 Da, polydispersity index of 1.6, and melt viscosity value of 74 cm^3/g was used, and commercial PCL Capa 6800, with a molecular weight of 80,000 Da was supplied by Ingevity CAPA®, UK. The HPLC-grade methanol and acetonitrile were procured from Finar chemicals, India.

2.2 Experimental Methods

2.2.1 Preparation of Algae Extract

Algae biomass residue powder was subjected to an eco-friendly extraction technique to obtain algal extract rich in bioactive molecules and the extraction protocol has been described in the below section.

2.2.1.1 Optimization of De-oiled Algal Biomass Ultrasound-Assisted Extraction Procedure Using Response Surface Methodology (RSM)

In the present study, optimization of ultrasound-assisted solid-liquid extraction of de-oiled algal biomass (DAB) powder based on antioxidant activity (in terms of DPPH free radical scavenging activity) was studied by RSM. The design experiments were performed using an ultrasound probe sonicator (Biologics, Inc. USA). Based on the preliminary experiments

(data not shown), four probable independent variables with upper and lower limit ranges are selected and summarized in **Table 2.1**, such as solvent (ethanol) concentration (x_1), solvent to solid ratio (x_2), extraction time (x_3), and ultrasonic frequency (x_4) for optimization of algal extract in terms of maximum antioxidant activity, the response parameter (Y= antioxidant activity). Millipore water was used to adjust the ethanol concentration, and the heat released during ultrasound extraction was controlled by placing a sample container inside a cool water bath (20 °C). Besides, the upper surface of the sample container was covered with aluminum foil to suppress the ethanol evaporation; however, a hole was made as per the probe diameter at the center for inserting the ultrasound probe. The Design-Expert (version 11, Stat-Ease, Inc. USA) software was employed to obtain the effects of independent factors on response following the RCCD model. A total of 30 experiments were carried out, as listed in **Table A1**, and the factor effectiveness on responses was analyzed at a 5% significance level. The obtained second-order polynomial equation by the five-level experimental RCCD model was as follows:

$$y = \beta_0 + \sum_{j=1}^{n} \beta_j x_j + \sum_{j=1}^{n} \beta_{jj} x_j^2 + \sum\sum_{j=1}^{n} \beta_{ij} x_i x_j + \varphi \quad \text{.....(1)}$$

The coefficients of the polynomial equation are β_0 (constant), β_j (linear effects), β_{jj} (quadratic effects), and β_{ij} (interaction effects), whereas x_i and x_j are the coded independent variables and φ is constant. The response parameter, antioxidant activity is denoted as 'y'. The information provided in **Table 2.1** is related to chapter 3.

Table 2.1. Independent variables with their coded and actual values.

Independent Variables	**Unit**	**Symbol**	**Level of factor**				
			-2	-1	0	+1	+2
Ethanol concentration	% (v/v)	x_1	25	43.75	62.5	81.25	100
Solvent to solid ratio	mL/g	x_2	5	12.5	20	27.5	35
Extraction time	min	x_3	1	3.75	6.5	9.25	12
Ultrasonic frequency	kHz	x_4	35	38.75	42.5	46.25	50

2.2.1.2 Extraction of Optimized De-oiled Crude Algae Ethanolic Extract

The green extraction of the de-oiled algae residue powder (provided by TERI, India) of *Dunaliella tertiolecta* is depicted in **Figure 2.1**. Here, 1 gm of the standardized particles of the de-oiled algae biomass residue (passing through a 40-mesh sieve) was added into 12.5 mL of extracting solvent ethanol-water (81.25%) and kept under shaking overnight, before being subjected to ultrasound-assisted extraction. An ultrasonicator probe (Biologics, Inc., USA) was used for the extract preparation, and sonication was conducted for 9.25 min, at room temperature, 35 kHz frequency.

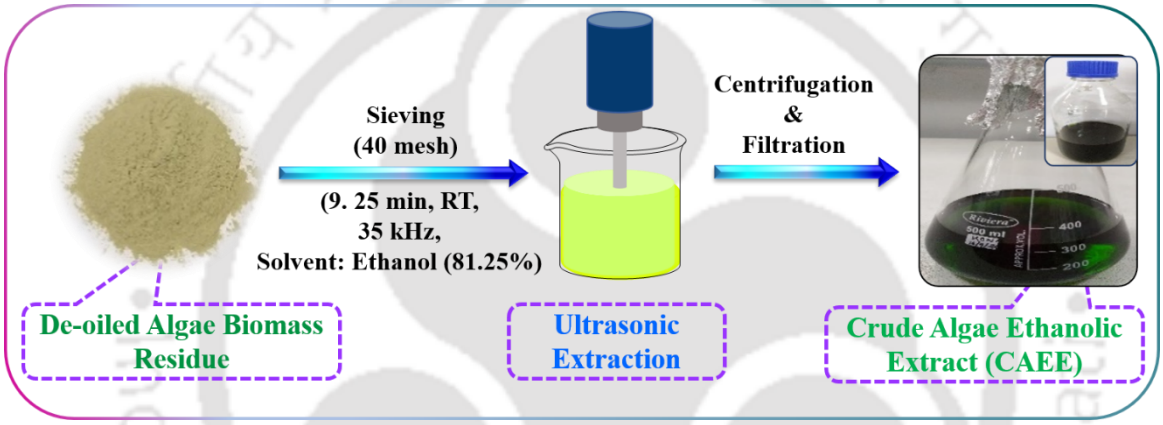

Figure 2.1: Schematic of steps of extraction of algae extract from algae biomass residue.

Thereafter, the suspension was subjected to centrifugation at 5000 rpm for 5 min to separate the solid part from the solution, and finally, filtration was conducted using Whatman filter paper no. 3 for obtaining the clear transparent, green-colored crude algae ethanolic extract (CAEE) without any particles. Finally, the obtained extract was kept at − 20 °C in the dark until further use.

2.2.2 Development of Biopolymer-based Edible Films as Primary Packaging Material

2.2.2.1 Fabrication of Chitosan-based Bio-composites Active Edible Films

The films were prepared by a solution casting technique, as described in **Figure 2.2**. The concentrations of chitosan (CS, medium molecular weight, Sigma Aldrich, (USA)) (1 g/100 mL filmogenic solution) and acetic acid (Finar, India) (0.3%) were kept constant.

Afterward, the incorporation of CAEE into the CS solution was followed by varying the amount of CAEE at concentrations of 0, 4, 8, 12, 16, 20, 24, and 28 mg g^{-1} of CS. The solution was magnetically stirred for 24 h at room temperature. The developed filmogenic solution was kept under a vacuum drier for stabilizing the air bubbles generated from the solution for 2 h. Thereafter, the solution was spread over Teflon plates (140 cm dia) and dried at 40 °C for 24 h inside a hot air oven. A digital micrometer (Indi-6156, India) was used to measure the average film thickness by taking 10 random measurements on the film surface.

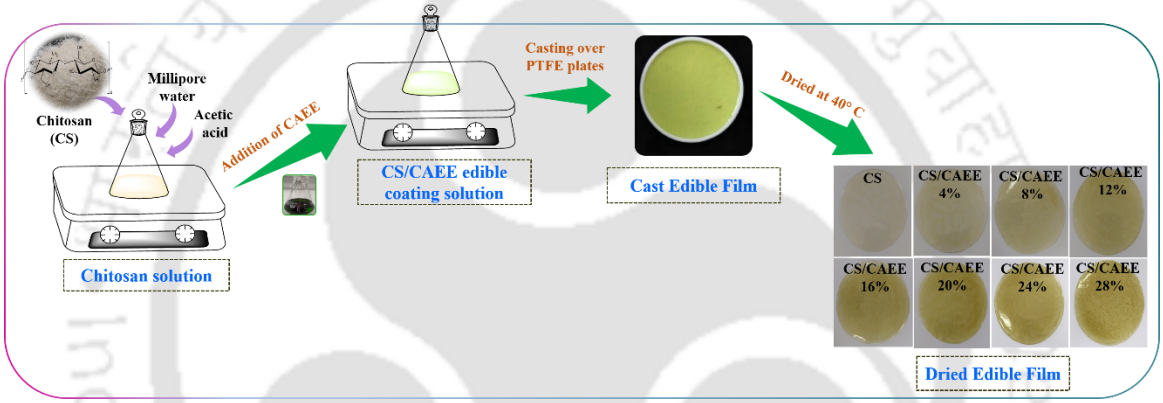

Figure 2.2: Flowsheet of preparation of the chitosan-based edible active film.

2.2.2.2 Fabrication of Guar Gum-based Bio-composites Active Edible Films

A fixed concentration of guar gum (GG) powder was added to the film-forming solutions (1 g/100 mL), where Millipore water was used as a dissolving solvent. The film-forming solutions were heated at 60 °C, for 2 h with a stirring speed of 800 rpm. After 15 min of stirring, a constant amount of glycerol (30% w/w of GG) was added to all the bio-composite formulations. Subsequently, upon cooling to room temperature a constant amount of CAEE at a concentration of 4 mL/100 mL film-forming solution was added. The TEO was added at varying concentrations of 0, 0.5, 1, and 2 mL/100 mL of film-forming solution after 10 min of stirring to develop control, EF B, C & D films. After the addition of TEO, the solution was again stirred for another 30 min. After that, the film-forming solution was

subjected to homogenization at 4000 rpm for 10 min to obtain a homogeneous solution (**Figure 2.3**).

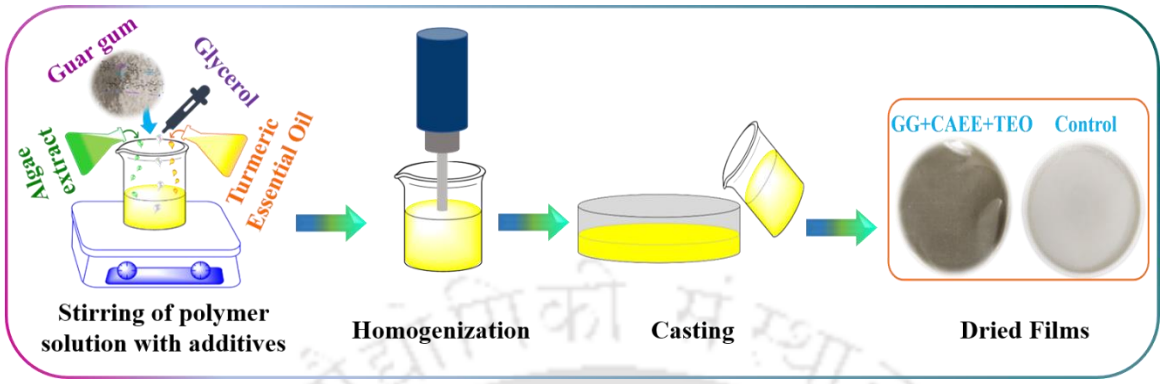

Figure 2.3: Flowsheet of preparation of the guar gum-based edible active film.

A total of six types of GG-based edible film were developed, namely control, EF A, EF B, EF C, EF D, and EF E as depicted in **Table 2.2** which is related to chapter 5. The control film was developed in absence of bio-fillers CAEE and TEO. Further, EF A film contained bio-filler CAEE along with GG and glycerol, and EF E consisted of TEO, GG, and glycerol to compare and understand the effect of CAEE and TEO separately on the edible film property. After homogenization, the solution was kept under vacuum for 5-10 min at room temperature for stabilizing the entrapped air bubbles. Finally, the solution was cast on Teflon plates and dried under a hot air oven as mentioned in section 2.2.3.1.

Table 2.2: Composition of guar gum-based edible films.

Sample Designation	**Guar gum (g/100 mL)**	**Glycerol (wt.%)**	**CAEE (mL)**	**TEO (mL)**
Control	1	30	-	-
EF A	1	30	4	-
EF B	1	30	4	0.5
EF C	1	30	4	1
EF D	1	30	4	2
EF E	1	30	-	2

2.2.3 Development of Biopolymer-based Edible Coating Formulation and Coating on Fresh Produce

2.2.3.1 Development of Chitosan-based Edible Coating Formulation

The edible coating formulations were prepared by dissolving 1 g of CS (for 100 mL filmogenic solution) into a mild (0.3%) acetic acid solution and continuously stirred for 24 h over a magnetic stirring plate at room temperature (**Figure 2.4**). The optimized CAEE with the highest antioxidant activity, obtained by RSM analysis (81.25% ethanol concentration, 12.5 (mL/g) solvent to solid ratio, 9.25 min of extraction time, and 35 kHz frequency), was added to the CS solution with varying concentrations of 0, 2, and 4 mL/100 mL of the coating solution and stirred for another 30 min for proper mixing. After mixing, the developed coating solutions were allowed to stand for 1 h without agitation, followed by keeping under vacuum for 15 min to stabilize the air bubbles generated during formulation. Three types of coating formulation were prepared for this study, namely, neat chitosan (nCS), CS/CAEE 2%, and CS/CAEE 4%, respectively. Control samples were prepared by dipping them into pure Millipore water.

2.2.3.2. Coating of Chitosan-based Formulation on Fresh Produce

The developed edible coating solution was applied to tomatoes (*S. lycopersicum L*., Pusa Ruby var.) using a simple dip-coating technique. The coating was executed in triplicates with a batch size of 4 kg tomatoes (**Figure 2.4**). Tomatoes (red with a trace of yellow color matured) were collected from the local market of IIT Guwahati. The tomatoes were dipped into a 0.2% sodium hypochlorite solution for eliminating extraneous matter and surface contamination of the fruits. Afterward, the tomatoes were transferred and submerged into Millipore water to remove traces of sodium hypochlorite solution. Finally, after completion of sorting and washing, fruits were allowed for air-drying for 2 h at room temperature. Subsequently, tomatoes were dipped into the coating solution for a time interval of 5 min.

After the completion of dipping time, fruits were kept over perforated trays for dripping out excess solution and allowed to dry for 30 min and were stored under ambient conditions (27-30 °C, 60-70% RH). Similarly, other fresh produce such as green chili, potato, and onion were also coated (**Figure 2.4**) and stored at room temperature for 7 days and 60 days, respectively.

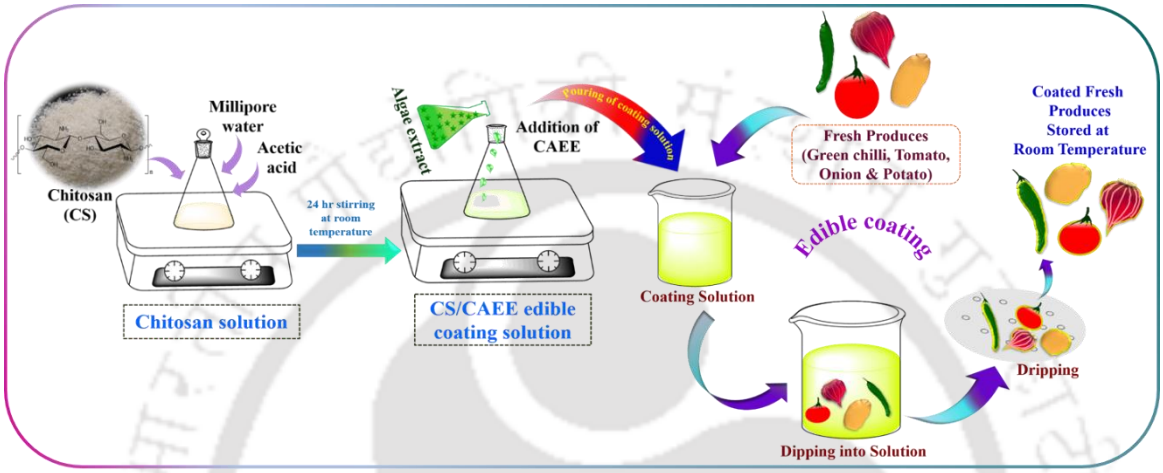

Figure 2.4: Schematic on the preparation of edible coating solution and coating on fresh produce.

2.2.3.3 Optimization of Guar gum-based Edible Coating Formulation for Shelf-life Extension of Cut Potato

The RCCD model with six center points and three factors or independent variables i.e., GG (X_1, g), CAEE (X_2, mL), and TEO (X_3, mL) were used to optimize the GG-based edible coating formulation for cut potatoes. Based on the preliminary experiments, the range of independent variables, X_1, from 0 to 2 g/100 mL, X_2, from 0 to 1 mL/100 mL, and X_3, from 0 to 1 mL/100 mL, were selected (**Table 2.3**). The detailed study related to Table 2.3 has been described in chapter 6. Besides, the concentration of the following additives i.e., glycerol (30%, w/w of GG), L-ascorbic acid (0.1%, w/w of GG), and calcium chloride anhydrous (0.01%, w/w of GG) was added into the coating formulations at a constant concentration. The optimization of coating formulation was performed based on the chosen

response variables or dependent factors such as oxygen transmission rate (OTR), carbon dioxide transmission rate (CTR), water vapor transmission rate (WVTR), the total color difference (ΔE), visible mold, and overall acceptability. The mass of GG, CAEE, and TEO was accurately measured for preparing 250 mL of coating solution according to the obtained design experiment described in chapter 6. The coating solution was prepared as mentioned in section 2.2.3.2. In addition, food additives i.e., calcium chloride and L-ascorbic acid with calculated mass were dissolved in solvent i.e., Millipore water before the addition of GG. After homogenization, the coating solution was kept undisturbed for stabilizing the entrapped air bubble. The obtained second-order polynomial equation by the five-level experimental RCCD model is like **Equation 1**. The OTR, CTR, and WVTR values were determined using the following equations:

$$OTR_{req} = \frac{W \times R_{O_2}}{A_p \times (Y_{O_2}^{O} - Y_{O_2}^{i})} \quad \text{.....(2)}$$

where, OTR was the oxygen transmission rate in cm^3/m^2 h atm, and R_{O2} was the respiration rate on the first day of storage. The terms W and A_p were the mass of cut potatoes in kg (~ 0.05 kg, per batch) and the surface area of the cut potato, estimated by assuming the cut potato as a rectangle, respectively. The term Y_{O2} was the concentration of O_2 (Volume fraction). The superscript 'o' and 'i' corresponded concentration outside (O_2 = 20.9%) and inside (O_2 = 0%) the fruit, respectively.

$$CTR_{req} = \frac{W \times R_{CO_2}}{A_p \times (Y_{CO_2}^{i} - Y_{CO_2}^{o})} \quad \text{.....(3)}$$

where, CTR was the carbon dioxide transmission rate in cm^3/m^2 h atm, and R_{CO2} was the respiration rate on the first day of storage. The term Y_{CO_2} was the concentration of CO_2 (volume fraction). The superscript 'o' and 'i' corresponded concentration outside (CO_2 = 0.03%) and inside (O_2 = 100%) the fruit, respectively.

$$WVTR_{req} = \frac{W \times TR}{A_p \times (Y^i_{H_2O} - Y^o_{H_2O})} \quad \text{.....(4)}$$

where, WVTR was the water vapor transmission rate in g/m^2 h of the coated potato. The term Y_{H_2O} was the concentration of water vapor (volume fraction). The superscript 'o' and 'i' corresponded to concentration outside (70±10 % water vapor) and inside (100% water vapor) the fruit, respectively.

Table 2.3: Independent variables of guar gum-based coating with their coded and uncoded values.

Independent Variables	Unit	Symbol	Level of factor				
			-2	-1	0	+1	+2
Guar gum (GG)	g/100 mL	X_1	0	0.41	1	1.60	2
Algae ethanolic extract (CAEE)	mL/100 mL	X_2	0	0.20	0.5	0.80	1
Turmeric essential oil (TEO)	mL/100 mL	X_3	0	0.20	0.5	0.80	1

2.2.3.4 Guar Gum-based Edible Coating on Cut Potatoes

Firstly, the potatoes were collected from (Kufri Jyoti) local IITG market and rinsed with water followed by washing the outer surface to remove dirt and unwanted matter. After cleaning potatoes were subjected to peeling and cutting. The average dimension (L×W×H) of the cut potato was 4×2×2 cm. Here, the dip coating technique was followed to coat the cut potatoes. Around 1 kg of cut potatoes was dipped into the coating solution for 5 min and then placed over perforated plastic plates for dripping out of excess coating solution for 30 min. The control groups consisted of the same amount of cut potatoes dipped into Millipore water. Finally, all treated and untreated cut potatoes were dried and kept at room temperature (27-30 °C, 60-70% RH) for seven days.

2.2.4 Isolation of Cellulose Nanocrystals (CNC) from Algae Biomass Residue

The provided ABR contained several extraneous substances along with cellulose. Therefore, pre-treatment was carried out to remove the unwanted organic and inorganic

contents. The extraction of cellulose from ABR was done by the method of El Achaby et al. (2018) [92] with few modifications as depicted in **Figure 2.5**. The ABR was subjected to continuous washing with water and ethanol for the removal of dirt, excess fat, and chlorophyll pigment. The pre-washed and dried biomass was successively treated with 5 wt.% each of sodium hydroxide, hydrogen peroxide, and sodium hypochlorite solution, respectively, and refluxed at 80 °C for 2 h under rigorous stirring conditions. The 5 wt.% of the chemical reagents were selected based on the few trials. Finally, the neutral mass was dried at 60 °C for obtaining the dried cellulose. Extracted algal cellulose was subjected to acid hydrolysis with 50 wt.% sulphuric acid (H_2SO_4) under valorous magnetic agitation (~700 rpm) at room temperature for 4.5 h for isolation of CNCs. To arrest the reaction, an adequate amount of chilled deionized water was added after the stipulated time. Centrifugation was conducted at 10,000 rpm for 15 min to wash out the acidic solution, followed by dialysis using cellulose acetate membrane (molecular weight cut = ~14 kDa, Sigma Aldrich) against filtered water for obtaining neutral pH. Afterward, the neutral suspension was subjected to centrifugation for separating the substantial parts. Finally, the precipitated mass was freeze-dried at ~ − 96 °C to obtain the CNCs powder.

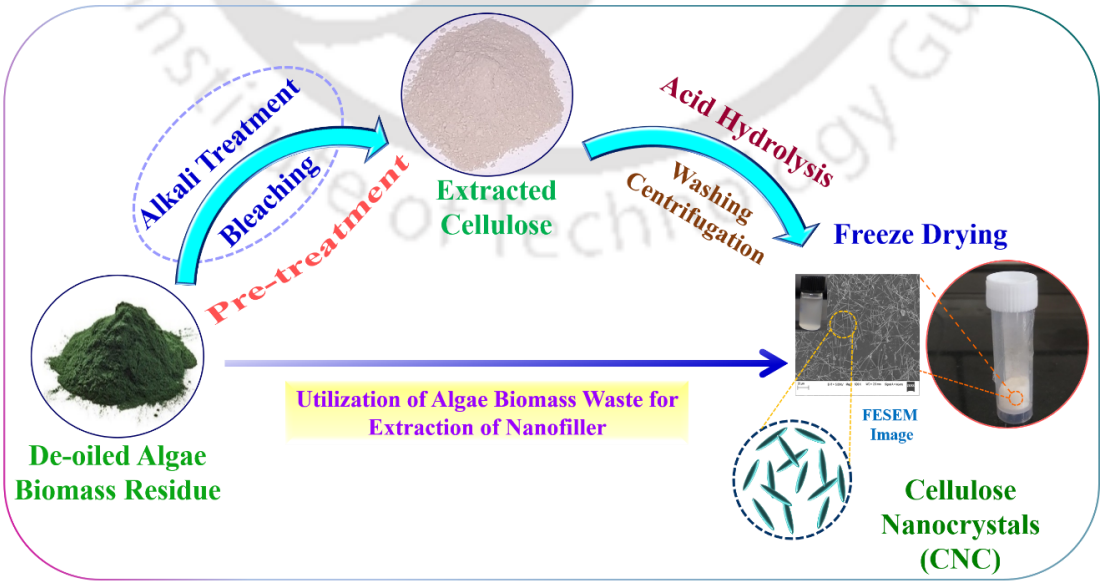

Figure 2.5: Schematic of isolation of cellulose nanocrystals from algae biomass residue.

2.2.5 Development of Biopolymer-based Secondary Packaging Material

2.2.5.1 Fabrication of PLA/algae and PLA/CNC Bio-composites

The WABR and CNC-loaded bio-composites were compared to check the effective crystallization of the bio-fillers. The PLA/CNC bio-nanocomposite films were prepared with PLA granules (500 mg) and a varying amount of CNCs (0–2 wt.%) via the solution casting method. The PLA granules and the CNC powder were vacuum dried at 40 °C (for 24 h) for the removal of any adsorbed moisture before the processing of the bio-composite films. The addition of CNCs into the polymer matrix was done by the repeated solvent exchange method [93]. Finally, the CNC dispersed polymeric suspension (in chloroform) was subjected to magnetic stirring for 7-8 h, at room temperature, followed by casting on a glass Petri plate. All the films were subjected to evaporation inside a laminar hood and dried under a vacuum. The WABR was prepared by washing ABR using Millipore water several times, followed by heating at 60 °C for 1 h. The whole mass was then subjected to drying at 40 °C overnight in a hot air oven. The PLA/WABR bio-composites were prepared in the same manner as mentioned for the preparation of the PLA/CNC films. Details of the composition of the bio-composite films have been summarised in **Table 2.4** which is related to chapter 7**.**

Table 2.4: Composition of the developed PLA-based bio-composites.

Sample Name	PLA (wt.%)	CNC (wt.%)	WABR (wt.%)
Neat PLA	5	-	-
PLA/CNC0.5	4.5	0.5	-
PLA/CNC1	4	1	-
PLA/CNC2	3	2	-
PLA/WABR0.5	4.5	-	0.5
PLA/WABR1	4	-	1
PLA/WABR2	3	-	2

2.2.5.2 Fabrication of PCL/algae and PCL/CNC Bio-composites

The WABR was utilized as a bio-filler into the PCL matrix (PCL/WABR) for drawing a comparison with the *Dunalliela tertiolecta* extracted CNCs incorporated PCL bio-nanocomposites (PCL/CNC). Further, the WABR was prepared as per the previously mentioned section 2.2.6.1. The bio-composites were formulated with varying concentrations of bio-fillers (0, 0.5, 1, and 2 wt.%) by the solvent casting technique as mentioned in section 2.2.6.1. Besides, 500 mg of total mass (polymer with bio-filler) was mixed to develop one formulation (**Table 2.5**). The neat PCL (nPCL) film was prepared without the addition of a bio-filler. For instance, Millipore water, acetone, and chloroform were utilized as the solvent. In the next step, the polymer and bio-filler were added into chloroform to prepare a bio-filler dispersed polymer solution under magnetic stirring for 7-8 h at room temperature followed by casting over a glass Petri plate. Finally, films were vacuum-dried at room temperature after evaporation of the solvent under a laminar air hood. The films developed using the data of Table 2.5 is described in chapter 7.

Table 2.5: Composition of the developed PCL-based bio-composites.

Sample Name	PCL (wt.%)	CNC (wt.%)	WABR (wt.%)
Neat PCL	5	-	-
PCL/CNC0.5	4.5	0.5	-
PCL/CNC1	4	1	-
PCL/CNC2	3	2	-
PCL/WABR0.5	4.5	-	0.5
PCL/WABR1	4	-	1
PCL/WABR2	3	-	2

2.2.5.3 Fabrication of Curcumin Loaded CNC Incorporated PLA Bio-composite Films

The bio-composite films PLA/CNC and curcumin (CUR) incorporated PLA/CNC/CUR were fabricated using a solvent casting method with the help of a customized casting

machine. The PLA/CNC bio-nanocomposite solution was prepared as mentioned in section 2.2.5.1. The solvent used to dissolve PLA granules was chloroform. Upon completion of mixing, the solution was kept in undisturbed condition for 10-15 minutes to stabilize the air bubbles. Thereafter, the solution was poured on the glass plate of the casting machine, and a blade attached to the machine spread the solution over the surface of the glass plate. The casting of the solution was performed at room temperature however, the casted film on the glass plate was subjected to a temperature of 40 ºC for 30 min for drying. The concentration of PLA in films was 5 wt.% and CNC was varied at 0, 0.5, 1, and 2 wt.%, which is detailed in **Table 2.6**. No bio-fillers were added to the neat PLA (nPLA) film. Other sets of bio-composites were prepared with the addition of CUR to PLA and PLA/CNC matrix. The concentration of CUR (2 wt.%) was kept constant in all types of film. The CUR was dissolved in chloroform and mixed with a specified mass of CNC (0, 0.5, 1, and 2 wt.%) and the CNC dispersed solution was added to PLA dissolved in chloroform solution and subjected to magnetic stirring for 6-7 h and the same step was followed as mentioned above for casting and drying. A PLA/CUR bio-composite film was prepared to compare the effectiveness with the CNC-loaded PLA/CUR bio-composite. Details of the composition of the bio-composite films have been summarised in **Table 2.6** which is related to chapter 8.

2.2.5.4 Fabrication of Curcumin Loaded CNC Incorporated PCL Bio-composite Films

The PCL/CNC and PCL/CNC/CUR bio-composite films were prepared as mentioned in section 2.2.5.3. However, in this case, all types of films were dried at room temperature. The films were subjected to vacuum drying at room temperature for evaporation of the entrapped solvent. The same composition, which is mentioned in **Table 2.6**, was used to

fabricate PCL-based bio-composite, however, instead of PLA, PCL was selected as the polymer matrix.

Table 2.6: Composition of the developed PLA-based CNC and curcumin incorporated bio-composites.

Sample Designation (wt.%)	PLA (g)	CNC (g)	Curcumin (g)
nPLA	5	-	-
PLA/CNC 0.5%	4.975	0.025	-
PLA/CNC 1%	4.95	0.05	-
PLA/CNC 2%	4.9	0.1	-
PLA/CUR	4.9	-	0.1
PLA/CUR/CNC 0.5%	4.875	0.025	0.1
PLA/CUR/CNC 1%	4.85	0.05	0.1
PLA/CUR/CNC 2%	4.8	0.1	0.1

2.3 Migration Study of Secondary Packaging

2.3.1 Migration Testing on PLA/CNC and PLA/CNC/CUR Bio-composites

Study of migration is one of the most relevant and important property of any type of packaging material when applied on real food system. The migration of small particles, lower molecular weight compounds, and fractionated or degraded molecules must be under specified standard limit and should not contain any toxicity in case of food packaging.

2.3.1.1 Overall Migration Testing for PLA/CNC Films

Three types of food simulants i.e., water, acetic acid 3% (v/v), and ethanol 15% (v/v) were selected to perform the overall migration test as per the standard protocol (EU No. 10/2011) [94]. The surface area of the test film sample was 100 cm^2 which was weighed and fully immersed into the migration test cell (Migracell MC 60 B, Fabes, Munich). The test cells contained 100 mL of food simulant at a ratio of film weight to simulant volume of 1:10. The test cells were hermetically sealed and inserted in a preheated temperature-controlled

hot air oven at 70 °C, for 2 h. After the specified incubation period, the films were removed, and the simulant was transferred to a pre-weighed flask. The simulant was evaporated using a rotary evaporator (Buchi R-3, Switzerland). Next, the flask weight was measured to determine the mass of migrants which was migrated from the film using an analytical balance precision of ±0.1 mg. The weight of the dried removed film from the test cell was noted to determine the overall migration value (mg/dm^2). The following equation was used to determine the overall migration value:

$$M = \frac{(m_a - m_b)}{S} \times 1000\ mg/dm^2 \quad \text{.....(5)}$$

where M is the overall migration into the simulant, in milligrams per square decimetre of the surface area of the sample intended to encounter foodstuffs, m_a is the mass of the test sample after removal of simulant (g), m_b is the mass of residue from the food simulant (g), S is the surface area of the test specimen intended to encounter foodstuff. For each film sample, three experiments in replicates were performed and the final migration value showed the average of the three replicas.

2.3.1.2 Specific Migration Test for Curcumin Loaded PLA Films

The specific migration test for curcumin from PLA/CUR and PLA/CNC/CUR bio-composites was performed similar way as in the case of the overall migration test. In this case, ethanol 15% was selected as a food simulant for PLA/CNC/CUR films. All the films were fully immersed in the migration test cells as mentioned in section 2.3.1.1. The test cells were kept at 40 ºC and the samples were collected at 0, 6, 9, 12, 24, 36, 48, and 120 h time intervals. The concentration of migrant (curcumin) in collected samples was determined using the UV-Vis spectrophotometer (Perkin Elmer Lamda 25, USA) at 428 nm. To make up the volume of the simulant in the test cell after collecting the sample at each time interval, the same amount of 15% ethanol was added.

2.3.2 Migration Testing on PCL/CNC and PCL/CNC/CUR Bio-composites

2.3.2.1 Overall Migration Testing for PCL/CNC Films

The overall migration test for PCL/CNC bio-composites and neat PCL film was performed as mentioned in section 2.3.1.1. Here, the test cells containing sample film were kept at room temperature (25±2 °C) during the experiment for 10 days. After completion of the specified experimental time, the film samples were removed, and the subsequent steps were performed as mentioned in section 2.3.1.1.

2.3.2.2 Specific Migration Test for Curcumin-loaded PCL Films

The migration of curcumin from PCL/CUR and PCL/CNC/CUR film was performed as mentioned in section 2.3.1.2. Here, ethanol 15% was used as the food simulant and the migration test cells were kept at 7 °C. The samples were collected at the time interval of 0, 6, 12, 24, 36, 48, 60, 72, 84, 96, and 108 h, and the concentration of curcumin was measured by UV-Vis spectrophotometer as mentioned in section 2.3.1.2.

2.3.3 Migration Kinetics of Specific Migrant Curcumin

Specific migration kinetics study of curcumin from the active bio-nanocomposite films were performed and analyzed using four different mathematical models. These models have been described in below section:

2.3.3.1 Zero-order Model

$$M_t = M_0 + k_0 t \quad \text{.....(6)}$$

where, M_t is the concentration of active agent/specific migrants migrated during the time t, M_0 is the initial concentration of active agent/specific migrants, k_0 is the zero-order migration rate constant, and t is the time in h.

2.3.3.2 First-order Model

$$ln\left(1 - \frac{M_t}{M_\infty}\right) = -k_1 t \quad \text{.....(7)}$$

where, M_t is the concentration of active agent/specific migrants migrated during the time t, M_∞ is the concentration of active agent/specific migrants migrated at equilibrium, k_1 is the first-order migration rate constant, and t is the time in h.

2.3.3.3 Higuchi Model

$$\frac{M_t}{M_\infty} = kt^{1/2} \quad \text{.....(8)}$$

where, M_t is the concentration of active agent/specific migrants migrated during the time t, M_∞ is the concentration of active agent/specific migrants migrated at equilibrium, k is the first-order migration rate constant, and t is the time in h.

2.3.3.4 Korsemeyer-Peppas Model

$$\frac{M_t}{M_\infty} = kt^n \quad \text{.....(9)}$$

where, M_t is the concentration of active agent/specific migrants migrated during the time t, M_∞ is the concentration of active agent/specific migrants migrated at equilibrium, k is the first-order migration rate constant, t is the time in h, and n is the diffusion exponent.

2.4 Characterization of Bio-fillers and Developed Bio-composite Films

2.4.1 Compositional Analysis of ABR

The α-cellulose content of the ABR was determined using chemical assay by the method of Loader et al., 1997 [95]. Further, the moisture, total solids, and ash contents of the ABR were analyzed according to the method of Van Wychen and Laurens (2016) [96] with modifications. ABR powder of 100 mg was taken in a crucible and kept in a muffle furnace (Box furnace, VB Ceramic consultants, India) with the temperature ramping program starting from room temperature to 105 °C, holding at 105 °C for 12 min, ramp to 250 °C at 10 °C/min, holding at 250 °C for 30 min, ramp to 575 °C at 20 °C/min, holding at 575 °C for 180 min and finally dropped to 105 °C. Afterward, the crucible was taken out and kept

in a desiccator for cooling to room temperature. Finally, the weight was measured and total solid (TS) and moisture content was calculated using the following equations:

$$\%\, Total\ Solid = \frac{(Weight_{crucible+dry\ sample} - Weight_{crucible})}{weight_{samples\ as\ received}} \times 100 \ldots\ldots\ldots\ldots\ldots\ldots\ldots\ldots (10)$$

$$\%\, Moisture = \frac{(Weight_{crucible+dry\ sample} - Weight_{crucible})}{weight_{samples\ as\ received}} \times 100 \ldots\ldots\ldots\ldots\ldots\ldots\ldots\ldots (11)$$

2.4.1.1 Inductively Coupled Plasma Mass Spectroscopy (ICPMS)

Several major and trace elements present in the ABR, and isolated CNC were quantified using the inductively coupled plasma mass spectroscopy (7800 ICP-MS, Agilent Technologies, USA) using He (auxiliary gas) and Ar (plasma gas) gases at the flow rate of 0.90 L/min and 15 L/min, respectively, and the nebulizer speed for sample injection was 0.10 rps at a flow rate of 1.03 L/min at 1550 W. The samples were digested using an Advance microwave digestion system (ETHOS EASY, USA) before introducing to the ICP-MS for analysis. The bio-filler was digested using an acid mixture of nitric (HNO_3) and hydrochloric acid (HCl) at a ratio of 50:50, as per the inbuilt digestion system library. The ICP-MS system was attached with an autosampler (SPS4 Autosampler, USA) unit that introduces the sample to the nebulizer where Ar and He were introduced.

2.4.2 Biochemical and Structural Characterization of Algae Extract (CAEE) and Developed Films

2.4.2.1 Determination of the chlorophyll content of CAEE

The chlorophyll content of CAEE of the dried spent algae biomass was measured via UV-Vis spectrophotometer (PerkinElmer, USA) at wavelengths (λ) of 663 and 645 nm. The concentration of total chlorophyll (Total Chl), chlorophyll a (Chl 'a'), and chlorophyll b (Chl 'b') was determined using the following equations [97]:

$$Total\ Chl = 8.02 \times A(663) + 20.2 \times A(645) \ldots\ldots\ldots\ldots\ldots\ldots\ldots\ldots\ldots\ldots\ldots\ldots\ldots\ldots (12)$$

$$Chl\ 'a' = 12.7 \times A(663) - 2.69 \times A(645) \ldots\ldots\ldots\ldots\ldots\ldots\ldots\ldots\ldots\ldots\ldots\ldots\ldots\ldots\ldots (13)$$

$$Chl\,'b' = 22.9 \times A(645) - 4.68 \times A(663) \text{.....(14)}$$

The yield of chlorophyll from the CAEE using green solvent via ultrasonic extraction was calculated as given below equation:

$$Yield\ (mg/ml) = \left[\frac{Chlorophyl\ lcontent\left(\frac{mg}{ml}\right) \times volume\ of the\ solvent\ (ml)}{Weight\ of\ dried\ spent\ algae\ biomass\ (g)}\right] \text{.....(15)}$$

2.4.2.2 Nuclear magnetic resonance (NMR) analysis of CAEE

The proton (^{1}H) and carbon (^{13}C) NMR spectra of CAEE were recorded by the Bruker (ASCENDTM 600 MHz) NMR spectrometer attached with TCI Cryo Probe. The concentrated extract of CAEE of ~70 mg was dissolved in two different solvent (0.7 mL) separately, deuterated chloroform ($CDCl_3$) and deuterated methanol (CD_3OD) containing internal standard tetramethylsilane (TMS - 0.03% (v/v)), respectively. After filtering the with PTFE (0.25µm) micron filter the solution was subjected to analysis. The ^{1}H and ^{13}C spectra were measured in ppm range of 0 to 10 (32 scans) and 0 to 200 (900 scans), respectively.

2.4.2.3 Matrix Assisted Laser Desorption/Ionization Time of Flight (MALDI TOF) Mass Spectroscopy Analysis of CAEE

The CAEE was mixed with matrix solvent 2,5-dihydroxybenzoic acid (DHB), prepared by dissolving in methanol (10 mg/mL) with 0.1% TFA. The sample was prepared at a ratio of 1:6 (matrix: CAEE), which means 1 µl of matrix solution was added to 6 µl of analyte solution (CAEE). The MALDI TOF MS analysis was performed by Bruker Autoflex Speed spectrometer at an accelerating voltage of 19 kV (per spectrum around 2000 laser shots). The sample with matrix solution was placed over a stainless-steel plate and dried before being subjected to analysis. The spectrum reproducibility was checked by taking measurements at five different spots on the sample.

2.4.2.4 Determination of β-Carotene in CAEE

The amount of β-carotene present in the optimized extract was determined using high-performance liquid chromatography (HPLC) according to the method of Das et al., 2017 [98] with slight modification. The HPLC apparatus (Ultimate 3000, Thermo Scientific) equipped with a UV detector and C18 column (Hypersil Gold) were used for the analysis. A mixture of methanol and acetonitrile (90:10) was used as the mobile phase with a constant flow rate of 0.5 mL/min. The injection volume was 30 µL, and the detection was performed at 277 nm at room temperature (25 °C). The identification of β-carotene was performed by comparing the retention time with the standard samples.

2.4.2.5 Determination of Antioxidant capacity of CAEE and Films

The free radical scavenging property of the CAEE and the developed CS-based bio-composites/active edible films was quantified using the DPPH (2,2 diphenyl-picrylhydrazyl, Aldrich, USA) free radical scavenging activity method according to Dudonné et al., 2009, with slight modification [99]. In this study, ethanol was used as a reference instead of methanol. The DPPH solution was prepared by dissolving in ethanol (50 mg/L) and 3 mL of it was added to 1 mL of algae extract solution. Similarly, the film extract solution (1 mL) was mixed with 3 mL of DPPH solution and kept under dark place at room temperature for 30 min. Finally, the absorbance was measured at 517 nm. The percentage of DPPH free radical scavenging activity was measured according to the following equation:

$$DPPH\ Scavenging\ Activity(\%) = \frac{Abs_{DPPH} - Abs_{Sample}}{Abs_{DPPH}} \times 100 \ldots\ldots\ldots\ldots\ldots\ldots(16)$$

where, Abs_{DPPH} indicates absorbance of pure DPPH solution and AbS_{sample} implies absorbance of sample solutions.

2.4.2.6 Determination of Total Phenolic Content of CAEE and Films

The total phenolic contents of CAEE were determined by Folin-Ciocalteu (Himedia, India) method [66]. A small quantity of extract (500 µL) was mixed with 2.5 mL of Folin reagent (Distilled water: F-C reagent = 10:1), followed by the addition of 2 mL of sodium carbonate (Himedia, India) (7.5%, diluted in distilled water) into the mixture after 5 min. The absorbance of the solution was measured at 740 nm after the incubation period of 2 h in dark. The result was determined using standard gallic acid (Himedia, India) curve and reported in terms of µg of gallic acid/mL of extract.

2.4.2.7 Color Parameters of CAEE and Films

The color co-ordinates of CAEE and developed films were determined by using a colorimeter (Datacolor 550, Datacolor Technology Suzhou Co., Ltd., China) controlled by the Datacolor tools software program. The color values L*, a*, and b* are indicators of lightness, degree of redness (+a) to greenness (-a), and yellowness (+b) to blueness (-b). The total color difference (ΔE) and yellow index (YI) of the film was determined using equation 17. The result of CAEE and film samples were obtained in triplicates.

$$\Delta E^* = [(\Delta L^*)^2 + (\Delta a^*)^2 + (\Delta b^*)^2]^{0.5} \quad \text{.....(17)}$$

$$YI = \frac{(142.83 \times b)}{L} \quad \text{.....(18)}$$

2.4.2.8 Transparency of Developed Films

The ultraviolet and visible light barrier properties of the edible films were determined according to Fang et al., 2002, using a UV-Vis spectrophotometer (PerkinElmer, USA) [80]. Film samples with the length and width of 10.0 cm, 1.5 cm respectively, were placed in the cuvette for allowing the light beam to pass through the film surface. The film transparency was measured at transmittance mode with the scan wavelength range between 200 and 800 nm.

2.4.3 Physicochemical Characterization of Developed Films

2.4.3.1 Field Emission Scanning Electron Microscope (FESEM)

The surface morphology of the bio-fillers and the films were analysed by field emission scanning electron microscopy (Sigma 300, Zeiss, Germany). The samples were made conductive by placing them inside a gold sputtering system (SC7620, Quorum) to coat the surface. The particle size including their length and the diameter were calculated by the ImageJ software.

2.4.3.2 Atomic Force Mass Spectroscopy (AFM)

The surface topography and morphology of developed edible film were analysed using AFM (Aglient, Model 5500 series) with silicon cantilever having a spring constant of 42 N/m at a resonance frequency of 320 kHz. The film samples were cut with the size of 1 cm × 1 cm and dried under vacuum. AFM images were analyzed with WSxM software (version 4.0 Beta 9.3).

2.4.3.3 Thermogravimetric Analysis (TGA)

The thermal stability of the bio-fillers and the films was determined using a thermogravimetric analyzer (TGA-4000, PerkinElmer, USA) under N_2 atmosphere at 50 mL/min flow rate and temperature range of 30-700 °C at the rate of 10 °C/min using 7-8 mg sample.

2.4.3.4 Fourier Transform Infrared Spectroscopy (FTIR)

The de-oiled algae biomass residue powder, CAEE, and film samples were analyzed using attenuated total reflection Fourier transforms infrared (ATR-FTIR) spectroscopy (Spectrum One, PerkinElmer, Inc., USA) to examine the change in functional groups during extraction. The obtained spectra were recorded in the range of 4000-500 cm^{-1}, with a resolution of 4 cm^{-1}, and an accumulation of 16 scans.

2.4.3.5 X-ray diffraction (XRD)

X-ray diffraction measurement of the bio-fillers was recorded by Xray diffractometer (Rigaku Smart Lab, Japan). The X-ray was generated by a CuKα radiation source. The wavelength (λ) of the incident X-ray was 1.54 Å. The intensity was recorded within the 2θ range of 10-40° with a sampling step angle and a scan rate of 0.02° and 20° /min, respectively. The crystallinity index (I_{Cr}) was calculated by the following equation:

$$Crystallinity\ Index\ (I_{Cr}) = \frac{Area\ of\ crystalline\ peaks}{Area\ of\ crystalline\ peaks + area\ of\ amorphous\ peaks} \times 10 \quad ....(19)$$

2.4.3.6 Wettability Analysis

The developed films were subjected to water contact angle measurement to estimate the surface wettability, using Kruss, DSA 25 Expert model (Germany). The film samples were cut in the form of (1×1) cm (L×B) square shape and pasted over glass slide using double-sided transparent tape. The instrument was operated at room temperature (27 °C), and water dropped amount at a single time as 2 µL distilled water with a drop rate 0.16 mL/min. Thereby the water dropping by syringe over the specimen was captured using a video mode, and measurement was made for different times using Young's Laplace equation.

2.4.3.7 Water Vapor Permeability (WVP)

Water vapor permeability of the active edible films was measured by a water vapor permeability tester (Mocon, PERMATRAN-W® 1/50G) as per ASTM E398 standard protocol. The sample was vacuum dried for 2 h at room temperature before the analysis. The 50 cm^2 area was exposed for the test at 37.8±0.5 °C with a difference of 40% RH. Nitrogen gas (99.9% purity) was purged through the films during the analysis. The standard mode was selected to perform the test. After reaching the saturation point, the obtained WVTR values were noted. The WVP of the film was calculated using the following equation:

$$WVP = \frac{WVTR \times L}{\Delta P} \quad \text{.....(20)}$$

where, ΔP is the partial pressure difference of water vapor across the film in the test chamber, L is the average thickness of the film, and WVTR is the water vapor transmission rate.

2.4.3.8 Mechanical Properties

According to ASTM D-882, the tensile strength (MPa) and elongation at break (%) of developed films were determined using a universal testing machine (ZwickRoell Z005). Samples were prepared by cutting the film into rectangular bars (10 mm × 50 mm) and fixed within the machine with a grip separation of 20 mm. The test speed was set at 5 mm/min obtained by using a cell load of 5 kN. The reported data were obtained after experimenting with triplicates.

2.4.4 Rheological Properties of Edible Filmogenic Solution

The rheological measurement of steady-state flow and dynamic viscoelasticity was conducted in a controlled stress rheometer (Anton Parr) with a cone and plate geometry (angle < 4°, diameter = 50 mm, gap = 0.215 mm). The measurement was carried out at room temperature, maintained by the Peltier system temperature controller. All the measurements were performed in triplicates.

2.4.4.1 Steady Shear Measurements

Steady shear experiments or the flow curves of the solutions were carried out at room temperature (25 °C) by varying the viscosity of the solutions as a function of shear rate (0.1-1000 s^{-1}). Experimental data were fitted to the Ostwald-de Waele model or power-law model to determine the Newtonian or pseudoplastic behavior of the solutions through the following equation:

$$\eta = m(\dot{\gamma})^{n-1} \quad \text{.....(21)}$$

where ‘m’ and ‘n’ were the fluid consistency coefficient and the flow behavior index, respectively.

2.4.4.2 Strain Sweep Measurements

Strain sweep measurements of the solutions were done to determine the linear viscoelastic region (LVER) by varying the strain amplitude at a fixed frequency value of 1.0 Hz at room temperature (25 °C), where the storage modulus, G′, and the loss modulus, G″ remain constant. Different rheological parameters are analyzed:

- G'_{LVER}, storage modulus at the critical strain
- γL, the critical strain
- tanδ, the ratio of loss to storage modulus which determines the liquid or solid behavior of the solutions
- the difference between the modulus, G″- G′ at a fixed strain value which depicts the reinforcing effect of the extract incorporation of the solutions in their viscous and elastic behaviors.

2.4.4.3 Frequency Sweep Measurements

The dynamic frequency sweep measurement was performed at room temperature (25 °C) by varying the frequency, range of 0.1-100 rad/s with a fixed strain value of 1% (in the LVER), which was determined from the amplitude sweep analysis. It determines the behavior of elastic and loss modulus with the increase in frequency and with the incorporation of extract.

2.4.5 Crystallization study

2.4.5.1 Differential Scanning Calorimetry (DSC)

The thermal properties of the PLA/WABR and PLA/CNC bio-composites were analysed by a differential scanning calorimetry (DSC214 Polyma, Netzsch, Germany) under N_2 flow, using 7-8 mg sample. The non-isothermal (two heating and one cooling cycles, from 25-200 °C, at 10 °C/min) and isothermal (heating from 25-200 °C at 50 °C/min, 5 min isothermal and rapidly cooled down to 110 °C at 300 °C/min and isothermal for 60 min)

studies were conducted to understand the detailed crystallization characteristic of the prepared films. Similarly, in case of PCL/WABR and PCL/CNC bio-composites, the non-isothermal (two heating and one cooling cycles, from 25-100 °C, and cooling from 100 °C to -100 °C at 10 °C/min) and isothermal (heating from 25-100 °C at 50 °C/min, 5 min isothermal and rapidly cooled down to 40, 45, and 50 °C, at cooling rate of 300 °C/min and isothermal for 60 min) studies were performed to understand the effect of bio-fillers on crystalline property of fabricated films. Moreover, the effectiveness of WABR and CNCs was confirmed by the improvement of the degree of crystallinity (ϕ(t)), which was estimated based on the heat flow data obtained from the DSC analysis by the following equation:

$$\phi(t) = \frac{\int_0^t (\Delta H_c)\, dt}{\Delta H_m^0} \quad \text{.....(22)}$$

where, t, ΔH_c and ΔH_m^0 represented time, enthalpy of the cold crystallized samples for PLA and enthalpy for isothermally crystalized samples for PCL, and enthalpy of fusion for 100% crystals of polymer, respectively. Here, the value of ΔH_m^0 for PLA and PCL was considered as 93 and 139.5 J/g, respectively [100, 101].

2.4.5.2 Kinetics Study by Melt Crystallization using Avrami Model

The isothermal crystallization kinetics can be depicted by the well-known Avrami theory. Based on the theorem, crystallinity as a function of time (ϕ(t)) and half time of crystallization ($t_{0.5}$) has been expressed by the following equations:

$$\frac{\phi(t)}{\phi^{\infty}} = 1 - exp[-k(t - t_0)^n] \quad \text{.....(23)}$$

$$log\left[-ln\left(1 - \frac{\phi(t)}{\phi^{\infty}}\right)\right] = nlog(k) + nlog(t - t_0) \quad \text{.....(24)}$$

$$t_{0.5} = \left(\frac{ln\, 2}{k}\right)^{1/n} \quad \text{.....(25)}$$

where, ϕ^{∞} indicated crystallinity after completion of crystallization, t_0 denoted induction period of crystallization, the dimensionality of the growing crystallites was represented by the Avrami exponent, 'n', and 'k' denoted the crystallization rate constant associated with nucleation and the growth of crystals.

2.4.5.3 Polarized Optical Microscopy (POM)

Polarized optical microscopy was conducted to characterize the growth rate and crystallization behaviour of the bio-composites using Nikon Eclipse Ci-POL (Japan) attached with a hot stage (THMS600, Linkam Scientific, UK), from room temperature to 200 °C at the rate of 50 °C/min, 5 min hold and rapidly cooled down to isothermal (125 °C) at the rate of 50 °C/min for 60 min for PLA/WABR and PLA/CNC biocomposites. Similar study was performed under an isothermal condition where the PCL/WABR and PCL/CNC were subjected to heating till 100 °C at a heating rate of 50 °C/min with a holding of 5 min and finally cooling down to 45 °C at a cooling rate of 50 °C/min and maintained the isothermal condition for ~60 min. The spherulite dimensions were measured using the ImageJ software.

2.4.5.4 Small-angle X-ray scattering (SAXS)

Small-angle X-ray scattering (Synchroton radiation as X-ray source, beamline BL-6A KEK Photon Factory, High-Energy Accelerator Research Organization in Tsukuba, Japan, λ at 0.150 nm, using Kapton films (DuPont-Toray Co. Ltd., Tokyo, Japan) for preparing the samples were performed to characterize the higher order crystalline behaviour of the films and the analysis was done at room temperature after isothermally quenching to 110 °C for 60 min for PLA/WABR and PLA/CNC film. In case of PCL/WABR and PCL/CNC film, quenching was conducted at 45 °C for 60 min. Igor Pro software was used to analyse the SAXS data.

$$q = \frac{2\pi Sin(2\theta)}{\lambda} \quad \text{.....(26)}$$

2.4.6 Antimicrobial and Biocompatibility Study of Filmogenic Solution and Films

2.4.6.1 Antimicrobial Activity

- ***Disc Diffusion Method***

The two most common food pathogens, namely Gram-negative *Escherichia coli*, and Gram-positive *Staphylococcus aureus* were used for the analysis of the antibacterial activity of neat chitosan (nCS) and CAEE incorporated formulated CS-based filmogenic/coating solutions. The freshly prepared bacterial culture suspension of about 100 µL was spread over the Luria-Bertani agar culture medium. The filter paper was cut using a paper cutter punching machine manually, followed by dipping into each bio-composite/filmogenic coating solution before placing it over the plate surfaces and incubated at 37 °C for 24 h [102]. The appearance of a clear inhibition zone diameter was recorded.

- ***Colony Counting Method***

The above mentioned two common food pathogens were used for the analysis of the antibacterial activity of developed primary and secondary packaging material i.e., GG-based edible flims, PLA/CNC, PLA/CNC/CUR, PCL/CNC, and PCL/CNC/CUR non-edible films, respectively. The experiment was performed as mentioned by Song et al., 2022 [103] with slight modification. Briefly, 5 mg of all the films were incubated with 1 mL of bacterial suspension in 24 well plates in triplicates at 37 °C and stored at 140 rpm for 24 h. Meanwhile, the bacterial suspension without the film sample was set as the control group. After that, the obtained bacterial suspension was serially diluted; 50 µL was taken and evenly coated on the agar plate; then, it was placed in a 37 °C incubator for 24 h for colony count. The inhibition rate (%) for bacteria was calculated by the following equation:

$$Inhibition\ Rate\ (\%) = \frac{A_1 - A_2}{A_1} \times 100 \quad \text{.....(27)}$$

where A_1 and A_2 represent the number of colonies in the control (without film) and test sample groups, respectively.

2.4.6.2 Cytotoxicity Study

- ***Seeding and Culturing of cell***

Dulbecco's Modified Eagle's Medium (DMEM) (Gibco™) was used to culture BHK-21 (Baby Hamster Kidney Fibroblast) cells (at passage-42). The fetal bovine serum (FBS) (10%) and Antibiotic-Antimycotic cocktail (1%) were also added to the DMEM and the culture medium along with cells were maintained at 37 °C in a humidified atmosphere with 5% CO_2. After staining with trypan blue stain (SRL), the cells were counted by Automated Cell Counter (Countess® II FL, Thermo Fisher Scientific). One day the before, cells were seeded (100 µL/well) in five 96 well plates.

- ***MTT assay***

The mitochondrial activity of BHK-21 cells seeded onto the bio-composite filmogenic/coating solutions and onto polymeric films of 1 cm^2 surface area was assessed by enzymatic conversion of tetrazolium dye MTT (3-(4,5-dimethylthiazol-2-yl)-2,5-diphenyltetrazoliumbromid after the time intervals of 8, 16, 24, 48, 72 h. The samples were prepared of 10% (v/v) concentration in plain DMEM (Standard culture media without serum) in which plain DMEM was used as control. 100 µL of each sample and control was added to all the plates in four replicates after removing seeding media (Standard culture media) followed by incubation at 37 °C under the humidified atmosphere with 5% CO_2 for different time intervals (8, 16, 24, 48, 72 h). Meanwhile, MTT stock solution of 5 mg/mL was prepared in PBS and stored at 4 °C. After the incubation period of respective plates, all the samples were removed and 100µl of MTT solution diluted in plain DMEM to 0.5 mg/mL was added and incubated at 37°C in a humidified atmosphere with 5% CO_2 for 3 h. Afterward, MTT solution was discarded and 100µL of DMSO was added to each well

and plate incubated at 37 °C in a humidified atmosphere with 5% CO_2 for 10 min to dissolve the formazan crystals. Cell viability was determined by taking absorbance at 570 nm using a 96 well plate reader (Thermo Fischer Scientific). Graphs were plotted using the closest absorbance values of three replicates out of the four replicates of each sample.

2.4.7 Shelf-life Study

2.4.7.1 Surface Morphology of Fruits

The surface morphology of coated and control fruits during 30 days of storage period was characterized both ways, that is, visually as well as by the field-emission scanning electron microscope (Sigma 300, Zeiss, Germany). The surface of the tomatoes was cut by a commercial knife and lyophilized at −96 °C. The freeze-dried samples were made conductive by placing them inside a gold sputtering system (SC7620, Quorum). The selected surfaces were free from decay areas for surface morphology analysis under field emission scanning electron microscopy (FESEM).

2.4.7.2 Color and Gloss Properties of Fruits

The color coordinates of coated and control fruits during storage days at an interval of 5 days were evaluated using a colorimeter (Datacolor 550, USA). The L*, a*, and b* are color parameters that indicate lightness, redness to greenness, and yellowness to blueness, respectively. Besides, the gloss values at a lower (20°) and higher angle (85°) were determined using a colorimeter. The color and gloss values were measured after calibrating the reflectance of a color spectrophotometer with a black trap, white tile, and green tile. An ultra-small area view (USAV) aperture plate with an illuminated and measured sample area of 6.5 mm, wherein 2.5 mm area was used during analysis. The pulsed xenon lamp was the illuminating source. The data color tool's software was used to measure the color and gloss values. During the color and gloss measurement, decay portion of the tomato surface was neglected.

2.4.7.3 Weight Loss (%)

One common indication of fruit respiration during postharvest storage is weight loss [30]. The control and coated tomato fruits were weighed at regular intervals during storage. The results of the percentage of weight loss were determined using the following equation:

$$Weight\ loss\ (\%) = \frac{Initial\ weight - Final\ weight}{Initial\ weight} \times 100 \quad \text{.....(28)}$$

2.4.7.4 Determination of Total Soluble Solid Content and pH

The chopped tomatoes of ~50 g weight was crushed in a mixture grinder (M/s Philips, India), and the mixer was centrifuged at 5200 rpm for 10 min at 20 °C. The supernatant (juice) was used to determine the total soluble solid content with the help of a hand refractometer (ERMA RHB-32ATC, China). The measurements were taken at 25 ± 0.5 °C and expressed as the percentage (%) of weight loss. A commercial digital pH meter (Eutech pH 700, Eutech Instruments, Thermo Scientific) was used to determine the pH values of tomatoes during storage. The pH probe electrode was placed into a beaker containing 10 mL of juice to measure the pH value.

2.4.7.5 Determination of Titratable Acidity

Approximately 10 g of tomato juice was diluted with 250 mL Millipore water. Afterward, the mixture was titrated against 0.1 N NaOH solutions using a phenolphthalein indicator to detect the endpoint. The volume of NaOH was expressed as ‘g’ of citric acid/100 mL of homogenate. Titratable acidity was calculated by the following equation:

$$Titratable\ acidity\ (\%) = \frac{v \times 0.064 \times N \times 100}{m} \quad \text{.....(29)}$$

where, v is the amount of NaOH solution consumed, N indicates normality of NaOH solution (0.1 N), and m is the weight of juice.

2.4.7.6 Determination of Reducing Sugar

The reducing sugar content was measured by 3,5-dinitro salicylic acid (DNSA) assay according to the method by Khatri et al., 2020 [104], with slight modification. The DNSA solution of ~1 mL was mixed with 2 mL of diluted tomato juice (10 times) and boiled at ~95 °C for 5 min. After cooling down to room temperature, the absorbance of the resultant solution was measured using an UV-Vis spectrophotometer (Perkin Elmer, USA) at 540 nm. The D-glucose (200-1000 mg/L) standard curve was prepared to calculate the reducing sugar content of the samples. The experimental results were expressed in the percentage of reducing sugar of mg D-glucose equivalent per 'g' of the sample.

2.4.7.7 Determination of Antioxidant Activity

The free radical scavenging activity of coated and uncoated samples was determined by the DPPH assay. About 1 mL of juice was mixed with 3 mL of DPPH solution. The DPPH solution was prepared in ethanol (50 mg/L). The absorbance of the mixtures was measured at 517 nm using a UV-Vis spectrophotometer (PerkinElmer, USA) after the completion of 30 min incubation period. The antioxidant activity of stored fruits in terms of DPPH scavenging activity was calculated using Equation 9.

2.4.7.8 Determination of Lycopene Content

The amount of lycopene present in tomatoes during storage was quantified by the HPLC and spectrophotometer method according to the reported literature with slight modification [32-34]. The HPLC system equipped with a UV-vis detector, and C18 column was used for the analysis. A mixture of methanol and acetonitrile (90:15) was used as the mobile phase, with a constant flow rate of 1.0 mL/min, and the detection was recorded at 472 nm under room temperature for 30 min. The actual peak of lycopene was identified by comparing the retention time with the standard lycopene solution (**Figure A1**). For sample preparation, ~10 g chopped tomato was mixed using a mixture grinder and freeze-dried at −96 °C. After

that, 0.01 to 0.6 g of the dried sample was mixed with 20 mL of an organic solvent mixture of ethanol, hexane, acetone, and BHT (1:2:1:0.002) and stirred at 180 rpm, for 15 min under dark conditions. Subsequently, 3 mL of Millipore water was added and stirred at 180 rpm followed by 5 min incubation without agitation. The separated uppermost hexane layer was collected for analysis. The lycopene content was estimated using the following formula under an UV-vis spectrophotometer [105].

$$Lycopene\ (g/kg) = (x/y) \times A_{503} \times 3.12 \quad \text{.....(30)}$$

Where, x, y, and A_{503} represents the volume of hexane (mL), the weight of the sample (g), absorbance, respectively and 3.12 is the extinction coefficient.

2.4.7.9 Determination of Ascorbic acid

Ascorbic acid (AA) was estimated by a UV-Vis spectrophotometer according to Barros et al. (2007) method with slight modification [106]. Around 100 µL of juice was mixed with 10 mL of 1% (w/v) metaphosphoric acid and incubated at ambient conditions for 45 min. Next, 1 mL of this mixture was mixed with 9 mL of DCPIP solution, and the absorbance was measured at 515 nm.

2.4.7.10 Determination of Firmness

The firmness of tomatoes was measured with five fruits from each batch and the measurement was taken on two different surfaces of each fruit using a texture analyzer (TA.XT Plus, Stable Microsystem). The 5 mm diameter cylindrical probe was used for the measurement with a speed of 20 mm min^{-1}. The texture analyzer measured the maximum force on the skin penetration and the results were expressed in Newton (N).

2.4.7.11 Determination of Respiration Rate

The evolution of carbon dioxide (CO_2) during storage of tomatoes was measured with a slight modification of the Kim and Min (2017) method [107]. Around 100 g of tomato was placed into a separate aluminum bag (100 mL) which was subjected to nitrogen purging to

maintain an inert environment, followed by sealing with an electric vacuum sealer (Ionix instruments, India). The bags were stored at room temperature and punctured on a particular storage day to measure the amount of CO_2 evolved. The bags were punctured using a 1 mL needle with the help of a rubber septum to ensure that no air could enter from the surroundings and that the CO_2 generated inside the bag headspace was analyzed by the gas analyzer (Lab think, China).

2.4.7.12 Microbiological Analysis

The microbiological analysis of tomatoes was performed at the initial and the end of the storage day to observe the microbial behavior of stored tomatoes. The tomatoes were chopped using sterile accessories like a knife and other containers to avoid cross-contamination. Around 10 g of chopped tomato were added to 15 mL sterile peptone water (0.1 g/100 mL) and homogenized for 5 min. The serial dilutions were prepared using sterile peptone water inside a sterile chamber. Subsequently, 50 µL of each sample was placed into a sterile Petri plate, followed by the addition of nutrient media (Plate count agar (PCA) for mesophiles and psychrophiles; and Potato dextrose agar (PDA) for psychrophiles). The sample with media-containing plates was rotated in the clock and anti-clockwise direction to ensure proper mixing. Finally, the plates were incubated for mesophiles (2 days at 30 °C), psychrophiles (5 days at 10 °C), and yeast and molds (3 days at room temperature) counts [108, 109]. Colonies were counted, and the results were expressed as log CFU/g of tomato. All experiments were performed in three replicates.

2.4.7.13 Sensory Evaluation

The overall acceptability of stored tomatoes on 0, 5^{th}, 15^{th}, and 30^{th} day of storage was evaluated through five-point hedonic scale sensory evaluation techniques (9-Excellent, 7-Very good, 5-Good, 3-Fair, 1-Poor) [110]. The predominant sensory attributes i.e, taste, flavor, and acceptability were evaluated by ten panelists between 25-32 y of age group from

our laboratory at Indian Institute of Technology Guwahati (India). Firstly, the participants were subjected to screening based on their consumption prevalence of red tomato. The stored tomatoes were served as the sample with code name over a tray with a glass of water and cracker to refresh taste buds between samples.

2.4.8 Statistical Analysis

Analysis of variance (ANOVA) was performed on the data sets using SPSS 26.0 software and significant effects ($p<0.05$) were noted. Significant difference among the means was determined by Tukey's test.

CHAPTER 3

EXTRACTION AND CHARACTERIZATION OF ALGAE AND ITS EXTRACT INCORPORATED CHITOSAN-BASED CAST FILM FOR EDIBLE ACTIVE PACKAGING

The concept of sustainability and the substitution of non-biodegradable packaging for biodegradable one has gained gigantic interest. The objective of the present study is to re-value the bio-waste "de-oiled green algae biomass (DAB)" of Dunaliella tertiolecta using a green approach and development of bio-degradable chitosan (CS)-based edible active bio-composite films and coating for prolonging the shelf-life of fresh produces. The ultrasound-assisted green extraction was conducted using food-grade solvent ethanol for obtaining the bio-actives namely "crude algae ethanolic extract (CAEE)" from DAB. Response surface methodology was used for optimizing the process of extraction. The edible films (CS/CAEE) and coating solutions were developed by incorporating CAEE with varying concentrations (0 to 28%). The CAEE was subjected to MALDI-TOF-MS, NMR, and other biochemical analyses and found as rich in DPPH antioxidant activity (~40%). The CS/CAEE films were fabricated using the solvent casting method and characterized for several biochemical and physicochemical (FESEM, TGA, FTIR, XRD, WVTR, UTM, and Rheological) characterizations. The addition of CAEE into the CS-matrix reduced maximum film transparency (~20%) water vapor permeability (~60%), improved crystallinity (~24%), tensile strength (~25%), antioxidant activity (~27%), and exhibited UV-Vis blocking properties as compared to control film. Besides, the developed coating solutions and CAEE showed biocompatibility with BHK-21 fibroblast cells and antimicrobial activity against common food pathogens.

Outcome: Mondal, K., Bhattacharjee, S. K., Mudenur, C., Ghosh, T., Goud, V. V., & Katiyar, V. (2022). *Development of antioxidant-rich edible active films and coatings incorporated with de-oiled ethanolic green algae extract a candidate for prolonging the shelf life of fresh produce. RSC advances*, *12*(21), 13295-13313.

V. Katiyar & **K. Mondal** "*A chitosan-based de-oiled green algae extract additivated edible packaging formulation*", Patent file no. 202131013653.

Graphical Abstract

This schematic chart describes the processing steps involved in obtaining crude algae ethanolic extract and its various characterization and processing steps for the development of chitosan-based edible films and their characterization.

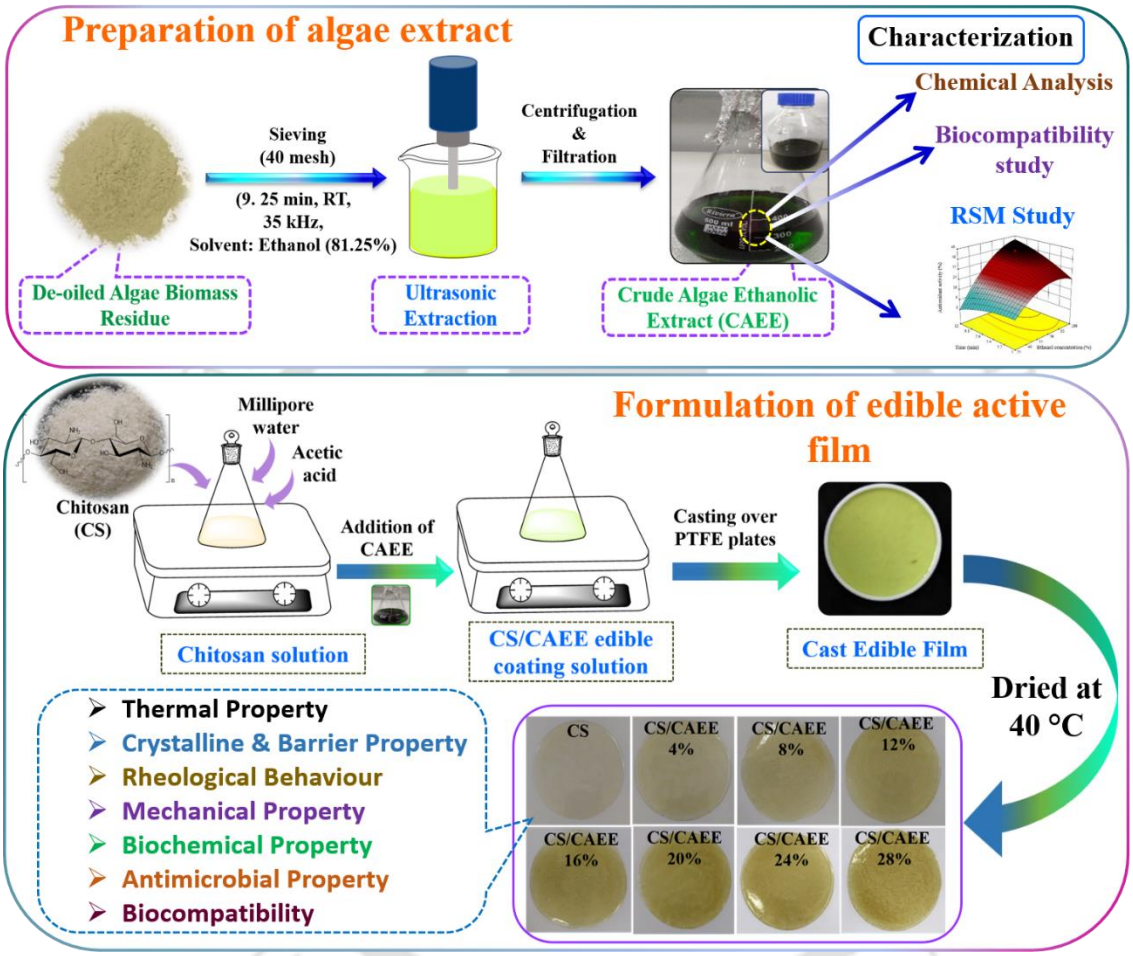

3.1 Introduction

Active and edible packaging is an emerging concept aimed to deliver quality and safe food along with prolonged shelf-life while at the same time mitigating environmental hazards caused by non-biodegradable food packaging waste. Besides, providing barrier properties, this innovative packaging acts as one of the preservation methods. The improved functionality of this packaging material is due to the incorporation of active substances such as antimicrobial agents, antioxidants, and others, which are not available in conventional packaging [111-114]. In this context, chitosan, a biodegradable, non-toxic, bio-based with good film-forming properties and bio-compatible polymer, obtained from the deacetylation of chitin, found in crustaceans and insects [115], has received much attention for the development of active and edible food packaging material [8]. Chitosan-based films and coating have wide antimicrobial properties against Gram-positive, Gram-negative, yeast, and molds, which is due to the presence of cations that led to surface damage in the microbial cell via interacting with anions present on it [116]. Besides, chitosan can restore essential oils and bioactive compounds into their structure, which diversify its application in controlled-drug delivery and food coating system [117,118]. Nevertheless, the restricted use of chitosan-based films in food packaging is due to their inherent poor barrier and mechanical properties, which make them hydrophilic and brittle, which is undesirable for a food packaging material where high strength, control of moisture, and gas transfer is essential [119]. To overcome these limitations bio-fillers such as oil, lipids, fatty acids, waxes, proteins, polysaccharides, and various plant extracts have been added to chitosan for obtaining improved physicochemical and structural properties [120]. However, the addition of oils and lipids adversely affects the mechanical properties of chitosan by altering the three-dimensional network structure [121]. Further, the incorporation of proteins and polysaccharides into the chitosan films sometimes provides

incompatibility thereby restricting their use. In this regard, Ferreira et al., 2009, [122] have reported whey protein-rich surfaces are more hydrophobic than chitosan. However, enhancing the protein amount decreased the mechanical strength and elongation. Furthermore, the concept of developing selected biopolymer-based multi-layered films, and composites as biodegradable packaging material gained a lot of attention due to their improved mechanical, and other properties, whereas higher cost limited its use [123,124]. In this context, a promising strategy has been made to address all the limitations and urge to develop novel sustainable packaging material via utilizing the concept of green technology where various biomaterials from different agri-based waste have been utilized as a key factor for fabricating eco-friendly packaging material [125,126]. In this regard, various plant-based extracts such as banana peel extract [127], pomegranate peel extract [117], mutra leaf extract [128], extract of a pine nutshell, peanut shell, jujube leaf [129], and others have been used as bio-filler in chitosan matrix and the associated literature has reported about the improvement in antioxidant and other functional properties of developed bio-composites. Recently, one study has reported about the addition of spice extract into chitosan film enhances different characteristic properties of the film and extends the shelf-life of the food material [130]. Besides, Lorenzo, et al., 2018, stated the non-toxicity of the plant extract at a higher dose level as compared to doses taken through daily diets [131].

Dunaliella tertiolecta is a green microalga mostly studied for bio-energy production [132]. Besides, it has potential use in the pharmaceutical and food industry as a healthy food supplement due to its bioactive compounds [133-137]. Therefore, this chapter focuses on the ultrasound-assisted green technology-based liquid extraction of bioactive compounds from *Dunaliella DAB*, and the development of chitosan (CS) based on active edible bio-composite films and coating. The ultrasound-assisted crude algae ethanolic extract (CAEE) was optimized in terms of DPPH antioxidant activity using the RCCD

model and used in varying concentrations as a bio-filler/food additive in the chitosan matrix to obtain active edible packaging material with improved several physicochemical and functional properties. Further, the developed filmogenic solution was applied to a real food system as a primary packaging material in form of active edible coating, targeting to extend the shelf-life. Moreover, several physicochemical and functional properties of developed films were studied.

3.2 Results and Discussion

3.2.1 Compositional and Elemental Analysis of the ABR

The α-cellulose content of ABR was found to be 19.7±1.6 % which is supported by the literature that green algae have significant cellulose content within the range of 20-30 wt.% [138], indicating ABR as a good source of cellulose. However, the cellulose content varies based on internal and external factors including culture conditions and algae species [139]. The total solid, moisture, and ash content of the ABR was found to be 94.9 ±1.7 %, 5.1±1.7 %, and 47.3 ± 1.4 %, respectively. The ash content indicated the presence of an enormous amount of inorganic matter which agrees with the literature [140]. More than twenty elements were detected in the ABR via ICPMS analysis, but those having concentrations equivalent to 1 ppm, or more were considered including Mg, P, Fe, Si, Na, K, and others (**Table 3.1**). All the elements were found to be under the permissible safe limits based on the available standard literature. Further, this finding corroborated the ash content result.

3.2.2 Optimization of CAEE Extraction

3.2.2.1 Response Surface Analysis and Model Fitting

Based on the preliminary investigation (data not shown), four independent variables were selected to perform the experimental design for optimizing the process of ultrasound-assisted extraction of DAB. The range of independent variables has been depicted in **Table**

3.2. The RCCD model was used to investigate the effect of independent variables on the response parameter, antioxidant activity.

Table 3.1: Elemental analysis of the algae biomass residue by the ICPMS analysis.

Sl. No.	Elements Name	Quantity (ppm)	Permissible limit of the element	Reference
1.	Sodium (Na)	2.218±0.01	<2300 mg/day (daily intake of food)	[141]
2.	Magnesium (Mg)	130.713±0.65	380mg/day (daily intake of food)	[142]
3.	Aluminum (Al)	1.500±0.02	0-95 mg/day (daily intake of food)	[143]
4.	Silica (Si)	3.926±0.04	3.9-10.1 mg/kg body weight /day in food (≥ 65 years) 4.9-13.2 mg/kg body weight /day in food (18-64 years) 18.5-74.2 mg/kg body weight /day in food (Infant) 18.5-39.4 mg/kg body weight /day in food (Toddlers) 10.2-31.2 mg/kg body weight /day in food (3-9 years)	[144]
5.	Phosphorous (P)	29.337±0.59	700-800 mg/day for adults (>19 years old) (daily intake in food)	[143]
6.	Sulfur (S)	1.014±0.23	0.7 mg/kg (daily intake of food)	[145]
7.	Potassium (K)	1.919±0.02	2.7 mg/kg body weight /day in drinking water	[146]
8.	Vanadium (V)	1.249±0.01	6.5-11 µg/day (infants, children, and adolescents) 6-18 µg/day(adults)	[147]
9.	Iron (Fe)	7.284±0.12	10-50 mg/day (minimum daily intake)	[148]
10.	Strontium (Sr)	1.015±0.01	4 mg/day (daily intake)	[149]

The correlation between independent factors (solvent concentration (x_1), solvent to solid ratio (x_2), extraction time (x_3), and ultrasonic frequency (x_4)) and dependent variables as a percentage of antioxidant activity (y) was developed in terms of a second-order polynomial equation and analyzed by response surface regression. The obtained quadratic polynomial equation of the response surfaces is as follows:

$$y = 31.94 + 6.18x_1 - 0.96x_2 - 1.02x_3 + 0.77x_4 - 0.86x_1x_2 + 1.89x_1x_3 - 0.41x_1x_4 - 0.95x_2x_3 + 0.07x_2x_4 - 1.30x_3x_4 - 2.32x_1^2 + 0.10x_2^2 - 0.64x_3^2 - 0.44x_4^2 \quad \text{……(24)}$$

The ANOVA of the response parameter for the quadratic polynomial model has been inserted in **Table 3.2.** The obtained regression coefficient (R^2) for the response parameter using the RCCD model was 0.98, which predicted the preferable fitting of an experimental model to the real data.

Table 3.2: Analysis of variance of the regression parameters.

Response	**Sources**	**Sum of squares**	**Degree of freedom**	**F**	**P**	**R^2**	**Adj R^2**
Antioxidant Activity (y)	Regression	1247.37	14	76.04	<0.0001	0.98	0.97
	Lack of fit	16.02	10	5.16	0.04		
	Pure error	1.55	5				

3.2.2.2 Analysis of Response Surfaces and DPPH Antioxidant Activity

Free radical formation occurs when a hydrogen atom is eliminated from the double bond of any molecules resulting in accelerate oxidation and unstabilizing of the system [150]. Therefore, the scavenging of free radicals is essential. In this context, the use of antioxidants can suppress the oxidation rate by inhibiting chain initiation reactions [151]. One of the most applied methods to determine the antioxidant activity in CAEE is DPPH

free radicals scavenging activity. The antioxidant activity in CAEE varied from 10.3% to 39.8%, which is related to the types and levels of antioxidants recovered at each extraction stage [152]. The interaction effects among independent variables on DPPH antioxidant activity have been described in **Figure 3.1**.

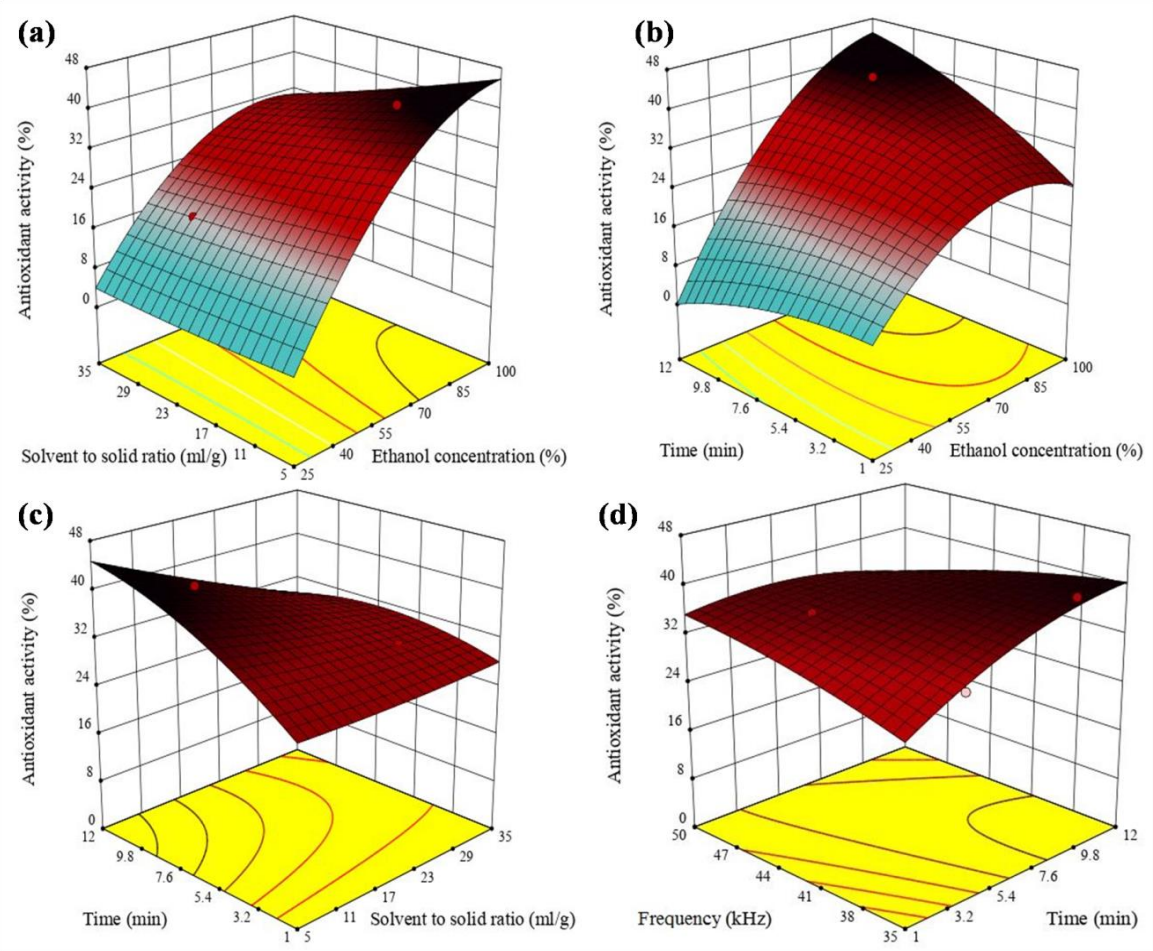

Figure 3.1: Response surface plots for the effects of (a) ethanol concentration and solvent to solid ratio, (b) ethanol concentration and time, (c) solvent to solid ratio to extraction time, and (d) ultrasonic frequency and time on antioxidant activity of CAEE.

3.2.2.3 Optimization, Prediction, and Validation of Parameters

The solid-liquid extraction conditions for maximizing the antioxidant activity in CAEE from DAB powder were optimized. The optimum extraction condition was obtained using multiple regression analysis and model fitting (**Equation 24**) based on the highest

desirability values. The optimized condition has been summarized in **Table 3.2**. The highest predicted antioxidant activity obtained (**Table 3.2**) in de-oiled algae biomass extract (y) is 39.46%. In this context, the optimized condition for exhibiting maximum antioxidant activity is found to be 81.25 % (v/v) extracting solvent concentration, 12.5 mL/g solvents to solid ratio, 9.25 min of extraction time, and 35 kHz frequency. The validation of predicting model is executed by performing the lab-scale experiment using optimized parameters (**Table 3.3**). The predicted models are found as significantly effective for optimizing the extraction process, and no significant difference is observed between the experimental and predicted values on DPPH antioxidant activity.

Table 3.3: Optimized condition of antioxidant activity with the predicted and experimental value.

Sample (Algae extract)	**Ethanol concentration (%)**	**Solvent to solid ratio (mL/g)**	**Time (min)**	**Frequency (kHz)**	**Antioxidant activity (%)**		
					Desirability	Predicted	Experimental
y	**81.25**	**12.5**	**9.25**	**35**	0.95	39.46	40.88

3.2.3 Biochemical Analysis of Bio-filler CAEE

The ultrasound-assisted extraction from de-oiled algae biomass residue has been schematically described in chapter 2 (**Figure 2.1)**. The CAEE was rich in antioxidants with 40±1.41% DPPH radical scavenging activity, total phenolic content of 515.72±4.67 µg/g, total flavonoid content of 151.75±2.05 µg/mL, and total chlorophyll content of 23.81±1.1 mg/mL, respectively. Further, the optimized algae extract CAEE contains13.6 mg/L of β-carotene, which was determined by the HPLC technique, indicating that CAEE is a rich source of β-carotene. The yield of chlorophyll was 238.14 mg/mL which indicating ethanol acted as a superior chlorophyll-extracting solvent [153]. In addition, the percentage of chlorophyll ‘a’ (15.63±0.16) in CAEE was higher as compared

to chlorophyll ‘b’ (8.19±0.09). Moreover, the obtained results indicates that CAEE is rich in antioxidants and polyphenols. The color coordinates L, a*, and b* values of CAEE were 72.62±0.04, −4.1±0.01, and 59.29±0.05, respectively. The negative value of a* is attributed to the green color of the extract, which is due to the presence of pigment chlorophyll, whereas the higher positive value of b* indicates to yellow color which may be due to the presence of carotenoids such as beta carotene and others which is the most available pigment found in the green algae [154].

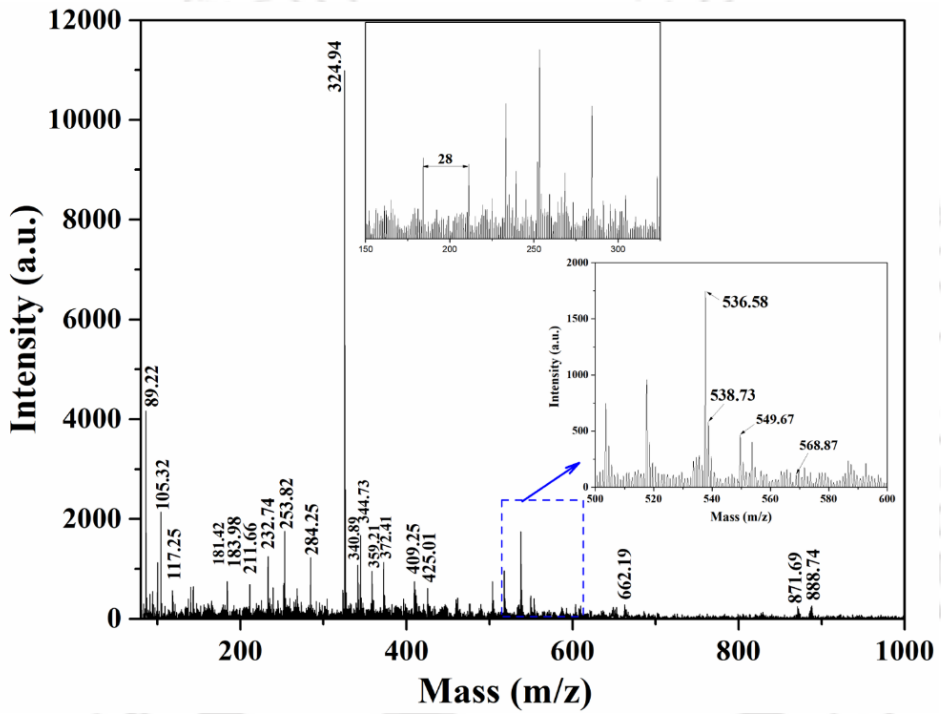

Figure 3.2: MALDI TOF MS spectra of crude algae ethanolic extract (CAEE).

3.2.4 MALDI TOF MS Analysis of CAEE

Matrix-assisted laser desorption/ionization mass spectroscopy is one of the methods for the structural identification of organic matter of any biological sample. A series of masses m/z of CAEE was observed from the MALDI TOF MS spectrum and have been depicted in **Figure 3.2**. The obtained peak at lower m/z value i.e., 89.22, 105.32, 11.25, and 181.42 indicates presence of proteins including alanine, serine, valine, and tyrosine, respectively [149]. Besides, masses m/z at 183.98, 211.66, 232.74, 253.82, 258.21, 284.25, 324.94,

340.89, 344.73, 359.21, 372.41, 409.25, 425.01 corresponded to protonated hexose sugar, sulfated hexose sugar, Magnesium ion (Mg+) attached with a hexose sugar, uronic acid, two hexose sugar, two pentose sugar with Mg+ ion, di-saccharide (heptose and pentose), deprotonated di-saccharide (hexose and heptose) associated with a sodium ion, and sugars linked with other ions like Na, Mg, P, S, etc. The mentioned metals present in de-oiled algae biomass were also detected by ICPMS analysis as reported in previous section 3.2.1. The observed peak at m/z 662.19 might be related to the tetra-saccharide of two sugars i.e., both pentose and hexose. The mass deltas between peaks were observed consecutively at 1-2, 14, 18, and 28 Da corresponding to degrees of saturation and ring structures, polymeric chains ($(CH_2)_n$), loss of water molecule, and deprive of CO bond from esters of lactone [155]. Further, the m/z value in the range between 500 to 600 is predominantly responsible for carotenoids. MALDI spectra were highlighted and intensified for masses m/z at 536.58, 538.73, 549.67, 568.57, and 593.86 representing the presence of carotenoids such as β-carotene along with its derivatives, zeaxanthin and deprotonated astaxanthin which is like the reported literature by Fraser et al., 2007 [156]. The identified peaks at m/z 871.69 and 888.74 corresponded to chlorophyll a or pheophytin and astaxanthin esters [156].

3.2.5 NMR Study of CAEE

3.2.5.1 ^{1}H NMR

The proton (^{1}H) NMR spectra of obtained algal extract (CAEE) of *Dunaliella tertiolecta* in two different solvent chloroform ($CDCl_3$) and methanol (CD_3OD) attributed to several peaks in the spectrum which possibly due to the presence of various compounds and its derivatives including exopolysaccharide, carotenoids, and proteins (**Figure 3.3**). The spectrum describes chemical shifts (ppm) and corresponding functional groups. Both spectra predicted the presence of α, β-anomeric carbon of hexose or pentose based on the chemical shift at 5.1 to 5.4 and between 4.8 to 4.9 ppm, respectively. The ppm value at 2.3

was attributed to the presence of uronic acid which was also found in the MALDI TOF MS spectrum [34]. The presence of halide and N-H groups was attributed to 3.0 ppm and 1.3 ppm. Further, chemical shifts at 2.0 and 2.8 ppm attributed to the functional groups related to acetyl amine of hexose or pentose sugar moiety [157]. Moreover, along with polysaccharides other functional groups attributed to the alkene, alkyne, aliphatic, aldehyde, and aromatic compounds are found in the spectrum which is clearer in the magnified graph (**Figure 3.3a**). It is well known that *Dunaliella* species can accumulate quite a good quantity of pigments mainly chlorophylls and carotenoids [154]. Among chlorophylls, chlorophyll a is predominant whereas β-carotene, astaxanthin, and fucoxanthin are mostly found in this species. The signals between 6-6.9, 2.0, 1.5, and 1.0 ppm are attributed to polyene $(CH=C\text{-}CH_3)_n$, vinyl CH_3, CH_2, and iso dimethyl attached to a cyclic ring, respectively [158]. In this context, the presence of β-carotene and astaxanthin pigments was also confirmed due to these signals. The observed chemical shift at 7.13 ppm in doublet form in both the NMR spectrum is related to olefinic protons of fucoxanthin [154].

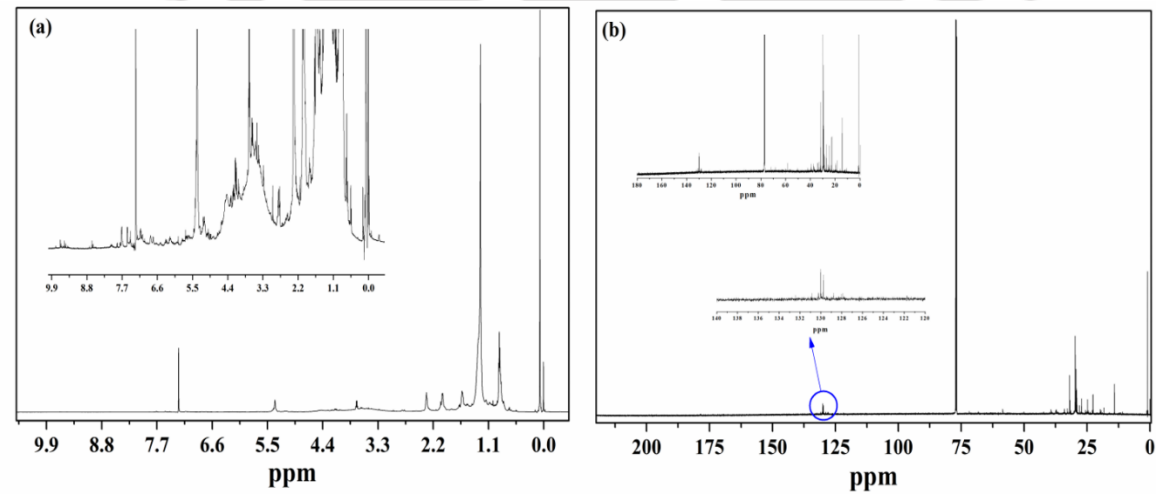

Figure 3.3: (a) ^{1}H NMR spectra of CAEE in $CDCl_3$ solvent (b) ^{13}C NMR spectra of CAEE in $CDCl_3$ solvent.

Further, ^{1}H NMR spectra predicted the presence of proteins such as alanine and tyrosine in CAEE due to the appearance of chemical shifts at 3.62, 1.47, 2.30, 2.34, and 7.14. This finding is in corroboration with obtained mass from the MALDI TOF MS spectrum. In this context, a similar observation has been reported by Iglesias et al., 2019 [154].

3.2.5.2 ^{13}C NMR

The ^{13}C NMR analysis of CAEE was carried out to confirm the presence of carotenoids, polysaccharides, and proteins and the absence of intensified saturated and unsaturated fatty acids. As conferred from **Figure 3.3b,** none of the intensified peaks was found in the range of 170 to 175 ppm in both the spectrum of CAEE dissolve in $CDCl_3$ (**Figure 3.3b**) and CD_3OD which is mainly corresponding to saturated carbonyl carbons, oleic, linoleic, alpha-linolenic acid, acyl chains [154]. This result indicated the absence of saturated and unsaturated fatty acids which are commonly found in algae. The occurrence of this result is expected as de-oiled algal biomass was utilized for the present study. The presence of peaks between the 120 to 140 ppm range corresponded to C11, C7, C5, C15, C10, C14, C12, and C8 of carotenoids [159]. Further, the presence of olefinic groups was also confirmed by the observed peak range from 127-132 ppm [154]. The presence of carbohydrates was assigned to the peak range from 60 to 106 ppm whereas proteins like alanine and tyrosine correspond to the carboxylic group at 178.3, 58.5, 16.9, 59.5, 122.3, and 131.0 ppm. The presence of aromatic, amine and sulphonic groups was identified in the spectra. The presence of aromatic compounds was also following the result supported by ^{1}H NMR analysis. Further, NMR analysis is corroborated by the MALDI-TOF findings.

3.2.6 Chitosan-based Edible Film Characterization

3.2.6.1 Visual Aspect and Color Parameters

The CS-based films represented homogeneity and an absence of insoluble particles regardless of the CAEE concentration, as shown in **Figure 3.4**. The color parameter values

corroborated the difference in the visually observed yellow color intensity in bio-composite films. In general, the L* and a* values decreased and b* values increased as a function of increasing CAEE concentrations (**Figure 3.4a, b**), where L*, a*, and b* corresponded to lightness, green, and yellow color, respectively. However, in this study, a negative a* value was observed which was attributed to the presence of pigments of chlorophyll. The increment in negative a* value with increasing the CAEE concentration was observed maximum in 12% CAEE concentration followed by reduction and finally positive value was obtained with the highest bio-filler loading (**Figure 3.4b**). The increment in negative a* values might cause the increasing concentration of chlorophyll or carotenoids in higher loading bio-composites, which is like a visual observation of bio-composite films. The positive a* value might be due to the occurrence of carotenoid derivatives during the drying of the film. In this regard, reported literature says active films containing natural-colored pigments could be responsible for changing the values of the color coordinates. Wang et al., 2013 reported a reduction in L* value and an increment in a* and b* values in CS-based film after the incorporation of tea polyphenols as compared to control film [160].

3.2.6.2 Transparency of the Films

The transparency of a film describes its optical nature which is another important parameter for food packaging. Since food is a complex system and many of them are sensitive towards light i.e., UV-Vis (ultraviolet-visible). It can be conferred from **Figure 3.4c** that the neat CS (nCS/control) film presented higher transparency as compared to bio-composites. The incorporation of CAEE into the CS matrix improved the barrier of light transmission to visible and ultraviolet (<400 nm) regions. The addition of the extracts in the films reduced transmittance values in the UV and visible light region (400-800 nm), showing a significant reduction of these values for visible light around 650 nm, whereas no blocking properties were found in nCS film. Interestingly, the improvement of blocking property was observed

with increasing the bio-filler concentration. In this regard, the presence of phenolic compounds in CAEE could be attributed to providing UV-Vis blocking properties to the edible active films [161].

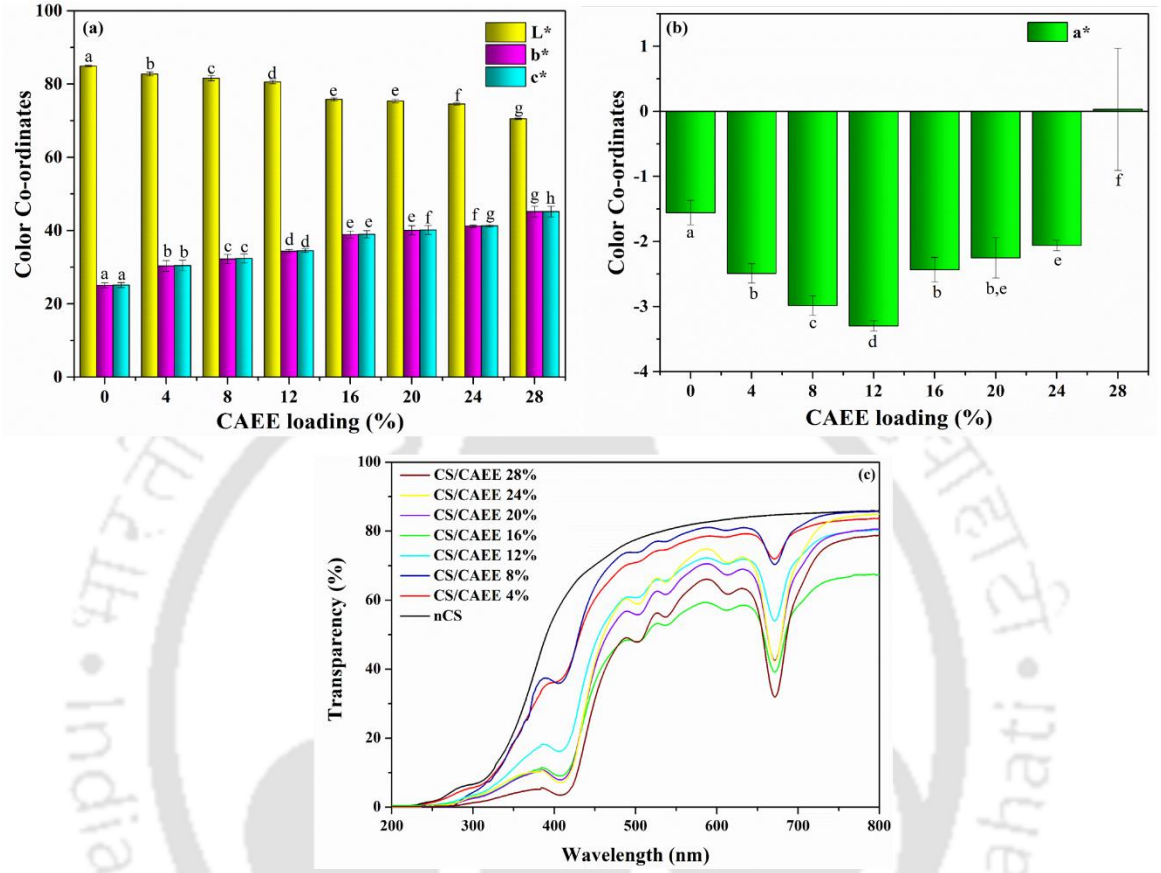

Figure 3.4: Color coordinate values of (a) L*, b*, & c* (b) a*, and (c) UV-VIS light transparency of CAEE incorporated edible active films (bio-composites) along with control film.

3.2.6.3. Thermal Stability of Films

The thermogravimetric (TGA) and derivatives (DTG) thermograms of the control and bio-composite films are presented in **Figure 3.5a, b**. The two steps degradation was recorded in each of the samples. The first stage of degradation was recorded around 50-100 °C (about 5% decomposition for each film) which could be attributed to the loosely bounded water evaporation from the polymeric structures. The second step of degradation was observed between 270-320 °C and it could correspond to the decomposition of CS molecules and

CAEE [127]. The predominant mass loss was recorded in the second degradation stage at around 270-305 °C and it was because of the denaturation of CS-polymeric organization and bio-filler. In the second stage, bio-composite films showed a slight reduction in mass loss as compared with nCS film which could be due to the formation of strong and heavy interactions via hydrogen bonding between CS molecules with phenolic compounds of CAEE [127].

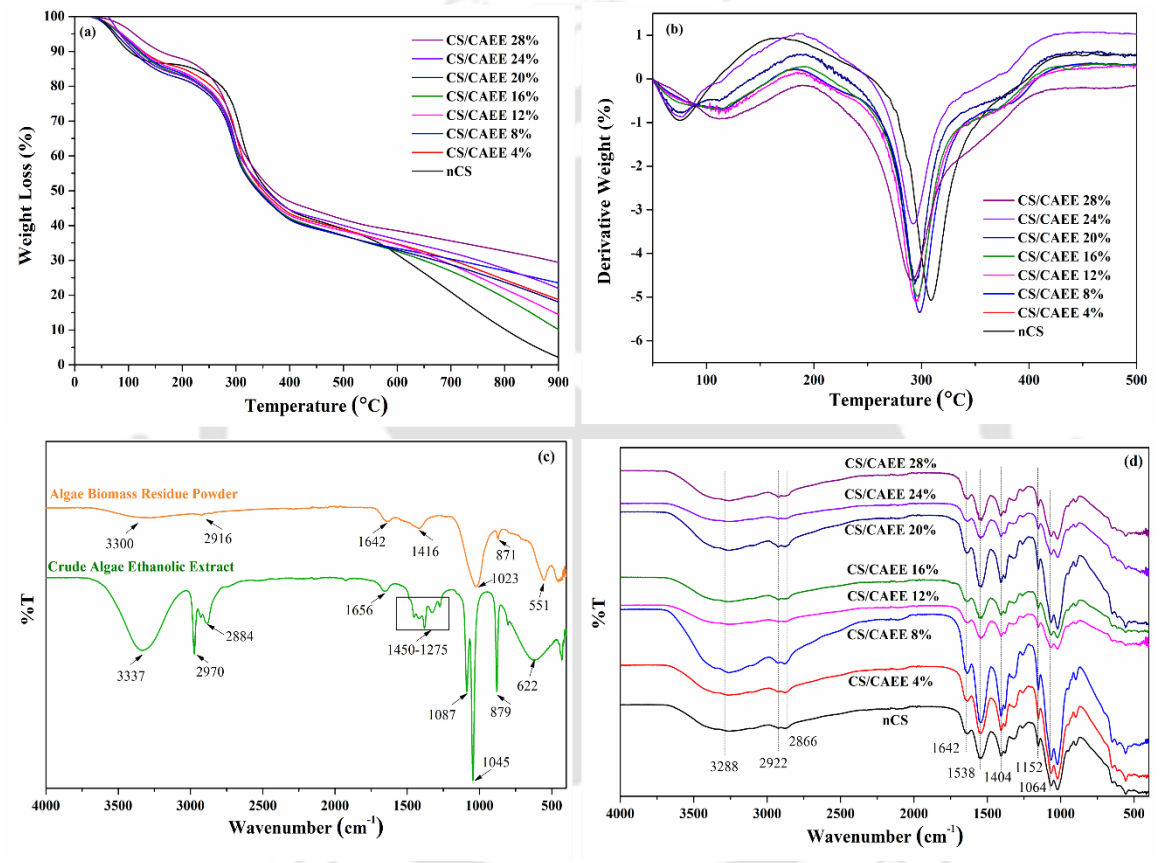

Figure 3.5: (a) Thermogravimetric, and (b) derivative thermogram of CAEE incorporated edible active films (bio-composites) along with control film, (c) FTIR spectrum of de-oil algae residue powder and CAEE, and (d) FTIR spectrum of developed bio-composite films with control.

The temperature at 5% (T5%) and 10% (T10%) mass loss has been reported in the Table A2, described bio-composite showed higher temperature as compared to nCS film in both cases. Furthermore, the maximum temperature of the first degradation of the control film

was ~75.5 (**Table A2**) whereas the incorporation of CAEE increased temperature to 106.8 and 113.8 °C in bio-composites. The increment in onset degradation temperature of bio-composite films might be related to moisture release effect and thermal stability. The addition of CAEE might potentially modify the moisture content or release characteristics of the chitosan matrix. Moisture release can affect the degradation temperatures observed in the bio-composite films, as the evaporation of moisture can lead to a shift in the onset of degradation. Besides, CAEE compounds can act as antioxidants or heat-resistant agents, preventing or slowing down the degradation of the chitosan matrix at elevated temperatures. This type of similar observation was reported where the incorporation of sweet potato extract, banana peel extract, and others tailored the thermal stability in developed bio-composites [127,162].

3.2.6.4. FTIR Analysis

FTIR analysis of de-oiled algae biomass residue powder (**Figure 3.5c**) depicts the functional groups present on the surface of the residual *Dunalliela* biomass. The observed broadband ~3300 cm^{-1} belonged to –NH and –OH groups [163]. The frequency band at ~2916 cm^{-1} was attributed to –CH stretching. The bands at 1643 and 1416 cm^{-1} corresponded to the carbonyl (C=O) group and the –C=S group the stretching vibrational [164]. The other lower region peaks were assigned to C-N and –C=S groups. The FTIR spectrum of CAEE (**Figure 3.5c**) exhibited a broad absorption peak of ~3337 cm^{-1} attributing to –OH stretching. However, the observed absorption bands in the de-oiled algae biomass residue powder and the extract were different. A strong absorption peak was observed at 2970 cm^{-1} corresponding to C–H symmetric stretching vibrations of the polyphenols. The presence of a band at 2884 cm^{-1} and 1656 cm^{-1} might be attributed to ethanol and amide I, or C=O stretching of proteins or carboxylic acid, respectively. The presence of a band at 1276, 1327, and 1380 cm^{-1} could be related to CH_2 vibration, amide

III, and symmetric $CH_3(CO)$ vibration of 1,8-Cineole, respectively. Further, the possibility of the presence of polysaccharides could be attributed to the occurrence of the band at 1087, and 1045 cm^{-1}. The observed band at 879 cm^{-1} corresponds to the $–CH_2$ stretching vibration of 1,8-Cineole or ethanol. **Figure 3.5d** depicts the spectrum for nCS and developed bio-composite edible films. The nCS displayed a wide absorption peak centered at 3288 cm^{-1} which could be associated with stretching vibrations of N–H and O–H. The occurrence of the peak at 2922 and 1642 cm^{-1} might be attributed to C–H asymmetric stretching due to methylene groups and the C=O stretching vibration of the residual amide bond. The absorption band at 1538 and 1404 cm^{-1} corresponded to amide II and amide III, while the peak at 1152 cm^{-1} was attributed to C–H and 1064 cm^{-1} was ascribed to C–O stretching vibration [102]. Moreover, the incorporation of CAEE into the CS matrix exhibited variation in intensity however, the frequency was unalerted.

3.2.6.5. Possible Mechanism of Developed CS/CAEE Films

The probable mechanism of fabricated CAEE-incorporated CS-based bio-composite films has been depicted in **Figure 3.6a**. One of the potential candidates for developing edible films or bio-composites is CS due to its bio-compatible, adequate film-forming property, high molecular weight, and charge density. The presence of amino (NH_2) and hydroxyl (OH) groups in the CS chain play a major role in the development of bio-composites via hydrogen, covalent, and amide bonding. The addition of mild acetic acid is required to dissolve CS and the NH_2 groups on CS molecules undergo partial protonation, resulting in the formation of positively charged ammonium ions (NH_3^+). Since the extent of protonation depends on various factor such as acetic acid, pH, pKa (acid dissociation constant) of the CS and acetic acid. The presence of both NH_2, and NH_3^+ reduces the electrostatic repulsion within the CS molecules and enhances the binding affinity with added bio-filler CAEE [127].

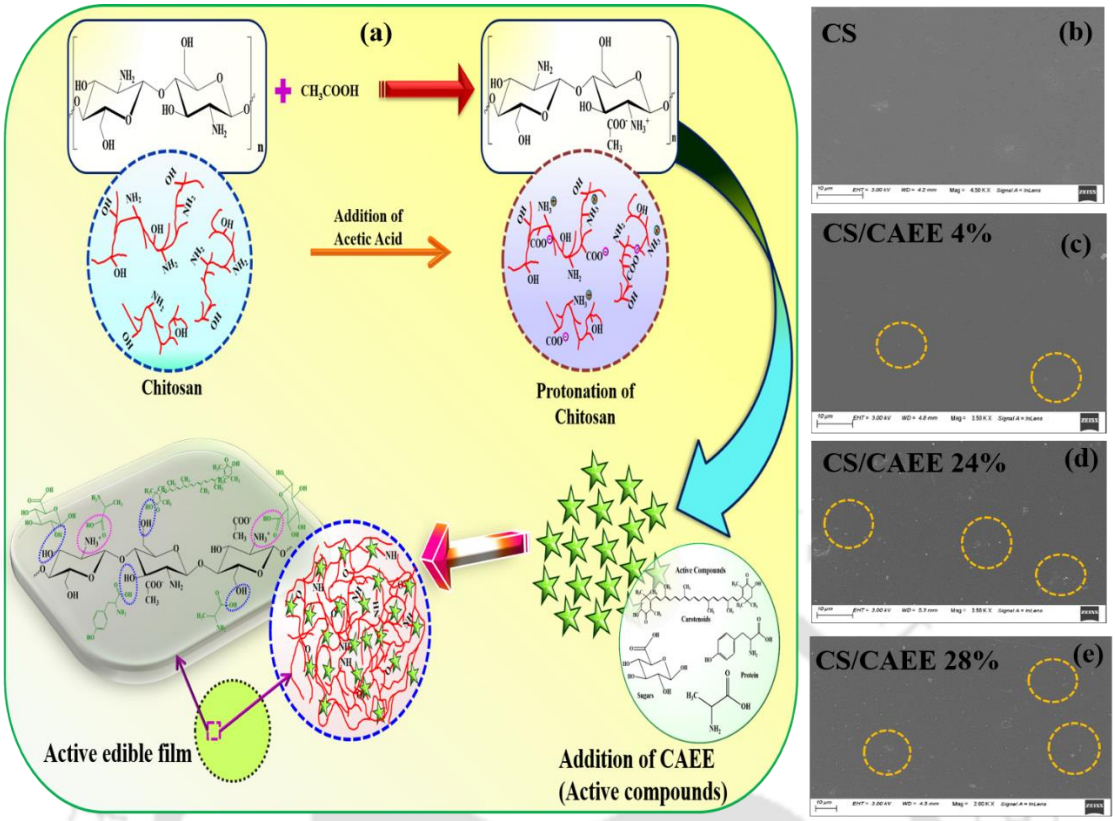

Figure 3.6: (a) Probable mechanism of CS/CAEE bio-composite film formation, and (b-e) surface morphology of developed bio-composite films with control.

Further, CAEE contains an adequate number of bioactive molecules predominantly, polyphenols such as carotenoids, proteins, polysaccharides, and sugars. These active molecules are strongly attached to the protonated chitosan chain via hydrogen bonding (dotted blue circle in **Figure 3.6a**) and amide bonding (marked as the dotted magenta circle in **Figure 3.6a**) as demonstrated in **Figure 3.6a** and form the grafting between active molecules and polymer matrix. The amide bonding majorly occurs between protein molecule and cationic CS chain as proteins contain a carboxylic group in their structure which is highly attracted towards the cationic amine group thereby a strong interaction occurs. This statement is corroborated with the findings of FTIR analysis of developed CS-based films as discussed in section 3.2.6.4. In this context, Deshmukh et al., 2021 reported the strong interaction of filler to CS matrix while Chlorella biomass was added via bridging and patching phenomenon [102]. The formation of grafting by intermolecular interaction

and encapsulation was reported while active compounds were incorporated into the pectin matrix [126].

3.2.6.6. Surface Morphology of Films

The surface characteristics of nCS and CS/CAEE bio-composite films are presented in **Figure 3.6b-e**. As seen from **Figure 3.6b**, a smooth, compact, and without the presence of cracks or pores surface morphology was observed for control which was in association with the visual observation results. Nevertheless, the addition of CAEE in bio-composite films exhibited irregular surfaces. The CS/CAEE films showed particles (range of particles 22 to 120 in number) on the surface captured by FESEM (**Figure 3.6c-e**). The fabricated films exhibited heterogeneous surface roughness which was increased with the addition of a higher CAEE concentration. Around 25 no. of particles were observed in the bio-composites whereas a more than 120 no. of particles was detected in the highest loading of 28% CAEE (**Figure 3.6e**). It could be speculated that the bridging phenomenon was formed inside the bio-composites where CAEE molecules partly bonded with CS chains and the rest of the CAEE molecules attached to another CS chain [96]. The increased roughness was due to the occurrence of a higher number of bioactive molecules including polyphenols, protein, sugar, amino acids, and polysaccharides. Almost similar surface morphologies were revealed after the addition of algae biomass and seaweed from the SEM micrographs in other reported works of CS-based and gelatin-based composite films [102, 165]. Presence of non-toxic minerals such as sodium, magnesium, calcium, potassium, and sulphur along with oxygen, nitrogen, and carbon were found by energy-dispersive X-ray spectroscopy (EDX) in bio-composites (**Figure A2**). In this context, the presence of mentioned elements arose from the organic sources of CAEE containing polysaccharides, carotenoids, proteins, and sugars. Moreover, homogeneous distribution of particles was observed in bio-composites.

3.2.6.7. XRD Analysis of Developed Films

Figure 3.7a depicts the X-ray diffraction pattern of the nCS and developed bio-composite films. The characteristic peak was observed at 9.69° and 20.54° which correspond to the plan [020] and [115], respectively. An increasing trend of crystallinity was observed after the addition of CAEE. A maximum improvement of ~22% crystallinity was obtained in the highest loading of CAEE (I_{CR} = 64%) as compared to nCS film (I_{CR} = 42%). The enhancement in the percentage of the crystalline index might be due to strong intermolecular hydrogen bonding between bio-filler (CAEE) and polymer matrix (CS). Further, peak shifting was not observed in any of the sample XRD patterns thereby indicating no structural changes occurred after the addition of bio-filler with varying loading.

3.2.6.8. Water Vapor Permeability of Developed Films

Figure 3.7b depicts the water vapor permeability (WVP) of the developed edible bio-composite films and the effectiveness of the addition of CAEE. A significant reduction was observed in WVP values in bio-composites due to the addition of CAEE. Further, the reduction was found to be highest with increasing the CAEE concentration from 4 to 28%. The highest reduction of ~60% was obtained in bio-composite films with a 28% addition of CAEE as compared to control film. Moreover, the improvement in WVP might be due to strong intermolecular hydrogen bonding between CS-matrix and bio-filler (CAEE) which probably allowed the formation of crosslinking due to which reduction in free space occurred inside the polymer matrix because of the lowered rate of diffusion of water vapor molecules happened through the bio-composite edible films. The observed findings were in association with the results of improved crystallinity of bio-composites by XRD. Further, before the analysis, films were dried at 100 °C for 2 h, this step could have an impact on slowing down the diffusion rate of water molecules due to crosslinking which led to a

reduction in chain mobility thereby minimizing the WVP through the film surface [166]. The observed result is corroborated with the FTIR analysis which also postulated the interaction between CS-matrix and CAEE attributed to the shortage of free hydrophilic moieties including amino and hydroxyl groups to bind with water, thereby minimizing the water vapor diffusion rate [167].

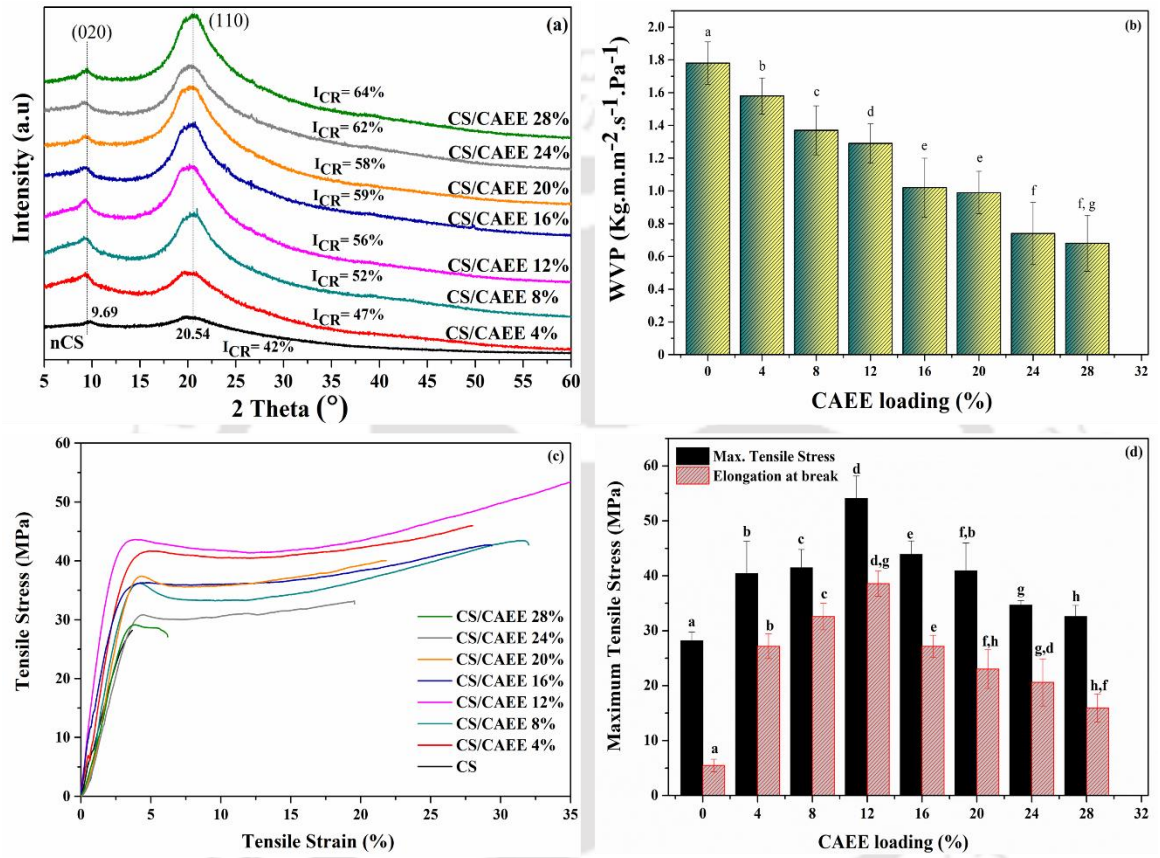

Figure 3.7: (a) XRD pattern, (b) water vapor permeability, (c) stress-strain curve, and (d) maximum tensile stress and elongation at break of developed bio-composite films with control.

3.2.6.9. Mechanical Properties of Developed Films

The consequence of incorporating CAEE into the CS-polymer matrix on the mechanical behavior of CS/CAEE bio-composite edible films was investigated regarding tensile strength (TS) and elongation at break (%E). The obtained stress-strain curve of edible films has been shown in **Figure 3.7c**. The increasing trend of CAEE content was observed with

an addition from 4 to 28%, which led to a significant increment in the TS, from 28.62 to 54.1 MPa. Further, a significant increment in %E of bio-composites was observed upon the addition of CAEE till 12% loading, beyond that slight reduction occurred (**Figure 3.7d**). The improvement in the mechanical property could be related to the uniform and homogeneous distribution of CAEE particles with CS-matrix which is attributed to the improved tensile strength. Besides, the reduction in %E, at higher loading of CAEE might occur due to the formation of strong hydrogen bonding between filler and polymer matrix which could cause the reduction in chain mobility into the system. However, increasing CAEE concentration beyond 12% led to a slight reduction in both TS and %E in the resulting CS/CAEE films, values were higher in comparison to the control. Furthermore, the reduction in mechanical behavior beyond 12% CAEE incorporation attributed to the weak intermolecular interaction between matrix and filler due to the formation of agglomeration which provides discontinuities in the polymeric matrix, and the formation of heterogeneous structure led to the loss of cohesion in the developed edible films. A similar type of result was also reported in the literature where the addition and increment of green algae *Ulva armoricana* content from 0 to 30% in polyvinylalcohol (PVA) matrix did not significantly improve TS, however, the sharp reduction was reported for % E [168]. Chiellini et al., 2008 reported the reduction in TS and %E in PVA/algae composite films with higher loading of around 30% algae powder into the matrix [168], which might be caused for the formation of improper cross-linking or bonding between algae powder and PVA matrix as a result the cohesion property of the developed film was compromised, leading to a decline in its mechanical strength and stretchability.

3.2.6.10. Rheological Behavior of filmogenic solutions

- **Strain Sweep Measurements of Developed Chitosan-based Bio-composites Filmogenic Solutions**

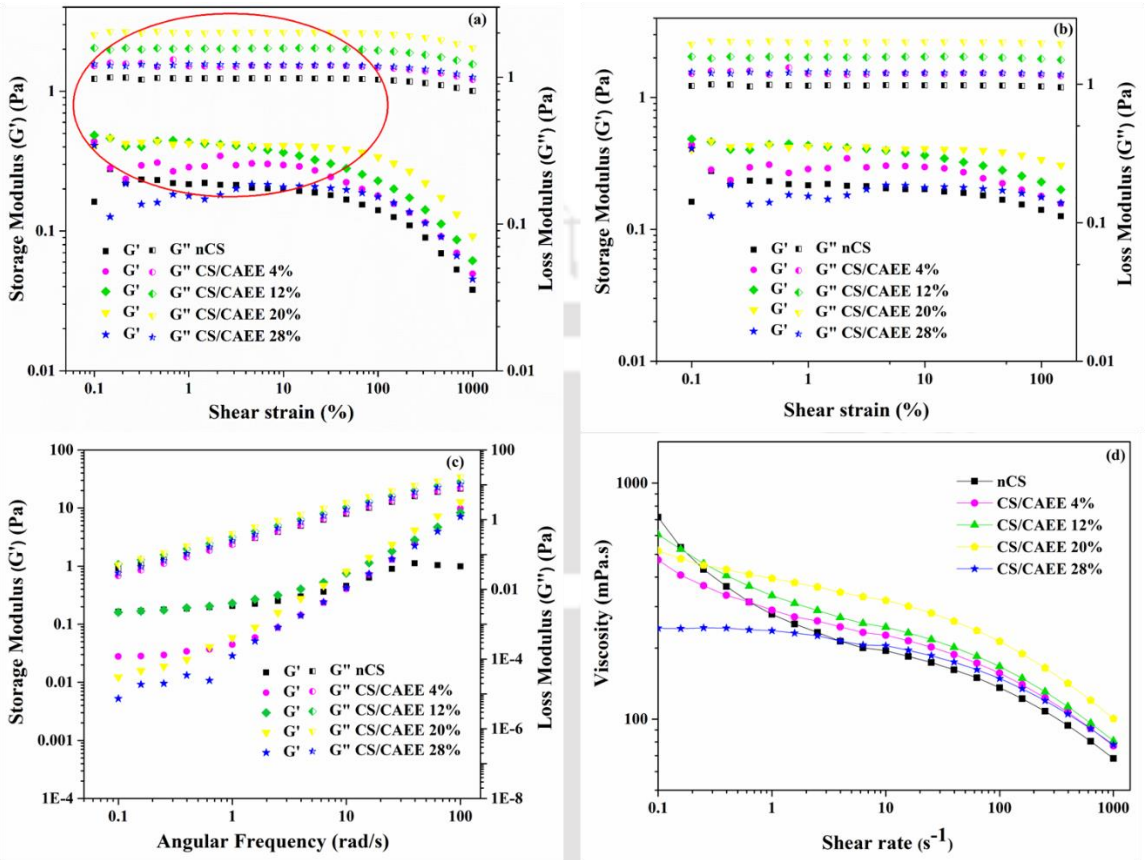

Figure 3.8: (a) Strain sweep parameters of G′ and G″ modulus at f = 1 Hz, (b) emphasizing of LVR, (c) frequency sweep parameter of G′ and G″ modulus, and (d) flow curve of developed bio-composite films with control.

The strain sweep measurements helped to determine the LVR (Linear viscoelastic region) of developed filmogenic solutions, where G′ (Storage modulus) and G″ (Loss modulus) remained constant and independent of applied strain. This measurement also imparts information regarding the structural strength of the material based on the length of the LVR region, i.e., the stable solution might remain longer in the LVR region as it is more resistant to applied force than an unstable one. The representative curve of the G′ and G″ moduli of all the solutions against applied strain have been depicted in **Figure. 3.8a,b**. It is evident

from the curve in all cases G″>G′, indicating all the samples showed liquid-like behavior under the LVR region. Overall, the elasticity (G′) decreased over time with increasing the shear strain for all the samples including the control. However, the addition of CAEE significantly improved the elastic behavior as compared to the control (nCS) which is more significant at higher strain. Further, a significant increase in G'_{LVR} values with increasing filler concentration from 4% to 20 % was observed, whereas, at a higher concentration of CAEE (28%), the G'_{LVR} dropped down but not below than control value as described in **Table 3.4** at a fixed shear strain of 1%. Besides, at lower shear strain similar trend was visualized for all the samples except higher loading of CAEE (28%), where a slight reduction of G′ was observed. Additionally, the non-linearity of the G′ and G″ modulus under applied strain detects the end limit of the LVR region [117].

Table 3.4: Strain sweep parameters measured at room temperature with f = 1 Hz: Critical strain (γ_L), G′ modulus at the LVR limit (G'_{LVR}), G″ modulus at the LVR limit (G''_{LVR}), loss factor value (tanδ) and the difference between G″ and G′ moduli at 1% strain.

Sample	γ_L (%)	G'_{LVR} (Pa)	G''_{LVR} (Pa)	tanδ	G″-G′ (Pa)	Power law model (n)	R^2
nCS	31.6	0.21	0.97	4.49	0.75	0.32	0.996
CS/CAEE 4%	46.4	0.28	1.18	4.14	0.90	0.31	0.991
CS/CAEE 12%	68.1	0.43	1.56	3.61	1.13	0.37	0.990
CS/CAEE 20%	99.9	0.42	2.00	4.72	1.58	0.40	0.996
CS/CAEE 28%	147	0.17	1.22	6.88	1.05	0.23	0.994

Moreover, the G″ value of CAEE incorporated polymeric solution increased as compared to the control solution indicated viscous nature. The G″ values showed significant improvement from 0.97 (nCS) to 2.0 (CAEE 20%) Pa with increasing the CAEE

concentration from 4 to 28%, however at 28% CAEE addition G″ decreased sharply but higher than control. One of the important parameters of oscillatory rheology is loss factor or loss tangent (tanδ = G″/G′) which indicates the characteristics of the material if tanδ > 1 indicates the viscous nature of the sample as G″ > G′, the sample is elastic when tanδ < 1 (G′ > G″) and samples behave intermediate phase of highly concentrated polymer solution and a real gel when tanδ > 0.1, where the sample is not a true gel [169]. The tanδ value of all the filmogenic solutions of the present study is greater than 1 which predicted the concentrated and viscous nature of the polymeric solution. Incorporation of CAEE into the polymeric matrix decreased the tanδ value for 4% and 12% CAEE (4.14 & 3.61) with increasing the filler loading as compared to control (4.49) that was expected as addition these specified concentrations of CAEE improved elasticity of the CS-based filmogenic solution. However, the addition of 20% and 28% CAEE significantly increased tanδ value as the G'_{LVR} value was less, among this higher concentration (28%) was significant. The discussed parameters from sweep strain measurement also supported by the G″- G′ values at a specified shear strain of 1% showed incorporation of CAEE increased the viscous property of the bio-composite filmogenic solutions. The strain sweep measurement showed the influence of added filler, CAEE on the rheological properties of chitosan-based bio-composite solutions. The observed significant effect might be correlated to the major interaction between the phenolics groups of CAEE and cationic groups (NH_3^+) of chitosan via hydrogen, covalent and hydrophobic bonding. The effect was more with increasing the bio-filler content up to 20%. Sometimes, no great effects on rheological behavior were found after the addition of extracts like grape seed, and jabuticaba peel extract in the polymeric matrix due to the use of a small range of extracts [170]. However, other studies showed the influence of incorporated extract on the rheological properties of the chitosan matrix like the result obtained from the present study.

- **Frequency Sweep of Measurements of Developed Chitosan-based Bio-composites Filmogenic Solutions**

While the strain sweep measurements give information about the structural stability of the solutions against an applied deformation, the frequency sweep tests classify the samples as gel, concentrated, or dilute solutions, depending on the storage and loss modulus behavior over the frequency range. If G′> G″ is all over in the frequency range, the samples are classified as gels. For samples with G″> G′ and at a higher frequency, the storage and loss moduli got closer to each other; it is classified as diluted solutions; if G″> G′ and the moduli intersect inside the frequency range, the solution is concentrated. From the frequency sweep curve (**Figure 3.8c**), it is observed that all the samples can be considered as diluted polymer solutions as already described in the strain sweep tests by the tanδ values (tanδ > 1) in **Table 3.5**. The crossover frequency parameters, obtained from frequency sweep curves are listed in **Table 3.5**. Between nCS and CS/CAEE 4%, a shift in crossover frequency ($\omega_{crossover}$) was observed from 1 to 63.1 rad/s and an increased value of $G'_{crossover}$ from 0.207 to 7.367 was also observed. No crossover point was noticed for CS/CAEE 20% and CS/CAEE 28% samples.

Table 3.5: Frequency sweep parameters measured at room temperature for angular frequency ($\omega_{crossover}$) and storage modulus ($G'_{crossover}$) at the crossover point.

Sample	$\omega_{crossover}$ (rad/s)	$G'_{crossover}$ (Pa)
nCS	1	0.207
CS/CAEE 4%	63.1	7.367
CS/CAEE 12%	0.6	0.205
CS/CAEE 20%	-	-
CS/CAEE 28%	-	-

- **Steady Shear Flow Properties of Developed Chitosan-based Bio-composites Filmogenic Solutions**

The flow curve of formulated nCS and CAEE incorporated developed bio-composites filmogenic solution has been depicted in **Figure 3.8d**, where it shows the viscosity of each filmogenic solution against the shear rate at room temperature. A non-Newtonian pseudoplastic (shear thinning) behavior was obtained in control (nCS) as well as in the CAEE-incorporated bio-composites, as a result viscosity values decreased with increasing the shear rate. This type of behavior is quite possible to occur in the case of polymeric solutions. The occurrence of pseudoplastic behavior was due to the alignment or orientation of polymeric molecules towards the direction of flow where apparent viscosity decreases under increasing the shear rate which leads to the formation of higher-order alignment of the polymeric chain towards applied stress. Further, the incorporation of CAEE reduced the viscosity in bio-composites as compared to nCS from 717.66 to 242.98 mPa s (**Figure 3.8d**). The obtained results indicated the addition of CAEE weakens the intramolecular polymeric bonds of chitosan and acetic acid. The overall viscosity was decreased with increasing the CAEE concentration, however the improvement in viscosity was noticed in the case of 12% and 20% as compared to 4% CAEE, however, this increment was overcome by the significant reduction of viscosity with the highest CAEE (28%) concentration as compared to control. As mentioned earlier, CAEE contains various phenolic compounds such as carotenoids, pheophytin, chlorophyll, β-carotene, and astaxanthin which loosen the bond interaction among polymeric chains as polyphenols are rich in hydroxyl group (–OH) which could create space between polymeric chains thereby increasing mobility of the chains by providing free space [171]. In this context, similar observations of a reduction in viscosity with the addition of polyphenols such as pomegranate seed extract [117], grape seed extract [170], mutra leaf extract [60], apple skin [172], and green tea extract [173] into

CS-based film-forming solution was reported in the literature. Besides, the flow behavior index (n) obtained by plotting viscosity as a function of shear rate and using the power-law model represents pseudoplastic behavior when the 'n' is from 0 to 1 and values beyond 1 following a Newtonian behavior [117]. The 'n' values in this study ranged from 0.32-0.40 as shown in **Table 3.4**, indicating the pseudoplastic behavior of all the filmogenic solutions which is corroborated by observed steady flow behavior. Further, the increase in CAEE concentration in polymeric solution led to increasing 'n' values except at higher concentrations (28%) where a slight reduction was noticed however, the addition of CAEE did not alter the pseudoplastic behavior of filmogenic solutions.

3.2.6.11. Antioxidant Activity and Total Phenolic Content of the Developed Films

One of the common methods for the determination of antioxidant activity is DPPH free radicals scavenging activity where DPPH acted as a reducing agent or electron donor. The deep violet color of the DPPH radicle converted to transparent color in the presence of an antioxidant and the absorbance was recorded at 517 nm to calculate the percentage of DPPH antioxidant activity [81]. **Figure 3.9a** depicts the percentage of free radical scavenging activity and/or antioxidant activity of CAEE-incorporated bio-composite films. The control film exhibited moderated scavenging activity of ~21.01%. However, remarkable improvement in DPPH antioxidant activity was observed in developed edible CS/CAEE edible films. The DPPH radical-scavenging activity of the bio-composite films was increased gradually to 28.81%, 31.85%, 33.86%, 36.92%, 40.16%, 44.21%, and 48.23% with the increasing concentration of CAEE from 4 to 28%, respectively. The rise in antioxidant activity could be attributed to the presence of phenolic compounds and a small fraction of the $–CH_2–$ group in CAEE [174]. However, the bio-composites provided preferable antioxidant properties, which indicated the presence of CAEE phenolic hydroxyl groups in the film. The presence of polyphenols in CAEE was previously confirmed by

MALDI TOF and NMR analysis and available adequate DPPH free radical scavenging activity of CAEE (~40%) supported the results of antioxidant activity of edible films. Therefore, this analysis exhibited addition of CAEE enhanced the antioxidant property of CS-polymer, significantly. Similar findings of improvement in antioxidant activity after the incorporation of fruit extract and seed oil in CS-based edible film were reported in the literature [174,175].

The total phenolic content (TPC) of CS/CAEE bio-composite films was determined by the Folin-Ciocalteu phenol reagent method. The TPC of the films has been shown in **Figure 3.9b**. The control film exhibited a TPC of 97.96 µg gallic acid/g film. Moreover, the increasing TPC was observed in the bio-composite with increasing CAEE loading. The highest TPC obtained in bio-composites was 423.50 µg gallic acid/g film which was ~38 times greater than the control. Therefore, it can be postulated that the presence of phenolic compounds was responsible for desirable DPPH antioxidant activity in films, and which showed an increasing trend with enhancing the bio-filler (CAEE) concentration and corroborated with the result obtained in DPPH antioxidant activity [176].

3.2.6.12. Antimicrobial Activity of Formulated Active Edible Filmogenic Solution

Antibacterial activity against Gram-negative *E. coli* and Gram-positive *S. aureus* was individually tested for each formulation of CS-based CAEE incorporated filmogenic or edible coating solution as the solution was applied directly on the real food system (green chili) for coating. The antimicrobial activity was evaluated using the disc diffusion zone method. The appearance of inhibition zones around the sample confirmed the antimicrobial activity. The accompanying pictures of the tested samples are shown in **Figure 3.9c**. All the filmogenic solutions along with nCS showed clearly visible inhibition zone against both the food-borne pathogen. However, a slight increment in inhibition zone diameter was

observed in bio-composites in comparison to the control neat chitosan solution. The initial concentration of *E. Coli* was 2×10^9 cfu/mL and *S. aureus* was 4.5×10^9 cfu/mL.

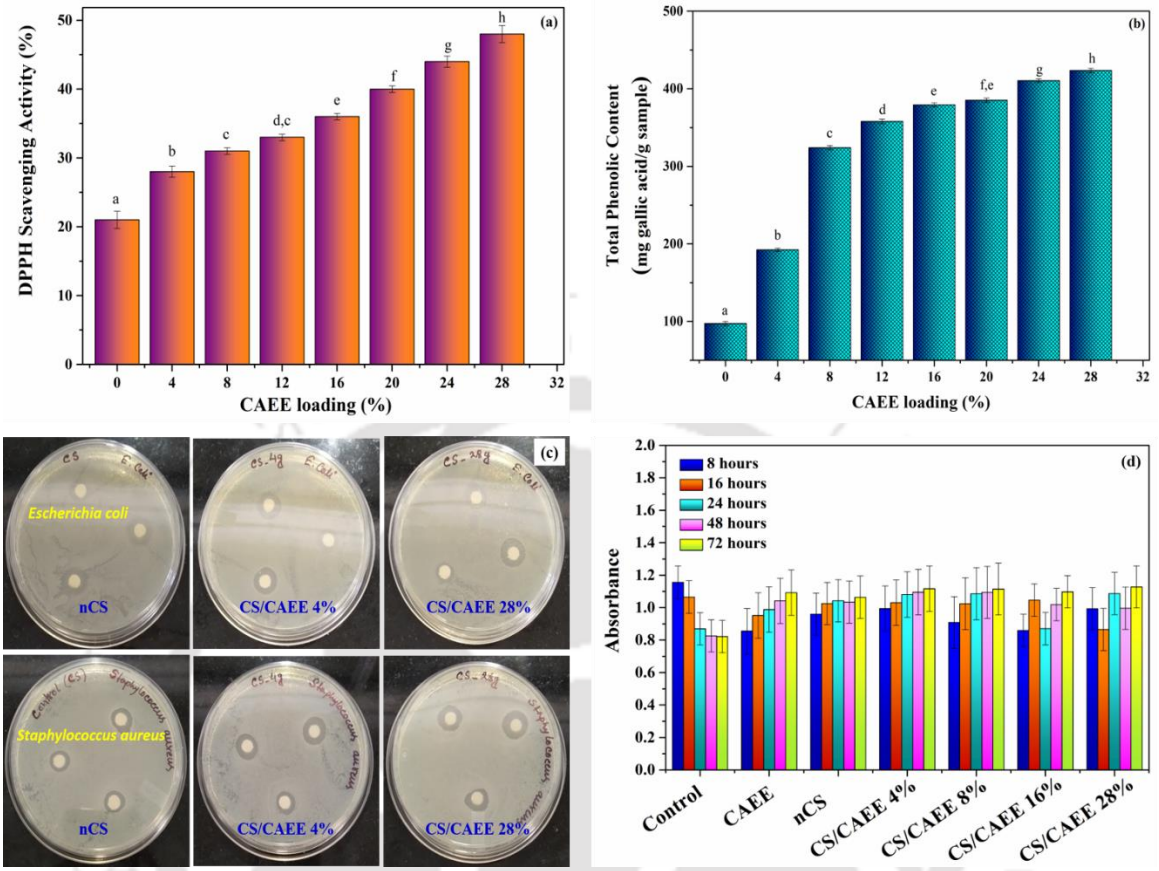

Figure 3.9: (a) Antioxidant activity, (b) total phenolic content, (c) antimicrobial activity, and (d) biocompatibility (MTT assay) of developed bio-composite films with control.

3.2.6.13. Biocompatibility of Formulated Active filmogenic Solutions

The cell viability of developed coating solutions by MTT assay has been depicted in **Figure 3.9d**. The obtained results describe the proliferation of BHK-21 cells over all the filmogenic bio-composite/coating solutions (nCS, CS/CAEE 4%, CS/CAEE 8%, CS/CAEE 16%, CS/CAEE 28%) as well as on CAEE till 72 h incubation whereas, a decreasing trend of cell viability was accounted in case of control without filmogenic solution. This assay suggests formulated bio-composites/coating solutions were biocompatible and no adverse effect was observed at the end of the study in both bio-filler (CAEE) and coating solution, respectively

which indicates the formulated coatings considered as non-toxic material and could be explored in the field of edible packaging. The representative images of BHK-21 cells adhered to filmogenic solution and CAEE after 72 h incubation under a bright-field microscope have been visualized in **Figure A3** with control and it signified the biocompatible nature of the formulated edible coating solutions and bio-filler.

3.3 Summary

The present study involves the successful utilization of algae biomass waste by extracting the algae extract which is rich in antioxidants and fabrication of chitosan-based edible active bio-composites incorporated with CAEE as bio-filler as primary packaging material. The antioxidant-rich CAEE was obtained by ultrasound-assisted sustainable extraction from waste de-oiled green algae biomass (*Dunaliella tertiolecta*) using response surface methodology. The extract, CAEE was rich in antioxidants and various bioactive compounds predominantly carotenoids, proteins, and polysaccharides. The developed CAEE incorporated edible films displayed superior antioxidant activity, total phenolic content, water vapor barrier property (max. ~ 60% reduction), thermal stability, crystallinity (~64%) and tensile strength (~54.1 MPa). An excellent UV-Vis light-blocking property was observed in the developed edible active film due to the strong interaction of polyphenols with the polymer matrix. The rheological property of the filmogenic solution exhibited stable shear thinning (viscous liquid) behavior. The cell line study suggested developed coating material was bio-compatible and non-toxic. Therefore, the developed film and the filmogenic formulation can apply to the real food system as a primary packaging material.

CHAPTER 4

SHELF-LIFE STUDY OF TOMATO, ONION, AND POTATO USING CHITOSAN AND ALGAE EXTRACT INCORPORATED (CS/CAEE) EDIBLE PACKAGING

De-oiled crude green algae ethanolic extract (CAEE) incorporated chitosan (CS)-based edible coating material was formulated and applied on red tomatoes, green chilies, potatoes, and onions, aiming to minimize postharvest loss and prolong the shelf-life with improved quality attributes. The coating materials were developed by mixing aqueous CS (1 wt.%) solution in a mild acetic acid medium (0.3 % v/v) with CAEE at varying concentrations (0%, 2%, and 4% w/v). Millipore water was used as a control coating material for drawing the comparison. The coating was applied on fresh produce by following the simple dip coating technique. The coated and control tomatoes, green chilies, potatoes, and onions were stored for 30, 10, and 60 days, respectively, under ambient conditions (27-30 °C, 60-70% RH). The results indicated that the tomatoes coated with CS/CAEE 4% coating formulation exhibited superior effectiveness for extending the shelf-life with improved physicochemical properties such as DPPH antioxidant activity, reducing sugar, lycopene, ascorbic acid content, and firmness by restricting faster respiration and ripening rate during ambient storage. Further, the shelf-life of chilies, potatoes, and onions was extended without altering the quality as compared to uncoated fresh produce. Therefore, the formulated coating could be applicable for prolonging the shelf-life of fresh produce.

Outcome: Mondal K, Goud V. V, & Katiyar V. (2022). *Effect of Waste Green Algal Biomass Extract Incorporated Chitosan-Based Edible Coating on the Shelf Life and Quality Attributes of Tomato*. ACS Food Science & Technology, IF:1.718, 2(7), 1151-1165.

Graphical Abstract

The below graphical abstract represents the steps for the preparation of edible coating solution and a step-by-step procedure for edible coating of fresh produce using the dipping technique and shelf-life study of the coated sample through various physicochemical and other properties.

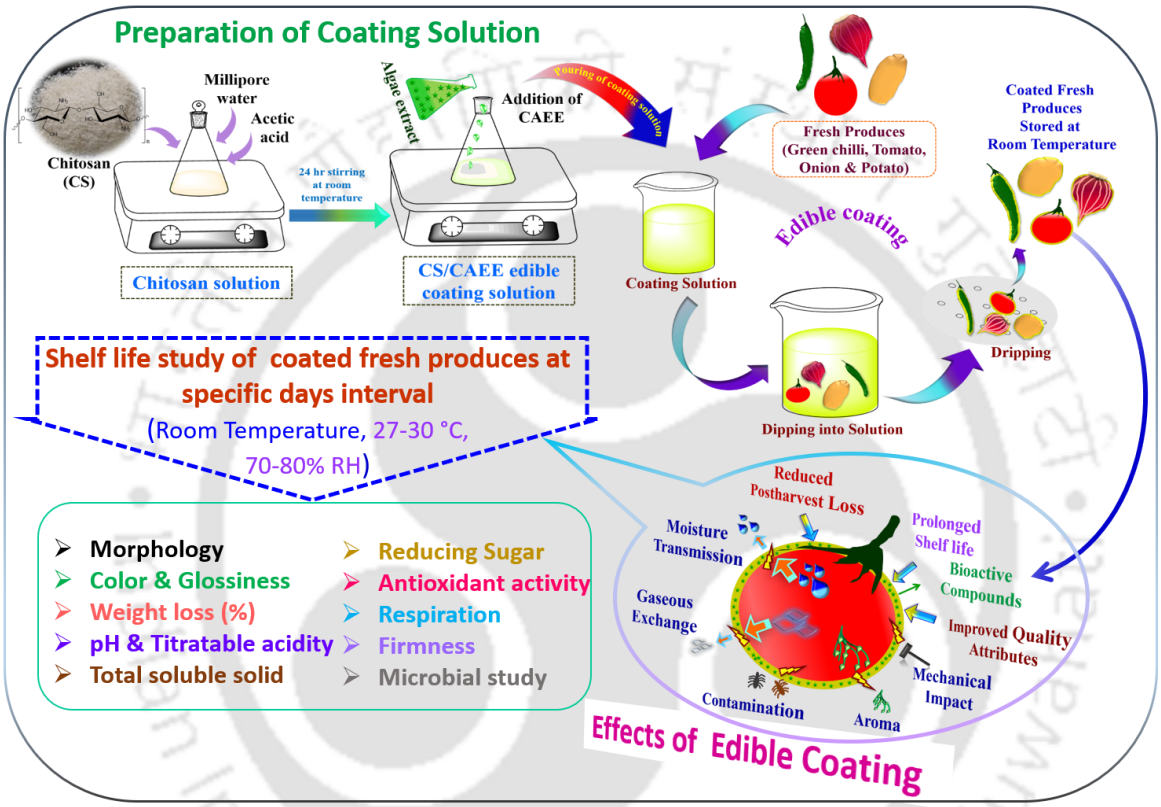

4.1 Introduction

The demand for green consumerism with quality, safety, and extended shelf-life of fresh produce has drawn attention to investigating and developing advanced technology. The prime concern associated with fruits and vegetables is postharvest losses, responsible for lowering the economic values due to improper storage and transportation [177]. In this context, biopolymer-based edible coatings can provide a feasible alternative to the expensive storage system for prolonging the shelf-life of perishables thereby reducing postharvest losses [178-181]. Generally, environmentally benign natural polymers are applied as an edible coating on fresh produces that creates a thin layer outside the fruit surface [182]. This layer also provides a modified atmosphere surrounding the fruits, which helps control the gaseous and moisture transmission rate of fruits and vegetables resulting in prolonging the shelf-life [182,183]. In this context, chitosan is one of the foremost edible polymers which can be used in edible coating owing to its inherent nature of non-toxicity, biocompatibility, bio-degradability, antimicrobial activity, and film-forming ability [5,182-185] as mentioned in the chapter 3.

Among various fresh produce, tomato (*Solanum lycopersicum L.*) fruit is a highly consumable one that slows down the risk of cancer and cardiac diseases [186, 187]. It is a rich source of various bioactive compounds such as lycopene [188]. However, being a climacteric fruit, it is highly perishable and has shorter shelf-life due to faster ripening, higher respiration, and transmission of gaseous and water vapor rates [189]. The higher respiration rate accumulates lycopene faster at the deep red stage, as a result brings maturity quicker and shortens the shelf-life [190]. Therefore, different storage techniques such as low temperature (6-20 °C), controlled (2.5% O_2, 5.0% CO_2), and modified atmosphere (10% O_2 & 10% CO_2) packaging are used for extending the storage life of tomato [184,186]. However, chilling injury, skin contraction, and the expensive nature of these

technologies limit their use [185]. In this regard, literature on chitosan-coated tomatoes stored under lower temperature has reported the effectiveness of coating, by which the various physicochemical properties including respiration, ripening, weight loss, titratable acidity, total soluble solid content, and others has been controlled, which has extended the shelf-life and quality attributes of tomato [82]. In addition, the inherent antimicrobial activity of chitosan reduces the microbial load on fresh produces. Therefore, chitosan as an edible coating biopolymer is highly recommended use for enhancing the shelf-life of fruits and vegetables [22].

In this chapter, the waste *Dunaliella tertiolecta* biomass extract (CAEE) incorporated chitosan-based edible coating formulation was applied on fresh produce (tomato, chili, potato, and onion) to determine the effectiveness of the formulated coating on shelf-life extension at ambient condition storage. Here, based on the results obtained from chapter 3, the edible coating formulations were prepared by dissolving chitosan (CS) (1wt.%) into a dilute acetic acid solution (0.3%) under vigorous stirring at room temperature (24 h) with the varying concentration of CAEE (0 to 4%). Further, the purpose of direct incorporation of CAEE into edible coating solution is to retard the oxidation (oxidative and hydrolytic) phenomenon, deliver bioactive compounds for quality value-addition, and improve the shelf-life of coated fresh produce, since the CAEE is a rich source of antioxidants (~40% DPPH free radical scavenging activity), predominantly, β-carotene, and others as obtained from the result of chapter 3 [187]. The previously mentioned fresh produce (tomato, chili, potato, and onion) were coated by using a simple dip-coating technique and stored for 30, 10, and 60 days at ambient conditions (27-30 °C, 60-70% RH). Further, the prime focus of this study is to extend the shelf-life of fresh produce by keeping them at room temperature instead of storing them under preferable cold storage conditions. The foremost reason behind this objective is to bring a simple, cost-effective technology to the agronomists

when addressing the problem of the unavailability and affordability of cold storage houses. Several physicochemical and biochemical assays were performed to characterize the changes that occurred in stored fruits. The physicochemical changes of tomatoes during storage with and without coating have been studied in detail in this chapter.

4.2 Results and Discussion

4.2.1 Effect of Coating Efficiency on Physicochemical Parameters of Tomatoes During Storage

4.2.1.1 Surface Morphology

The visual observation of control and coated fruits throughout the storage days has been depicted in **Figure 4.1a-d**. The observations were recorded at 0, 15, and 30th days during storage. The decay was visible in control fruits before 15 days of storage, whereas all coated fruits were fresh. The occurrence of black rot in nCS-coated fruits was noticed after 20 days of storage. However, no such decay was observed in CS/CAEE-coated fruits. Though, surface shrinkage was noticed after the 26th day of storage (data not shown) in CS/CAEE 2% bio-composite coated samples. Neither decay nor shrinkage occurred in CS/CAEE 4% coated fruits which could be attributed to the antimicrobial property of CAEE. The presence of bioactive compounds such as β-carotene in CAEE could be one of the reasons for contributing antimicrobial properties, and since the concentration of CAEE was higher in CS/CAEE 4% coated samples as compared to 2% CAEE, the occurrence of decay rate was minimum. This result suggested that CS/CAEE 4% bio-composite formulation might provide optimum physicochemical properties to the coated fruits by creating a modified environment outside the fruits that controlled the gas and moisture transmission. The visual observation was validated by correlating the images obtained from FESEM (**Figure 4.1e-h**) analysis. The cuticle layer of natural wax was visible in the zero-day control sample, which showed an uneven surface layer, as seen in the **Figure 4.1e**.

However, the zero-day coated sample showed a smooth surface that covered the cuticles of the tomato evenly. The surface of control tomatoes, after 30th days of storage, was found to be rough, and a diminishing wax layer was also noticed. The smooth surface was observed even after the end of the storage period in coated fruits however a shredded surface was found in nCS-coated fruits, which might be occurred because of decay.

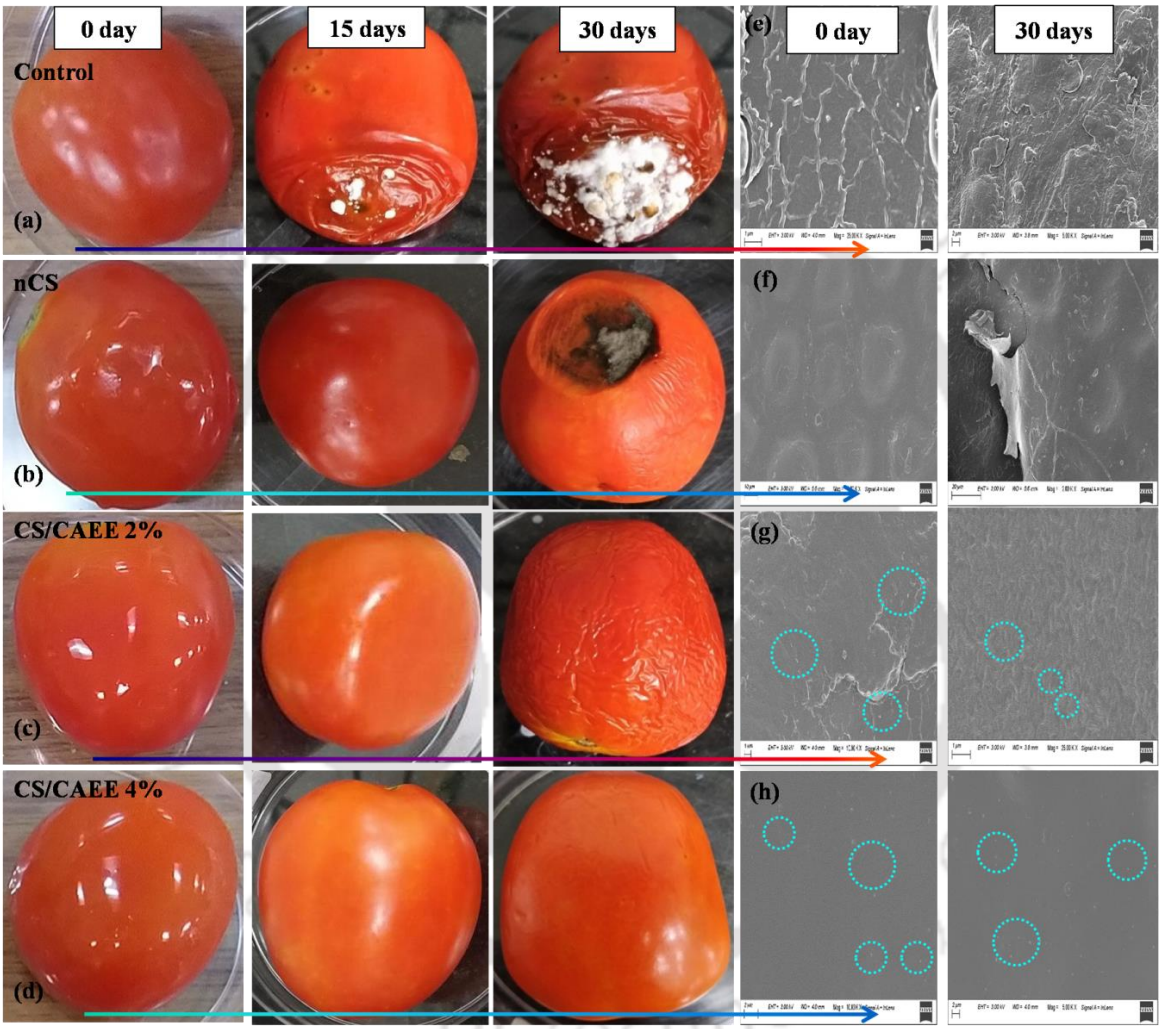

Figure 4.1: Visual observation of (a) control, (b) nCS (c) CS/CAEE 2%, (d) CS/CAEE 4%, and FESEM images of the same fruits (e to h) at specific storage days, respectively. The dotted circle refers to small particles of CAEE.

The samples coated with CS/CAEE exhibited a smooth surface as compared to the control, although small particles were observed over the surface due to the addition of CAEE on both 2% and 4% coated fruits (**Figure 4.1g,h**). At the end of the storage period, a shrinkage

surface was noticed by visual observation in samples coated with CS/CAEE 2%, which was in line with the FESEM analysis where an uneven surface was observed. However, visually, a smoother surface was noticed after 30 days of storage in CS/CAEE 4% coated fruits as compared to others, which could be due to the lesser moisture evaporation from the fruit surface to surroundings via blocking the pores on the fruit's skin. The overall observation indicated that CS/CAEE 4% edible coating formulation could be able to provide a better surface to stored tomatoes by controlling the gas and water vapor transmission rate. Besides, no such visual cracks or lumps were noticed in CAEE 4% coated fruits during storage, which indicated this coating could able to maintain the CO_2 and O_2 transmission rate. In addition, the observed smooth surface in CS/CAEE 4% coated fruits after the end of storage days could be related to the presence of antioxidant and antimicrobial properties of CAEE, which might have protected the plant cells of tomato by retarding oxidation and decay in fruits.

4.2.1.2 Color Parameters and Gloss Value

Changes in color parameters such as L^*, a^*, and b^* of fruits during storage are important attributes as visual quality affects consumer perception. The color measurements are expressed in terms of luminosity (lightness) L^* ($L^* = 0$ for black, and $L^* = 100$ for white), and the chromaticity parameters a^* (green/red) and b^* (blue/yellow); and as a*/b* ratio [191]. Since a^* measures redness, therefore this parameter is responsible for estimating the degree of ripeness, whereas b^* measures yellowness. Thus, a^*/b^* is one of the effective indexes for measuring the color changes in tomatoes during longer storage, which has been depicted in **Figure 4.2a.** Significant changes ($p<0.05$) were observed between coated and control fruits during 30 days of ambient storage. Here, the increasing behavior of color index a^*/b^* indicated fruits was getting ripened during storage [191] wherein, the rate of ripening in control fruits was higher as a^*/b^* values increased significantly from 0.90 to

1.18 ($p<0.05$). The *a*/b** value (~0.90) of coated and control tomatoes was similar on the initial day of storage, which indicated red color and similar maturity states of all the tomatoes.

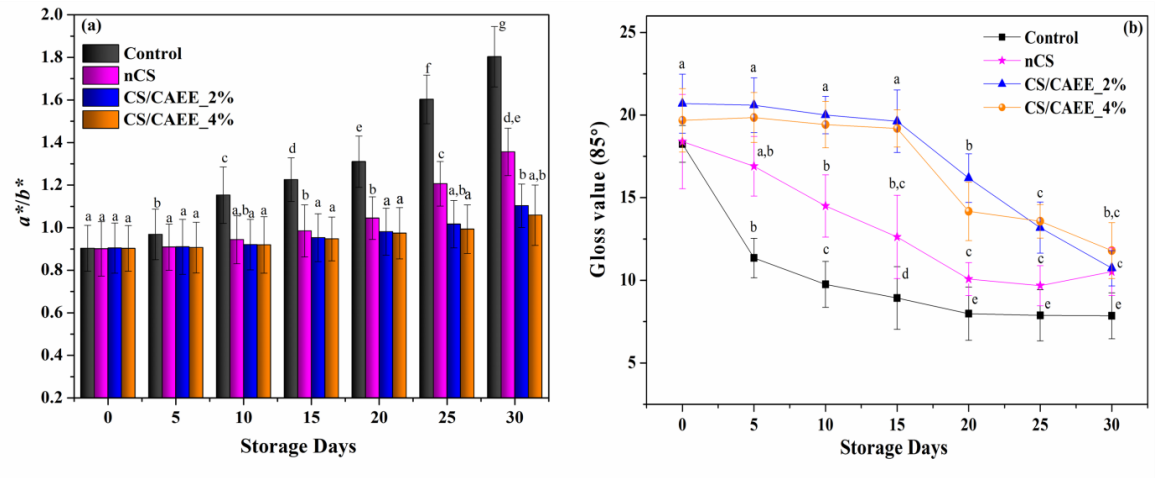

Figure 4.2: (a) The ratio of red and yellow color intensity (*a*/ b**) as a color index, and (b) glossiness at a higher angle (85°) of control and coated tomatoes during storage at 27-30 °C for 30 days. Each value is the average mean of three replicates, and vertical bars represent the standard deviation. The letters 'a-g' indicates significant differences ($p<0.05$).

Further, the *a*/b** value ~1.12 and ~1.20 indicated intense red firm to soft maturity levels, according to Arias et al., 2000 [192]. Moreover, no such changes were observed between nCS, and CS/CAEE coated fruits till the 10th day of storage ($p>0.05$), whereas the effective changes were noticed from the 15th day of storage ($p<0.05$). This observation indicated the occurrence of faster ripening in nCS-coated fruits than in CS/CAEE-coated samples. The insignificant ($p>0.05$) observation was noticed between 2%, and 4% CS/CAEE coated fruits till the 20th day, afterward, effective changes were observed ($p<0.05$). Furthermore, a declining trend of *L** and *b**, and an increasing trend of a* values, were observed during the storage of tomatoes. However, coated fruits showed a restricted reduction of *L**, which means keeping the brightness of fruit by stopping the conversion to the darker color,

whereas CS/CAEE 4% exhibited optimum retention, which could be due to CS-coating, which made the fruit's surface transparent for passing and reflecting the light. Further, the addition of CAEE could be able to control the ripening rate through its antioxidant activity. The progression of the color change was found significantly ($p<0.05$) slower in the developed edible bio-composite coated fruits as compared to nCS-coated and control samples. Therefore, the observed findings indicated coating restricted the color change of tomatoes from red to intense red, which might be ascribed to a reduction in the ripening process. The visual observation was in line with the colorimetric result.

Gloss is another physical parameter attributed to a shiny appearance. Generally, fruits and vegetables have either a glossy or dull appearance naturally. In the present study, the gloss values of the stored fruits have been shown in **Figure. 4.2b** & **Figure A4**. Here, the gloss parameters were measured at two different angles (20° and 85°) to determine the high and low gloss values. The gloss value at a lower and higher angle of control fruits reduced with the storage time, and a negative value was obtained, from 0.7 to -0.03 ($p<0.05$) and 18.3 to 7.9 ($p<0.05$) at lower (20°), and higher angles (85°), respectively, at the end of the storage. The coated samples showed a restricted reduction in gloss values ($p<0.05$) and provided an extra glossiness, due to which glossiness was maintained even after 20 days of storage. However, both control and coated fruits exhibited a declining nature of glossiness, wherein the gloss reduction rate was higher in control fruits. Further, CS/CAEE coated sample retained better glossiness ($p<0.05$) at a higher angle during the storage period, however slightly decreased at the end of storage. The retention of glossiness in CAEE-coated fruits could be ascribed to the presence of carotenoids [193]. Therefore, based on the obtained results, it could be postulated that CS-based coating maintained the glossiness of fruits while storing for a longer period by modifying the outer surface of the fruits, which could provide a better reflection of light.

4.2.1.3 Weight Loss

In general, coating restricts the evaporation of water from the fruit surface, thereby preventing surface shriveling of fruits during postharvest storage. However, the coating must provide a moderate water vapor transmission rate through the fruit surface to maintain the surface freshness [32]. In this study, the average weight loss (WL) was measured at 0, 5, 10, 15, 20, 25, & 30 days of storage, as depicted in **Figure 4.3a**.

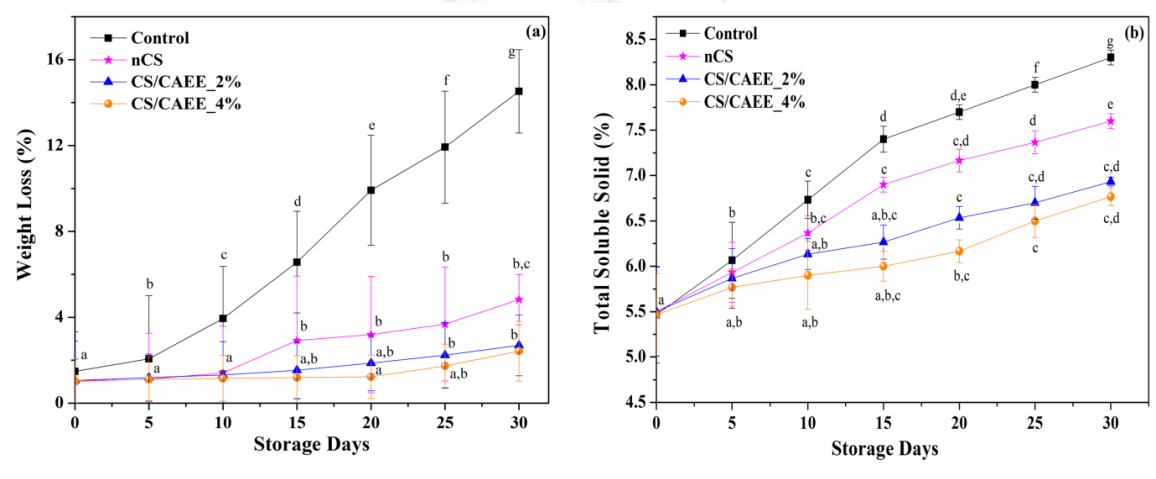

Figure 4.3: (a) Weight loss, and (b) total soluble solid content of control and coated tomatoes during storage at 27-30 °C for 30 days. Each value is the average mean of three replicates, and vertical bars represent the standard deviation. The letters 'a-g' indicates significant differences ($p<0.05$).

The WL in CS/CAEE-coated fruits was slower ($p<0.05$) as compared to nCS coated and control fruits. Among CAEE concentrations, 4% showed minimum weight loss. The maximum weight loss was found as 12.55% in control fruits ($p<0.05$) at the end of the storage days, whereas 4.76%, 2.69%, and 2.43% were recorded in nCS, CS/CAEE 2%, and CS/CAEE 4% coated samples, respectively. A significant ($p<0.05$) weight loss reduction was observed in control and coated fruits. Further, non-significant changes were observed between 2% and 4% CS/CAEE coated fruits ($p>0.05$). The observed minimum weight loss in coated tomatoes could be associated with the water vapor barrier property of the

developed coating material. Furthermore, according to the literature, the addition of bio-fillers such as grape seed extract, tea extract, and others to the CS-matrix provided effective water barrier properties [32]. In the present study, the addition of CAEE exhibited minimum weight loss therefore, it could be postulated that CAEE was a substance highly compatible with hydrophilic bio-polymer CS due to which, the developed coating layer could able to provide a superior water vapor barrier through strong intermolecular interaction between CAEE particles and CS-matrix.

4.2.1.4 Total Soluble Solid

The increasing trend of total soluble solid (TSS) content was noticed in control and coated fruits during the overall storage period. Further, the increment rate of TSS in the control tomatoes was effectively higher than in coated fruits ($p<0.05$) (**Figure 4.3b**). The difference in TSS content between control and coated tomatoes was significant ($p<0.05$), which increased to 3% in control fruits on the final day of storage. The TSS increased from 5.5 to 8.3% during 0 to 30 days of storage in control tomatoes, whereas CS/CAEE 4%, 2%, and nCS significantly retained the value from 5.5 to 6.8%, 6.9%, and 7.6%, respectively. Moreover, it could be anticipated based on the observation that CAEE-added coating was performed effectively to control the TSS content in tomatoes during storage. In general, during the storage of fruits, TSS content increases, which is a natural phenomenon, where starch, a storage polysaccharide converts to the simplest sugar. As a result, glucose is produced during ripening, which provides a sweet taste to fruits. Therefore, TSS content in fruits during postharvest storage needs to be under control for the prolongation of the fruit's shelf-life. The observed results could be attributed to the suppression of respiration and metabolic activity of fruits during storage [194]. The TSS of the CS/CAEE coated sample was significantly controlled ($p<0.05$), which could be related to the strong intermolecular bonding to CAEE with the CS-matrix, and the antioxidant property of CAEE. Further, the

increasing content of TSS in tomatoes could be related to the hydrolysis of complex carbohydrates to simple sugars. The enhancement of TSS content in tomatoes occurred during maturity and reached the highest at the deep-red stage [194], which is similar to the observed findings in this study.

4.2.1.5 Measurement of pH

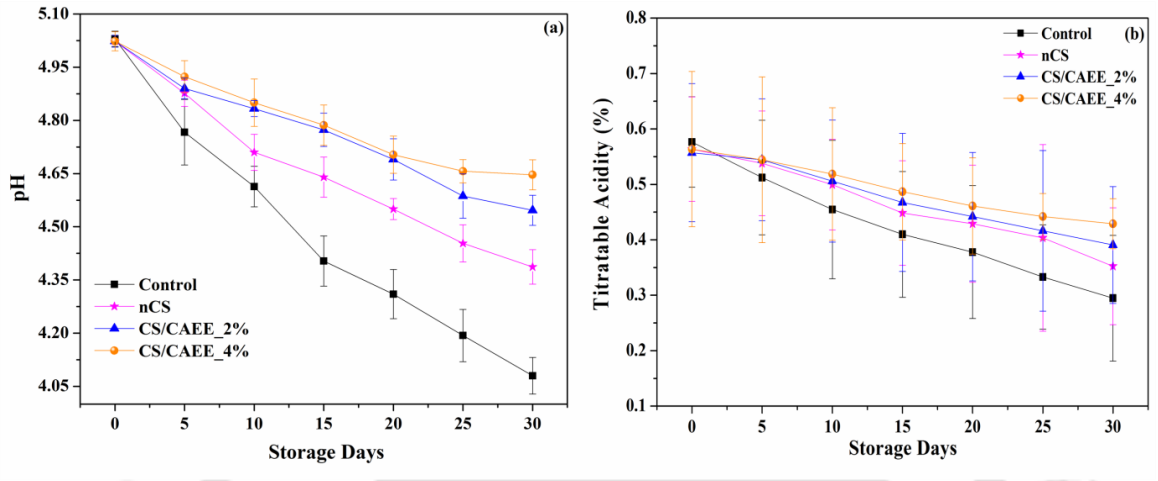

Figure 4.4: (a) pH value, and (b) titratable acidity of control and coated tomatoes during storage at 27-30 °C for 30 days. Each value is the average mean of three replicates, and vertical bars represent the standard deviation.

Fruit pH is another quality attribute to determine the freshness during storage. The pH value was measured at the interval of 5 days of storage. The obtained values were in the range of 5.02 to 4.07 ($p<0.05$). A declining trend (**Figure 4.4a**) was noticed in all types of samples, which was similar to the reported literature by Mustapha *et al.*, 2019 [195]. However, most of the reported literature has depicted the ripening of the fruit as one of the possible reasons for increasing the pH value during the storage of tomatoes. The control sample exhibited the highest decrement to 4.07 ($p<0.05$), whereas CS/CAEE 4% coated sample showed the least decrement to 4.65. However, the nCS-coated fruits also showed less reduction than the control. The probable reason for the reduction in pH value in this study could be the degradation of sugars by microbes, indicating microbial contamination occurred in the

control sample at a higher rate [79]. In this context, the process by which sugar is degraded by microorganisms known as microbial fermentation and during this process, microorganisms such as bacteria and yeast utilize the sugars present in the tomatoes as a source of energy. As a by-product of their metabolic activity, these microorganisms produce organic acids such as lactic acid and acetic acid which reduces pH. The CS-coated fruits reduced microbial load ($p<0.05$) due to the natural antimicrobial property of CS. Further, the addition of CAEE exhibited improved results due to the presence of antioxidants and antimicrobial agents.

4.2.1.6 Titratable Acidity

A declining trend was observed for titratable acidity (TA) in control and coated tomatoes during prolonged storage (**Figure 4.4b**). A higher decrement in TA value was observed in control fruits (0.57 to 0.29%) ($p<0.05$) as compared to coated fruits. However, the minimum reduction ($p<0.05$) in TA (0.56 to 0.43%) was observed in CS/CAEE 4% coated fruits during storage. The nCS-coated fruit also exhibited a lesser reduction of TA as compared to control samples. The reduction of TA during the storage of climacteric fruits could be attributed to the natural ripening process, where faster metabolic changes occurred in organic acid. Besides, the rate of reduction in TA also depends on metabolic activity. Furthermore, a controlled respiration rate occurs during the storage of fruits, when organic acids are less consumed as respiratory substrate, which could be responsible for providing a higher TA and lower pH value, and vice versa [32]. In some cases, the reduction of organic acid reduces the pH value, which could be ascribed to higher metabolic activity, maturation stage, harvesting type, and microbial decay [195]. In this context, a lesser reduction ($p<0.05$) in TA value was observed in coated fruits, attributed to the slower metabolizing activity of organic acids due to barriers in oxygen transmission, which reduced the rate of accumulation of sugar and controlled fruit ripening [195]. Further, the

addition of a higher concentration of CAEE could able to slow down the reduction of TA by controlling the ripening rate and metabolic activity, owing to the presence of antioxidants and bioactive compounds in CAEE.

4.2.1.7 Determination of Reducing Sugar

Another predominant key parameter for determining the quality attributes of fresh produces during storage is reducing sugar. According to the literature, an increment in the reduced sugar content in stored fruits indicates the breakdown of polysaccharides into soluble sugar or monosaccharide that is responsible for faster respiration, which helps in the quick ripening of fruits [196]. Therefore, controlling the range of reducing sugar during storage time is essential. The reducing sugar content was measured at the interval of 5 days of the total storage period as described in **Figure 4.5a**. The reducing sugar content in the control sample exhibited a significant ($p<0.05$) increment from 2.5 to 5.7% at the end of the 30 days of storage, whereas a sharp increment was noticed at 5 days of storage. However, no such sharp enhancement was observed in a coated sample in 5 days of storage ($p>0.05$). Further, a slight increment was noticed in nCS-coated fruits to 10 days of storage from 2.5 to 2.7%, whereas an almost constant reducing sugar content was observed in CS/CAEE-coated fruits till 15 days of storage, followed by a slight increment. The maximum reducing sugar content was found up to 2.9% and 2.8% ($p>0.05$) in CS/CAEE 2% and 4% coated samples at the end of storage days, respectively, which was insignificant ($p>0.05$) for each other. The nCS-coated sample increased the maximum reducing sugar content up to 3.8% at the end of storage. The present findings predict that coated sample was superior in controlling the reducing sugar level in tomatoes, wherein CAEE incorporated sample was more effective than others. The obtained results could be attributed to slower metabolic activity with suppressed respiration and slower degradation of polysaccharides to soluble sugars, which helped in controlling the reduced sugar content throughout the storage. This

finding corroborated the obtained results of TSS content in stored tomatoes, where the increment of TSS content was higher and faster in control fruits than in coated ones due to faster metabolic activity. Besides, strong intermolecular bonding between CAEE and CS matrix could be a possible reason for controlling the minimum increment of reducing sugar in CAEE-coated fruits.

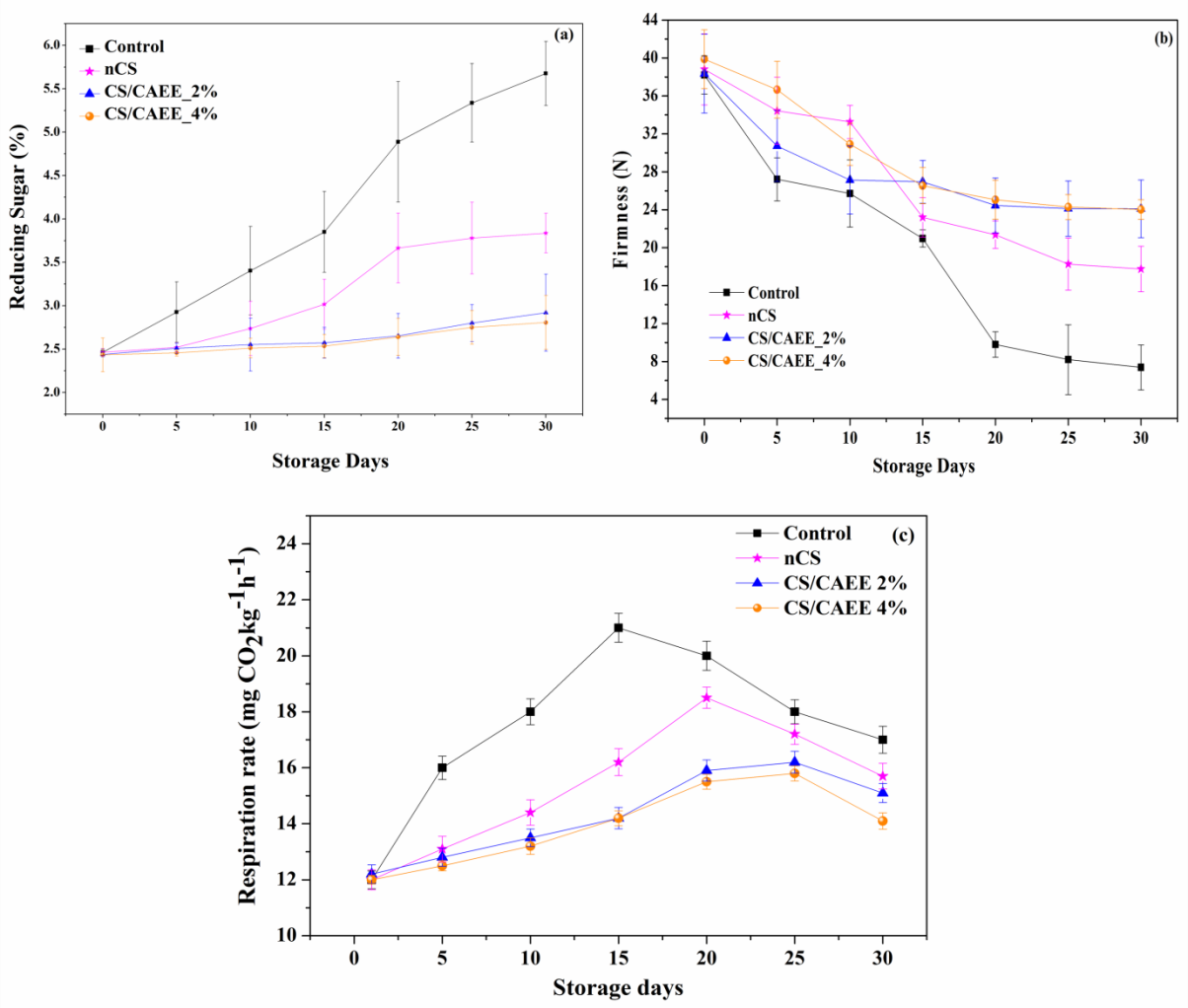

Figure 4.5: (a) Reducing sugar content, (b) firmness, and (c) respiration rate of control and coated tomatoes during storage at 27-30 °C for 30 days. Each value is the average mean of three replicates, and vertical bars represent the standard deviation.

4.2.1.8 Firmness

A declining trend of firmness was noticed in stored tomatoes during progressing storage time, where coated fruits exhibited remarkably slower reduction ($p<0.05$) as compared to control ones (**Figure 4.5b**). An intense firmness drop was noticed in control fruits, from 38 to 27 N ($p<0.05$), within 5 days of storage. Although no such reduction was observed in the coated fruits within 5 days, however, firmness dropped to below 27 N after 10 and 15 days of storage in nCS and CS/CAEE coated fruits, respectively. The control fruit firmness value was reached below 20 N within 15 days of storage which rendered the fruit soft and susceptible to mechanical and microbial damage. However, a similar type of reduction was observed in CS/CAEE-coated fruits after 25 days of storage. There was no significant firmness reduction noticed ($p>0.05$) between the CS/CAEE 2% and 4% coated fruits. In addition, the controlled reduction of fruit firmness in coated tomatoes could be attributed to the slowdown of the activity of cell wall degrading enzymes, namely, pectinesterase and polygalacturonase. These enzymes degrade the cell wall's polysaccharide pectin, which makes fruit soften [195]. In this context, modified atmosphere packaging by slowing down the ethylene production rate via controlling the passage of gasses could suppress this enzyme activity, as a result, retain fruit firmness for a longer time during postharvest storage [196]. In this regard, the edible coating could be one of the key aspects for extending the shelf-life of tomatoes by creating a modified atmosphere around the fruits, which could be able to protect fruits from softening and microbial infection and eventually would enhance the fruit's quality and marketability [197].

4.2.1.9 **Respiration Rate**

One of the key indexes for the determination of freshness and ripening conditions in fresh produce is by measuring the rate of respiration and ethylene production during storage. The higher respiration rate in fruits influences faster metabolic activity and the ripening process,

thereby decreasing the shelf-life of tomatoes. In this study, an increasing pattern of respiration rate in terms of CO_2 evolution was observed in all fruits, which was reduced afterward. This trend is like the reported literature on respiratory climacteric fruits pattern [198]. This similar type of observation has been reported by Ghaouth et al., 1992, where chitosan coating was applied to tomatoes [199]. A sharp increment of CO_2 evolution was observed at 15 days of storage in control fruits, followed by a reduction in respiration rate, which was significant as compared to coated fruits ($p<0.05$) (**Figure 4.5c**). On the other hand, coated fruits exhibited a slower rate of increment in CO_2 evolution, wherein CS/CAEE coated samples showed more significant ($p<0.05$) results than others. Further, an intense peak was observed in nCS-coated fruits after 20 days of storage, followed by a reduction in respiration rate, which was slower than the control ($p<0.05$). However, no such sharp peak was found in CS/CAEE-coated fruits. The present findings suggested that the incorporation of CAEE significantly delayed the respiration rate, wherein CS/CAEE 4% coated tomatoes exhibited effective results ($p<0.05$). Further, the slower rate of respiration in CS/CAEE coated fruits than in other fruits, indicated incorporation of CAEE into edible coating formulation improved the gas barrier property, which could be due to its antioxidants and antimicrobial properties. Besides, this property of CAEE could be able to protect fruits from oxidation and decay, which could help in suppressing the rate of fruits' respiration. However, a reverse trend has been reported in the literature, where the respiration rate of CS-coated fruits such as longan [199], and cherry tomato decreased gradually from the initial to final day during storage at a lower temperature, which was ascribed for the type, and maturity stage of fruits, where the fruits were entered to the senescence stage [32]. Moreover, the declination in respiration rate might be correlated with delayed senescence and reduction in susceptible decay [186]. A similar type of finding has been observed in reported literature, where they have reported uncoated fruits exhibited

an early rise of ethylene production, whereas 1.5% CS coated fruits delayed respiration during five weeks of storage [186]. The delayed respiration in various types of coated fruits such as mango, strawberries, papaya, and grapes has been reported by several researchers [186]. This study also attributed that edible coating could extend the shelf-life of tomatoes by creating a modified environment outside the fruit by which respiration rate and gaseous passage could be controlled [32,195].

4.2.2 Coating Effect on the Antioxidant Properties of Tomatoes During Storage

4.2.2.1 Antioxidant Activity

The maximum DPPH free radical scavenging activity was observed in CS/CAEE 4% coated fruits at the end of the storage period. However, 2% CAEE exhibited maximum (82%) antioxidant activity at 20 days of storage, followed by a sharp reduction to 65% at the end of the storage period, which was significant ($p<0.05$) against other coated fruits. Further, a slight reduction to 69% was noticed in CS/CAEE 4% coated fruits at the end of storage ($p<0.05$) after reaching a maximum antioxidant activity of 75% at 20 days of storage (**Figure 4.6a**). Nevertheless, a decreased antioxidant activity of up to 38% was observed in control fruits at the end of the storage after showing a maximum of 69% activity after 10 days, which was significantly lower ($p<0.05$) than coated fruits. This drastic drop occurred in antioxidant activity in control fruits might be occurred due to a higher rate of respiration which was in line with the observation of an increasing amount of reduced sugar during storage due to faster ripening. Moreover, a similar increment of antioxidant activity was noticed in nCS-coated fruits after 10 days of storage (73%), which was reduced to 61% at the end of the storage. This value was also significantly higher ($p<0.05$) than control fruits and lowers ($p<0.05$) than CAEE-coated fruits. In addition, CS biopolymer also contributed a moderate amount of antioxidant activity, due to which nCS-coated fruits were able to provide a better result as compared to the control. Moreover, the addition of CAEE

enhanced the scavenging activity, which might be due to the presence of β-carotene, carotenoids, polyphenols, and other bioactive compounds, which slowed down the respiration rate effectively in stored CS/CAEE-coated fruits than others. In this context, the antioxidant activity of CAEE 4% coated fruits was higher in comparison to 2% due to higher concentration. Besides, the coating layer partially seals the pores on the fruit's surface, which might be ascribed to a reduction in respiration rate. Generally, the antioxidant activity of tomato fruit is the inherent characteristic that remains in it due to the presence of bioactive compounds such as carotenoids, ascorbic acid, and polyphenols [186]. Although, other factors such as climacteric conditions, plant species, growing technique, harvesting time, and postharvest storage conditions influence the antioxidant activity. Therefore, the delayed increment of antioxidant activity in CS/CAEE-coated fruits during storage could be attributed to the suppression of the ripening process. Additionally, some other possible factors, such as the amount of beta-carotene, vitamin C, and E, also might influence the antioxidant activity [186].

4.2.2.2 Lycopene Content

The richness of the red color in tomatoes is owing to the presence of lycopene, which builds up into chromoplasts, and increases with fruit maturity and ripening, as a result, the dark red color is achieved [105]. The accumulation and synthesis of lycopene are faster due to the higher rate of respiration at the deep-red stage. Therefore, the accretion of a higher concentration of lycopene is an indication of faster respiration occurring in tomatoes. The present study exhibited that the lycopene concentration in stored tomatoes was increased significantly ($p<0.05$) from the initial to the final day of storage. However, a higher concentration of lycopene was accumulated in control fruits ($p<0.05$) than coated tomatoes (**Figure 4.6b**), which could be assigned for the faster ripening rate in stored fruits, which caused faster synthesis of lycopene [186]. The highest lycopene concentration was

observed in control fruits at 0.23 g/kg whereas nCS, CAEE 2%, and CAEE 4% coated fruits exhibited 0.18, 0.15, and 0.14 g/kg at the end of the storage, respectively. Further, no significant ($p>0.05$) changes were observed during the initial five days of storage in coated fruits. Moreover, a similar observation of lycopene content in stored tomatoes was noticed by the spectrophotometer (**Figure A5**).

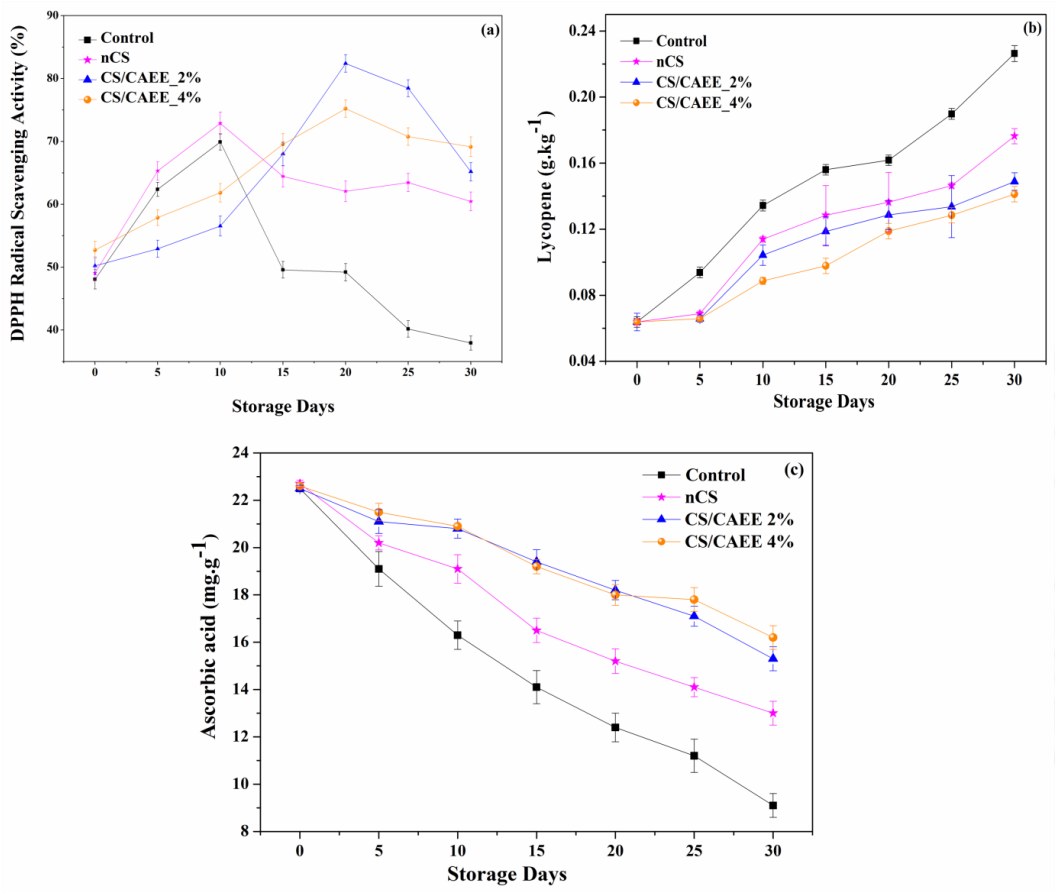

Figure 4.6: (a) DPPH free radical scavenging activity, (b) lycopene content, and (c) ascorbic acid content of control and coated tomatoes during storage at 27-30 °C for 30 days. Each value is the average mean of three replicates, and vertical bars represent the standard deviation.

In addition, during the ripening of tomato fruits, ethylene produces naturally, which helps to induce the enzyme, lycopene synthase, responsible for occurring lycopene synthesis in the cell tissue. Tomatoes coated with CS/CAEE 4% significantly lowered the rate of

lycopene accumulation than control and other treated fruits, suggesting the developed CS/CAEE bio-composite coating could be able to suppress the respiration rate, which eventually would reduce the ripening and ethylene production due to its antioxidant activity. This finding is corroborated by the DPPH free radical scavenging activity results, where antioxidant activity increased and then sharply decreased due to faster respiration.

4.2.2.3 Ascorbic Acid Content

The naturally present ascorbic acid (AA) is another bioactive compound responsible for providing antioxidant activity in tomatoes. A higher concentration of AA is present in green tomatoes, which decreases during the conversion of green to red color. The present study revealed a significant reduction ($p<0.05$) in AA content in control fruits from 22.4 to 9.06 mg/g at the end of storage (**Figure 4.6c**). However, the CAEE incorporation significantly ($p<0.05$) maintained AA acid level throughout the storage period in which CAEE 4% expressed maximum retention as compared to others. Further, insignificant ($p>0.05$) observation was noticed between 2% and 4% CAEE incorporation up to 20 days of storage. According to the literature, the natural reduction of AA content occurs in tomatoes during storage due to ripening, where AA is consumed as a respiratory substance and eventually converts to simple sugar [200]. Therefore, the obtained result indicated that tomatoes coated with a higher concentration of CAEE 4% were more promising in terms of lowering the degradation of AA content by controlling the rate of faster ripening, which could be due to its higher antioxidant activity. This observation is correlated with the previous findings of antioxidant activity and lycopene content, where control fruits exhibited less antioxidant activity, and higher lycopene content than coated fruits, which could be due to the occurrence of a faster rate of ripening. Also, the antimicrobial activity of CAEE and CS synergistically helped to control the decay, which had an impact on the respiration rate. In addition, dehydroascorbic (DHA) acid, an oxidized product of AA,

which is accumulated when AA degrades due to improper storage conditions and poor handlings, such as high-temperature storage, lower relative humidity, chilling injury, and mechanical damage of fruits [201]. AA is an extremely sensitive and easily oxidized substance. The accumulation of DHA in the stored fruits and vegetables indicates the degradation of AA. Based on this concept, this study indicated that lesser accumulation of DHA occurred in CAEE-coated fruits than in control fruit as a minimum reduction of AA was noticed in CAEE-coated fruits during storage, which could be the result of restricted respiration and oxidation rate that might be related to the antioxidant activity of added bio-filler (CAEE). Interestingly, DHA can transform to AA after consumption with the help of reducing agents. However, there is a possibility of irreversible oxidation, where it forms diketogulonic acid, which does not have the activity of vitamin C. Therefore, minimum degradation of AA content in fruits is desirable as fresh produce is the prime source of vitamin C for human nutrition.

4.2.3 Coating Effect on Microbial and Sensory Properties of Tomatoes During Storage

4.2.3.1 Microbiological Analysis

The microbiological analysis of control and coated samples have been incorporated in **Table 4.1.** The mesophiles, psychrophiles, yeast, and mold counts in all the samples were performed at zero-day and at the end of the storage days (30 days). From **Table 4.1**, it can be stated that the control sample exhibited a significantly ($p<0.05$) higher microbial load for mesophiles, psychrophiles, yeast, and mold counts than coated tomatoes. The occurrence of dense colonies in control fruits prohibited the appearance of a single colony. Therefore, visual colony counting was not possible. However, 1 log reduction of the microbial load was obtained in nCS-coated fruits, which were significantly lower ($p<0.05$) than control fruits but higher than CS/CAEE-coated fruits. In this context, the reduction in microbial load was due to inherent antimicrobial nature of CS-biopolymer. The presence

of the cationic amine group as a positive charge is responsible for providing antimicrobial properties to the CS biopolymer, which allows it to bind with the cell wall of the microorganism, and subsequently, disrupt and damage the cell metabolites [201]. A 2-4 log cycle microbial load reduction was noticed ($p<0.05$) in CAEE 4% coated fruits, which might be associated with the synergistic effect of the antimicrobial property of CAEE and CS biopolymer. The richness of antimicrobial properties in CAEE could be attributed to the presence of antioxidants, namely, β-carotene, and the higher loading of CAEE (4%) exhibited an optimum reduction in microbial load than lower loading (CAEE 2%). Therefore, this finding suggested that CAEE could be used as an active bio-filler and an antimicrobial agent for controlling the microbial load during the prolonged storage of fresh produces.

Table 4.1. Microbial analysis of coated and control fruits during storage days.

Sample	**Mesophile Counts (Log CFU/g)**		**Psychrophiles Counts (Log CFU/g)**		**Yeast and Mold counts (Log CFU/g)**	
	0 day	30 day	0 day	30 day	0 day	30 day
Control	6.11±1.2	***	6.98±0.3	7.94±0.3	7.03±0.4	***
nCS	5.68±0.8	6.89±0.7	5.74±0.3	6.46±0.5	6.81±0.1	7.19±0.3
CS/CAEE 2%	4.85±0.8	5.80±0.5	5±0.4	6.11±0.1	6.02±0.3	6.92±0.4
CS/CAEE 4%	4.39±0.9	5.21±0.4	3.30±0.2	4.58±0.5	3.76±0.4	4.45±0.3

'***' indicates uncountable, each value is the average mean of three replicates and '±' indicates the standard deviation

4.2.3.2 Sensory Evaluation

The sensory evaluation of the coated and control tomatoes has been depicted in **Figure 4.7** and **Table A3**. The control, nCS, and CS/CAEE coated fruits were examined for sensorial properties, specifically for taste, flavor, and overall acceptability throughout the storage at ambient conditions. An insignificant result ($p>0.05$) was obtained on the initial day of

storage in all types of coated tomatoes, as illustrated in **Figure 4.7** and **Table A3**. Further, no such significant ($p>0.05$) changes were observed in control and coated fruits till the fifth day of storage in terms of taste and flavor. However, a significant reduction in taste, flavor, and overall acceptability was noticed in the control ($p<0.05$) as compared to treated fruits at 15 days of storage (**Table A3**). This sharp fall down of organoleptic score in control fruits was because of microbial decay due to which taste, and flavor was not determined. Since, after 7 days of storage, surface dryness and microbial contamination were visualized on the control tomato (data not shown). This observation corroborated the morphological evaluation. Further, decay was noticed in nCS-coated fruits after 20 days of storage, resulting in a reduction of the sensory score ($p<0.05$) on the final day (30^{th} day) of storage than in CAEE-coated fruits (**Figure 4.7**).

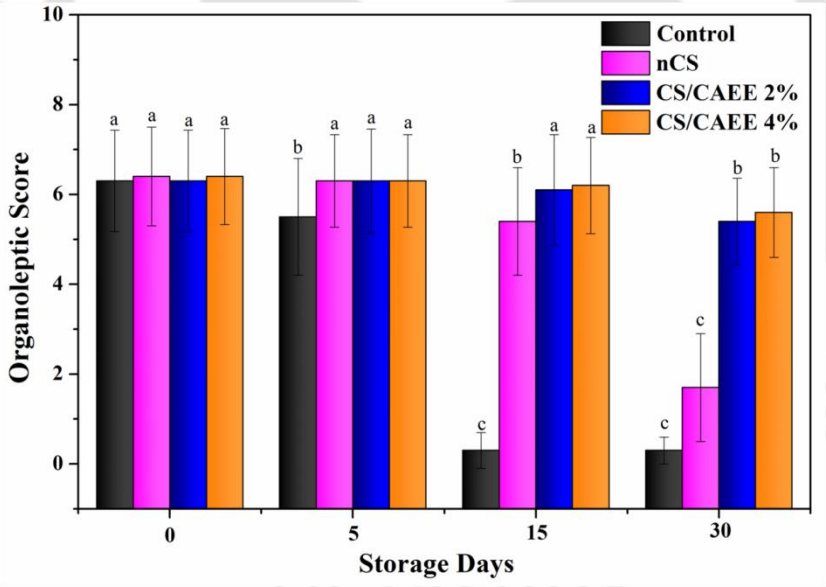

Figure 4.7: An organoleptic score of tomato stored under ambient conditions (27-30 °C, 60-70% RH). Error bars represent the standard deviation.

Further, changes were also observed between 2% and 4% CAEE-coated fruits ($p<0.05$) in terms of overall acceptability at the end of the final storage period, where surface shrinkage was observed in 2% CAEE-coated fruits in comparison to 4% CAEE coated tomatoes. Although, an insignificant difference was found in 2% and 4% CAEE-coated fruits in terms

of taste and flavor. Thus, the CS/CAEE 4% coating improved the acceptability of tomatoes by minimizing microbial contamination, rancid taste, and putrid smell and by controlling moisture loss, resulting in the absence of surface shrinkage, which could broaden acceptable appearance.

4.2.4 Coating Efficiency on Physiological Characteristics of Green Chili

Evaporation of moisture from the fresh produce is the reason for the occurrence of shrinkage on the surface of the produces. Biopolymer-based films and coatings such as starch, CS, and alginate exhibited significant improvement in retarding weight loss in fresh produce [195]. A minimal WL was obtained from coated green chilies which were able to maintain a fresh appearance after 10 days of storage at the ambient condition in comparison to the control (**Figure 4.8a)** The difference in weight loss in coated and control samples was significant. The highest loss of weight ~9% was observed in control samples as compared to the coated chilies, which was in the range of 5–6%. Importantly, the loss percentage was less in bio-composites as compared to nCS coating as well as control. Therefore, this result indicated incorporation of CAEE improved the water vapor barrier property on real food systems which is corroborated with the described VWP of the developed CS/CAEE active edible films. The reduction in weight loss in bio-composites might be due to the strong interaction between bio-filler and polymer matrix as discussed earlier. The minimum WL was found in 4% CAEE-added bio-composite film. However, increasing weight loss during storage could be attributed to trans-evaporation and respiration which is the natural process where coating effectively minimizes the rate of loss. Basically, during the respiration process, a carbon molecule is usually lost from the fruits and causes weight reduction [202]. Moreover, similar types of results were reported by Xing et al. 2011, in the case of bell peppers [203].

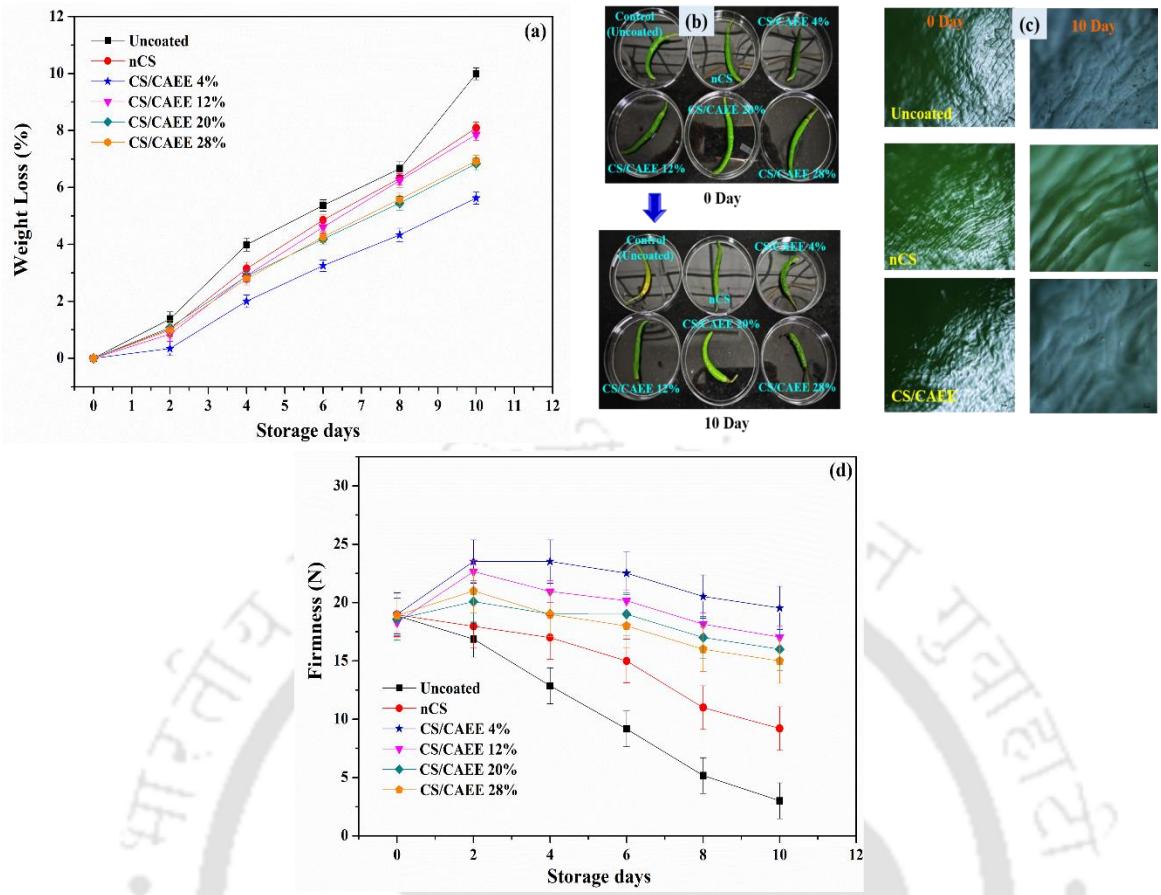

Figure 4.8: (a) Weight loss, (b) visual observation, (c) polarized optical microscopic observation, and (d) firmness of coated and control green chili during ambient storage.

In addition, during the ripening of chili fruits, the synthesis of carotenoid pigments occurs, (capsanthin and capsorubin exclusive to this genus) [199]. This process is accompanied by a sharp decrease in chlorophyll because of the degeneration of chloroplast into chromoplast. Respiration of the chilies causes fruit ripening. The coated chilies showed minute changes in color values (L*, a* & b*), indicating a delay in respiration and senescence thereby prolonging the shelf-life as shown in **Table A4**. Generally, the coating treatment suppressed the change of green discoloration by partially inhibiting the chlorophyll degradation during storage which could be confirmed from the observation of less a* values in the chilies (**Table A4**). The coated and control samples were shown an increasing trend of L* and b* values with progress in senescence during storage whereas, coated samples

exhibited a slower increment rate. However, the change in color during storage in chilies also depends upon the maturation, presence of carotenoid content, species, composition, and other factors [200]. The coating formulation incorporated with CAEE exhibited remarkable retention in the color parameter as compared to the control and nCS coated sample which suggested the addition of CAEE tailored the physicochemical properties of CS-matrix by building strong intermolecular hydrogen bonding between the hydroxyl group of active molecules of CAEE with polymer matrix. In this context, similar observations were reported on a variety of peppers [198, 202]. The visual appearance of coated green chilies along with uncoated ones has been depicted in **Figure 4.8b**.

It was crystal clear that the control sample exhibited surface dryness and wilting effect during storage at ambient conditions whereas, coated samples appeared fresh. However, a higher concentration of CAEE (28%) was less effective as compared to a lower concentration which might cause due to the agglomeration of CAEE particles inside the polymer matrix. Further, the microstructure of stored samples was captured under a polarized optical microscope (POM) where surface roughness was observed in control as compared to coated sample (**Figure 4.8c**). Although, some particles were visualized over CS/CAEE coated sample due to the addition of CAEE.

Reduced firmness in fresh produces signifies the inferior quality of fruits which causes due to respiration. In this context, the modified atmosphere at the exterior of the food surfaces exhibited retention in firmness when exposed to high levels of carbon monoxide [201]. The occurrence of softness in fruits is correlated to mechanical damage, microbial contamination, and moisture loss. In the present study, the measured firmness value dropped for uncoated and coated chili with increasing storage. However, a slow reduction was observed in bio-composites as to control and nCS-coated chilies while stored at ambient conditions (**Figure 4.8d**). The optimum result was observed for 4% CAEE loading.

In addition, when fresh produce undergoes aerobic respiration during storage, enable the production of superoxide radicals which helps to disturb the cell wall structure and allow pectinase enzyme to access cell wall polysaccharide such as pectin to degrade and causes softness in produces thereby reducing the post-harvest life [197]. Therefore, the combination techniques could adequately be used to preserve the firmness of green chilies during postharvest storage.

4.2.5 Coating Efficiency on Physiological Characteristics of Potato and Onion

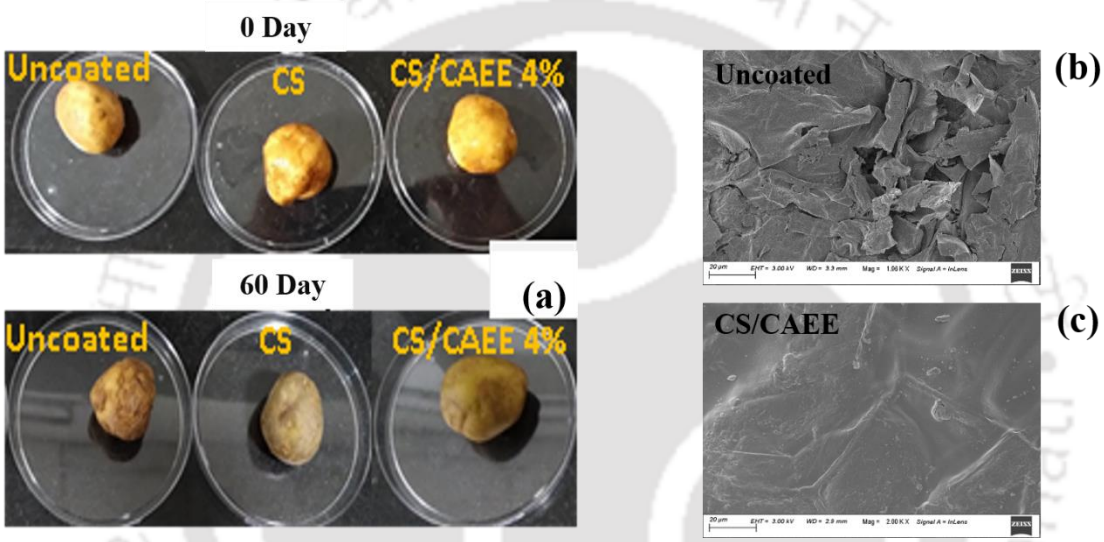

Figure 4.9: (a) Visual observation, and surface morphology under FESEM of (b) uncoated, and (c) CS/CAEE coated potato during storage at room temperature.

The effectiveness of the edible coating was observed in coated potatoes as compared to the control. A smooth and shiny surface was visualized in coated potatoes during storage at room temperature as depicted in **Figure 4.9a**. The microscopic image of the potato surface during storage also revealed the occurrence of smooth and homogeneous surfaces whereas, the uncoated sample exhibited rough and uneven surface morphology. This observation indicated coating of the biopolymer-based bio-composite solution developed a layer over the potato surface keeping the surface smooth and glossy.

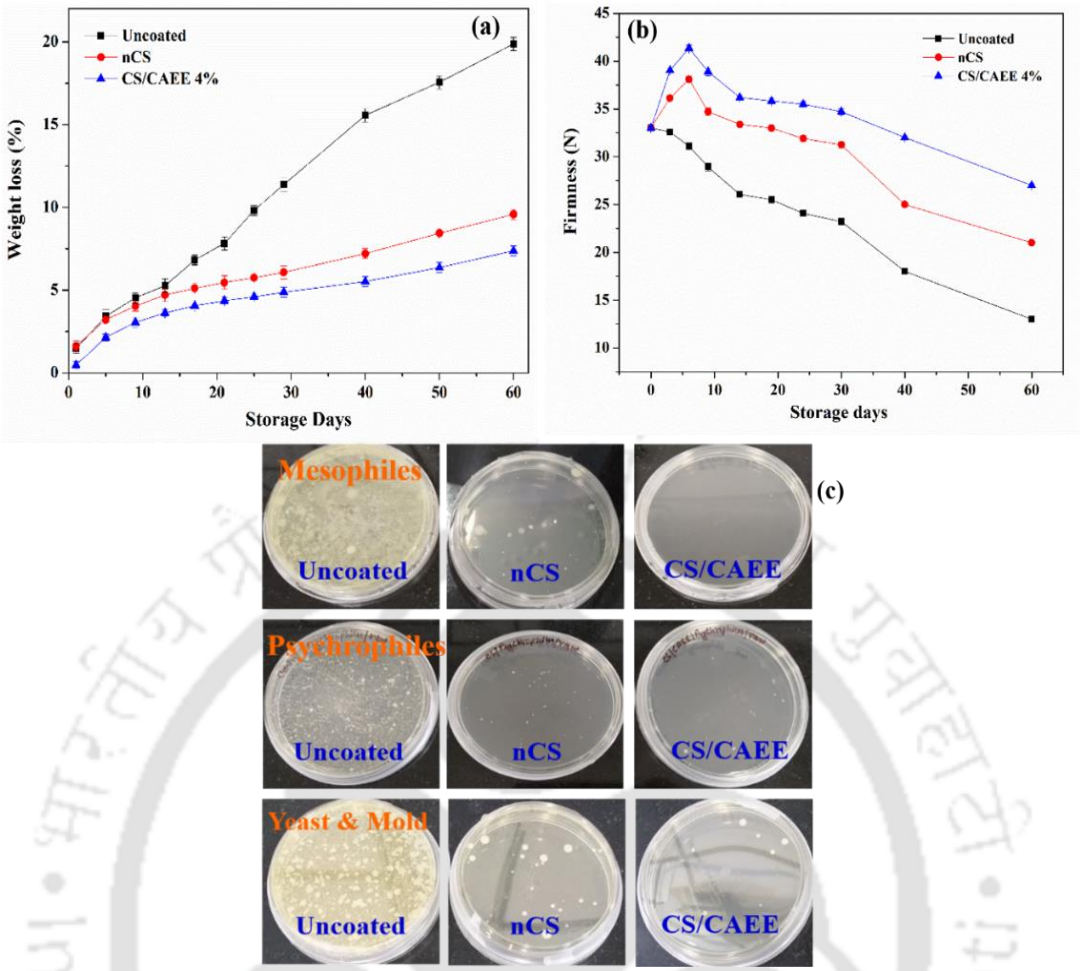

Figure 4.10: (a) Weight loss, (b) firmness, and (c) microbial analysis of uncoated and coated potato during storage at room temperature.

Besides, CAEE-incorporated coating material helped to control the moisture and firmness loss optimally in potatoes as compared to others *via* controlling the moisture and gaseous transmission (**Figure 4.10a,b**). The enhancement of the shelf-life of potatoes by edible coating was also achieved by keeping the fresh produce from microbial attack. **Figure 4.10c** depicts the mesophiles, psychrophiles, yeast, and mold counts when plated at the end of the storage days. The occurrence of less colony in the CS/CAEE coated sample as compared to others indicated the antimicrobial nature of CS and CAEE.

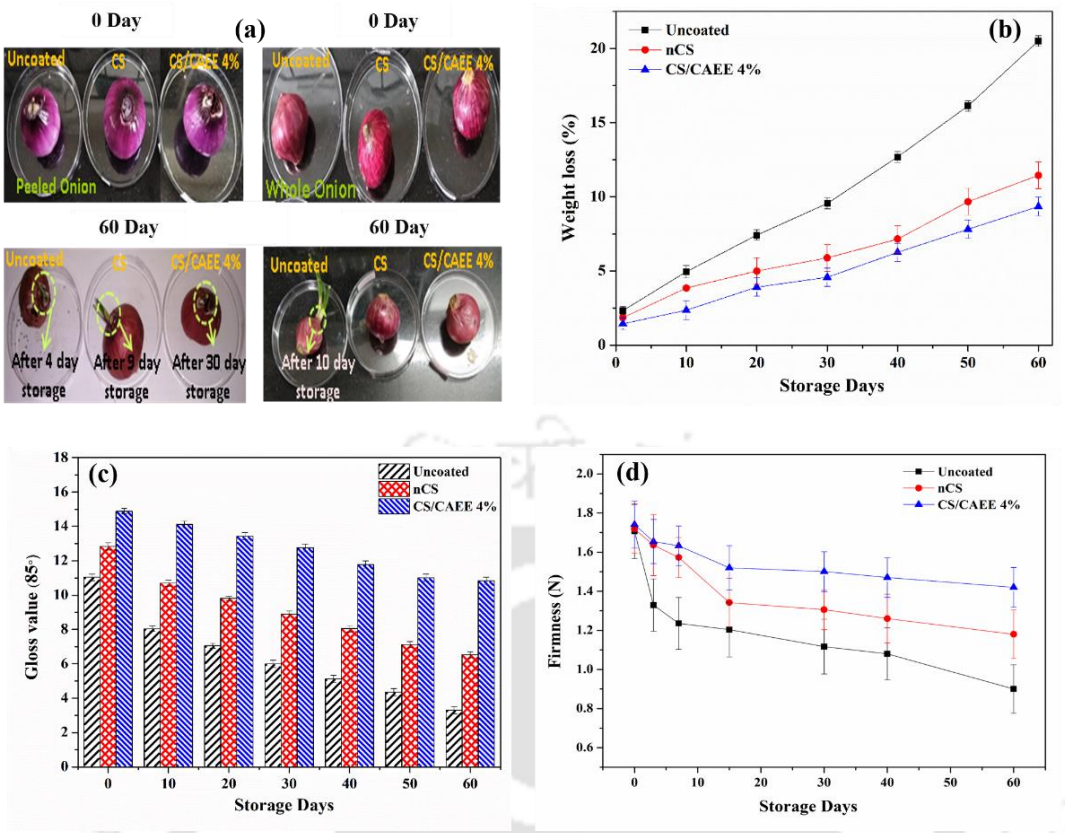

Figure 4.11: (a) Visual observation, (b) weight loss (c) glossiness, and (d) texture of stored onion.

Furthermore, a noteworthy and interesting outcome is observed in coated onion, where the delayed appearance of sprouting was observed in coated than uncoated onion during storage as picturized in **Figure 4.11a**. The polysaccharide-based edible coating formulation with added bio-filler slowed down the sprouting by one month, whereas sprouting was started in uncoated onion within ten days of storage. The reason behind the reduction in sprouting rate could be possibly due to restrictions in enzyme activity in stored onions through controlling the water vapor and gaseous (O_2 & CO_2) transmission rate. Generally, sprouting causes major problems in stored onions which affects the onion bulb quality. Therefore, it is necessary to inhibit sprouting in stored onions for longer storage. Besides, the developed edible coating protects onion from massive moisture loss. Further, the coating has helped to maintain the texture during storage. Therefore, it can be postulated

that the coating layer helped to control moisture loss and gaseous exchange which protects the quality and shelf-life. Besides, the coating helped to protect against the loss of bioactive compounds or nutraceuticals from fruits and vegetables. Furthermore, this coating provided a glossy surface appearance as compared to uncoated fruits and vegetables which helped to enhance consumer appeal. In this regard, the edible coating can be used as an alternative to minimize post-harvest loss and farmers' economic loss.

4.3 Summary

The present study involved the successful novel formulation of algae extracts incorporated with CS-based edible coatings (CS/CAEE 4%) for prolonging the shelf-life of fresh produce such as tomatoes, onions, potatoes, and green chilies. The 4% CAEE incorporated CS-based bio-composite coating enhanced the shelf-life of tomatoes, onions, potatoes, and green chilies by around 30, 60, and 10 days, respectively, under ambient storage conditions. The presence of antioxidant and antimicrobial activity of CAEE due to the presence of various bioactive components, predominantly β-carotene, could protect the fresh produce from oxidation and microbial decay during storage. Besides, the inherent antioxidant and antimicrobial properties of CS biopolymer and CAEE could be capable to retain and improve various physicochemical and biochemical properties of coated tomatoes. Therefore, the developed coating could be a promising solution for extending the shelf-life and arresting the post-harvest losses of fresh produce. Further, this simple technology would be easily accessible to agronomists for keeping fruits fresh longer after harvesting.

CHAPTER 5

DEVELOPMENT OF GUAR GUM-BASED ANTIMICROBIAL AND ANTI-BROWNING FILMS USING ALGAE EXTRACT AND TURMERIC ESSENTIAL OIL

Edible films are manufactured from natural, renewable, nontoxic, and biodegradable polymers and are safe alternatives to plastic food packaging. Despite ongoing research, biopolymer-based edible films still are not of the quality to ensure total commercial replacement of synthetic packaging materials. The study aims to compare the effectiveness of some novel methods employed to improve edible film properties. These include the dispersion of algae extract (CAEE) into guar gum (GG), and glycerol-based edible films that are further reinforced with turmeric essential oil (0-2% v/v) to enhance the film's physical properties. The films were characterized by measurement of film morphology, thermal stability, moisture content, water dissolvability, FTIR Spectroscopy, opacity, color properties, water vapor permeability, tensile properties, and antimicrobial activity. The CAEE and turmeric oil preserved their antimicrobial activity inside the films, which bestowed the films with an active packaging function. Control GG films had acceptable tensile and barrier properties that were further improved. All other film properties, such as opacity, dissolvability, and moisture content, that should be designed for specific applications, were successfully modified with the methods used. Our results confirmed the successful application of CAEE, and TEO incorporated emulsion film formation to edible films in manufacturing GG films for packaging.

Outcome: Mondal K, Goud V. V, & Katiyar V. "*Development of guar gum-based antimicrobial and anti-browning films using algae extract and turmeric essential oil*." (Under Preparation)

Graphical Abstract

The below schematic depicts the preparation of guar gum-based edible films incorporated with algae extract and turmeric essential oil and various characterizations of developed active edible films.

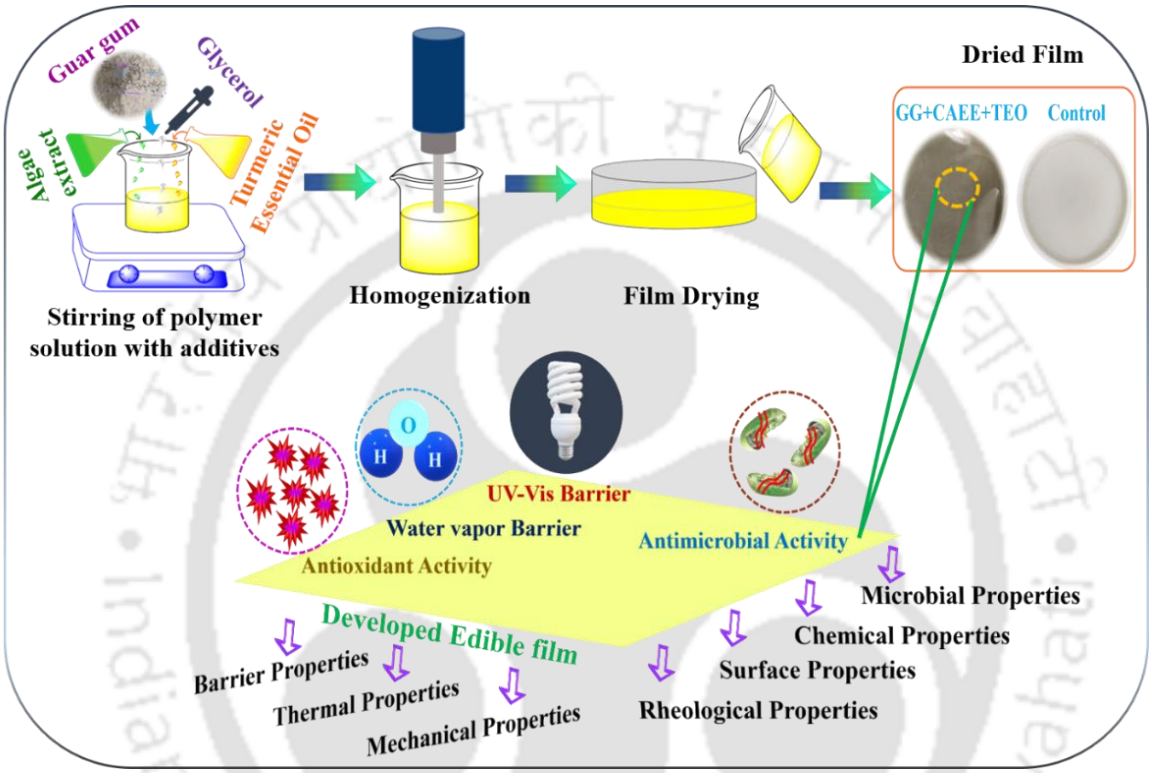

5.1 Introduction

The utilization of polysaccharide-based edible films as a food packaging material has gained much interest due to their sustainable and eco-friendly characteristics [204]. Guar gum (GG) is a natural, nonionic, hydrophilic polysaccharide, that is extensively used in the food industry as a thickener and stabilizer [35,205,206]. GG has been shown to form homogenous edible films that are almost completely water-soluble due to the presence of many hydroxyl groups it carries [35]. On the contrary, GG-based films are lacking some physicochemical properties including barrier, antioxidant, antimicrobial, and mechanical properties, despite their other unique functions [35]. Researchers have reported on the phosphate cross-linking of GG to enhance hydrophobicity [26]. However, there are methods to overcome these shortcomings. For example, increasing film hydrophobicity *via* the incorporation of essential oils (EOs) and plant extracts into the film matrix retards moisture transfer [87].

Turmeric essential oil (TEO) is another intriguing natural compound that is used in various biological fields and it is derived from the roots of *Curcumin longa*. Turmeric plants are well known since ancient times due to their medicinal properties. The TEO has a watery viscosity and bears a yellow color. This oil is appreciated for its distinct fresh, woody but spicy aroma. Moreover, TEO is composed of various therapeutic bioactive compounds like zingiberine, phellandrene, limonene, curcumin, ketone, 1,8-cineole, β-turmerone, ar-turmerone, and α-turmerone [207]. Owing to the presence of various bioactive compounds, TEO acts as an antiseptic, antifungal, antimicrobial, carminative, analgesic, bactericidal, astringent, febrifuge, sedative, insecticidal, tonic, nervine, and fungicidal agent. Therefore, TEO would serve as a superior antimicrobial and antioxidant agent as well as could provide an anti-browning activity. Therefore, by incorporating of TEO into the edible film matrix, it is possible to use the films as a carrier of oil-soluble functional agents. Consumptions of

such edible films or the release of oil-soluble components into the food system can contribute additional nutritional benefits and protect food from oxidative rancidity and microbial spoilage [35].

In addition, algae are also a rich source of various bioactive compounds, and the extract of de-oiled algae (CAEE) contains a sufficient amount of β-carotene along with other bioactive compounds as discussed in chapter 3. Further, the incorporation of algal extract into the polysaccharide-based polymer matrix i.e., CS improved its optical properties i.e., UV-Vis light blocking properties and other characteristics properties such as water vapor barrier, mechanical, antioxidant, and antimicrobial properties. Therefore, the addition of CAEE into GG polymer could improve physicochemical and biochemical properties in the developed film. Moreover, the reason behind the addition of CAEE along with TEO is to obtain synergistic effects which would provide effective characteristic properties to the developed edible films. Generally, the addition of property modifiers or food additives in the polymeric matrix is required to achieve desired physical and mechanical characteristics [24]. To fulfill this purpose, most commonly plasticizers are incorporated into the films. Besides, having more advantageous properties of edible films, it gets brittle and fragile to stress without the presence of plasticizers [24]. Glycerol is the most frequently used plasticizer in edible films, and it is employed here as the plasticizer for this study [27].

This chapter focuses on the development of antimicrobial and antioxidant-rich GG-based active edible bio-composite films. In order to obtain superior antioxidant and antimicrobial properties, algae extract (CAEE) and turmeric essential oil (TEO) were added to the polymer matrix. The concentration of CAEE was kept constant, which was based on the previous preliminary experiment, whereas TEO concentration was varied from 0 to 2%. For drawing comparisons among developed films, total of six types of the film was fabricated using the solvent-casting method. A control film was prepared which contained

GG-gum and glycerol and the rest of the films were named edible film (EF) A, B, C, D, and E, respectively, as described in chapter 2 (**Table 2.2**). For the ease of the reading and understanding, the composition of developed bio-composites films is mentioned in this section again. The developed films EF A, B, C, and D are comprised of same concentration of GG (1g), glycerol (30 wt.%), and CAEE (4 mL) whereas the TEO concentration is varied. The TEO is absent in EF A formulation whereas 0.5, 1, 2 mL of TEO present in EF B, C, and D formulation, respectively. The EF E formulation contains 2 mL of TEO along with other ingredients except CAEE. Glycerol was added as a plasticizer to all the film formulations. Also, to check the individual effects of bio-fillers such as CAEE and TEO, two films namely EF A and EF E were developed which contain separate CAEE, and TEO, respectively. Moreover, various physicochemical and biochemical properties of developed active films were studied.

5.2 Results and Discussion

5.2.1 Surface Morphology

Surface morphologies of developed films were observed by Field emission scanning electron microscopy (FESEM), (**Figure 5.1a**) respectively. Images of control films exhibited smooth, and homogeneous surfaces with the presence of some pitting and biopolymeric aggregates. the addition of CAEE in the edible films exhibited irregular surfaces. The bio-composite film showed many tiny particles on the surface film. A smooth layer on the film surface is observed in EF B, C, D & E film which may due to the addition of TEO. However, no surface cracks or pores were found in any of the film samples indicated uniform mixing of the ingredients and homogeneous dispersion of TEO in the films. However, few works of literature reported on the presence of pores in EOs added films where a reduction in solvent evaporation rate was observed due to the formation of a layer that forms the pore. The pore formation in the gelatin/EO blend was reported which

was believed to facilitate due to the volatility of the EOs. A similar observation in sago starch/GG film incorporated with EOs exhibited roughness with the addition of carvacrol, as reported by Dhumal et al., 2019 [83]. The addition of TEO into the GG matrix produced roughness in the film surface, and the maximum roughness was created by the TEO. The film's roughness property was also confirmed by the AFM images (**Figure 5.2**). The root mean square (RMS) roughness value was found to be in increasing order with the addition of more quantities of TEO from 25.72 to 79.35 nm.

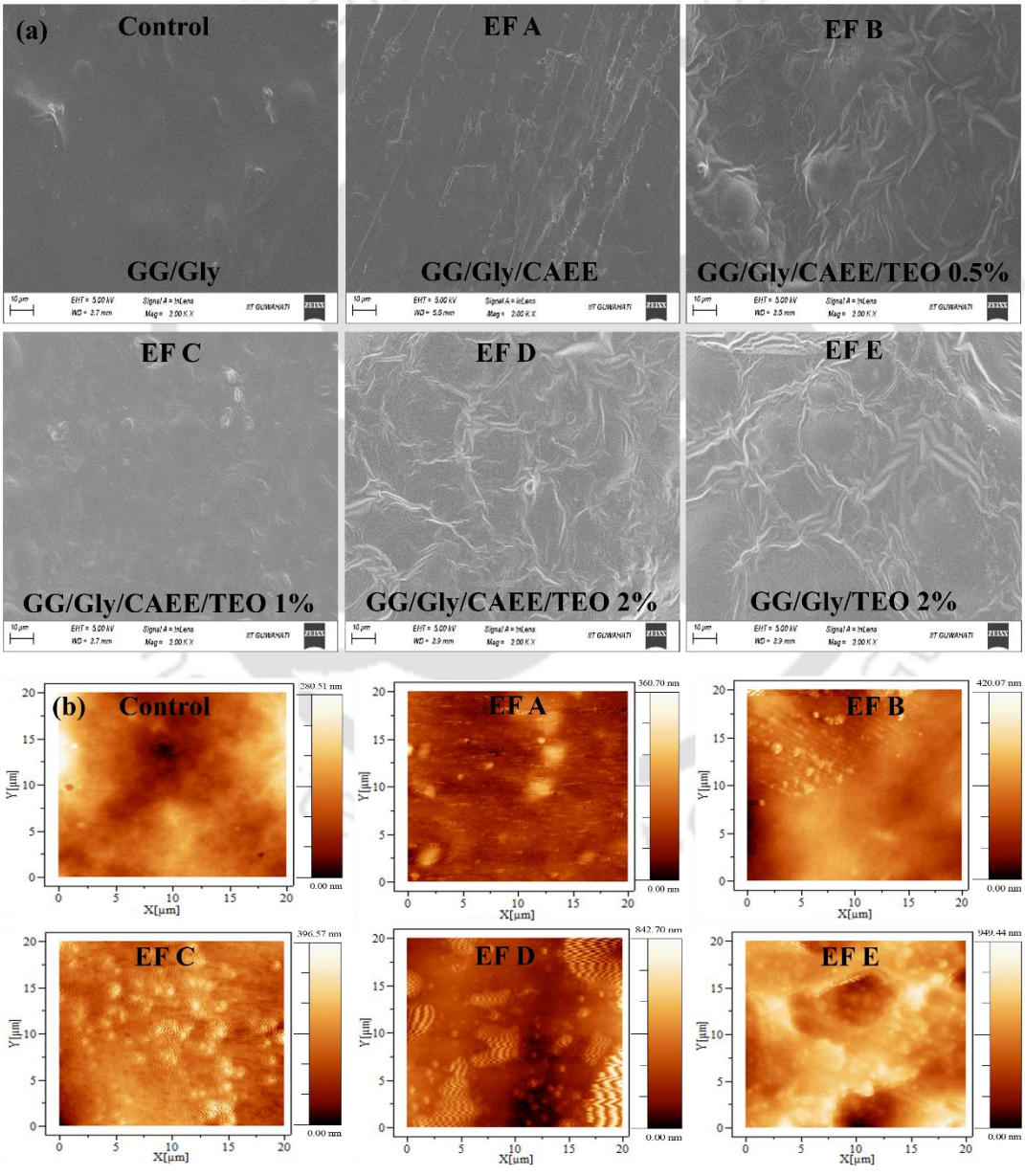

Figure 5.1: (a) FESEM images, and (b) AFM images of developed GG-based edible films.

5.2.2 FTIR Analysis

FTIR analyses provide the investigation of interactions between functional groups of the chains and can be recognized as shifts in the spectrum. FTIR spectra of the films are given in **Figure 5.2**. Two prominent peaks observed in control film FTIR spectra can be summarized as follows; in the region from 3650 to 3000 cm^{-1} which is normally associated with the stretching vibration of the O–H bond [34] and in the region 3000-2800 cm^{-1} that is assigned to C–H bond stretching. Another absorption band was centered around 1645 cm^{-1} which is related to the bending vibration of O–H. Peaks occurring between 1200 and 900 cm^{-1} centred around 1015 cm^{-1} correspond to stretching vibration of C–O–H bonds which the film has in excess due to guar gum being a galactomannan polymer [34].

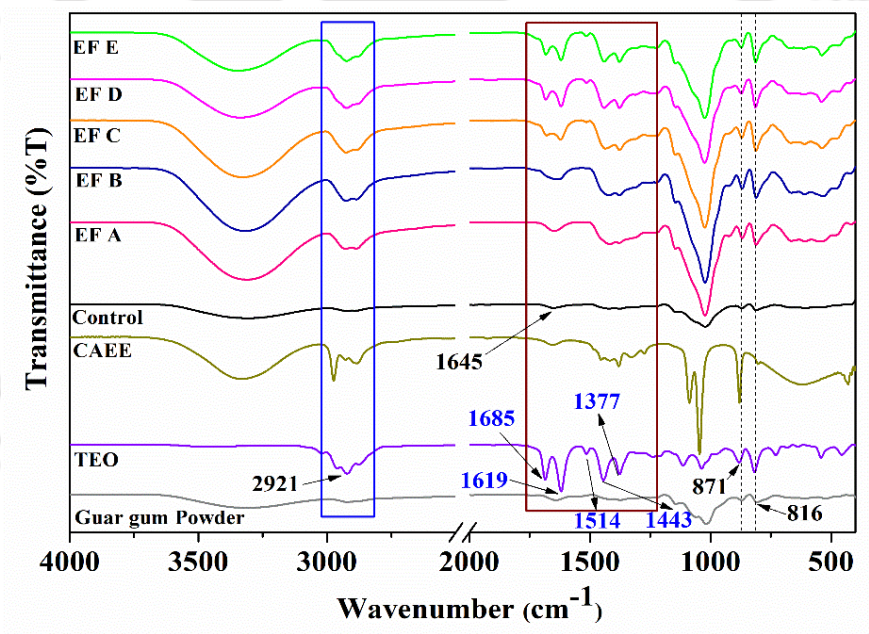

Figure 5.2: FTIR spectra of guar gum powder, turmeric essential oil, and developed edible films.

A strong absorption peak was observed in CAEE at 2970 cm^{-1}, corresponding to C–H symmetric stretching vibrations of the polyphenols. The presence of bands at 2884 and 1656 cm^{-1} might be attributed to ethanol and amide I, or C=O stretching of proteins or carboxylic acid, respectively. The presence of bands at 1276, 1327, and 1380 cm^{-1} could

be related to CH_2 vibration, amide III, and symmetric CH_3(CO) vibration of 1,8- cineole, respectively. Further, the possibility of the presence of polysaccharides could be attributed to the occurrence of bands at 1087 and 1045 cm^{-1}. The observed band at 879 cm^{-1} corresponds to the $–CH_2$ stretching vibration of 1,8-cineole or ethanol. Further, in the case of TEO, peaks were observed at 1685 and 1619 cm^{-1} corresponding to C=O and C≡N stretching vibration. 1514 cm^{-1} represents polyphenol skeletal (aromatic) stretching and C – O – C stretching vibrations of aromatic structure, confirming the presence of turmerone. However, peaks at 13771cm^{-1} confirm the availability of alkanes or CH_3 bending due to the presence of curcuminoid (curcumin). The peak at 1443 corresponds to C≡N stretching. Peaks observed at 1115 and 1034 cm^{-1} are due to C–O–C stretching. The addition of CAEE yielded no substantial changes in FTIR spectra, possibly related to the low concentrations employed (4%), however, the intensity of the peak was increased. Furthermore, the incorporation of TEO exhibited the appearance of new chemical shifts, which indicated noteworthy changes in the chemical structure of guar gum by forming the covalent bonds between TEO, CAEE, and polymer matrix.

5.2.3 Optical Properties

The developed GG film was transparent without any color, but the addition of TEO made the film yellowish, and the color intensity increased as the TEO content increased. However, the CAEE/TEO bio-composite film was still transparent enough to be seen through the other side of the film. The surface color values of the control and developed bio-composite films are shown in **Figure 5.3** &**Table A5**. As expected from the appearance of the film, the control film showed high L* and low a* and b* values. The addition of CAEE and TEO decreased L* and a* and increased the b* value of the GG film in such ways that the L* value decreased linearly, a-value decreased, and the b* value increased. However, the addition of CAEE did not show any significant change, which might be due

to the addition of a lower concentration. Consequently, the total color difference (ΔE) increased with the increase in the TEO concentration (**Figure 5.3**). The increased b* and a* values indicate the rise in redness and yellowness, respectively. The increased total color difference (ΔE) of the composite films was mainly due to the increased yellowness by the addition of TEO. Like the b* value, the YI of the GG film was significantly increased by the addition of TEO, and the increase of YI was dependent on the TEO concentration. Similar effects of curcumin addition on the surface color of gelatin and PLA-based films have been reported in literature [208,209].

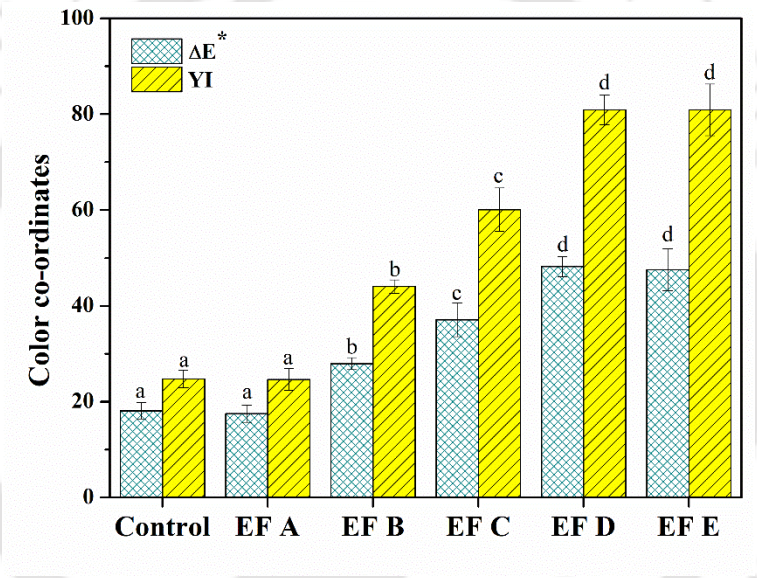

Figure 5.3: Total color difference (ΔE), and yellow index (YI) of developed edible films.

The transparency of a film describes its optical nature and is another important parameter for food packaging. This is especially important since food is a complex system and many foods are sensitive toward the light, i.e., UV-Vis. It can be conferred from **Figure 5.4** that the control film presented higher transparency as compared to the bio-composites. The incorporation of CAEE into the GG matrix improved the barrier of light transmission to the visible and ultraviolet (<400 nm) regions. EF A film showed a ~12% reduction after the addition of CAEE. Further incorporation of TEO in EF B, C, & D film showed UV-light blocking property which is depicted in the figure. The occurrence of a flat line in the region

of 200-330 nm indicated a higher UV-light blocking capacity of bio-composites due to the addition of TEO. Increasing TEO concentration in film significantly reduced transparency by 32%. However, EF E film with the highest TEO concentration and without CAEE showed an 11% reduction in transparency, the lesser reduction might be associated with the absence of CAEE. This observation also indicates the addition of CAEE into the GG matrix synergistically reduces the transparency of the developed bio-composites.

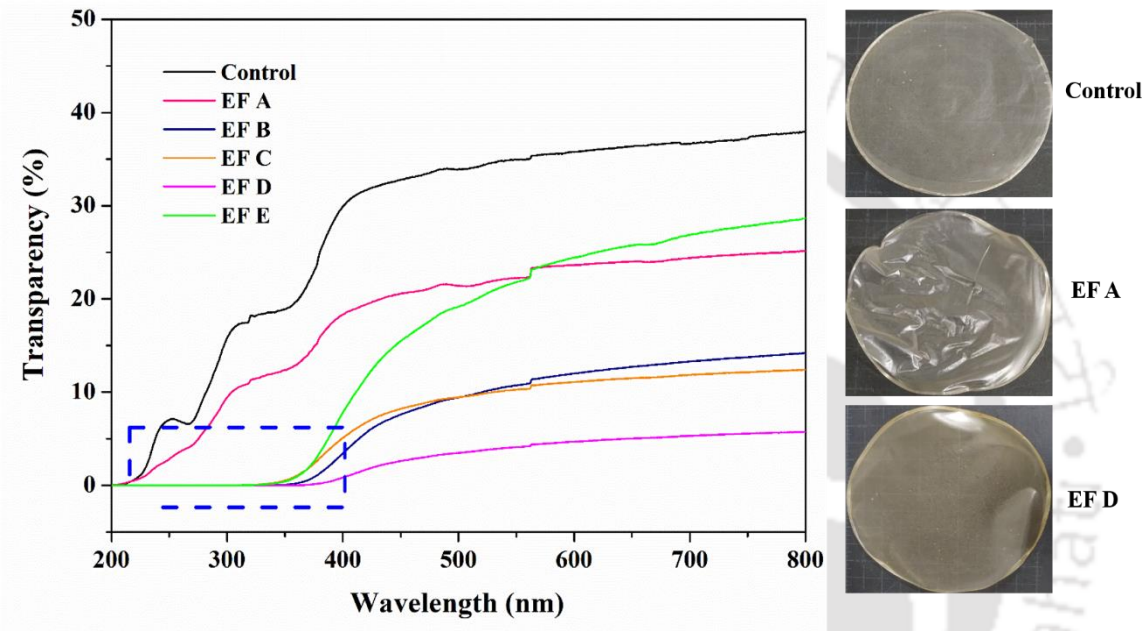

Figure 5.4: Transparency of developed guar gum-based edible films along with digital images of films.

5.2.4 Water Vapor Transmission Rate

Control of moisture transfer between the food and its environment or separate portions of a multi-component food is one of the primary functions of food packaging, particularly owing to the dominant role of water on the rate of deteriorative reactions [34]. Consequently, water vapor transmission (WVTR) constitutes one of the most widely studied properties of edible films [210]. Relative humidity (RH) of the film environment directly affects the WVTR which increases as films are stored at higher RH [34]. **Figure 5.5** depicts the WVTR of the developed edible bio-composite films and the effectiveness

of the CAEE, and TEO addition. The incorporation of CAEE reduced WVTR by ~6%, whereas the addition of TEO along with CAEE exhibited a higher reduction with increasing TEO concentration maximum by ~35%. This observation could be attributed to the strong intermolecular hydrogen bonding between the GG matrix and bio-filler (CAEE), which probably allowed the formation of crosslinking, due to which the reduction in free space occurred inside the polymer matrix because of the lowered rate of diffusion of water vapor molecules through the bio-composite edible films. Dispersion of a maximum of 1.5% TEO exhibited higher reduction which could be due to the proper dispersion of oil particles sought out the film. Water transfer occurs through the hydrophilic portions of the films. This explains why permeability strongly depends on the hydrophilic-lipophilic ratio of the films [34]. The rate of water transfer declines due to an increased tortuosity that raises the resistance against water transfer through the film. Tortuosity of the films is enhanced when the amount of oil phase is increased, or oil droplet sizes are reduced.

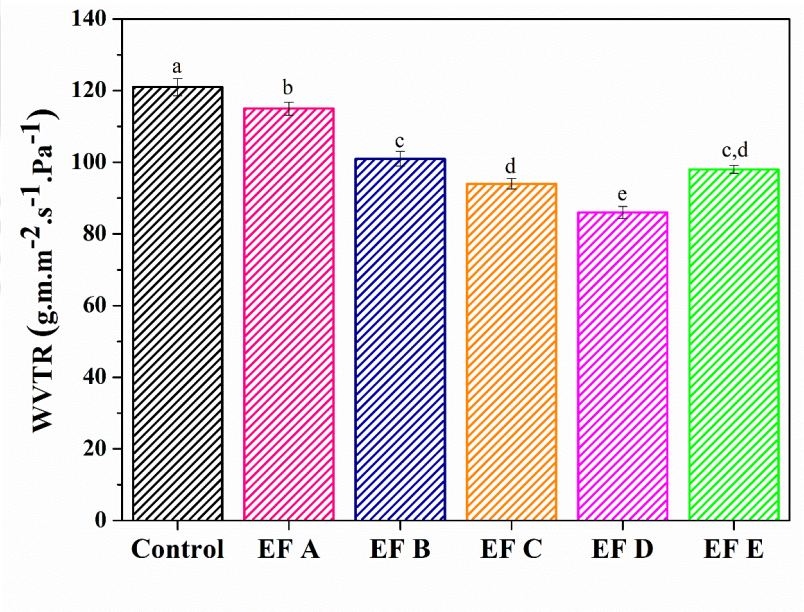

Figure 5.5: Water vapor transmission rate of developed guar gum-based edible films.

5.2.5 Water Contact Angle

Information about surface water wettability is essential in investigating the adhesive and cohesive properties of films for better spreading of the coating on the solid surface and evaluating food-coating compatibility. Contact angle (CA) is the most basic method to evaluate wettability and can be defined as a measure of affinity between the liquid and the solid surface [34]. When the liquid is water, the contact angle becomes a measure of the hydrophilicity of the film surface. Oil inclusion, along with decreasing film dissolvability, also made the film surface more resistant to water wetting, which enabled reliable measurement of contact angles. An increase in TEO content from 0.5% to 1.5%, expectedly, led to improved film surface hydrophobicity as observed by an increase in CA (**Figure 5.6**). A decrease in surface wettability with the addition of hydrophobic materials such as essential oils has been reported in several studies [34]. This result also explains the increase in contact angle with curcumin addition. The CA reading was noted down after 10 sec of water drop on the surface. The control film showed CA ~50.6°, which was increased by a maximum of 70° after the addition of TEO (EF D). However, EF E film contains 1.5% TEO and had a contact angle less than EF D, and C but higher than the control film which might be due to the absence of CAEE which helped to increase the surface roughness. Moreover, the addition of CAEE and TEO enhanced surface hydrophobicity which might be due to the increase in roughness of the edible films, and the roughness is also supported by AFM.

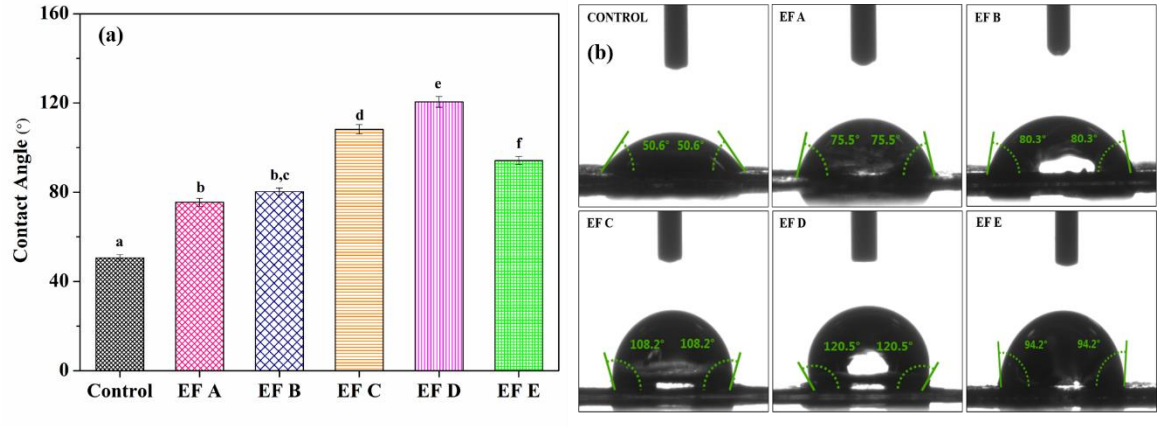

Figure 5.6: (a) Contact angle value, and (b) recorded image of developed guar gum-based edible films after 10 sec time intervals.

5.2.6 Mechanical Properties

The mechanical properties of GG-based developed edible films are depicted in **Table 5.1**. A significant reduction of TS in the bio-composites film was observed as compared to the control (6.58±0.34 MPa). The EFD film impregnated with 1.5% TEO and 4%CAEE displayed the lowest value (2.68±0.21 MPa). This significant decrease might be due to plasticizing or lubricating effect of TEO. However, all the other combinations of films exhibited TS values in the range of 5-6 MPa. The EF A film which contains CAEE without TEO exhibited reduced TS (4.76±0.16), which might be attributed to the weak molecular interaction such as hydrogen bonding between the polymer matrix and polyphenolic compounds of algae extract. A slight improvement was observed in EF B film (5.21±0.25) when CAEE and a lesser amount of TEO (0.5%) were added. It was also noticed that increasing TEO concentration with fixed CAEE concentration reduced the TS value as shown in **Table 5.1**. The addition of EO reduces the interactions between polymer-polymer chains and provides a flexible domain within the film matrix resulting in a decrease in TS and an increase in EAB [211]. On the other hand, the addition of EOs can create heterogeneous thin film structures with discontinuities in the film, and EO droplets

impregnated in the film can be deformed at room temperature, thereby decreasing the TS values [212].

Table 5.1: Mechanical properties of developed edible films.

Sample	Tensile Strength (MPa)	Young's Modulus (MPa)	Elongation at break (%)
Control	6.6±0.3	30.2±0.5	40.5±1.3
EF A	4.8±0.2	27.3±0.9	45.4±1.3
EF B	5.2±0.3	28.2±0.2	50.3±1.8
EF C	4.7±0.2	25.2±0.3	55.7±1.2
EF D	2.7±0.2	18.5±0.2	58.9±1.5
EF E	4.8±0.2	26.4±0.2	56.2±1.5

In contrast, the elongation at break (EAB) values was higher in developed bio-composites (EF A, B, C, D, & E) than in the control film (40.45±1.34) which might be due to the weak intermolecular interaction between polymer matrix and added CAEE and TEO. The maximum EAB value obtained in EF D is 58.89±1.54%. The increasing flexibility of the GG/CAEE/TEO films might be associated with the reduction in glass transition temperature (T_g) of the developed composites and the chain mobility caused by the plasticizing effect of TEO. The EAB values of edible films of EF A, B, C, D, & E were 45.40±1.25, 50.26±1.81, 55.65±1.23, 58.89±1.54, and 56.23±1.45, respectively. The stiffness of the polymer is determined by Young's Modulus (YM). The developed bio-composites exhibited reduced YM than the control film (30.24±0.51) after being impregnated with CAEE and a combination of CAEE and TEO as depicted in **Table 5.1**. The lowest YM value was obtained in EF D film (18.48±0.21). Several reported studies exhibited a reduction in YM with the addition and increasing concentration of EO [83].

5.2.7 Thermal Properties

The thermal degradation of guar gum powder, TEO, and developed films including control film, and CAEE/TEO incorporated bio-composites are shown in **Figure 5.7**. The results indicate that there are three steps of degradation in all developed films, the first in a temperature range of 40-100 °C, the second step in the range of 150-230 °C, and the third step in the range of 260-365 °C. However, two-step of degradation is observed in GG powder, the first in a temperature range of 40-100 °C, and the second in the range of 290 to 330 °C, which is associated with polysaccharide guar gum. A single-step degradation is found in the case of TEO in the range of 170-250 °C. The weight loss in the 40-100 °C temperature range could be associated with the evaporation of residual water in the films. The second degradation might be due to the evaporation of low molecular weight components in the films probably including glycerol and water in glycerol as well as aroma compounds from essential oil. The third step and the maximum degradation in the temperature range of 260 to 365 °C could be associated with guar gum. Notably, no other separate degradation peak was observed in the TEO-incorporated composite film, which indicated homogeneous mixing of TEO with the polymer and other fillers. The 10% weight (T_{10}) loss occurred at a higher temperature in TEO-incorporated film than in control and EF A films as described in the table. Interestingly, 90% weight loss (T_{90}) occurred at lower temperatures in TEO-incorporated films (EF B, C, D, and E) than in control and EF A. The results indicated the addition of TEO initially showed thermal stability but with increasing temperature degradation occurred at a faster rate. Therefore, the incorporation of TEO enhanced the biodegradability of the developed edible films. The addition of CAEE (EF A) exhibited faster weight loss initially at a lower temperature (84 °C) followed by slow degradation which generated around 10% char residue after the completion of the cycle

than control and other films. Therefore, the incorporation of TEO enhanced the biodegradability of the developed edible films.

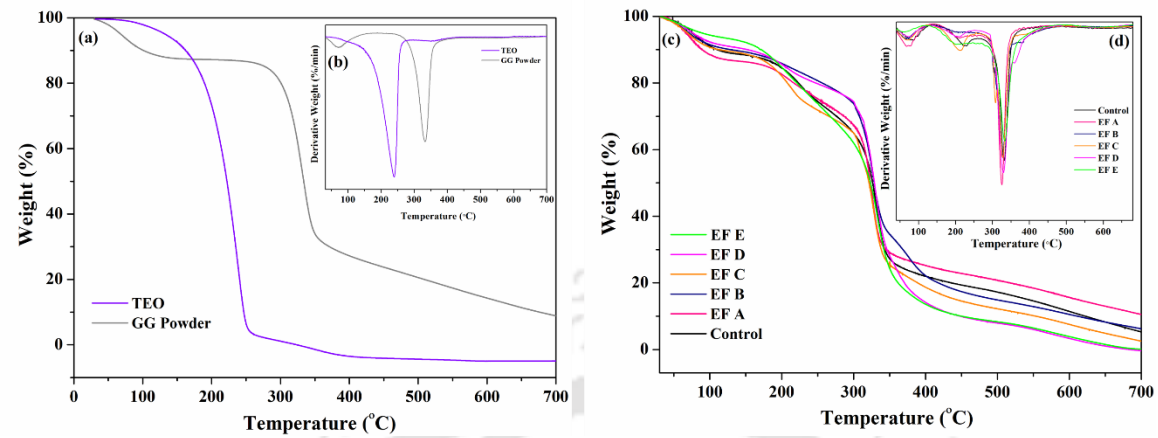

Figure 5.7: (a) TGA, (b) DTG thermograms of guar gum powder and turmeric essential oil, (c) TGA, and (d) DTG thermograms of developed edible films.

5.2.8 Rheological Behavior of Filmogenic Solutions

- ***Strain Sweep Measurements of the Developed Edible Film-Forming Solution***

Strain sweep measurements were performed and helped to determine the LVR (linear viscoelastic region) of developed filmogenic solutions, where G′ (storage modulus) and G″ (loss modulus) remained constant and independent of the applied strain. This measurement also imparts information regarding the structural strength of a material based on the length of the LVR region, i.e., a stable solution might remain longer in the LVR region as it is more resistant to applied force than an unstable one. The representative curves for the G′ and G″ moduli of all the solutions as plotted against the applied strain are depicted in **Figure 5.8a**. It is evident from the curve that in all cases G″ > G′, indicating that all the samples showed a liquid-like behavior under the LVR. Overall, the elasticity (G′) decreased over time with increasing the shear strain for all the samples, including the control. However, the addition of TEO significantly improved the elastic behavior compared to the control and EF A, which was more significant at higher strain. Moreover, the higher G″ value of the CAEE-incorporated polymeric solution compared to the control solution indicated its

viscous nature. The G″ values showed a significant improvement from 3.2 (Control) to 16.8 (EF C) Pa with increasing the TEO concentration from 0 to 1%; however, TEO concentration above 1%, G″ value decreased sharply, though it was higher than the control. One of the important parameters of oscillatory rheology is the loss factor or loss tangent (tan δ= G″/G′), which indicates the characteristics of the material; whereby tan δ > 1 indicates a viscous nature of the sample as G″> G′, the sample is elastic when tan δ < 1(G′ > G″), and the sample is in an intermediate phase of a highly concentrated polymer solution and a real gel when tan δ > 0.1, but where the sample is not a true gel [169]. The tan δ value of CAEE and TEO incorporated filmogenic solutions in the present study was greater than 1 except for the control and EF A. This result predicted a concentrated and viscous nature of the polymeric solution for samples EF B to E, whereas the control sample showed a highly concentrated solution but not a true gel. The incorporation of TEO into the film-forming solution increased the tan δ value.

- ***Frequency Sweep Measurements of the Developed Edible Film-Forming Solution***

While the strain sweep measurements give information about the structural stability of the solutions against an applied deformation, the frequency sweep tests classify the samples as a gel, concentrated, or dilute solution, depending on the storage and loss moduli behavior over the frequency range. If G′ > G″ is true all over the frequency range, the samples are classified as gels. For samples with G″ > G′ at a higher frequency, the storage and loss moduli are closer to each other, and it is classified as a dilute solution; if G″ > G′ and the moduli intersect inside the frequency range, the solution is considered to be concentrated. From the frequency sweep curve (**Figure 5.8b**), it could be observed that all the samples could be considered as diluted polymer solutions, as already described in the strain sweep tests by the tan δ values (tan δ> 1). The crossover frequency parameters, obtained from frequency sweep curves are listed in **Table 5.2**. Between the control and TEO-incorporated

filmogenic solution, a shift in the crossover frequency ($\omega_{crossover}$) was observed from 72.6 to 5.76 rad s^{-1} and an increased value of $G'_{crossover}$ from 14.2 to 19.2 was also observed. However, a reduced value was noticed in EF A sample.

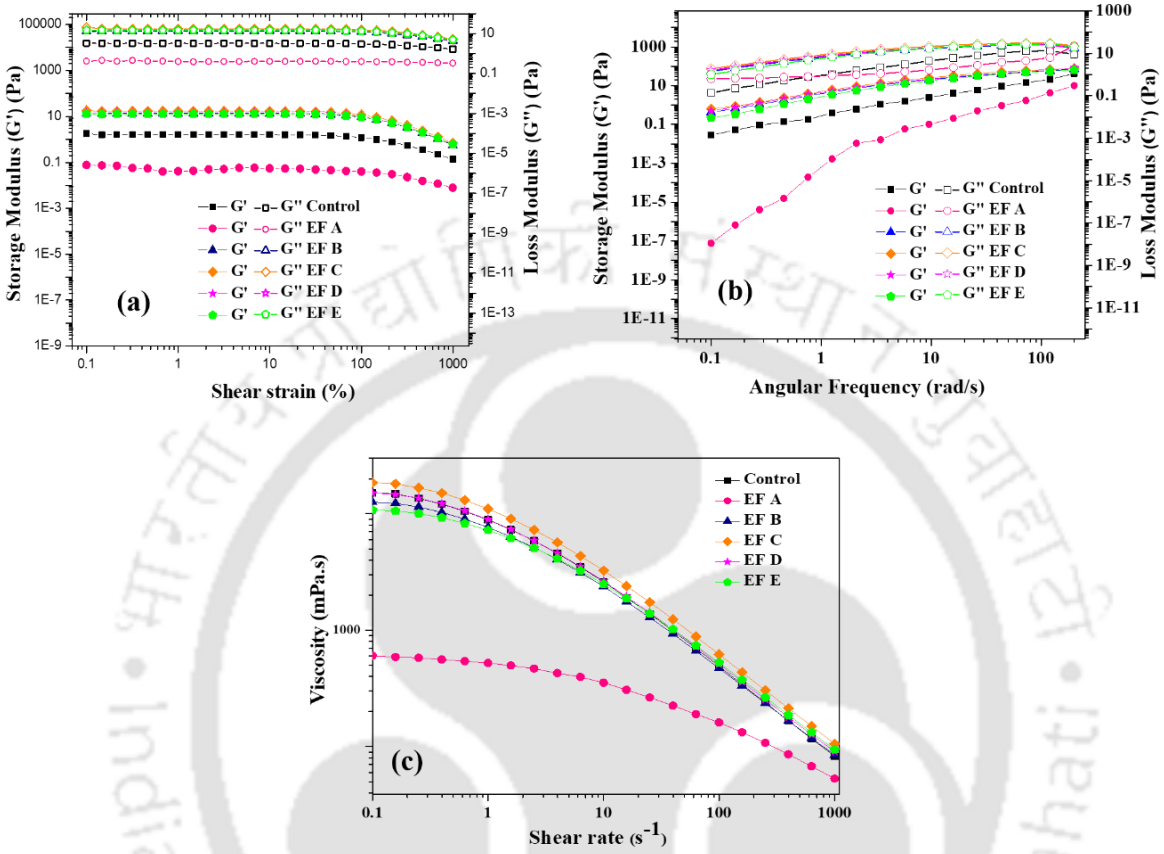

Figure 5.8: (a) Strain sweep parameters of the G′ and G″ moduli at f =1 Hz, (b) frequency sweep parameters of the G′ and G″ moduli, and (c) flow curves of the developed guar gum-based bio-composite filmogenic solutions together with the control.

- ***Steady-state Behavior of the Developed Film-Forming Solution***

The steady-state flow behavior of the FFSs could affect the spread-ability, uniformity, and mechanical properties of the bio-composite films. As shown in **Figure 5.8c**, all the FFSs displayed a pseudoplastic (or shear-thinning) behavior as the viscosity decreased with the increase of shear rate from 0.1 to 1000 s^{-1}. The reduction in viscosity with increasing shear rate might be due to the interruption in polymer chain entanglement which leads to the orientation of the molecular chains to become more random, resulting in loose interactions

between adjacent chains, thus viscosity is reduced [213]. The addition of CAEE reduced the viscosity of EF A more than the control and others, which might be due to the presence of polyphenols loosening the bond interaction among the polymeric chains, as polyphenols are rich in hydroxyl groups (–OH), which possibly could create space between the polymeric chains, thereby increasing the mobility of the chains by providing free space [128]. However, the addition of 0.5% TEO along with CAEE (EF B) showed improved viscosity than EFA but not higher than control, whereas 1% TEO addition (EF C) displayed higher viscosity than control FFS and other bio-composite solutions. Although, the addition of 1.5% TEO with (EF D) or without CAEE (EF E) exhibited less viscosity than the control, wherein EF E significantly lowered the viscosity. The improvement in viscosity might be due to the formation of strong hydrogen and covalent bonding between TEO, CAEE, and polymer matrix. In this case, CAEE exhibited a synergistic effect along with TEO, thus viscosity enhanced. Further, the plausible reason for reduced viscosity in EF E (absence of CAEE) could be attributed to less interaction between the polymer chain and TEO. Besides, the flow behavior index (n) was obtained by plotting the viscosity as a function of the shear rate and using the power-law model indicating a pseudoplastic behavior when 'n' is between 0 to 1, with values beyond 1 following a Newtonian behavior [117]. The 'n' values in this study ranged from 0.35-0.45 as shown in **Table 5.2**, indicating the pseudoplastic behavior of all the filmogenic solutions, which was corroborated by the observed steady flow behavior. Further, the addition of CAEE slightly reduced the 'n' value in EF A whereas the addition of TEO with increasing concentration in the polymeric solution led to increasing '*n*' values. However, the addition of CAEE and TEO did not alter the pseudoplastic behavior of the filmogenic solutions.

Table 5.2: Frequency sweep parameters measured at room temperature for angular frequency ($\omega_{crossover}$) and storage modulus ($G'_{crossover}$) at the crossover point and flow behavior index of developed guar gum-based filmogenic solutions

Sample	$\omega_{crossover}$ (rad/s)	G′ (Pa)	Power law model (n)	R^2
Control	72.6	14.2	0.35	0.996
EF A	72.6	1.73	0.33	0.991
EF B	5.76	15.2	0.38	0.990
EF C	5.76	19.2	0.40	0.996
EF D	5.76	16.4	0.42	0.994
EF E	9.56	17.9	0.45	0.992

5.2.9 Antioxidant Activity

One of the common methods for the determination of antioxidant activity is DPPH free radicals scavenging activity, where DPPH acts as a reducing agent or electron donor. The deep violet color of DPPH radicals is converted to transparent color in the presence of antioxidants, and the absorbance is recorded at 517 nm to calculate the percentage of DPPH antioxidant activity [81]. **Figure 5.9a** depicts the percentage of free radical-scavenging activity and/or antioxidant activity of the CAEE and TEO-incorporated edible films. The control film exhibited a moderate scavenging activity of ~18.59%. However, a remarkable improvement in DPPH antioxidant activity was observed in the developed edible films after the addition of CAEE and TEO. TEO exhibited higher capacity than CAEE with increasing concentration. However, the addition of CAEE long with TEO enhanced the antioxidant capacity significantly. The DPPH radical-scavenging activity of EF A, B, C, D & E films increased gradually to 31.85%, 38.47%, 61.02%, 71.97%, and 50.46%, respectively. The rise in antioxidant activity could be attributed to the presence of phenolic compounds and a small fraction of the $–CH_2–$ group in CAEE. Besides, TEO is rich in bioactive compounds. The RSA of the developed edible film was evaluated using the DPPH radical

[DPPH•] method. **Figure 5.9b** displays the reduction in free radical scavenging activity of edible films with time. Control film exhibited the lowest reduction in RSA (20% at equilibrium), while EF A, B, C, D & E displayed 48%, 60%, 74%, 79%, and 69% RSA, respectively. The highest RSA was observed in EF D film among others, leading to a 79% reduction of the DPPH• free radicals at equilibrium. Further, the increasing antioxidant activity was obtained with increasing TEO concentration. However, EF E film without CAEE displayed less activity than EF D, indicating the presence of significant antioxidant activity in CAEE. The possible reason for effective antioxidant activity in TEO-incorporated edible film might be associated with the presence of bioactive compounds such as turmerone, curcumin, and others. It is noteworthy that, with the time procced reduction in RSA was observed till equilibrium was reached.

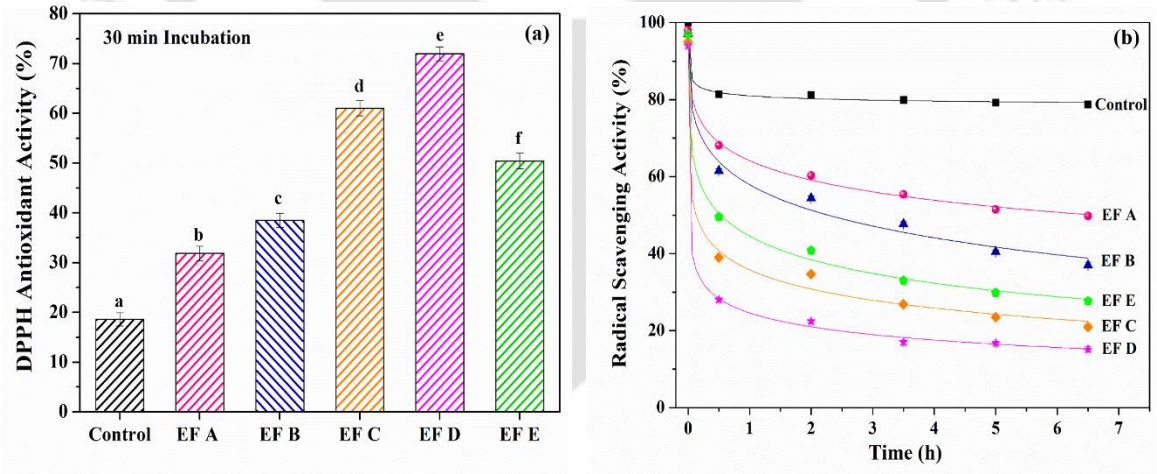

Figure 5.9: (a) DPPH Antioxidant activity of developed film, and (b) radical scavenging activity of developed edible films with time (lines drawn for eye guides).

5.2.10 Antimicrobial Activity

The antimicrobial activity of edible films against two typical pathogenic bacteria, *E. coli*, and *S. aureus*, was investigated using the colony counting method, as shown in **Figure 5.10**. The control film which contains neat guar gum without bio-fillers when incubated with bacteria, exhibited very weak antimicrobial activity for both pathogens. However, the

addition of algae extract (CAEE) in EFA film showed moderate (50%) inhibition whereas, the addition of TEO with increasing concentration into GG matrix along with constant CAEE (EF B, C, & D) displayed increasing antimicrobial behavior with 65 to 95% inhibition rate for *E. coli* and 60 to 90% for *S. aureus*, respectively. The EF E film impregnated with only a higher percentage of TEO exhibited effective antimicrobial activity. The addition of CAEE improves antimicrobial activity moderately due to the presence of polyphenols mainly β-carotene.

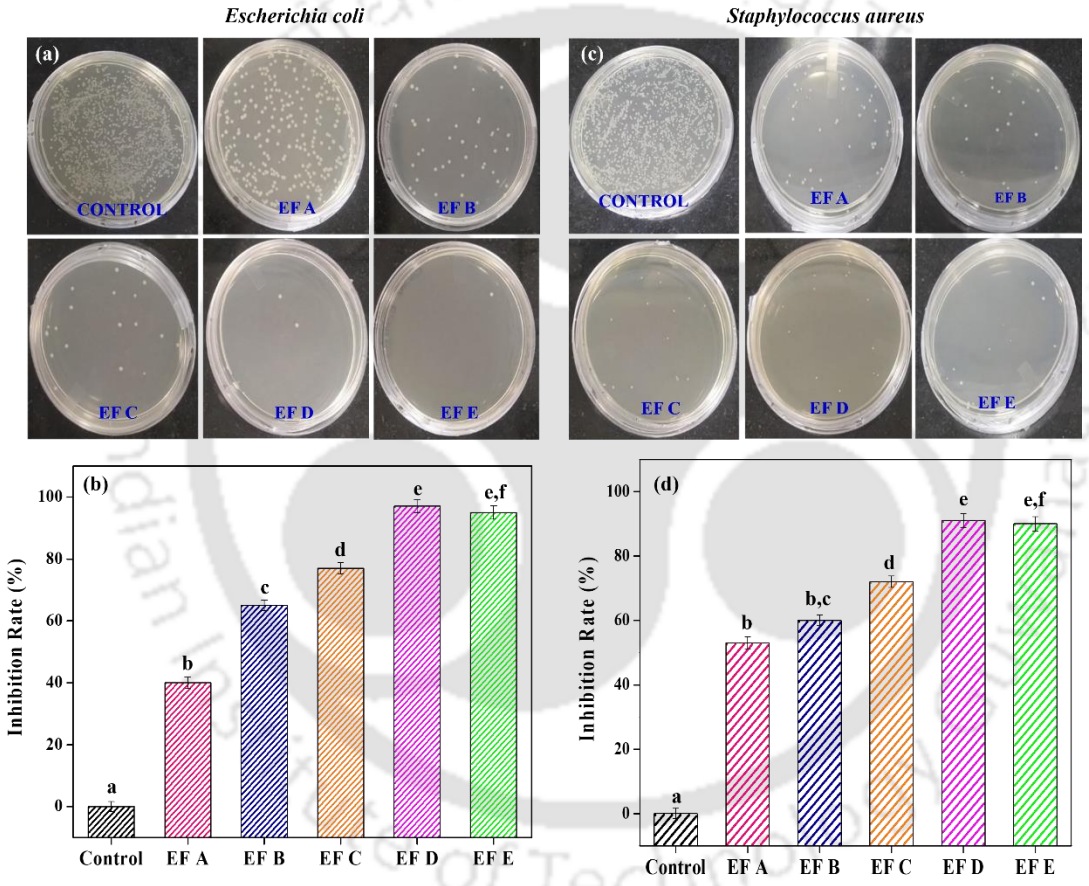

Figure 5.10: Antimicrobial activity of *E. coli* (a, b), and *S. aureus* (c, d) in developed edible films.

The addition of TEO effectively displayed a strong inhibition rate which could be due to the presence of mainly curcumin, and turmerone. Further, increasing the concentration of TEO inhibited more bacterial colonies. A lower concentration of TEO together with CAEE

displayed good inhibition properties. Moreover, CAEE was more active against *S. aureus* (Gram Positive) than *E. coli* whereas TEO was for *E. Coli*, and the mixture significantly reduced both bacteria, as depicted in plate images. This indicates, developed films are antimicrobial and can be used as active films as well.

5.3 Summary

The present study tried to fulfill the purpose of developing edible active films and enhancing the effectiveness of physicochemical properties which currently lag behind the commercial alternatives. Utilization of waste algae biomass and incorporation of algae extract to develop guar gum-based edible emulsion films with the dispersion of turmeric essential oil exhibited promising approaches in this regard. The addition of TEO in GG/CAEE provided the UV-light blocking property which will protect light-sensitive food. The different film samples showed distinct film properties including surface wettability. The surface roughness and hydrophobicity were increased after the incorporation of TEO and CAEE. Increasing the concentration of TEO reduced surface wettability by decreasing water dissolvability. Further, CAEE and TEO addition superiorly increased the antimicrobial activity by slowing down the two most popular food pathogens (*E. coli* & *S. aureus*) growth. The water vapor transmission rate was significantly decreased with increasing the TEO concentration. The synergistic effect of TEO and CAEE was observed almost in the physicochemical properties of developed edible films. In this context, higher antioxidant activity was obtained in the optimum TEO and CAEE incorporated film sample. Moreover, the addition of TEO improved the mechanical property by enhancing the film flexibility. The outcome of this study emphasizes the potentiality of CAEE and TEO-incorporated edible films that can be tailored for specific applications as targeted food packaging material.

CHAPTER 6

OPTIMIZATION OF GUAR GUM-BASED ANTI-BROWNING COATING FOR SHELF-LIFE EXTENSION OF THE CUT POTATO

Edible coating formulations based on Guar gum (GG) (0-2 g/100 mL), algae extract (CAEE) (0-1 mL/100 mL), and turmeric essential oil (TEO) (0-1 mL/100 mL) were developed using a rotatable central composite design and its effect on the quality of sliced potato was studied at 27±3 °C for seven days. Besides, 30% glycerol, 5% calcium chloride, and 3% ascorbic acid (w/w) were added to the edible coating solution in constant quantity. The surface color, respiration rate, water vapor transmission rate, mold growth, and overall acceptability were analyzed after the 7th day of storage. The OTR, CTR, and WVTR of the coated sliced potato with GG concentration in the range of 0.5-1 g/100 mL in the coating formulation were lower than those of the control samples (coated with water). The higher concentration of GG showed a significant ($p < 0.001$) positive effect on OTR, CTR, and WVTR whereas, CAEE and TEO exhibited significant negative effects. The interaction between CAEE and TEO with GG showed significant effects on the WVTR value of coated cut potatoes. The optimized coating formulation (0.9 g/100 mL AG, 0.9 mL/100 mL CAEE, and 0.5 mL/100 mL TEO) maintained suitable internal gas composition to delay browning and drying and showed higher overall acceptability and shelf-life of 7 days at 27±3 °C compared to 2 days of control.

Outcome: Mondal K, Goud V. V, & Katiyar V. "Optimization of guar gum-based anti-browning coating for shelf life extension of the cut potato" (under preparation).

Graphical Abstract

The below schematic depicts the preparation of guar gum-based edible films incorporated with algae extract and turmeric essential oil along with other food additives and the application of the developed coating on potato cubes followed by a storage study of samples at room temperature to obtain the best coating formulation.

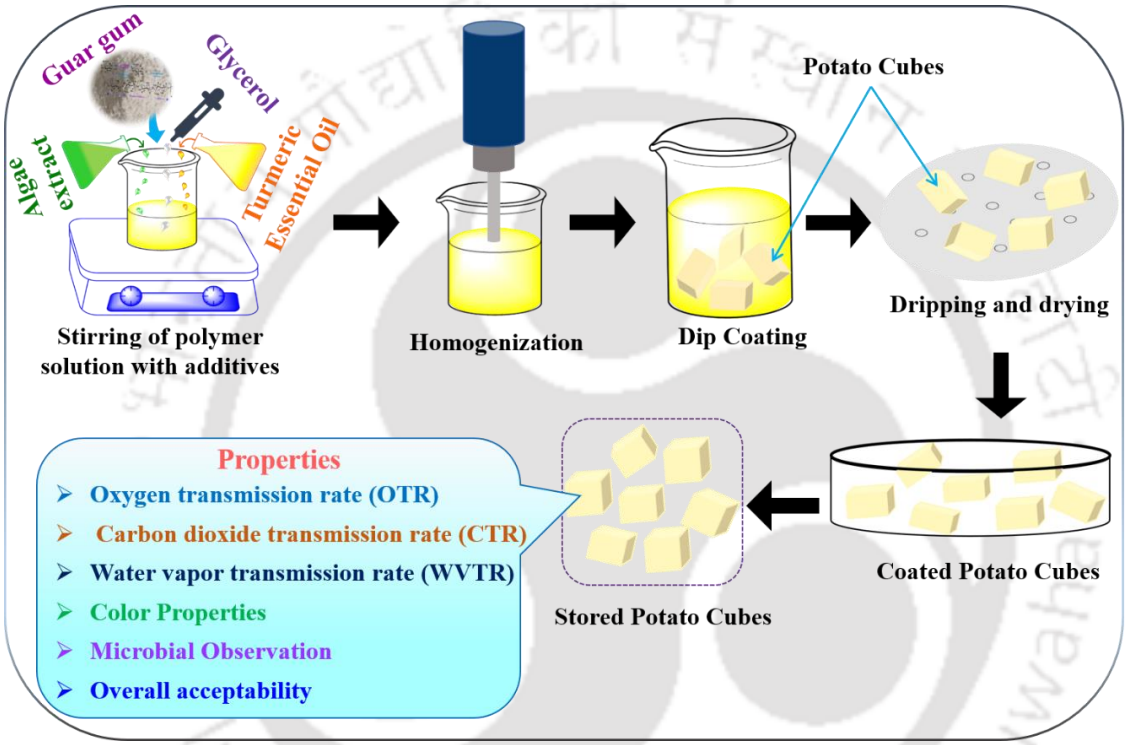

6.1 Introduction

Potato (*Solanum tuberosum L.*), is one of the most consumed agricultural products worldwide after rice, wheat, and maize. Most potato production is destined for commercial processing, followed by fresh table consumption and seed stock. The demand for potatoes for fresh markets and processing is year-round. It is the third-largest source of phenolic compounds in the human diet, after oranges and apples, due to its widespread consumption [214]. Potato polyphenols are considered antioxidants, anticarcinogenic, and antimutagenic agents [215] and effective against cancer cells in the human liver, colon, and prostate [216]. Colored flesh potatoes have higher antioxidant capacity compared with their white or yellow counterparts due to high levels of polyphenolic compounds [215]. Other important bioactive compounds of the potatoes are vitamin C and minerals [214]. Potato cultivars with yellow, purple- and red-colored flesh have high levels of flavonoids and carotenoids [213]. It is well understood that storing and processing foods change their physical and chemical structure, thus affecting their antioxidant activity. Potatoes are stored at low temperatures with high relative humidity [214]. The cut potatoes are prone to browning if stored under ambient conditions. In this context, low-temperature storage is preferred to store cut potatoes commercially until further use. However, this storage condition enhances the product cost of various potato-based products. For instance, the biopolymer-based edible coating can play a major role and possibly be applicable to extend the shelf-life of cut potatoes by arresting browning and microbial contamination. The inherent properties of edible biopolymers can be tuned by incorporation of EOs and plant or agricultural extracts. EOs are the secondary metabolite of aromatic plants, which has a wide range of biological activity and are generally recognized as safe (GRAS) elements by the FDA (American food and Drug Administration) [217].

This chapter emphasizes on the optimization of GG-based, algae extract (CAEE), and TEO-incorporated edible coating formulations to extend the shelf-life of cut potatoes by reducing browning and controlling the water vapor and gas transmission rate. Based on results obtained from chapter 5 and preliminary tests, the concentration range of GG, TEO and CAEE was selected. Further, calcium chloride as a crosslinking agent, glycerol as a plasticizer, and L-ascorbic acid as a source of vitamin C and anti-browning agent were added to the edible coating formulation. The optimization of edible coating formulation was performed by RSM using RCCD model. All the formulated solution were applied on cut potatoes at store for 7 days at room temperature. The aim of this work was to determine best edible coating formulation, developed by varying concentrations of GG, CAEE, and TEO for cut potatoes in order to reduce browning and prolong shelf-life.

6.2 Results and Discussion

6.2.1 Oxygen transmission rate (OTR)

The edible coating effect on the OTR, CTR, and WVTR values of cut potatoes due to the varying concentrations of GG, CAEE, and TEO are listed in **Table 6.1**. The coefficient of the regression equations for predicting the responses as a function of independent variables (GG, CAEE, and TEO) and their interaction parameters are depicted in **Table 6.2** including R^2 and lack of fit value. Generally, fruits should have a low oxygen transmission rate (OTR) as it would help to extend the shelf-life of the fresh perishables by reducing the carbohydrate breakdown and reducing early spoilage due to microbial and enzymatic effects. The coated fruits are expected to have a lower OTR value which would help in decreasing the rate of O_2 consumption and ethylene biosynthesis [218]. The effect of interaction parameters on OTR value has been depicted in **Figure 6.1**. In the present study, the OTR value of the control or uncoated cut potato was 39.38 cm^3/m^2 h atm.

Table 6.1: Response data of experimental table of guar gum formulation.

Run No.	X_1 (GG) (g/100 mL)	X_2 (CAEE) (mL/100 mL)	X_3 (TEO) (mL/100 mL)	OTR (cm^3/m^2 h atm)	CTR (cm^3/m^2h atm)	WVTR (g/m^2 h)	ΔE	Visible Mold	Overall Acceptability
1.	1.6 (1)	0.2 (-1)	0.8 (1)	50.92	132.68	16.81	67.56	0.8	1.1
2.	1 (0)	0.5 (0)	0.5 (0)	23.02	40.48	10.69	49.18	0	2.97
3.	1 (0)	0.5 (0)	0.5 (0)	24.41	45.61	7.26	50.11	0	2.96
4.	1 (0)	0.5 (0)	0.5 (0)	24.39	46.12	8.55	49.79	0	2.93
5.	1.6 (1)	0.8 (1)	0.8 (1)	47.09	110.61	14.89	59.18	0.02	1.01
6.	2 (1.68)	0.5 (0)	0.5 (0)	65.05	171.81	28.82	70.97	2.1	0
7.	1 (0)	0.5 (0)	0.5 (0)	24.33	73.59	8.35	48.61	0.07	2.95
8.	1.6 (1)	0.8 (1)	0.2 (-1)	34.62	93.83	16.1	52.45	1.81	1.11
9.	1 (0)	1 (1.68)	0.5 (0)	18.57	30.59	7.06	40.67	0	3.8
10.	1.6 (1)	0.2 (-1)	0.2 (-1)	39.43	112.07	21.89	54.57	3.98	0
11.	1 (0)	0.5 (0)	0.5 (0)	25.36	80.59	9.43	48.89	0	2.98
12.	0.4 (-1)	0.2 (-1)	0.8 (1)	26.07	88.02	28.76	56.45	1.26	1.57
13.	0.4 (-1)	0.2 (-1)	0.2 (-1)	33.69	95.37	31.15	58.56	1.69	1.6
14.	1 (0)	0.5 (0)	0.5 (0)	24.26	76.06	9.75	50.03	0	2.93
15.	0 (-1.68)	0.5 (0)	0.5 (0)	34.09	110.93	37.52	52.28	0.9	0
16.	1 (0)	0.5 (0)	1 (1.68)	23.77	98.92	11.23	53.34	0	0
17.	1 (0)	0.5 (0)	0 (-1.68)	26.30	50.51	16.74	51.47	1.71	0
18.	0.4 (-1)	0.8 (1)	0.8 (1)	27.48	67.90	26.12	48.12	1.21	0
19.	0.4 (-1)	0.8 (1)	0.2 (-1)	31.04	57.41	27.94	59.56	0.9	1.8
20.	1 (0)	0 (1.68)	0.5 (0)	27.78	114.88	17.85	49.67	1.59	0.5
Control	0 (-1.68)	0 (1.68)	0 (1.68)	39.38	115.79	20.57	65.55	4.8	0

However, a higher OTR value than the control was observed in the coated cut potato at a higher GG concentration from greater than 1 to 2 g/100 mL and the obtained values were in the range of 39 to 65 cm^3/m^2 h atm. Further, the optimum OTR value (65 cm^3/m^2 h atm) was obtained from the potato cube, coated with a higher GG concentration (2 g/100 mL). Further, a reduction in OTR value was noticed in potatoes coated with 0.5 to ≥1 g/100 mL GG, and a higher value was observed in potatoes coated with 0 to ≤ 0.5 g/100 mL GG. The lowest value of 18.57 cm^3/m^2 h atm was observed in potatoes coated with 1 g/100 mL GG. The reduction in OTR value in the range of GG concentration 0.5 to ≥1 g/100 mL could be attributed to the action of GG as the semipermeable membrane to O_2 exchange. Further, increasing the OTR value at a lower GG concentration (0 to ≤ 0.5 g/100 mL) might be due to a very thin coating thickness of GG failing to provide an appropriate barrier to O_2 transfer. On the other hand, a higher concentration of GG coating also increased the OTR value probably because of the thick coating, which might have caused the breakdown of the internal cell structure and anaerobic fermentation which could generate excessive heat and effective weight loss. Besides, not only polymer matrix, but bio-filler also influences controlling the various physicochemical property of coated fruits and vegetables. In this regard, several authors have reported on incorporating various types of extract in polymer material for edible coating [102], which helped to control the respiration rate of fresh produce. The plant or agricultural extracts are a rich source of polyphenols capable of arresting the generation of free radicles responsible for faster oxidation in oxygen-sensitive fruits and vegetables, enhancing the respiration rate. Increasing respiration rate deteriorates the quality and shelf-life of fruits and vegetables. Therefore, the addition of polyphenolic extract is preferable. The green algae ethanolic extract (CAEE) was added in the current study for edible coating formulation as a source of polyphenol-rich extract.

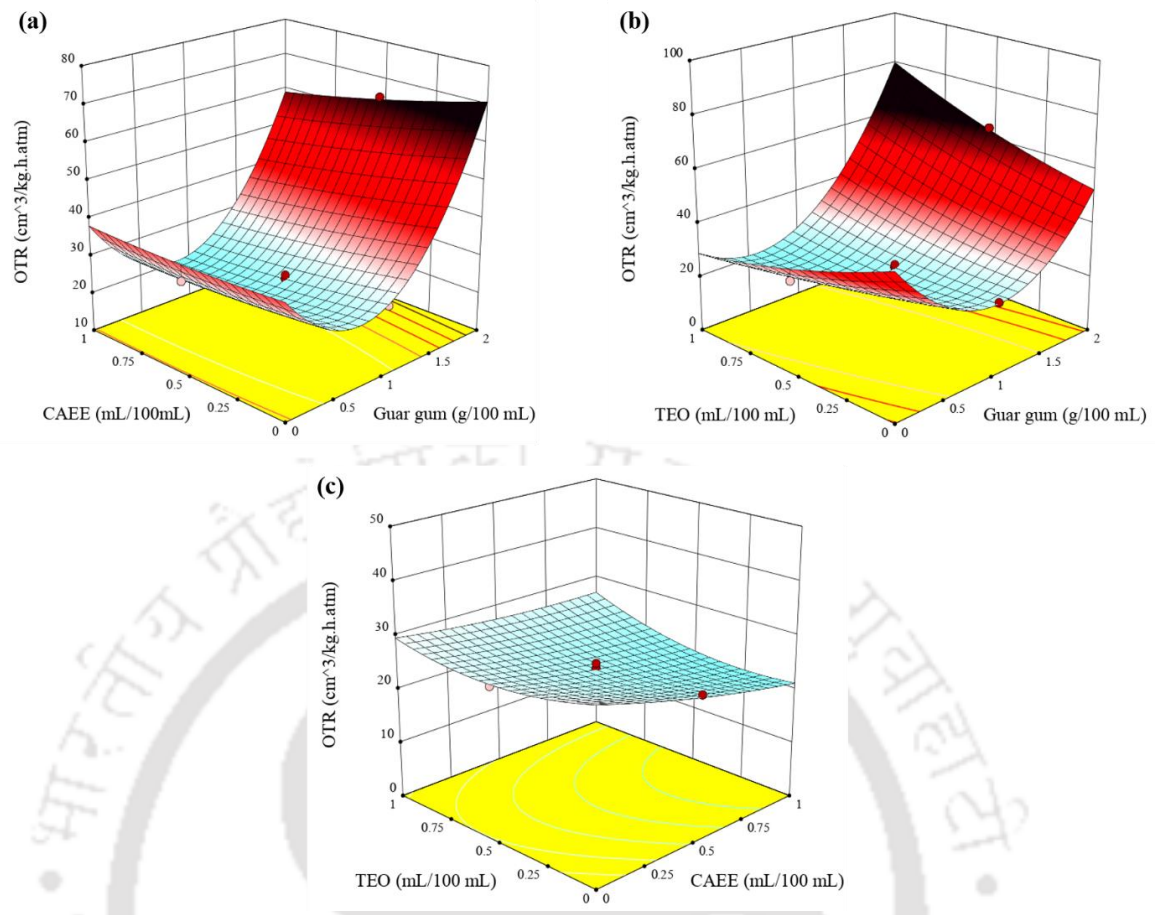

Figure 6.1: The effect of (a) algae extract and guar gum concentration, (b) turmeric essential oil and guar gum, and (c) algae extract and turmeric essential oil in the coating formulation on the oxygen transmission rate of cut potatoes after seven days of storage at room temperature.

The lowest OTR value (18.57 cm^3/m^2 h atm) was obtained in this study at a CAEE concentration of 1 mL /100 mL solution of the edible coating formulation. The potatoes coated with the formulation in absence of CAEE exhibited a higher rate of OTR. Although, the addition of ≤ 0.2 mL of CAEE showed a higher OTR value with a higher concentration of GG (50.92 cm^3/m^2 h atm), and a moderate range of value was found with a lower concentration of GG (26.07 cm^3/m^2 h atm). This observation indicates a low concentration of CAEE might not contain a sufficient amount of polyphenol to control the O_2 transmission rate in a higher concentration of polymer coating formulation. It was also noticed that the

addition of a higher amount of CAEE with a lower concentration of GG displayed a reduced OTR value.

The addition of EO has gained interest as a replacement for using toxic chemical agents as preservatives. The use of turmeric (*Curcuma longa*) in food and the addition of curcumin for the development of food packaging materials is common and widely used [34,174,206]. However, few studies have been done to explore the effect of TEO in edible coating applications. The TEO is a strong antimicrobial, antiseptic, antiallergic, antifungal, and antioxidant agent. The addition of TEO reduced the OTR value and exhibited effective performance when incorporated into a lower concentration of GG formulation. Furthermore, the lipophilic nature of the TEO might be the reason for to creation of a barrier membrane over the surface of the coated potatoes. The GG (linear and quadratic terms) displayed a significant ($p<0.001$) positive effect on OTR. The linear terms of CAEE exhibited a significant ($p<0.05$) negative effect on the OTR of potatoes, indicating increasing the concentration of CAEE decreases the OTR value. The interaction terms of GG and CAEE were not significant ($p = 0.38$). The effect of TEO was insignificant ($p = 0.44$) on interaction with CAEE.

Table 6.2: The coefficient of regression equations to predict the gas transmission rates, respiration rates, physical properties, and subjective quality scores of cut potatoes coated with different concentrations of guar gum, algae extract and turmeric essential oil.

Regression Coefficients	OTR (cm^3/m^2 h atm)	CTR (cm^3/m^2 h atm)	WVTR (g/m^2 h)	ΔE	Visible Mold	Acceptability
Intercept	24.19^{***}	60.53^{***}	8.93^{***}	49.31^{**}	0.0005^{***}	2.94^{**}
X_1-GG	7.75^{***}	17.78^{**}	-4.31^{***}	3.11^{**}	0.26^{**}	-0.13
X_2-CAEE	-1.86^{*}	-17.58^{**}	-2.32^{**}	-2.41^{*}	-0.47^{***}	0.38
X_3-TEO	0.62	8.93	-1.45	0.68	-0.58^{***}	-0.06
X_1X_2	-0.92	2.22	-0.23	-0.40	-0.26^{*}	0.30
X_1X_3	4.39^{**}	4.28	-0.26	4.16^{**}	-0.61^{***}	0.35
X_2X_3	0.63	1.75	0.56	-1.95	0.27^{*}	-0.37
X_1^2	9.61^{***}	27.84^{***}	9.06^{***}	5.11^{***}	0.60^{***}	-0.95^{***}
X_2^2	0.28	3.57	1.73^{*}	-0.71	0.35^{**}	-0.19
X_3^2	0.94	4.27	2.27^{**}	1.85	0.37^{**}	-0.95^{***}
R^2	0.97	0.89	0.96	0.88	0.97	0.87
Adjusted R^2	0.94	0.79	0.93	0.78	0.95	0.75
Lack of fit	0.001	0.73	0.02	0.0002	0.0001	0.0001

The significance at <0.05% level was indicated by '*', <0.01% level by '**', and <0.001% level by '***'.

6.2.2 Carbon dioxide transmission rate (CTR)

All the independent variables displayed a positive effect on the CTR value of coated potatoes except the linear term of CAEE. The linear term of CAEE showed an adverse effect ($p<0.01$), indicating increment of CAEE concentration reduced the CTR value of the potato. Further, the linear and quadratic terms of GG concentration exhibited a significant effect ($p<0.001$) on CTR, and TEO had a non-significant effect ($p = 0.07$). The effect of independent variables and their interaction on CTR values of coated cut potatoes has been

depicted in **Figure 6.2**. The CTR value of control potatoes was 115.79 cm^3/m^2 h atm. A higher CTR value (171.81 cm^3/m^2 h atm) was observed in potatoes coated with GG concentration 2 g/100 mL coating solution. The higher values of CTR in comparison to control were observed in potatoes at GG concentration in the range of >1 to 2 g/100 mL in the coating formulation. Further, the lower range of CTR was noticed in the range of 30 to 80 cm^3/m^2 h atm at the GG concentration of 0.4 to 1 g/100 mL coating solution. The higher CTR value could be attributed to the dense thickness of the coating layer outside the potato which might create complete sealing of passage of air between food and surroundings, as a result, anaerobic respiration occurred. This anaerobic respiration was responsible for high CO_2 evolution. Further, the incorporation of a higher concentration of CAEE reduces the CTR value which might be due to molecular interaction between the polymer matrix and CAEE polyphenolic components. Also, this type of interaction could restrict the polymer chain mobility which helps to reduce the OTR and CTR values [218]. Further, the interaction between the hydroxyl group of GG and the carbonyl group of CAEE and TEO establishes the esterification of GG, which did not reduce the amorphous region in GG matrix but could able to control the randomness of the polymer chain. Moreover, the presence of TEO contributes lipophilic moiety to the GG matrix which might create a rough path for easy transmission of gasses through the coating layer. Several authors have reported a similar reduced gas barrier property behavior of edible polymer coating where EOs (cinnamon, clove, lemon grass EOs) and plant extract was incorporated. Sometimes, the addition of a higher concentration of TEO enhances the CTR value which is probably due to the formation of a strong gaseous barrier between the food surface and surroundings which accelerates anaerobic respiration resulting in more CO_2 generation. Therefore, the ratio of polymer matrix and TEO should be such that it allows less transmission of O_2 and CO_2.

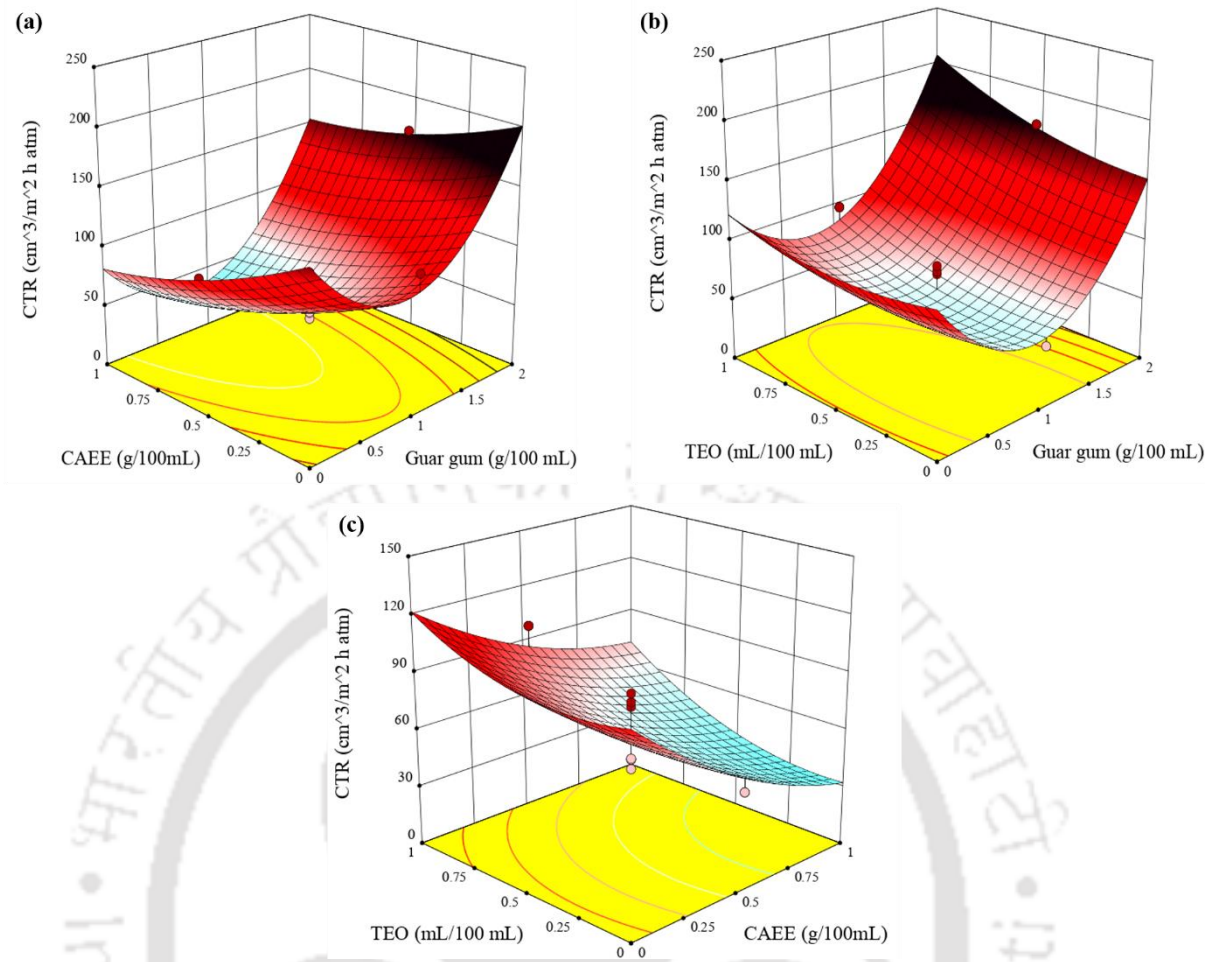

Figure 6.2: The effect of (a) algae extract and guar gum concentration, (b) turmeric essential oil and guar gum, and (c) algae extract and turmeric essential oil in the coating formulation on the carbon dioxide transmission rate of cut potatoes after seven days of storage at room temperature.

6.2.3 Water Vapor Transmission Rate (WVTR)

All the linear (X_1, X_2, & X_3) and two interaction coating parameters (X_1X_2 & X_1X_3) exhibited a significant negative effect ($p < 0.001$) on the WVTR value of coated potatoes. However, the effect of the TEO and interaction parameters was not significant. This observation indicated that increasing the concentration of GG, CAEE, and TEO decreases the WVTR values. The WVTR value of the control sample was 20.57 g/m^2 h. The minimum range of WVTR value (7 to 10 g/m^2 h) was observed in the potatoes coated with a GG concentration of 1 g/100 mL. The maximum WVTR value (37.52 g/m^2 h) was observed in

potatoes coated with 0.5 mL/100 mL of CAEE and TEO which could be due to the absence of GG and the presence of a lower concentration of TEO and CAEE might not be able to provide a semipermeable barrier. The WVTR of coated potato exhibited reduction with an increment of CAEE concentration which could be associated with the strong intermolecular hydrogen bonding between the GG matrix and CAEE, which probably allowed the formation of crosslinking, due to which the reduction in free space occurred inside the polymer matrix resulting in a lowered rate of water vapor molecules diffusion through the coating layer. Further, increasing the concentration of TEO reduced the WVTR value. This behavior could be attributed to the reduced binding ability and the increment of the tortuosity path for the vapor diffusion through the coated layer of the potato due to the presence of lipid globules [219]. Further at higher GG and lower CAEE concentrations, significant increment of WVTR was observed which might be due to lesser CAEE concentration could not be able to create strong intermolecular H-bonding. The presence of a higher amount of TEO also increased the WVTR value which might be due to the loss of interaction between TEO and GG-matrix, resulting in the widening of free space and increasing the ease of chain movement [220]. Further, an increment of ~20% WVTR value was observed in potato cubes coated with GG concentration 2 g/100 mL of the coating solution. It was noticed that in some cases GG concentration of more than 1 g/100 mL exhibited higher WVTR which could be due to the enhancement of the total hydrophilic group than the hydrophobic in the mixture of the coating formulation.

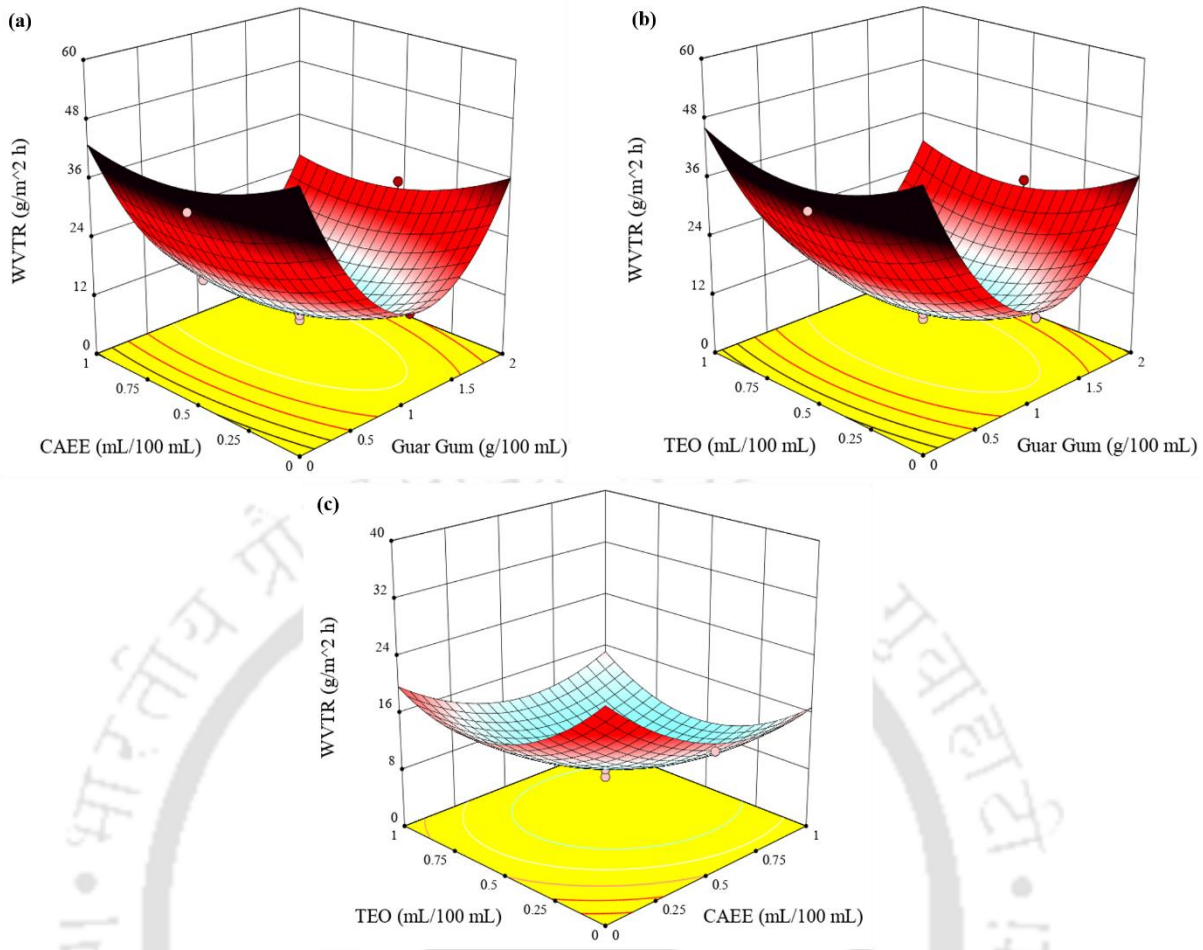

Figure 6.3: The effect of (a) algae extract and guar gum concentration, (b) turmeric essential oil and guar gum, and (c) algae extract and turmeric essential oil in the coating formulation on the water vapor transmission rate of cut potatoes after seven days of storage at room temperature.

6.2.4 Color Properties

Coating over any fruits and vegetables may mask their original color. Therefore, monitoring the total color difference (ΔE) is one important parameter. The storage study was performed for 7 days and a remarkable change in ΔE was observed between control and coated potatoes at the end of the storage study. The linear and quadratic terms of GG concentration exhibited significant positive effects on ΔE value ($p<0.001$) (**Figure 6.4**). However, linear, interaction, and quadratic terms of CAEE had a negative effect on ΔE value indicated increasing the CAEE concentration reduced ΔE value. Further, the

interaction parameter of GG&TEO displayed a negative effect. The ΔE increased steeply over the storage time in comparison to coated samples which showed a comparatively gradual increase after day 3 of storage (data not shown). The ΔE value of the control (uncoated) potato was 65.55 on the 7th day of storage which increased significantly from zero-day, whereas coated sample exhibited slow enhancement. The lowest ΔE value was observed as 40.67 in the cut potatoes coated with GG (1 g/100 mL), CAEE (1 mL/100 mL), and TEO (0.5 mL/100 mL).

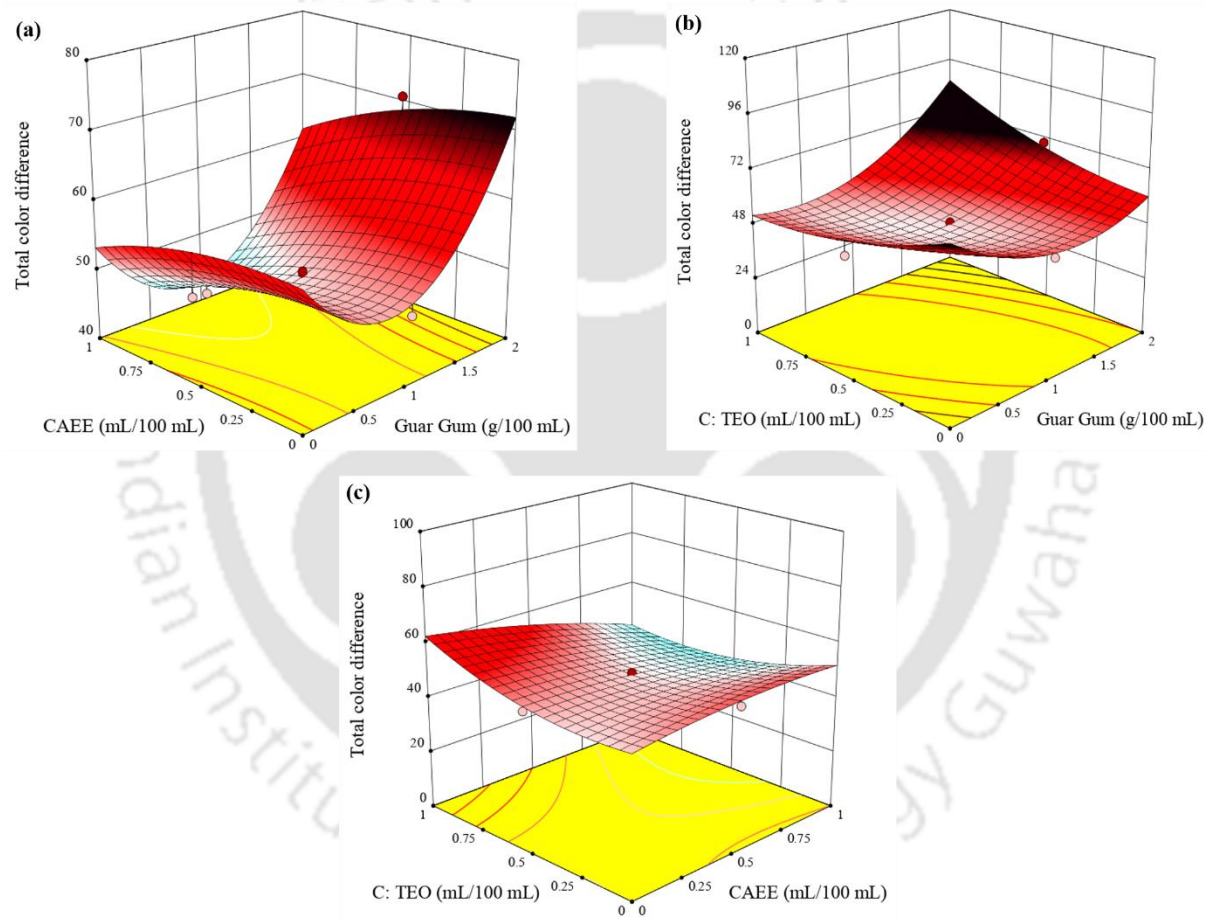

Figure 6.4: The effect of (a) algae extract and guar gum concentration, (b) turmeric essential oil and guar gum, and (c) algae extract and turmeric essential oil in the coating formulation on the total color difference of cut potatoes after seven days of storage at room temperature.

This observation could be attributed to the reduction in the polyphenol oxidase (PPO) activity, which is naturally present in potatoes and responsible for causing brown or black discoloration when gets oxidized. This oxidation occurs when PPO encounters O_2. Therefore, this observation indicated coating could be able to act as a semipermeable membrane and reduce oxidation by prohibiting the O_2 transmission rate. Besides, TEO is a rich source of polyphenols due to the presence of ar-turmerone, curlone, and ar-curcumin. Therefore, TEO might be acted as an anti-browning agent and suppress the polyphenol oxidase activity. However, the addition of a higher concentration of TEO accelerates the browning activity. Moreover, a synergistic effect was observed in potatoes coated with CAEE along with TEO, which effectively suppresses browning thereby minimum difference was obtained in ΔE value.

6.2.5 Visible mold appearance

The highest count of appearance of visible mold was observed in the control potato at 4.8 after 7 days of storage. **Figure 6.5** depicts the effect of interaction parameters on the visible mold count of coated cut potatoes during storage. It was observed that GG concentration (linear and quadratic) displayed a positive significant ($p<0.01$) effect on mold count. However, CAEE and TEO (linear) exhibited a negative significant (linear and interaction) effect ($p<0.001$) on coated potatoes. A positive significant effect was observed ($p<0.01$) for all quadratic terms of GG, CAEE, and TEO. The negative effect indicated increasing the concentration of CAEE and TEO reduced the visible mold count. This observation suggested the antimicrobial nature of CAEE and TEO. However, TEO displayed a strong antimicrobial effect than CAEE which could be due to the presence of the bioactive compound curcumin. Further, increasing the GG concentration enhanced the microbial count, possibly due to the composition of GG, a mixture composed of two carbohydrates of galactose and mannose. Therefore, GG acted as a rich source of food for the microbes.

There was no mold count visualized in potatoes coated with a higher concentration of TEO and CAEE with a lower concentration of GG.

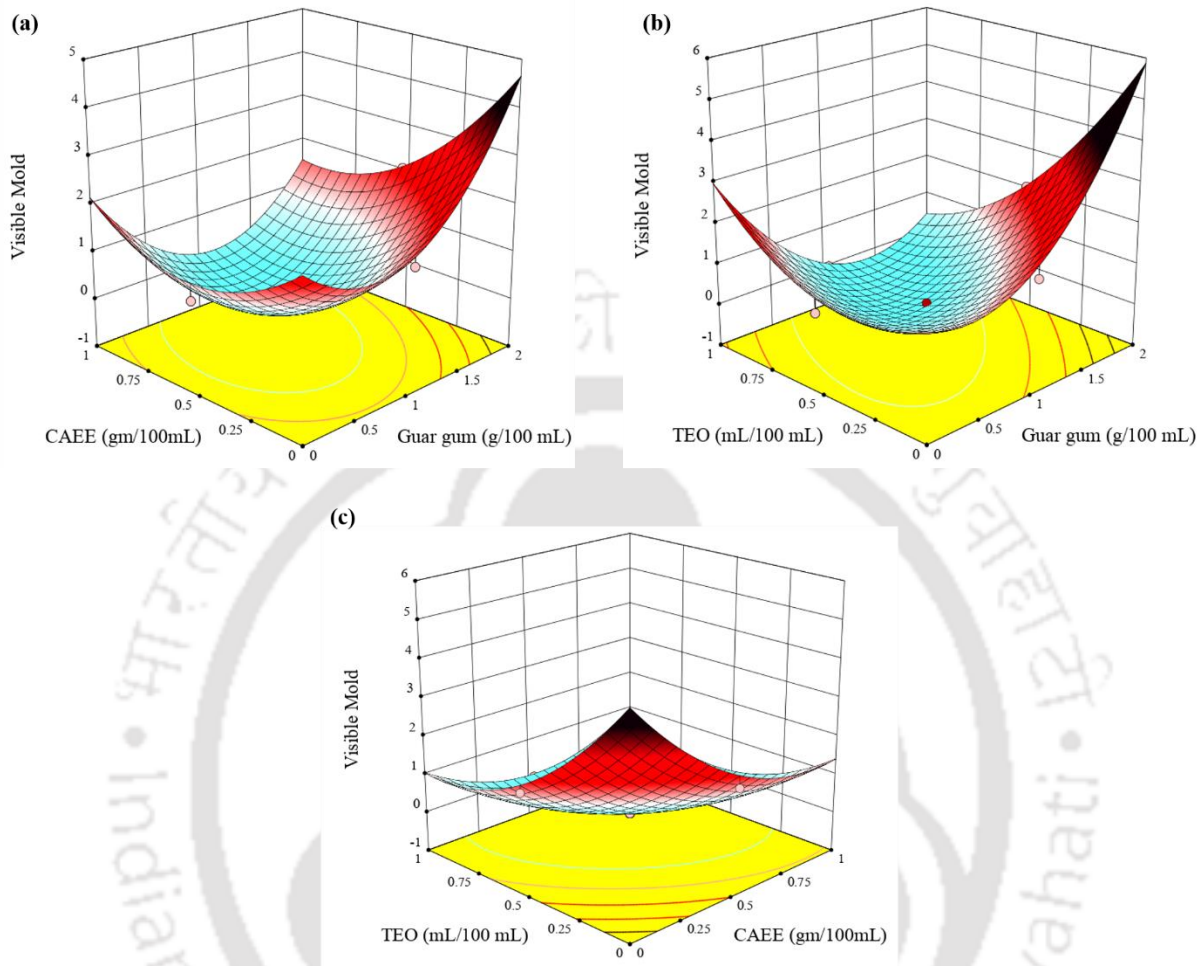

Figure 6.5: The effect of (a) algae extract and guar gum concentration, (b) turmeric essential oil and guar gum, and (c) algae extract and turmeric essential oil in the coating formulation on the visible mold of cut potatoes after seven days of storage at room temperature.

6.2.6 Overall Acceptability

The overall acceptability of the cut potato was based on the consumer's preference for the external appearance of the potato. The figure depicted the overall acceptability of potatoes as a function of GG and CAEE concentration. There was a significant ($p<0.001$) negative

effect (quadratic) and non-significant negative effect (linear) of GG and TEO observed in coated potatoes.

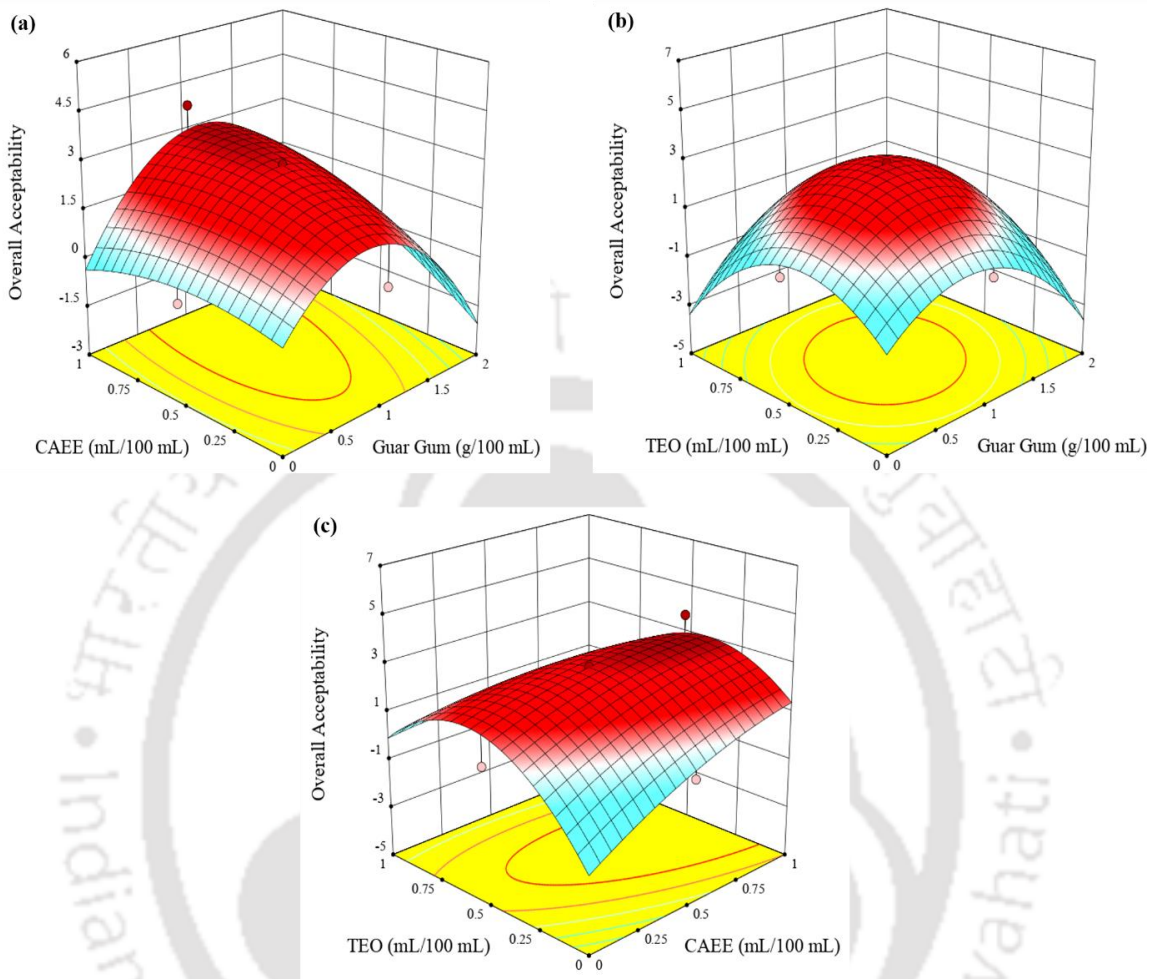

Figure 6.6: The effect of (a) algae extract and guar gum concentration, (b) turmeric essential oil and guar gum, and (c) algae extract and turmeric essential oil in the coating formulation on the overall acceptability of cut potatoes after seven days of storage at room temperature.

Further, the CAEE had non-significant positive (linear) and negative (quadratic) effects on the overall acceptability of potatoes. The control sample registered black color and mold count, hence was considered unacceptable (score 0 out of 5) after seven days of storage. Excessive weight loss and shrinkage and black coloration were observed in potatoes coated with a higher concentration of GG (>1 g/100 mL coating solution), which was

unacceptable. Further, a relatively higher acceptance value (score of 2.98 out of 5) was observed in potatoes coated with a GG concentration of 0.5 to 1 g/100 mL coating solution. The highest overall acceptance (3.8) was obtained in potatoes coated with GG, CAEE, and TEO concentrations of 1 g/100 mL, 1 mL/100 mL, and 0.5 mL/100 mL, respectively.

6.2.7 Optimization

The appearance of visible mold was significantly affected by the three factors namely, GG, CAEE, and TEO as well as their interactions (**Table 6.3**). The O_2 and CO_2 transmission rate, and WVTR of the coated samples are significantly correlated to the mold that appears on the coated potatoes. Therefore, based on the co-relation among responses the optimization was done by (i) minimizing the O_2 transmission rate, (ii) minimizing the CO_2 transmission rate, (iii) minimizing the WVTR transmission rate, (iv) minimizing the total color difference (ΔE), (v) minimizing the visible mold count, and (vi) maximizing the overall acceptability. The optimized condition was 0.9 g/100 mL GG, 0.9 mL/100 mL CAEE, and 0.5 mL/100 mL TEO with desirability of 0.91.

The obtained optimum concentration of GG, CAEE, and TEO a new coating formulation was prepared and applied on three batches of sliced potato using the dipping method as mentioned in the previous section and stored at room temperature (27±3 °C, 70-80% RH) for 7 days. The sliced potato was dipped into Millipore water and used as the control. The initial rate of respiration and water transmission was measured. **Table 6.3** depicts the observed and predicted values of the responses of cut potatoes coated with the optimized coating formulation. No such significant difference was observed between predicted and experimental values. The cut potatoes coated with optimum coating formulation showed no mold growth after seven days of storage and acceptability was higher to the panel. Therefore, the optimized coating formulation (0.9 g/100 mL GG, 0.9 mL/100 mL CAEE, and 0.5 mL/100 mL TEO) can be used to extend the shelf-life of cut potatoes without

browning defects up to seven days of storage at room temperature (27±3 °C, 70-80% RH) as compared to uncoated samples.

Table 6.3: The experimental and predicted rate of response parameters of cut potatoes coated with the optimized coating formulation (0.9 g/100 mL GG, 0.9 mL/100 mL CAEE, and 0.5 mL/100 mL TEO) after seven days of storage at 27±3 °C (room temperature) and 70-80% RH.

Response Parameters	Predicted	Experimental	Desirability
Oxygen transmission rate (OTR)	21.74	26.15	0.91
Carbon dioxide transmission rate (CTR)	40.84	37.63	
Water vapour transmission rate (WVTR)	9.38	11.21	
Total color difference (ΔE)	44.79	41.25	
Visible mold appearance	0.05	0	
Overall acceptability	3.16	4.7	

6.3 Summary

The significant effect of GG, CAEE, and TEO was observed on the O_2, CO_2, and water vapor transmission rate value of coated cut potatoes as compared to the uncoated control. Coating formulations containing GG concentration less than 0.5 g/100 mL were too thin to slow down respiration, ripening, senescence, and mold growth whereas, those with GG concentration greater than 1 g/100 mL resulted in too thick coating resulting in a high rate of O_2, CO_2, and H_2O transmission, and adversely affected the acceptability of cut potato following 7 days of storage at room temperature due to occurrence of black color. The optimized coating formulation was 0.9 g/100 mL GG, 0.9 mL/100 mL CAEE and 0.5 mL/100 mL TEO. Cut potatoes coated with the optimized formulation exhibited no mold

growth, and no surface black color generation and were highly acceptable to the panel member. Hence, the optimum formulation may be used to extend the shelf-life of the cut potatoes up to 7 days at 27±3 °C compared to the control cut potatoes which was unacceptable after one day of storage.

CHAPTER 7

DEVELOPMENT OF CELLULOSE NANOCRYSTALS (CNC) AND ALGAE BIOMASS INCORPORATED PLA AND PCL BIO-COMPOSITES FOR SECONDARY PACKAGING

Marine green algae biomass residue (ABR), a waste by-product of Dunaliella tertiolecta, left behind after the extraction of oil from the algal biomass, was utilized for the fabrication of cellulose nanocrystals (CNCs). The fabricated sulfuric acid hydrolyzed CNCs had needle-like morphology, with dominant cellulose type I polymorph and a high crystallinity index of 89%. Two types of bio-fillers i.e., Washed ABR (WABR) and CNC were used separately for the comparison of physicochemical properties between fabricated bio-composites. PLA/WABR, PCL/WABR, PLA/CNC, and PCL/CNC bio-composite films were developed via solvent casting technique with varying bio-filler loadings for comparing their effects on the crystallization behavior of PLA and PCL. FESEM, FTIR, XRD, and TGA were used to characterize the bio-fillers. The nucleating and crystallization behavior of the bio-composite films were confirmed using DSC, SAXS, and POM analysis which indicated better effectiveness of CNCs with a significant reduction in cold crystallization temperature in PLA bio-nanocomposite and enhancement in crystallization temperature in PCL bio-nanocomposite, and noteworthy increment in crystallinity and spherulite growth rate.

Outcome: Mondal K, Sakurai S, Okahisa Y, Goud V. V, & Katiyar V. (2021). "*Effect of cellulose nanocrystals derived from Dunaliella tertiolecta marine green algae residue on the crystallization behavior of poly(lactic acid)*." Carbohydrate polymers, IF:10.723, 261, 117881.

Mondal K, Sakurai S, Goud V. V, & Katiyar V. (2021). "*Utilization of microalgae residue and isolated cellulose nanocrystals: A study on crystallization kinetics of poly(ε-caprolactone) bio-composites*." International Journal of Biological Macromolecules, IF:8.025, 5191, 521-530.

Graphical Abstract

This schematic describes the isolation of cellulose nanocrystals from waste algae biomass residue and the fabrication of sustainable bio-composite films using separately two different bio-fillers CNC and algae waste powder by a solvent casting technique and their detailed characterization.

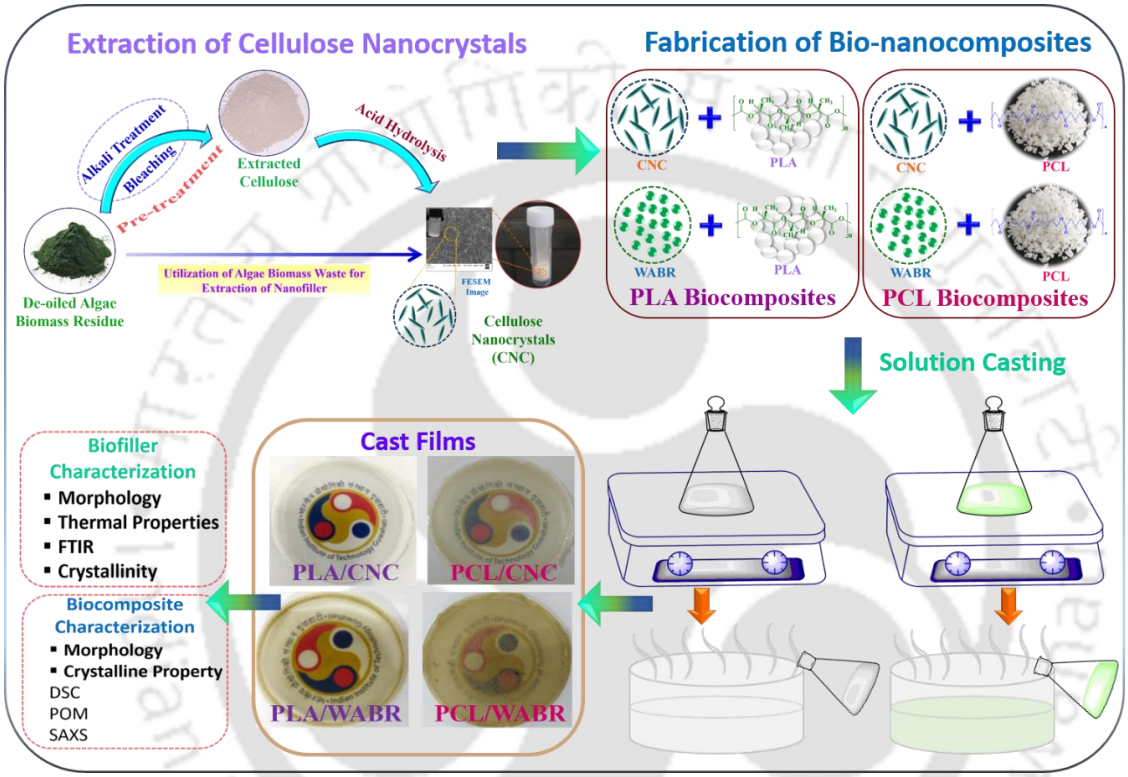

7.1 Introduction

'Algae' are complex organisms that represent one of the cheapest and vastly available sources for next-generation bio-filler [168]. In comparison to plant fibers, the cellulose content of algae is less [67]. The use of algae as an additive in the packaging industry is limited due to its unknown properties as a natural fiber in the polymer matrix. Nevertheless, algae have been employed in the pharmaceutical, food, agricultural and cosmetic industries for many years and it is a healthy source of various micronutrients [53]. Losic et al., (2009) reported diatom frustules as the main component of algal ash which could elevate a polymer's thermal stability and resistance [221]. Thus, the incorporation of microalgae in a polymer matrix can lead to the modification of polymeric properties. Further, utilizing algae will help in controlling the excess unnecessary bloom created over a water body. Predominantly, algae are cultured for biodiesel production by utilizing algal oil. However, the residual part of algae commonly known as the 'waste' or algae biomass residue (ABR) generates difficulties in waste disposal in the environment [222]. This algal waste can be utilized as a cellulosic source material for the extraction of cellulose nanocrystals (CNCs).

CNCs are a type of benignant bio-fillers and/or reinforcing agents, made up of an ordered crystalline structure and possess excellent physical characteristics. Several reports have been published establishing CNCs as non-abrasive, non-toxic, biodegradable, and biocompatible, and its use as bio-filler has a high impact on the development of bio-composites [223]. In addition, nanocellulosic materials have been derived from various algae including *Cladophora rupetris* [223], *Gelidium sesquipedale* [92], *Gelidium elegans* [224], and *Capsosiphon fulvescens* [225].

The rising concern regarding the minimization of plastic waste accumulation leads to an increasing interest in using biodegradable plastics as an alternative. However, the usage of biodegradable plastics for packaging and commodity applications has encountered many

limitations such as high manufacturing cost, processing difficulty, and poor inherent characteristics of the biopolymers. Nowadays, poly(lactic acid) (PLA) and poly(ε-caprolactone) (PCL) are being utilized by the packaging industry due to their biodegradability, biocompatibility, and other favorable characteristics [226, 227]. Nevertheless, the development of blends and composites of PLA and PCL requires tailoring their poor inherent characteristics such as barrier properties [226]. For instance, the incorporation of algal CNCs and natural fibers into the matrix material as a bio-filler helps to reduce the cost of the material as well as tunes its properties without altering its biodegradability.

In this chapter, ABR from *Dunaliella tertiolecta*, a green marine water microalga, was utilized to extract CNCs and the development of PLA/CNC and PCL/CNC bio-nanocomposite films. The fabricated films were characterized to observe the changes in their crystalline behavior. In order to compare the crystallization property, WABR (washed algae biomass residue) was also used as a bio-filler for developing PLA/WABR and PCL/WABR bio-composites. The bio-fillers were characterized for their physicochemical properties. This study focuses on the high-end utilization of algae waste as a natural fiber for the fabrication of bio-composites.

7.2 Results and Discussion

7.2.1 Extraction of Cellulose and Fabrication of CNCs

Algal cellulose is a mixture of crystalline and amorphous polymers [228], like other lignocellulosic substances. However, chemical treatment of cellulose is required for the removal of the amorphous components. Since these amorphous substances are associated with the cellulosic backbone, the physicochemical nature of the extracted cellulose depends on the chemical treatment. The alkaline and bleaching treatment was used to remove various soluble mineral salts, silica, ash, hemicelluloses, and lignin, resulting in an ease of

cellulose extraction from the ABR [223]. The removal of non-cellulosic components from ABR was confirmed visually *via* changing in color from green to a whitish suspension (**Figure 7.1a**). In this study, H_2SO_4-hydrolyzed CNCs displayed negatively charged sulfate groups on the surface of the nanoparticles via esterification. Accordingly, the yield of the obtained CNCs from the ABR was found to be 20-30%.

7.2.2 Morphological Properties

The morphological characteristics of the ABR, WABR, and isolated CNCs were investigated by FESEM. The surface of the ABR indicated an irregular geometrical shape with aggregated chunks of big and small particles, and a layered-type morphology (**Figure 7.1b**). Similar irregular surface morphology was observed in the WABR. Further, the smooth-layered surface indicated the presence of inorganic salts (**Figure 7.1c**) which was in accordance with the study conducted by Bulota & Budtova (2015) [140]. The layered flake-type morphology had also been reported for green, brown, and red algae [67]. The average diameter of the ABR particles was calculated to be ~3µm. The acid-hydrolyzed freeze-dried CNCs showed needle-like morphology (**Figure 7.2d**) with an average length of 520-700 nm, an average diameter of 30±5.2 nm, and a low aspect ratio of ~23. The higher loading of WABR enhanced the greenish tint in bio-composites (**Figure A6**). Homogeneous distribution of CNCs was observed inside the PLA matrix for 0.5 wt.% loading whereas, higher loading showed slight agglomeration (**Figure A7**).

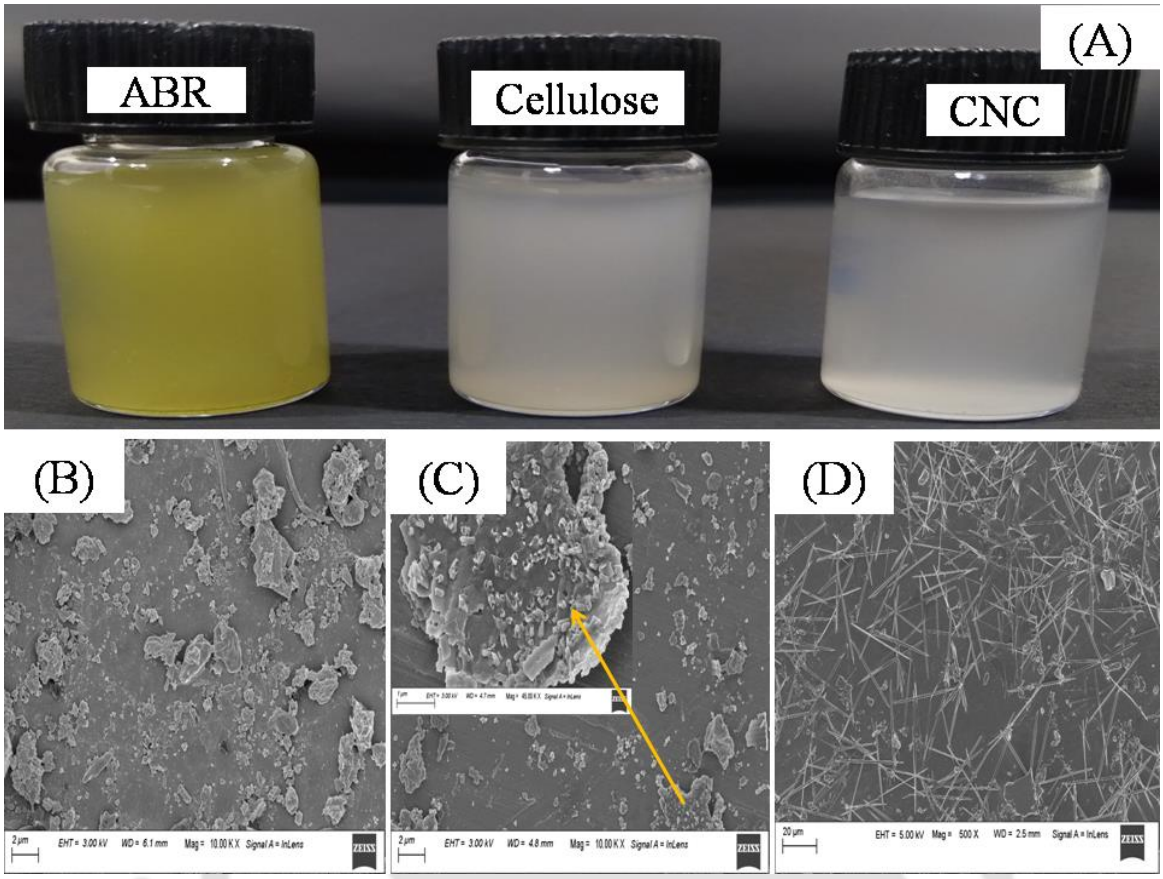

Figure 7.1: (a) Photographs of ABR, cellulose, and CNC suspension. FESEM micrographs of (b) ABR, (c) WABR, and (d) *Dunaliella* CNCs.

7.2.3 Thermal Properties of the Bio-fillers

TGA and derivative thermograms depict the thermal stability of the bio-fillers (**Figure 7.2**). The observed mass loss first occurred between 50-100 °C and was more prominent in ABR and WABR in comparison to extracted cellulose and CNCs. This mass loss probably arose due to the degradation of chlorophyll and adsorbed water [229], which was less in CNCs as most of the chlorophyll was removed during the extraction. The onset (T_{onset}) and maximum degradation temperature (T_{max}) for ABR, WABR, cellulose, and CNCs are summarized in **Table A6**. Thermal stability was improved in cellulose and extracted CNCs as compared to ABR and WABR due to the removal of the amorphous region. The double degradation behavior of ABR, WABR was associated with hemicellulose and lignin,

whereas two major weight losses, between 200-300 °C, and 300-400 °C were observed in CNCs due to the degradation of cellulose affected by H_2SO_4 hydrolysis [230].

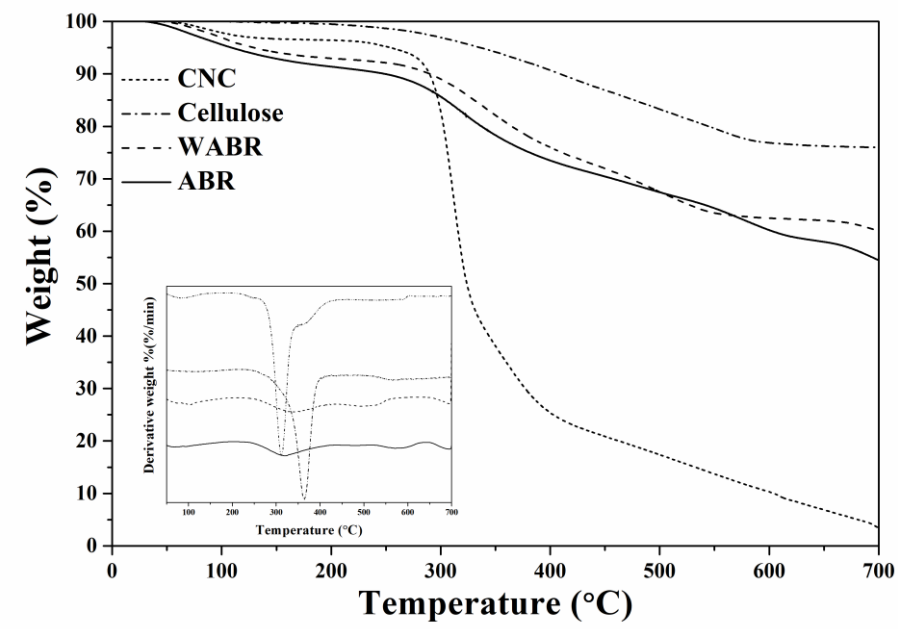

Figure 7.2: Thermogravimetric curves of ABR, WABR, cellulose, and CNCs from *Dunaliella tertiolecta.*

The second maximum degradation in algal cellulose at ~517 °C was observed which could be associated with lignin. However, the T_{onset} values of CNCs were lower than cellulose, due to the presence of sulfate groups on the surface of CNCs, which reduced their thermal stability. The residual mass of ABR, WABR, algal cellulose, and CNCs obtained after completion of the TGA cycle, was found to be 54%, 60%, 75%, and 3%, respectively. Cellulose had a high residual value due to the presence of inorganic component such as Si, Fe, Na, K, Mg, P, Cl, S, Sr and others which was not removed during pre-treatment and confirmed by ICPMS analysis. However, a trace amount of residual components was observed in CNCs as most of the inorganic salts were eliminated during acid hydrolysis. Faster degradation was observed in PLA/CNC bio-nanocomposites (**Figure A8**).

7.2.4 FTIR and XRD Analysis

FTIR analysis was conducted to determine the occurrence of chemical changes in the functional groups during the extraction process of the CNCs (**Figure 7.3**). The presence of aromatic (C=C) stretching of lignin in ABR and WABR was confirmed by the occurrence of the bands at 1416 cm^{-1} and 1528 cm^{-1}, and the band at 1228 cm^{-1} corresponded to C-O-C (aryl-alkyl ether) stretching, associated with hemicelluloses. However, these bands disappeared in CNCs, indicating the complete removal of lignin and hemicelluloses [223]. The presence of 1643 cm^{-1} and 2916 cm^{-1} absorbance bands indicated the stretching vibration of the O-H and C-H groups. The broad peak from 3400 to 3200 cm^{-1} region corresponded to the stretching vibration of O-H and adsorbed water. The band at 1022 cm^{-1} is related to the C-O-C pyranose ring associated with cellulose. The intensity of this peak increased gradually from ABR to CNCs due to the enhancement of cellulosic content and removal of the amorphous region. The band at 870 cm^{-1} corresponded to β-glycosidic linkages between anhydroglucose rings in cellulose, which completely disappeared in CNC and indicated the elimination of the amorphous region [231]. Moreover, FTIR analysis confirmed the effective extraction process for CNCs.

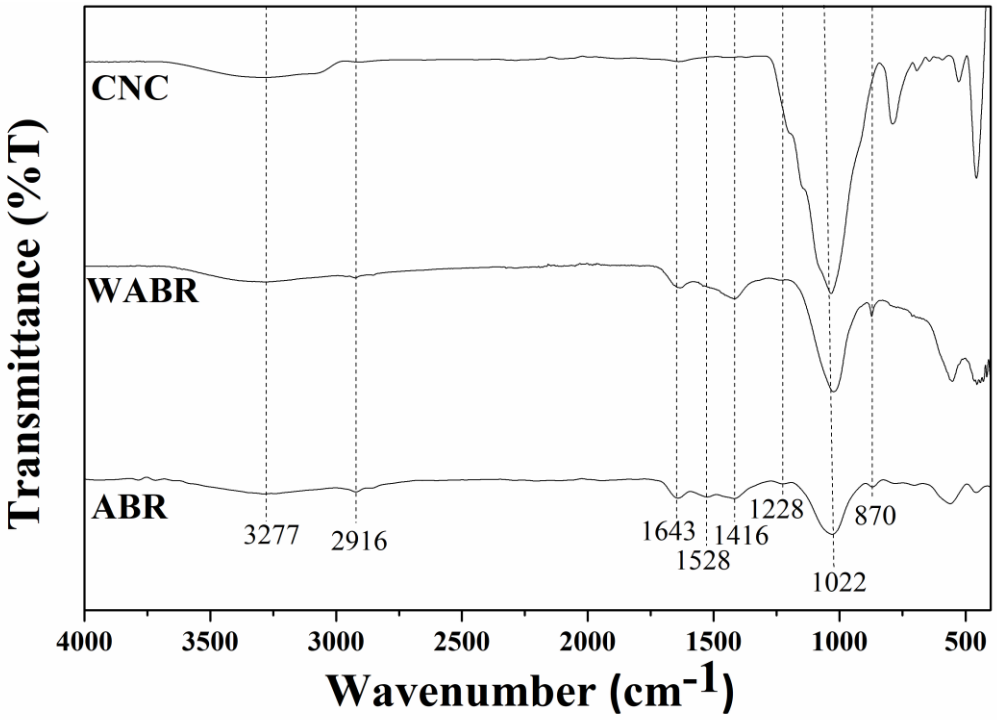

Figure 7.3: FTIR spectra of ABR, WABR, and CNCs obtained from *Dunaliella tertiolecta.*

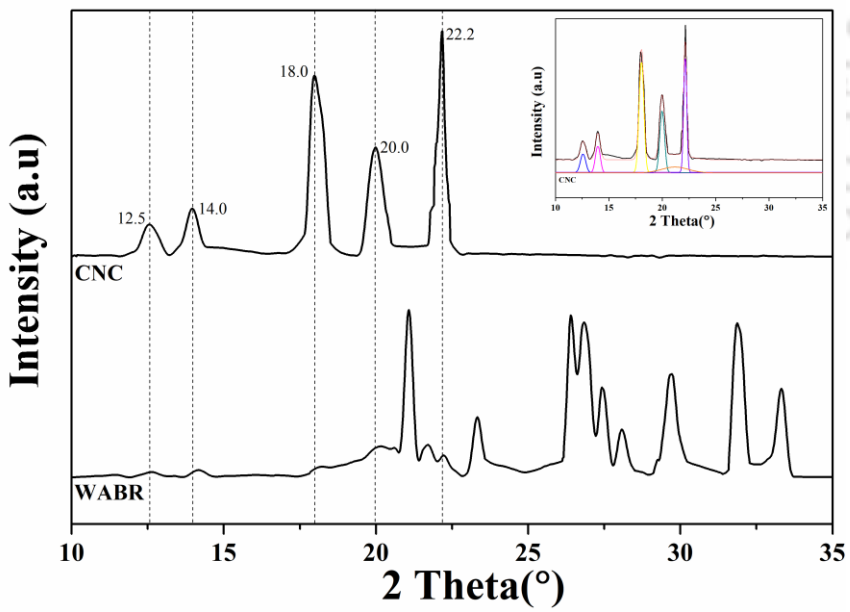

Figure 7.4: XRD diffraction patterns of WABR and CNCs obtained from *Dunaliella tertiolecta.*

Figure 7.4 represents the XRD patterns of CNCs and WABR. Several peaks of WABR were found in the XRD spectra corresponding to the presence of many inorganic elements and their salt crystals. The obtained result was vindicated by the ICPMS analysis (**Table**

3.1). However, along with these inorganic contents, a small amount of cellulose was also observed in WABR at 2θ = 12.5°, 14.2°, 18.0°, 20.0°, and 22.2°, corresponding to different polymorphs of cellulose [230]. The isolated CNCs showed intensified characteristics peaks at 2θ = 12.5°, 14.2°, 18.0°, 20.0° and 22.2°. According to the literature, peaks at 2θ = 14.2°, 18°, and 22.2° associated with cellulose I whereas, 12.5° and 20.0° represent cellulose II structure [231,232]. Interestingly, two different intensified cellulosic polymorphs were observed in CNCs as compared to WABR due to the removal of the amorphous region, among them cellulose I was predominant. The occurrence of different intensified cellulosic polymorphs in CNCs could be due to the pre-treatment processing step where celluloses were exposed to alkali and bleaching treatment repeatedly [232]. Further, for better understanding normalization of CNC spectra was evaluated (**Figure 7.4**). The I_{Cr} values of WABR and CNCs were determined as 74% and 89%, respectively. The I_{Cr} was significantly higher in CNCs in comparison to WABR, which might be due to the removal of amorphous and other impurities. Additionally, reported literature supported the findings since Cellulose I was found to be predominant in the fabricated CNCs and CNFs (cellulose nanofiber) from various algae [223].

7.2.5 Crystallization Behavior of the PLA Bio-composites

7.2.5.1 DSC Analysis

- ***Non-isothermal Study***

Non-isothermal DSC analysis was performed to reveal the effectiveness of the bio-fillers on the phase transition behavior of the bio-composites during the second heating process. The representative thermograms of the PLA/WABR and PLA/CNC bio-composites have been illustrated in **Figure 7.5a,b**. The glass transition (T_g), cold crystallization (T_{cc}), and melting (T_m) temperatures of neat PLA (nPLA) were found to be 58.2 °C, 135.8 °C, and 167.1 °C, respectively. The obtained T_g and T_m values of all the WABR bio-composites

were similar to nPLA (Table A7). However, the T_{cc} was found to be significantly variable in comparison to nPLA. The reduction in T_{cc} for 0.5, 1, and 2 wt.% WABR loadings was by 12.5 °C, 12 °C, and 13 °C, respectively, indicating the possible nucleation effects of WABR (**Figure 7.5a**), whereas the T_{cc} reduction was obtained in PLA/CNC bio-nanocomposites by 16.5 °C, 20.7 °C, and 24.3 °C, respectively (**Figure 7.5b**). In this context, the developed CNC bio-composites showed a higher reduction in T_{cc} as compared to reported grafted PLA/CNC nanocomposites where a maximum of 13.9 °C reductions were obtained for 3 wt.% CNC [192] which could be related to varying morphology, source material, and processing parameters of CNC.

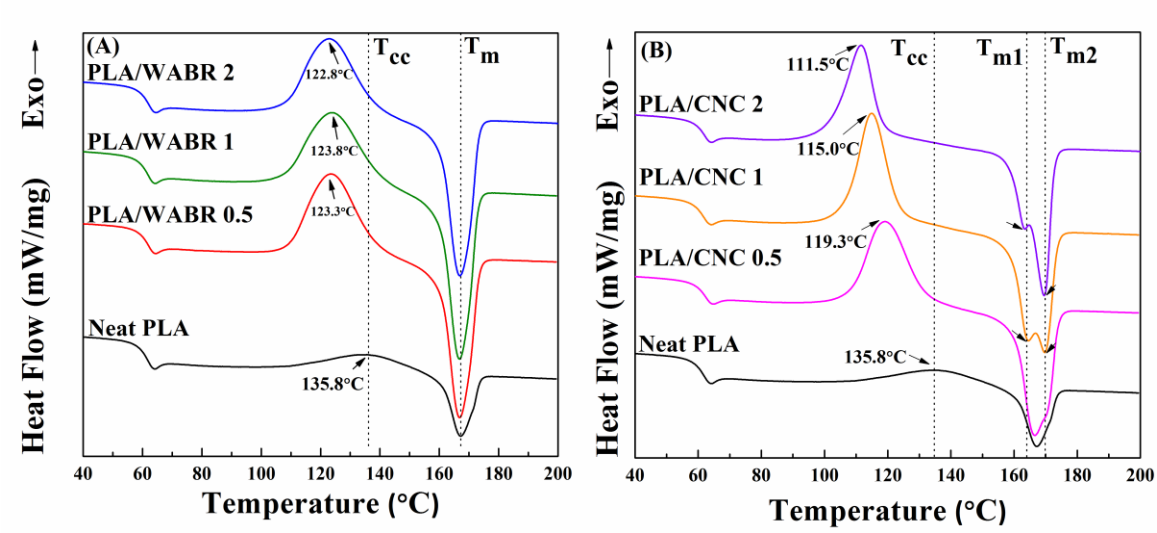

Figure 7.5: DSC non-isothermal thermograms of: (a) PLA/WABR bio-composites, (b) PLA/CNC bio-nanocomposites.

Further, the PLA/CNC bio-nanocomposite was highly effective in providing the crystallizing effect in comparison to the PLA/WABR. One of the probable reasons for the less nucleating effect of WABR might be the presence of the silica platelets, which possessed low surface energy. Interestingly, a double melting peak was observed in the PLA/CNC films (**Figure 7.5b**). These low (T_{m1}) and high (T_{m2}) temperature peaks corresponded to the α' and α crystals, indicating polymorphism of PLA [233]. For a

detailed understanding of the crystallization behavior, an isothermal crystallization kinetics study was conducted based on the significant changes in the T_{cc} values.

- ***Isothermal Study***

An isothermal crystallization study was conducted to understand the detailed influence of the bio-fillers on nucleation efficiency in the PLA matrix at 110 °C. It has also been reported in the existing literature that in the temperature range between 105-110 °C, the crystallization of PLA from the melt is maximum [100]. For this study, quick quenching was required for obtaining the desired crystallization temperature (T_c = 110 °C) from the melt state of the sample within a short time span which inhibits the formation of the crystals during the phase change from the amorphous melt state to the amorphous solid state. In regard to fulfilling the purpose special type of DSC apparatus was used, equipped with the liquid nitrogen cooling system at the cooling rate of 300 °C/min for quick quenching within seconds, other than conventional type DSC apparatus associated with moderate cooling which might allow crystal formation during the phase change due to slow cooling. The sample was left crystallized under specific T_c for 60 min and the heat generated during this crystallization process was recorded by a DSC instrument and plotted against time (**Figure 7.6a,b**).

The bio-composites showed rapid crystal formation under the isothermal condition against time, wherein, faster crystal formation was observed in the PLA/CNC bio-nanocomposites among others (**Figure 7.6 a,b**). The occurrence of the peak in nPLA was observed at ~18 min, whereas incorporation of 0.5, 1, and 2 wt.% bio-fillers led to quick crystal formation within the shortest time with increasing the bio-filler loading. The introduction of bio-fillers led to the formation of a sharp peak in comparison to nPLA which showed a broad hump-like peak. Further, the reduction in optimum crystal formation time confirmed the enhancement of the PLA crystallization rate. It was observed that CNCs were

more effective as a crystallizing agent than WABR. Moreover, the effectiveness of WABR and CNCs was confirmed by the improvement of the degree of crystallinity (ϕ(t)), which was estimated based on the heat flow data obtained from the DSC analysis using Equation no. 22. **Figure 7.6c** shows the ϕ(t) of all the films at different time intervals. The shape of the curve was sigmoidal which represented the occurrence of primary crystallization with nucleation and radial growth of the crystallites.

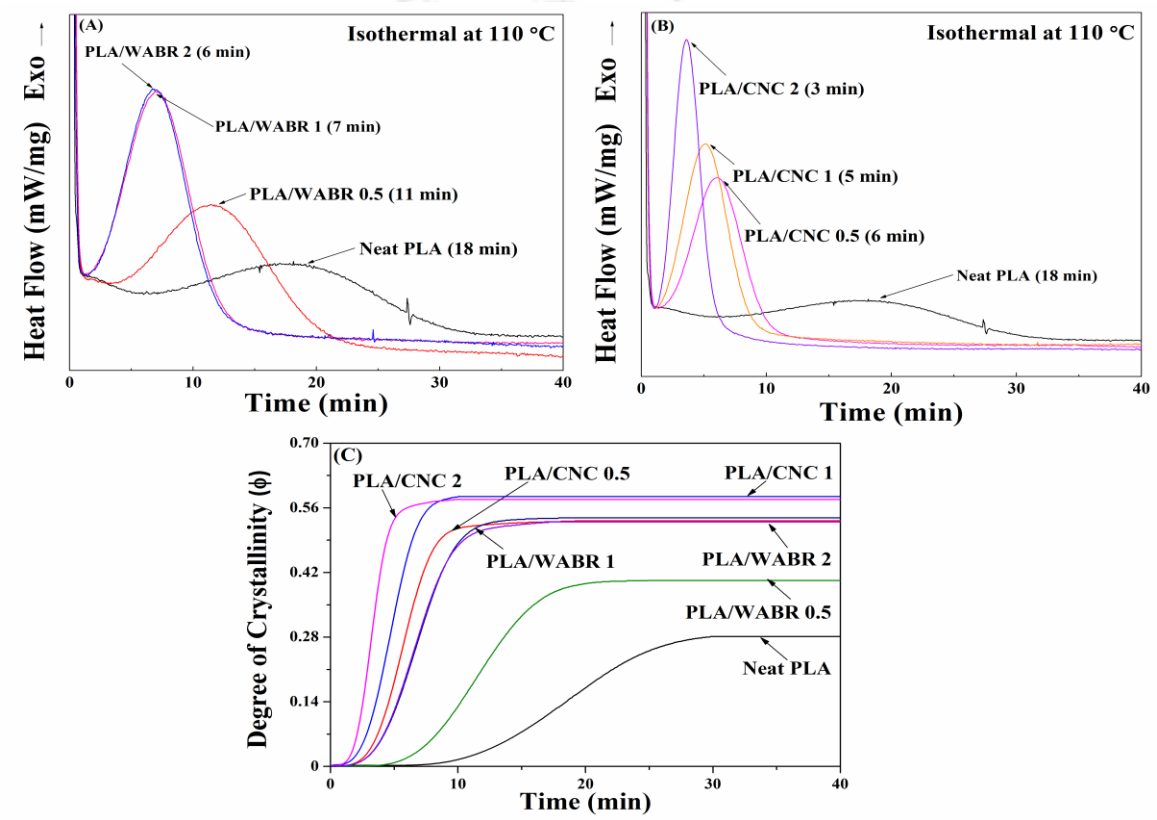

Figure 7.6: DSC time curves of the isothermally crystallized: (a) PLA/WABR, (b) PLA/CNC films, and (c) comparison of the degree of crystallinity among the bio-composites.

The next part of the curve consisted of the plateau region representing the secondary stage of crystallization. The estimated ϕ(t) of nPLA was found to be 28% which was enhanced up to 58% with the addition of 1wt.% of CNCs. The order of enhanced crystallinity of all the bio-composites was PLA/CNC1> PLA/CNC2> PLA/WABR1> PLA/CNC0.5>

PLA/WABR2> PLA/WABR0.5> nPLA. The order predicted that 1wt.% CNC loading would have the highest crystallization efficiency among all. However, 2wt.% CNC loading showed faster crystallization at the initial stage than others, however, the ultimate crystallinity was reduced (**Figure 7.6c**). The probable reason might be due to faster crystallization suppressing each other from growing or agglomeration of particles. The order confirmed CNCs were highly effective as a crystallizing agent than PLA and WABR. Additionally, this finding confirmed the improved compatibility between bio-fillers with the PLA matrix, as a result, rapid chain folding occurred during the crystallization process which reduced the time requirement. The isothermal crystallization kinetics can be depicted by the well-known Avrami theory. Based on the theorem, crystallinity as a function of time ($\phi(t)$) has been expressed using equations no. 23 & 24. All the mentioned parameters were enumerated from double log plots of the Avrami equation through the slope and intercept of the graph (**Figure 7.7a,b**). The primary crystallization was generally completed within 50% conversion. Based on this assumption and as the Avrami theorem focuses mainly on the primary crystallization, a 3-20% conversion range was chosen to obtain the best fitting curve according to Lorenzo et al., (2018) [234].

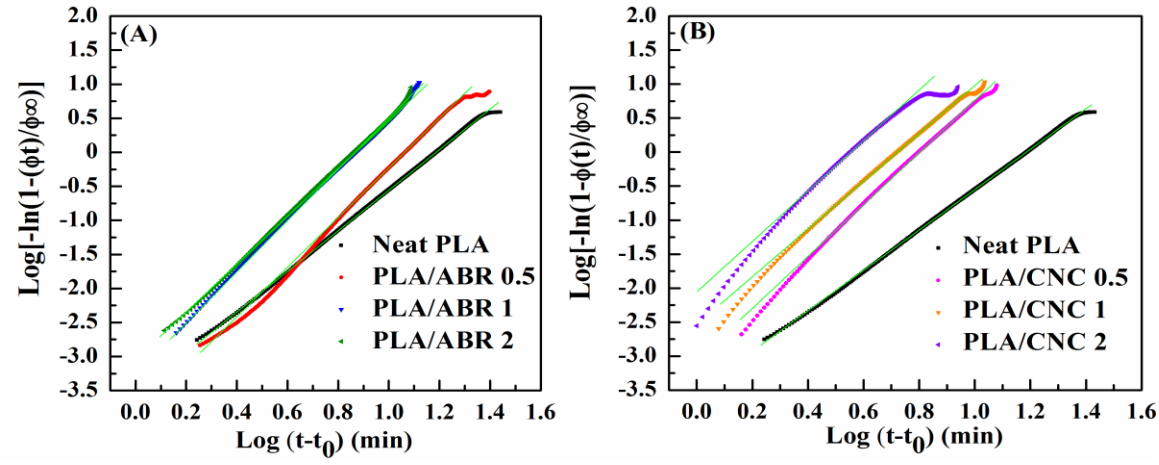

Figure 7.7: Avrami double log plot of (a) PLA/WABR bio-composites, and (b) PLA/CNC bio-nanocomposites.

A heterogeneous two-dimensional growth was observed for all the films based on the obtained 'n' value in the range of 2-3 and an increasing rate of 'k' value. The observed 'n' and 'k' values for the PLA/CNC were found to be increasing in order with the higher loading of CNCs, which confirmed the effectiveness of CNCs as nucleating agents (**Table A8**). This analysis suggested that increasing the CNC wt.% in the polymer matrix provided more nucleation sites. This signified that WABR was less effective in comparison to the CNCs in the PLA matrix. Therefore, from the detailed evaluation of the isothermal kinetics, it could be said that both CNCs and WABR could act as good nucleating agents, wherein CNCs were more effective due to their morphology, dimension, topography as well as the compatibility and interaction with the matrix material. Several pieces of literature have been reported on the crystallization behavior of PLA/CNC nanocomposites among them Gazzotti et al., (2017) reported the reduction in crystallinity in developed PLA/CNC nanocomposites via in-situ polymerization where cotton linters were used as CNC source material [235]. However, the crystallinity was improved in PLA/CNC via grafting and blending with higher loading of CNCs (20 wt.%) [236]. In the current study, algae-derived CNC showed much more effective nucleation and faster crystallization (6 min) with a minimum loading of 0.5wt.% which is significant in the reported literature [46].

7.2.5.2 POM Analysis

The POM study was conducted for observing the effect of bio-fillers on the crystallization process of PLA. The growth rate and nucleation density of the spherulites as a function of time were also evaluated (**Figure A9**). The POM analysis was conducted at 125 °C isothermal conditions. **Figure 7.8a,b** is the representative images of spherulites growth of bio-composites. Accelerated spherulite number and growth were noticed in the bio-composites as compared to nPLA. The POM images were taken at 4 min intervals to visualize the change in spherulites with time.

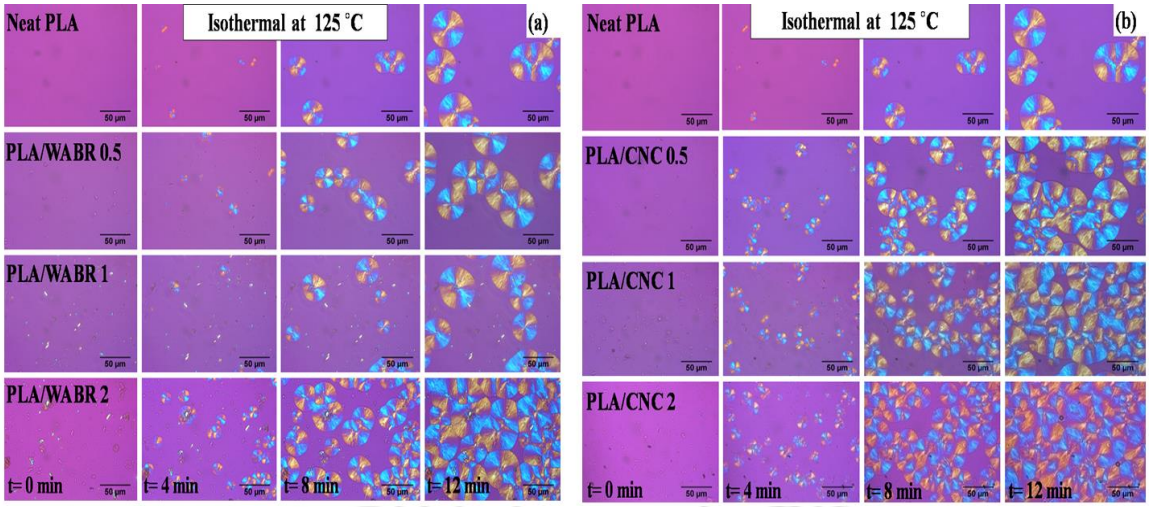

Figure 7.8: POM images of: (a) PLA/WABR bio-composites, (b) PLA/CNC bio-nanocomposites.

Further, enhanced nucleation density and an increased number of spherulites in PLA/CNC bio-nanocomposites indicated better compatibility between CNCs and PLA. Their needle-like morphology and aspect ratio could be accountable for the enhancement of better crystallization whereas, the larger particle size of WABR might be the possible reason for its less effectiveness. Heterogeneous nucleation was the cause for the occurring high crystal density. In comparison to nPLA, highly dense spherulites were observed in the bio-composites at the time interval of 12 min wherein the CNC-based films showed the highest density due to the availability of more nucleation sites (**Figure 7.8b**). Further, crystal density was enhanced with increasing bio-filler loading. The molecular chain entanglements hindered the growth of overlapped spherulites. The results confirmed that CNCs were more capable of imparting the PLA nucleation sites.

7.2.5.3 SAXS Analysis

Figure 7.9a represents the Lorentz-corrected SAXS profile of the bio-composites which was developed by correcting many factors including beam intensity, sample transmission, and background scattering [237]. Here, q denoted the scattering vector, 2θ was the scattering angle, and λ was the wavelength of the X-ray. The scattering vector was

determined using the Equation 26. Further, by multiplying with q^2, the scattering intensity I(q) was corrected as $q^2 I(q)$, known as the Lorentz-corrected SAXS profile.

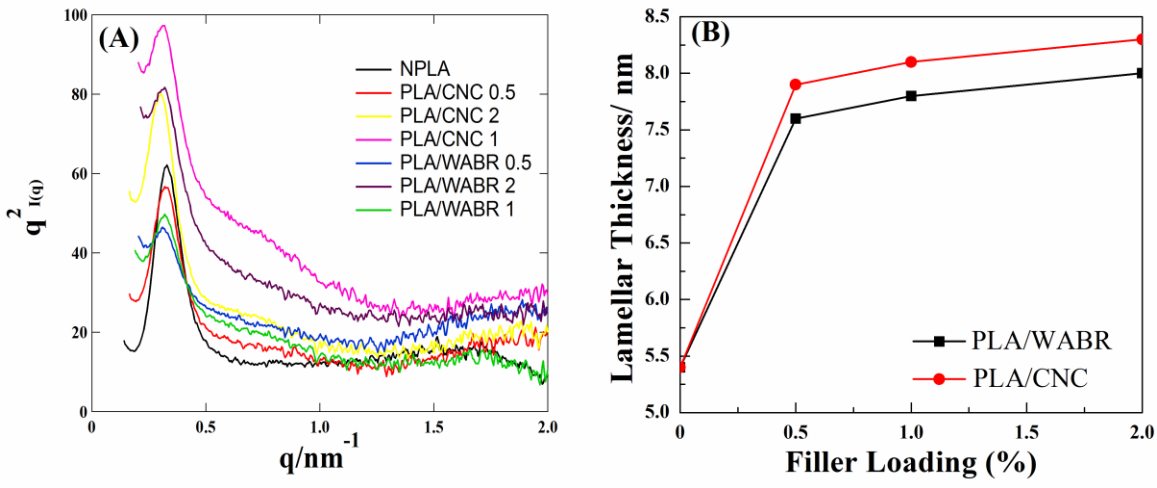

Figure 7.9: (a) SAXS profile of the developed bio-composites, and (b) Comparison of lamellar thickness among PLA bio-composites.

The difference in electron density between the crystalline and the amorphous phases represented the total scattering intensity which is also proportional to the volume fraction of the crystalline phase. Thus, the change in crystallinity was related to the change in scattering intensity. The SAXS peaks denoted the lamellar structure of the spherulites of PLA. A single clear scattering peak was observed from the SAXS profile for all the films, indicating the crystalline nature of bio-composites. The intensity of the peak for nPLA, 0.5, 1, and 2 wt.% CNC was 0.33, 0.32, 0.31, and 0.30 nm^{-1}, respectively. It was found that at higher bio-filler loading, the lamellar thickness value increased proportionally (**Figure 7.9b**, **Table A9 & Figure A8**) for the bio-composites, wherein the highest improvement was observed in the PLA/CNC bio-nanocomposites. Along with the SAXS profile, the different characteristic outcomes confirmed the better efficiency of CNCs in comparison to WABR as an effective nucleating and crystallizing agent.

7.2.6 Crystallization Behavior of the PCL Bio-composites

7.2.6.1 DSC Analysis

- ***Non-isothermal Study***

DSC analysis was carried out to investigate the effects of bio-fillers on the thermal properties of synthesized PCL. **Figure 7.10a,b** represent DSC thermograms of nPCL and its bio-composites. The obtained values of non-isothermal parameters have summarized in **Table 7.1**. The cooling scan of film samples has been depicted in **Figure 7.10a**. The crystallization temperature (T_c) of nPCL was 29.4 °C, which was improved in bio-composites, indicating effective nucleation. In this regard, the T_c value of PCL/WABR bio-composite increased by 5.7 °C, wherein PCL/WABR/1 provided the highest improvement. A similar trend was observed in PCL/CNC bio-nanocomposites, where T_c was enhanced from 29.4 °C to 35.1 °C with an increment of ~6.1 °C. Further, the PCL/CNC/0.5 bio-nanocomposite was shown the highest T_c among others. However, almost similar improvement was observed in PCL/WABR and PCL/CNC bio-composites. Moreover, the improved T_c indicates that CNC acted as a good nucleating agent in the PCL matrix thereby improving the crystallization process [238]. Interestingly, the analysis result suggested not only CNCs but WABR also acted as a nucleating agent. For instance, the enhancement in the T_c value indicated the occurrence of heterogeneous nucleation by the addition of bio-fillers. However, the melting temperature (T_m) was unchanged after the incorporation of bio-fillers (**Figure 7.10b & Table A10**). Similar observations have been reported in the literature that T_m values were almost independent after the addition of CNCs into the PCL matrix [239]. However, the addition of the tunicin whisker as filler into a different matrix such as plasticized starch and poly(ethylene oxide) based matrix materials showed insignificant effects on T_m [240]. Furthermore, the melting enthalpy (ΔH_m) of bio-composites was found in decreasing order as compared to nPCL which indicates the

reduction in crystallinity (**Table A10)**. One of the probable reasons could be the incorporation of organic fillers probably altering the PCL chain mobility which decreased the demand for the energy required for the melting of the films. Some study has supported about current finding, where the ΔH_m value of PCL composite decreased after the incorporation of cotton waste extracted CNCs and marine seaweed (*Ulva armoricana)* [241,242]. Moreover, for a better understanding of the effects of bio-fillers on the crystallization behavior of bio-composites, the isothermal crystallization kinetics study was conducted.

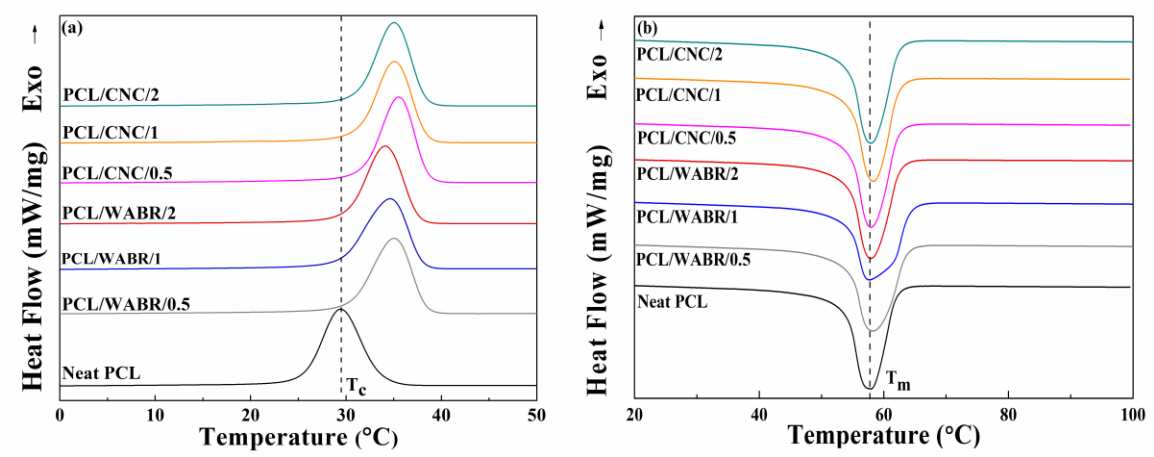

Figure 7.10: DSC non-isothermal thermogram of (a) first cooling scan, and (b) second heating scan of PCL bio-composites.

- ***Isothermal Study***

Isothermal crystallization kinetics was conducted for analyzing the crystallization and nucleation behavior of PCL bio-composites. Besides, this study investigated the crystalline behavior of both the bio-fillers CNC and WABR and their optimum crystallization temperatures. The crystallization exotherms of nPCL and bio-composites with varying temperatures have shown in **Figure 7.11**. The optimum crystallization temperature was 45 °C as shown in **Figure 7.11a,b**, for bio-composites with the highest bio-filler loading, where the exothermal peak shifted towards a shorter time region. However, 40 °C was the

optimum temperature for nPCL (**Figure 7.11c**) wherein subsequent addition of bio-fillers reduced the crystallization time and crystallization occurred before reaching 40 °C therefore, unable to obtain the peak at a cooling rate of 300 °C/min. Based on observations, the optimum temperature was selected as 45 °C for all the developed films for this study.

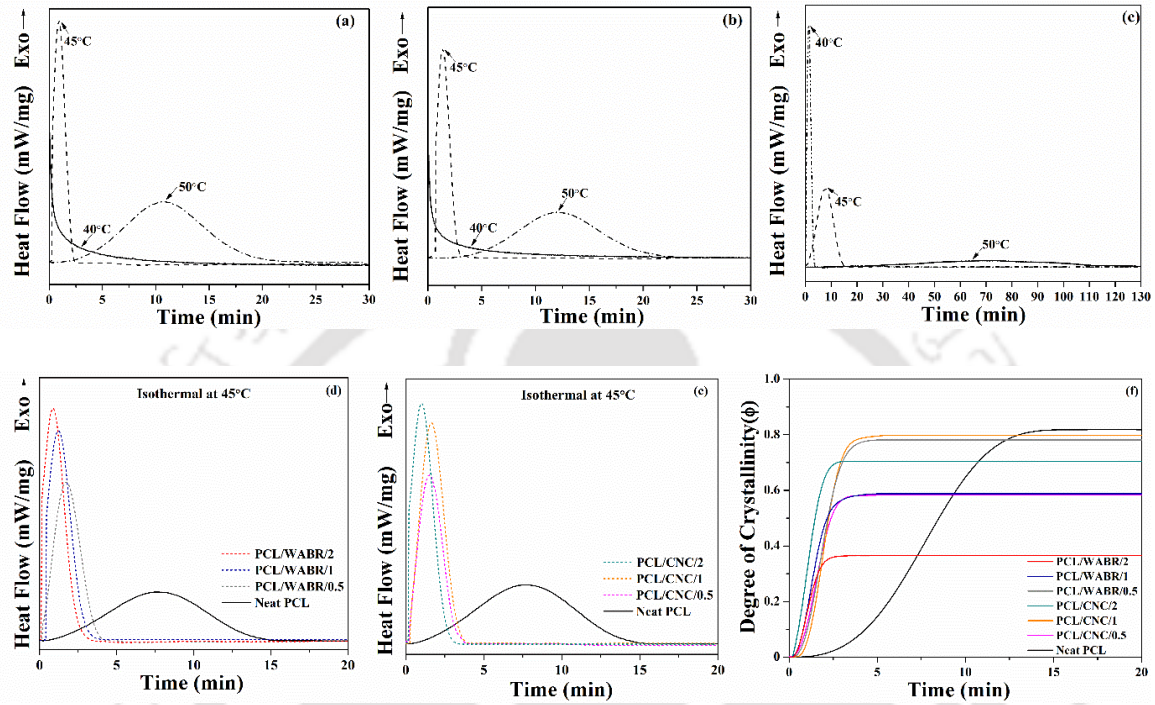

Figure 7.11: Isothermal crystallization exotherms of (a) PCL/CNC/2 bio-nanocomposites, (b) PCL/WABR/2 bio-composites, and (c) neat PCL with different crystallization temperatures; (d) PCL/WABR bio-composites, and (e) PCL/CNC bio-nanocomposites at 45 °C with various bio-filler content; and (f) comparison of degree of crystallinity among all bio-composites at 45 °C.

Figure 7.11d,e represents the exothermal peak of bio-composites against time where peaks shifted towards shorter time regions with increasing bio-filler loading. In contrast, a broad hump-like peak was visualized in the case of nPCL, which indicates a gradual increment in crystallization rate and formation of faster crystals due to the incorporation of a higher amount of bio-filler. The optimum crystal peak in nPCL was observed at ~8 min whereas, the addition of 0.5, 1, and 2 wt.% bio-fillers completed the peak formation within a few

minutes. Furthermore, the effectiveness of bio-fillers was determined by their degree of crystallinity ($\phi(t)$) which was estimated based on Equation 22. **Figure 7.11f** represents the curve of $\phi(t)$ with respect to time which was estimated under the isothermal condition. Each curve represents a sigmoidal shape that consists of a linear and nonlinear part corresponding to primary and secondary crystallization. The primary crystallization was caused due to the nucleation and radial growth of crystallites. Interestingly, the $\phi(t)$ of nPCL was highest at ~0.82 whereas reduced values were obtained for the bio-composites. However, the induction period of nPCL was more, indicating a slower rate of crystallization whereas a faster rate of crystallization was observed in bio-composites (**Figure 7.11f**). The induction period of nPCL was started at ~1.2 min whereas PCL/WABR was found at ~0.28, 0.13, and 0.21 min, and PCL/CNC bio-nanocomposites were shown at ~0.19, 0.38, and 0.13 with the addition of 0.5, 1, and 2 wt.% of bio-filler, respectively. The shorter induction period of bio-composites in comparison to nPCL indicated effective nucleation of the bio-fillers. Nevertheless, the ultimate crystallinity was decreased. The order of the $\phi(t)$ for nPCL and bio-composites is as follows: nPCL> PCL/CNC/1> PCL/WABR/0.5> PCL/CNC/2> PCL/WABR/1> PCL/CNC/0.5> PCL/WABR/2. In this context, reduction in ultimate crystallinity is higher in WABR bio-composites as compared to CNC bio-nanocomposites with increasing bio-filler content. For instance, the probable reason for decreasing in ultimate crystallinity could be the faster rate of crystallization, which eventually arrested the space for crystal growth. Further, since the bio-fillers acted as a good nucleating agent, the formation of the bulk number of crystals at a time could hinder individual crystals from growing, and overlapping of crystals might have occurred. Further, the algal extracted CNCs might restrict the PCL chain mobility *via* the formation of intermolecular hydrogen bonding between the hydroxyl group of CNCs and the carbonyl group of PCL. The contradiction in crystalline behavior might also depend upon bio-filler properties such as

morphology, and fabrication methods that might be responsible for enhancing the amorphous nature and offset of nucleation effect [243]. Some studies have reported the reduced crystalline behavior of acetylated CNCs incorporated PCL *Ulva armoricana* incorporated PCL matrix [242] and PCL nanofiber with CNCs where the insignificant effect of the nucleating agent was found due to higher electrostatic shear force [243]. In addition, reduced crystallinity was also observed in PCL/WABR bio-composites which might be due to the presence of inorganic elements. In this context, reported literature revealed that the presence of inorganic matter in the polymeric matrix can either increase or decreases the crystallinity by following two mechanisms. It can enhance heterogeneous nucletion as a result of increased crystallinity and melting temperature or reduced crystallinity via hindered chain mobility.

When $\log\left[-\ln\left(1-\frac{\emptyset(t)}{\emptyset^{\infty}}\right)\right]$ versus $log(t-t_0)$ is plotted at a particular crystallization temperature, a straight line generally appears. The slope and intercept of that line correspond to 'n' and 'k'. Further, the rate of the crystallization process can be predicted by calculating the half-time of crystallization ($t_{0.5}$) using Equation 25. All the kinetic parameters that were obtained from these isothermal exotherms using the Avrami model have been summarized in **Table A11**. **Figure 7.12a & b** represent the double log plot of PCL/WABR and PCL/CNC bio-composites.

The Avrami model is valid for the linear part of these curves corresponding to the primary crystallization. In addition, the primary crystallization generally completes within 50% conversion, based on this assumption, a 3-20% conversion range was selected to obtain the best-fitted curve according to Lorenzo et al., (2018) [234]. Besides, the two most important scenario of isothermal crystallization is the formation of nuclei at the early phase and observing the finite and constant nucleation rate. In the early stage, constant nuclei density was observed which subsequently changed by the bio-fillers activity and in the

second stage, thermal nucleation was started from the melt. The selection of time zero is critical and the time required for the complete crystallization process is more as compared to the time required for quenching. Further, a decreasing trend of the 'n' value was observed in bio-composites. The conversion of two to one-dimensional crystal growth was significant in PCL/WABR as compared to PCL/CNC bio-nanocomposites (**Table A11**), where 'n' values decreased gradually with increasing the bio-filler loading. The obtained 'k' values for bio-composites were found in increasing order with higher loading of bio-filler (**Table A11**), which predicted the effectiveness of WABR and CNCs as a nucleating agent since the 'k' value related to the nucleation efficiency of the bio-fillers.

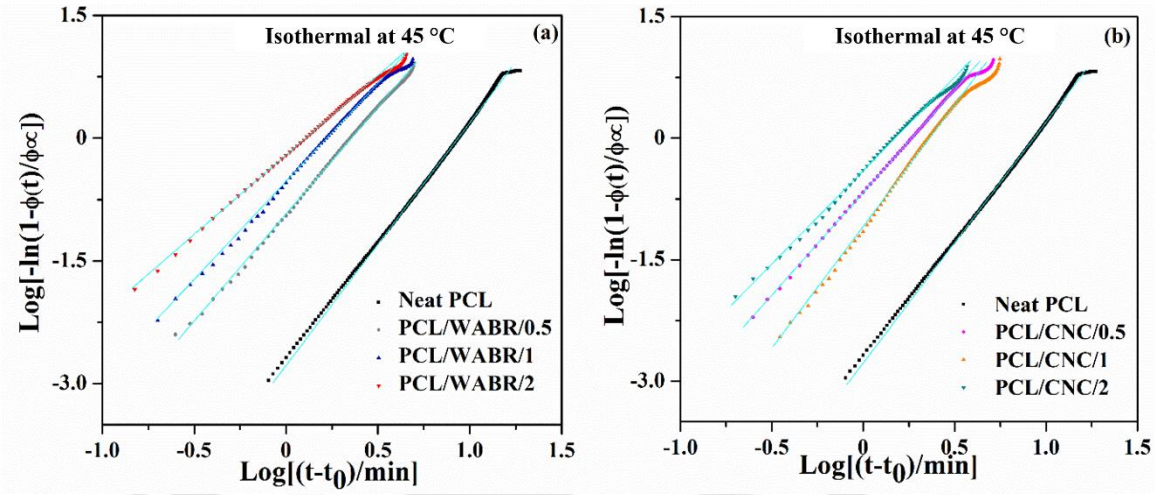

Figure 7.12: Avrami double log plot of isothermal crystallization at 45 °C (a) PCL/WABR bio-composites, and (b) PCL/CNC bio-nanocomposites.

Further, the gradual reduction in halftime ($t_{0.5}$) with increasing bio-filler content was noticed and the trend was similar for the bio-composites (**Figure A11**). Additionally, the various 'n' values correspond to the different nucleation types and crystal geometries [244]. The 'n' values were changed from 2.96 to 1.94 for PCL/WABR and up to 2.30 for PCL/CNC indicating the formation of axialites. Moreover, the reduction in 'n' value was observed which could be due to the formation of a large number of nucleation sites causing

the development of rapid crystals in a short time thereby hindering the possibility of developing three-dimensional spherulites, and as a result, reduced ultimate crystallinity.

7.2.6.2 POM Analysis

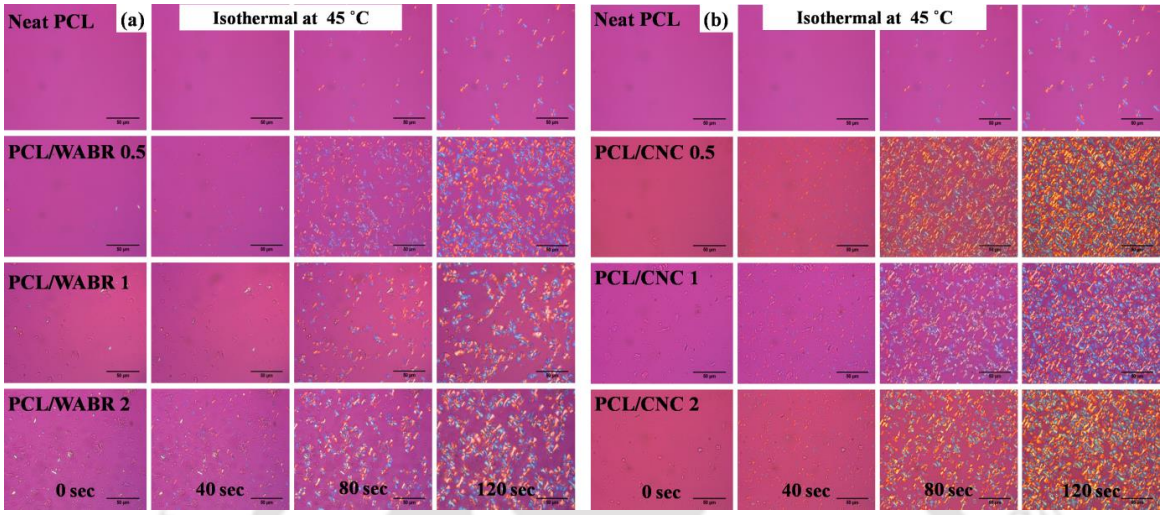

Figure 7.13: POM images of (a) PCL/WABR bio-composites, and (b) PCL/CNC bio-nanocomposites at the isothermal temperature of 45 °C with different time intervals (0, 40, 80, and 120 s).

The POM study was conducted to visualize the crystallization effect of WABR and CNCs in the PCL matrix. Additionally, this study allows obtaining information about nucleation density and the growth rate of spherulites as a function of time. POM observations were analyzed under the isothermal condition at 45 °C, where crystals formation might be delayed *via* slow folding of the polymer chains at specific crystallization temperature, which would allow a detailed visualization and mechanism of the crystallization process. **Figure 7.13a,b** depicts the captured POM images for PCL/WABR and PCL/CNC bio-composites. The occurrence of negative spherulites was found in the bio-composites along with nPCL. Moreover, the formation of negative spherulites indicated the insignificant effect of bio-fillers on spherulite formation without an extinction ring. Further, accelerated spherulite growth was observed in both bio-composites as the number of spherulites and density increased with time. The POM images were captured between

40 sec intervals for observing the changes in density, number, and orientation of crystals. The complete spherulites were visualized in the nPCL however, the number and density of spherulites were less with the measured time interval as compared to bio-composites (**Figure 7.13a,b**). On the contrary, incomplete spherulites were observed for bio-composites. However, the formation of incomplete spherulites was more significant in PCL/CNC bio-nanocomposites (**Figure 7.13b**). This observation suggested the formation of axialites rather than spherulites in bio-composites. It was noticed that increasing the bio-filler loading enhanced number of axialites and its density. The one-dimensional growth was noticed in the images (**Figure 7.13**). Further, the rapid axialite formation was observed against the time span. The probable reason behind the axialites formation could be due to the overlapping of spherulites during the rapid growth of nuclei as a result of the high crystalline nature of bio-fillers. Besides, the rate of formation of the nucleation site was so faster which could alter the mobility of the PCL chain and might provide more free spaces inside the polymer matrix. Further, better compatibility between bio-filler and polymer matrix could provide more free spaces. Since PCL is semi-crystalline in nature that might affect the formation of complete crystals. Moreover, axialites are two-dimensional lamellar aggregates. This study confirms the effectiveness of bio-fillers as nucleating agents with the formation of axialites, which lowered the crystallinity. In this context, [245] reported similar observations where multiwalled carbon nanotubes were used as a filler in the PCL matrix and reduced the crystallinity of the nanocomposites due to the formation of axialites.

7.2.6.3 SAXS Analysis

The Lorentz-corrected SAXS profile of bio-composites along with nPCL has represented in **Figure 7.14**. Here, 'q' denotes the scattering vector and is determined using an equation. SAXS profile, q^2 I(q) was obtained by multiplying q^2 with scattering intensity I(q). Further,

the change in scattering intensity represents the change in crystallinity [46]. Moreover, for a better understanding of the crystallization effect of bio-fillers into pristine PCL, the SAXS profile was drawn.

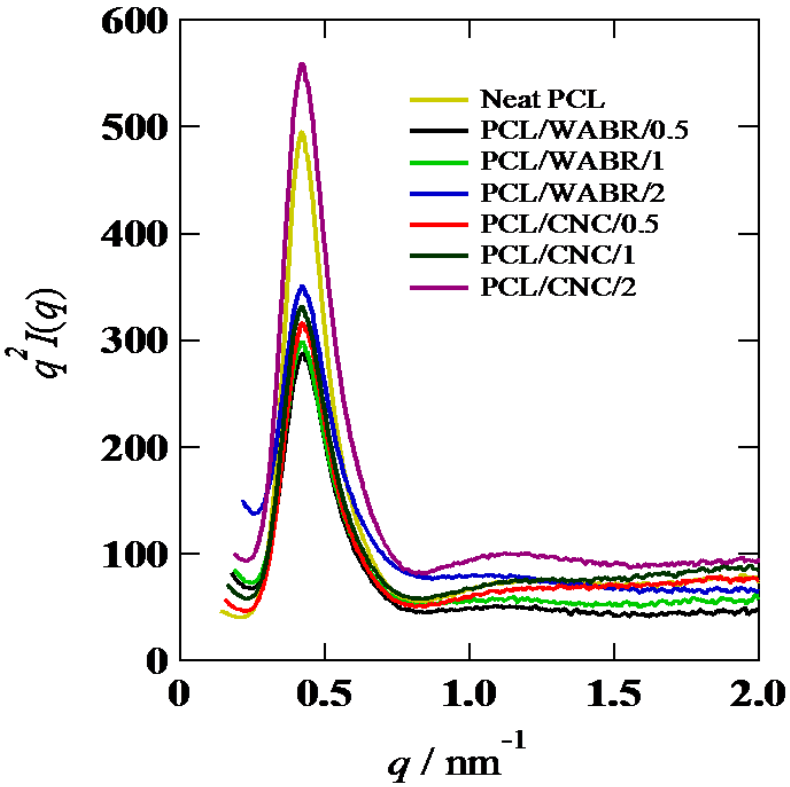

Figure 7.14: Lorentz-corrected SAXS profile of PCL/WABR and PCL/CNC bio-composites.

A single sharp scattering peak was found for bio-composites along with nPCL. The observed peak intensity was found at q=0.42 nm^{-1} for nPCL and PCL/CNC bio-nanocomposites, whereas q=0.43 nm^{-1} was observed for all PCL/WABR bio-composites. The scattering intensity, q was determined from the Lorentz-corrected profile. Furthermore, the SAXS profile at a crystallization temperature of 45 °C revealed the crystalline nature of bio-composites along with nPCL. The morphological parameters such as long period (D) was calculated to understand the crystalline behavior of bio-composites. The long period of the lamellar stacks was evaluated using the equation, $D = 2\pi/q^*$, where q* denotes the peak position from Lorentz-corrected. The calculated 'D' value of nPCL and all bio-

composites were 14.9 nm, which indicated no further improvement in crystallinity in bio-composites.

7.3 Summary

The algal biomass waste of *Dunaliella tertiolecta* would turn out to be a promising source for the development of highly crystalline CNCs. The raw fiber (WABR) could also be utilized as a bio-filler for tailoring the crystalline properties of PLA and PCL. The CNCs were displayed as effective nucleating and crystallizing agents which increased the degree of crystallinity in the PLA bio-nanocomposites by 30%. Moreover, WABR and algal CNCs could be utilized as effective nucleating agents. However, the formation of rapid nuclei within a short time reduced the ultimate degree of crystallinity in developed solvent-casted PCL/WABR and PCL/CNC bio-composites as compared to nPCL. The highest decrement in the degree of crystallinity was found in PCL/WABR/2 by ~58% and in PCL/CNC/2 by ~48%, respectively. Further, the addition of bio-filler slightly improved the thermal stability in bio-composites. The present study indicated that the utilization of a lesser quantity of bio-fillers could also deliver a change in significant characteristics. The developed films would be suitable for food packaging applications due to their excellent barrier properties achieved due to their improved crystallinity.

CHAPTER 8

STUDIES ON MIGRATION PROPERTIES OF ALGAL CNC AND CURCUMIN INCORPORATED PLA AND PCL BIO-COMPOSITES

Algal CNC and curcumin (CUR) incorporated PLA and PCL-based functional cast films were prepared using a customized casting machine. The CUR-incorporated bio-composite film was transparent with bright yellow color for PLA/CUR/CNC film; however, opaqueness was observed in the case of PCL-based film. The concentration of CNC was varied (0, 0.5, 1, and 2 wt.%) whereas, CUR concentration was kept constant to identify the effect of algal CNC on the film property. The developed bio-composite thermal, structural and chemical interaction was observed by TGA, FTIR, and, XRD. The CUR-incorporated bio-composites exhibited excellent UV-light blocking, antioxidant and antimicrobial properties. The water vapor transmission rate and surface wettability of the films were significantly reduced by the addition of CNC and CUR, however, lower concentrations of CNC exhibited better performance in both types of films. The overall migration study was conducted for specifically CNC-incorporated films in absence of CUR. Besides, specific migration of CUR from the developed films was performed using a food simulant and the kinetics study of CUR migration from the film was studied by various mathematical models. The addition of CNC enhanced the overall migration rate of the bio-composite films however, the migrant amount was within the specified limit. Furthermore, a higher rate of CUR migration was observed due to the addition of CNC from the PLA films as compared to the neat PLA matrix during storage at 40 °C whereas, a reduced rate of CUR migration was noticed from CNC incorporated PCL film as compared to neat PCL film during storage at 7 °C. The developed bio-composites were found as nontoxic or biocompatible against the BHK-21 cell line. Finally, the developed active and normal bio-composite films were used as secondary packaging material for the storage of cut potatoes and the study was performed at room temperature. The CUR-incorporated films exhibited improved shelf-life of cut potatoes as compared to others indicating CUR can be used as an effective active agent to develop active packaging material.

Outcome: Mondal K, Goud V. V, & Katiyar V. “Studies on migration properties of algal CNC and curcumin incorporated PLA and PCL bio-composites” (under preparation).

Graphical Abstract

The following schematic represents the fabrication of bio-nanocomposite films and curcumin-loaded bio-nanocomposite films using a customized solution-casting machine and various characterizations of developed films. Besides, the migration study of developed films has been performed and the developed films have been tested on cut potatoes.

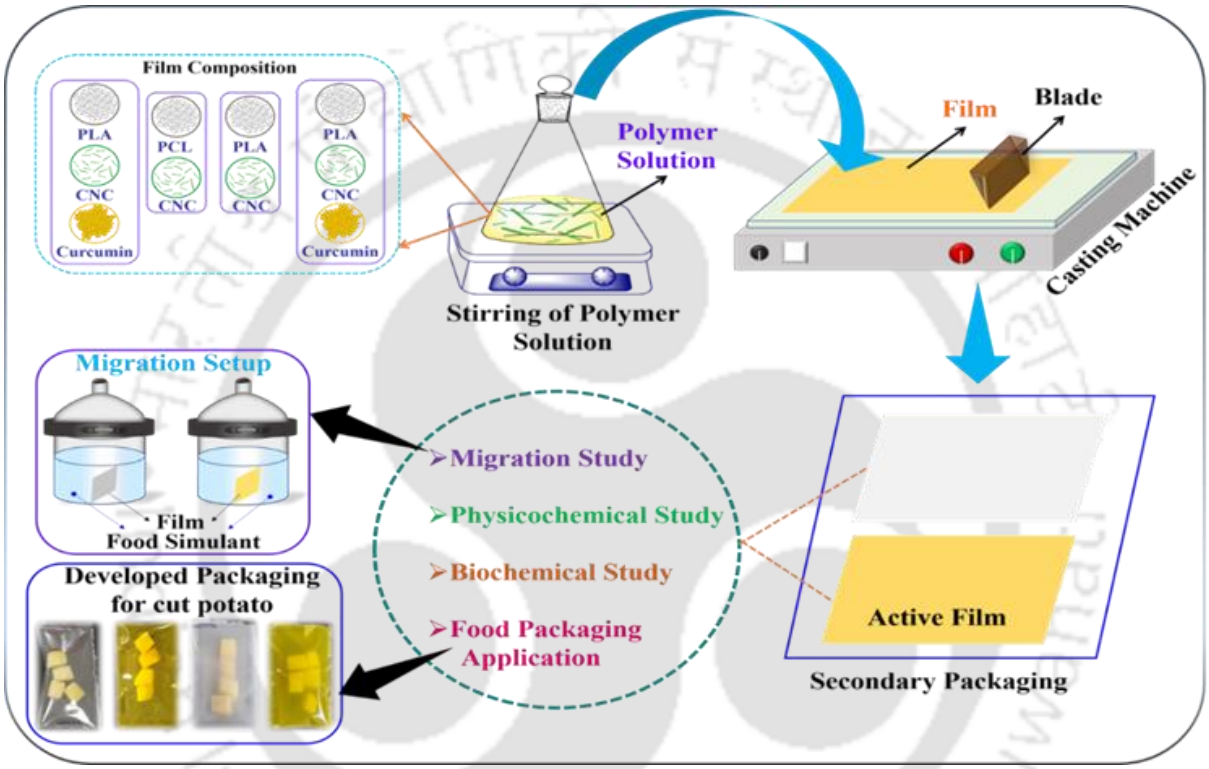

8.1 Introduction

Active secondary packaging materials have been designed where various antioxidant and antimicrobial substances are incorporated into packaging material to improve the quality and shelf-life of the food material. Incorporation of these low molecular weight chemical compounds enhances the functional properties of packaging material. The release of these active compounds from a package usually occurs through a slow and controlled way to maintain an adequate concentration of these substances in the packed food for a certain period. These substances also release from the food packages to the food material by migration phenomena as a result of diffusion, dissolution, and equilibrium processes [246]. Diffusion of chemical substances from polymers is a very complex process and is dependent on several parameters, such as concentration of substances in packaging film and food, film fabrication method, hydrophilicity and hydrophobicity of the polymer, volatility, and polarity of the substance, nature of the foods, temperature, and the period over which duration of contact occurs [246].

Furthermore, incorporation of bio-nanostructured materials can be considered an adequate alternative for tuning the primitive properties of biopolymers such as PLA and PCL. The improved characteristics of biopolymers would broaden its applications in food industry as food packaging material [247, 248]. Among other reinforcing materials, the use of biobased cellulose nanocrystals (CNCs) would be more fruitful due to their high aspect ratio, crystalline property, renewable and biodegradable nature, ease of recycling including combustion, high sound attenuation and comparatively easy processability due to their non-abrasive nature as discussed in chapter 7 [249]. On the contrary, the use of CNCs as reinforcing agents is limited due to the non-availability of commercial CNCs due to less production [247]. Besides, it is difficult to use CNCs with hydrophobic polymers like PLA, and PCL, as it tends to form a strong hydrogen bond. Therefore, it is required to transfer

CNCs from water to an appropriate solvent for producing and processing of PLA and PCL-based bio-composites [247]. In addition, many studies have reported the incorporation of various functional bioactive substances such as essential oil, plant extract, seed extract, and others to improve the inherent properties of biopolymer-based packaging films [209]. In this context, curcumin is one such functional or active material can be administered to the biopolymer matrices for improving the characteristic properties due to its significant antioxidant, antimicrobial, and compatible characteristics.

Curcumin (1,7-bis(4-hydroxy-3-methoxyphenyl)-1,6-heptadiene-3,5-dione) is a bioactive, hydrophobic compound obtained from turmeric (*Curcumin longa*). This functional compound has wide application not only as a coloring, and flavoring agent, but also provides clinical value, reduces various diseases, and has a pharmacological application, such as wound healing, antioxidant, anti-inflammatory, antimalarial, antitumor, anticancer, and antibacterial functions. It is considered a non-toxic and GRAS additive approved by the US FDA organization. Curcumin has been incorporated in various polymeric matrices such as low-density polyethylene, cellulose, carboxymethyl cellulose, agar, carrageenan, cellulose acetate, collagen, and gelatin for the production of functional films for biomedical and packaging applications. The inclusion of curcumin into the polymer matrix improved UV-Vis light blocking, oxygen, and water vapor barrier properties [209]. However, the migration of curcumin from the food packaging film has not been studied extensively.

In this chapter, two types of biodegradable/compostable PLA and PCL-based algal CNC incorporated bio-nanocomposites were developed. Separately, curcumin was incorporated in both PLA and PCL matrices to fabricate CUR-loaded PLA and PCL bio-nanocomposites. To draw the comparison and obtain the functional effects of curcumin, two types of film with and without curcumin-loaded PLA and PCL film was fabricated

using a solvent casting machine. The overall migration studies were conducted in three types of food simulant for the film sample's absence of curcumin to find whether the migrant amount was within the specified standard limit required for food packaging. Further, specific migration studies were performed for curcumin-loaded film samples to understand the nature of migration. In this regard, a migration kinetic study was conducted using different models to recognize the behavior of curcumin (migrant) from the films into food simulant.

8.2 Results and Discussion

8.2.1 Thermal Properties

The thermal stability of developed bio-composite films PLA/CUR and PLA/CNC/CUR along with neat PLA (nPLA) film was evaluated by TGA analysis and the resulting curve was shown in **Figure 8.1a,b**. A two-step thermal degradation was observed from the DTG curve. The first step of degradation occurred at around 100 ºC, which could be due evaporation of the remaining solvent in the film [209]. The second major weight loss was observed between 320-400 ºC. The maximum degradation (T_{max}) was noticed at 388 ºC in neat PLA film. The addition of CNC and CUR did not alter thermal stability effectively. However, CNC and CUR incorporation in the PLA matrix reduced the onset temperature of degradation (T_{on}) maximum by around 8 ºC and 12 ºC, respectively. Addition of 1 wt.% CNC with a fixed concentration of CUR reduced maximum T_{on} value. The addition of only CUR to the PLA matrix reduced T_{max} by 11 ºC, whereas CNC addition showed around 4 ºC reduction as compared to neat PLA. The analysis results indicated the inclusion of CNC and CUR slightly enhanced the degradation. The data obtained from the analysis has been depicted in **Table A12**. Similar results were reported in literature where the addition of CNC and CUR showed no significant impact on thermal stability [209, 250]. Further, a similar observation [206] was noticed after the addition of CNC and CUR in the PCL matrix

as ascribed in **Figure 8.1c,d**. The addition of CNC and CUR did not affect thermal activity in developed PCL/CNC and PCL/CNC/CUR bio-composite film.

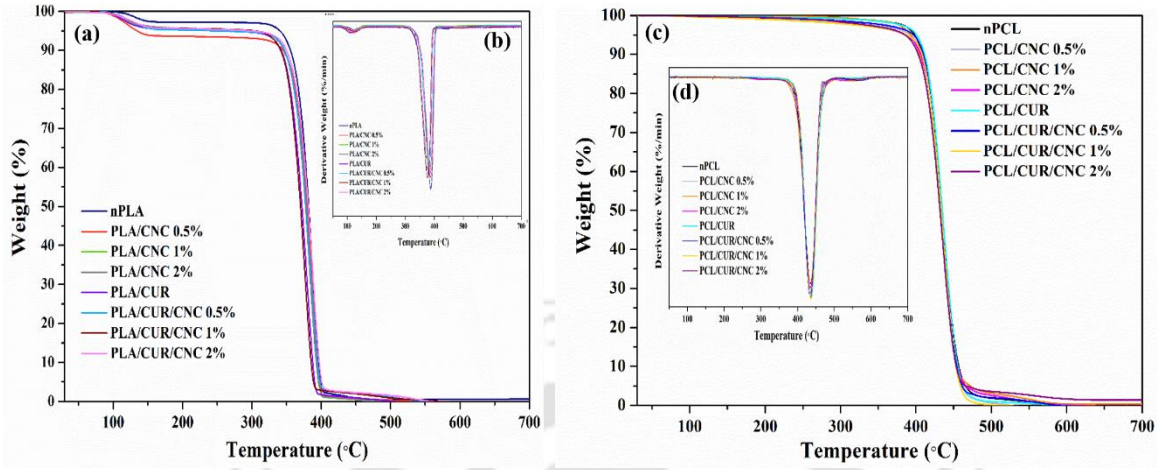

Figure 8.1: (a) TGA, (b) DTG curve of PLA bio-composite, (c) TGA, and (d) DTG curve of PCL bio-composite.

8.2.2 FTIR Analysis

FTIR spectroscopy was conducted to investigate the chemical structure and functional groups of bio-fillers in the polymer matrix. The FTIR spectra of the nPLA and PLA bio-composite films have been shown in **Figure 8.2a**. The developed films exhibited characteristic peaks at 869 and 753 cm^{-1}, which were attributed to the amorphous and crystalline phases of PLA, respectively [209]. The peaks found at 1183 and 1085 cm^{-1} were due to the symmetric and asymmetric stretching of the complex C–O–C group, respectively. The peaks observed at 1451 and 1361 cm^{-1} were due to the asymmetric and symmetric vibration of CH_3 deformation [232]. The peak at 1750 cm^{-1} was due to the C–O stretching vibration of the PLA ester group. The peaks observed around 2933 cm^{-1} referred to the stretching vibrations of a CH_3 group of saturated hydrocarbons. The CUR powder showed peaks at 3509 cm^{-1} ascribed to the O–H stretching vibration of the phenolic group present, and the peaks observed at 1627 and 1500 cm^{-1} corresponded to the carbonyl and ethylene groups, respectively [209]. Peaks shown in the range of 1500-1400 cm^{-1} were

ascribed to the C–O elongation of the O–H group [251]. The peak found at 1271 cm^{-1} was due to the C–O stretching of the ether, while the peaks at 959, 809, and 716 cm^{-1} were due to the C-H bending of alkene [251]. The absorption peaks of the PLA/CNC film spectrum were mainly due to the CH_3 stretching vibration at 2991 cm^{-1}. A strong absorption band was observed at 1751 cm^{-1} due to the C=O stretching from keto esters, as previously observed by Molinaro et al., (2013) [252]. The absence of formation of any new peak in the bio-composite films indicated no significant changes occurred in the chemical structure between PLA, CNC, and CUR except for changes in peak intensities. The FTIR analysis suggested that physical interaction occurred between PLA and bio-fillers.

The FTIR spectra of nPCL and the bio-composites have been depicted in **Figure 8.2b**. The addition of CNC and CUR into the polymer matrix did not show significant changes in peak position. The characteristics peak position of nPCL was intact in the developed bio-composites. In this context, a similar type of observation of PCL/CNC bio-nanocomposites was reported by Mi *et al*., (2014) [239]. However, a change in intensity was noticed in the developed bio-composites. It might be attributable to the occurrence of strong hydrogen bonding in the bio-composites. The nPCL spectrum showed characteristics peak at 2942 and 2862 cm^{-1} corresponding to stretching vibration of C–H and hydrocarbons [253]. Further, a sharp peak at 1720 cm^{-1} was identified in the nPCL spectrum, related to carbonyl groups (C=O). Besides, the bands from 1471 to 1044 cm^{-1} corresponded to the deformation of CH_2 of PCL. There was no occurrence of new peak formation in PCL bio-composites and changes in intensities again indicated strong physical interaction. Moreover, a similar observation was found in both PCL and PLA bio-composites.

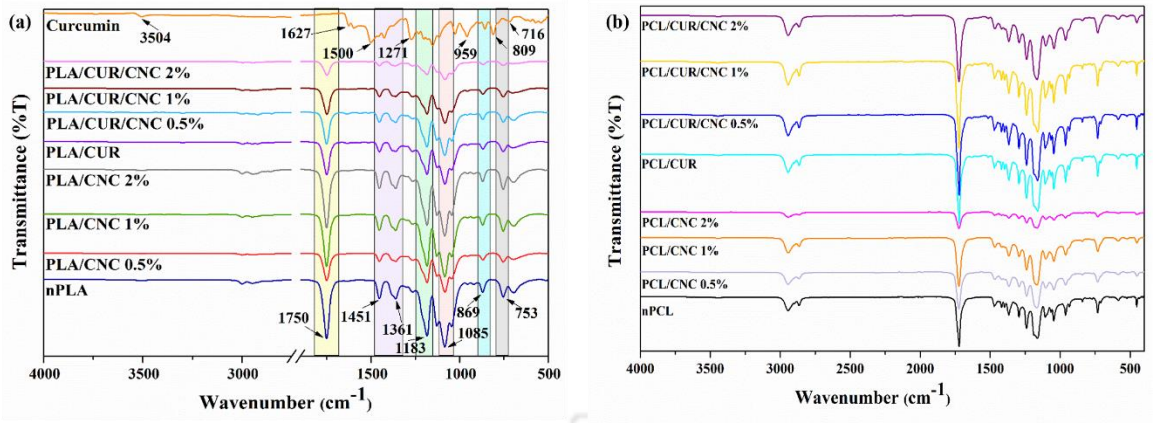

Figure 8.2: FTIR spectra of (a) curcumin, PLA, and (b) PCL bio-composite films.

8.2.3 Surface Color

The color properties data of the nPLA and developed film have been tabulated in the **Table A13**. The PLA film was transparent and the addition of CNC did not change the film color significantly. However, the addition of CUR changed the film color from transparent to bright yellow. Although, CUR incorporated PLA film was still transparent enough to be seen through the other side of the film. The nPLA film showed high L^* and low a^* and b^* values. The inclusion of curcumin decreased L* and a* values and increased the b* value of the PLA film at the same amount due to the addition of a fixed concentration of CUR. Therefore, the total color difference (ΔE) in CUR-incorporated PLA film was higher than nPLA and PLA/CNC bio-composite film as depicted in **Figure 8.3a**. The decreased a* and increased b* indicated the rise in greenness and yellowness, respectively. The increased total color difference (ΔE) of the bio-composite films was mainly due to the increased yellowness due to the addition of CUR. Similar to the b*, the yellow index (YI) of the PLA film was significantly increased by the addition of CUR. However, CNC did not change the surface color of the PLA/CNC bio-composite films. A slight reduction in ΔE and YI values was noticed in PLA/CUR/CNC 2% film as compared to other CUR incorporated films which might be attributed to the higher loading of CNC caused agglomeration inside the matrix. Since the CUR concentration was fixed for all the CUR-incorporated bio-

composite therefore, CUR was not the reason for the reduced value. The observed analysis is corroborated by the reported literature on the surface properties of PLA/CUR film [206]. In general, the PCL film is opaque in nature and the addition of CNC did not change the opacity in the developed film. However, the addition of CUR into the PCL and PCL/CNC matrix showed an increase in ΔE and YI values, the same as PLA films (**Figure 8.3b**).

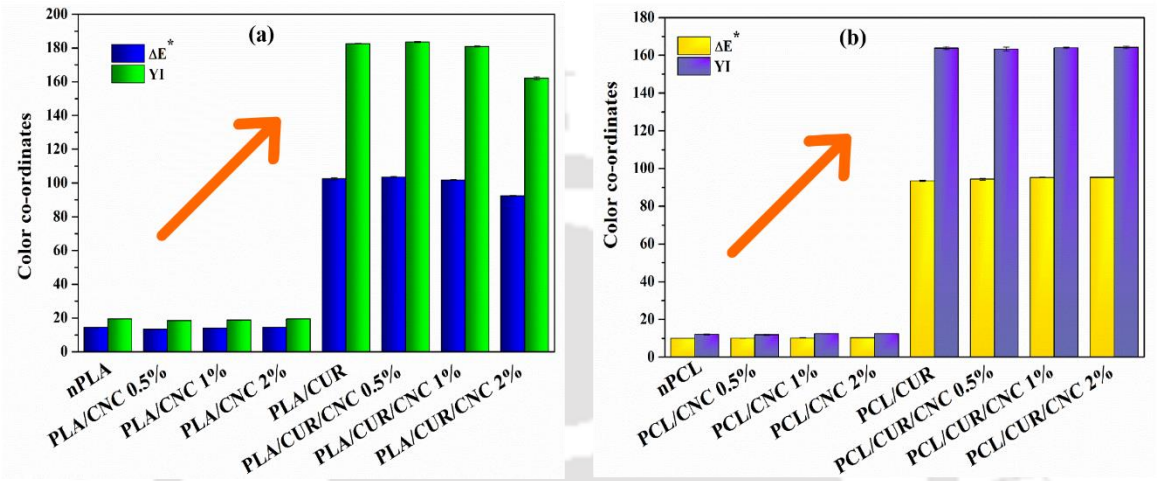

Figure 8.3: Color properties of (a) neat PLA, PLA/CNC, and PLA/CUR/CNC bio-composites, and (b) neat PCL, PCL/CNC, and PCL/CUR/CNC bio-composites.

8.2.4 Transparency

The transparency of packaging material plays a vital role as based on this property food samples are chosen to be packed as light-sensitive foods are also available and storing them for the future is a concern. Besides, consumer acceptance is another major factor, nowadays they like transparent packaged food so that they can see the product from outside. However, the transparency allows the UV rays in sunlight to penetrate the packaging and can adversely affect food quality and safety. The nPLA exhibited a higher transmittance (95%) than other bio-composites as depicted in **Figure 8.4a** which, indicated high transmittance for UV and Visible light. The transparency of the film was reduced after the addition of CNC and increased with higher CNC loading. This might be attributed to the presence of

CNC particles in the film matrix which hindered the passage of light partially though through this film UV and visible light can pass. Further, the addition of CUR into the PLA matrix significantly reduced the transparency and completely blocked the wavelength region of 200-500, which stopped the passage of UV light.

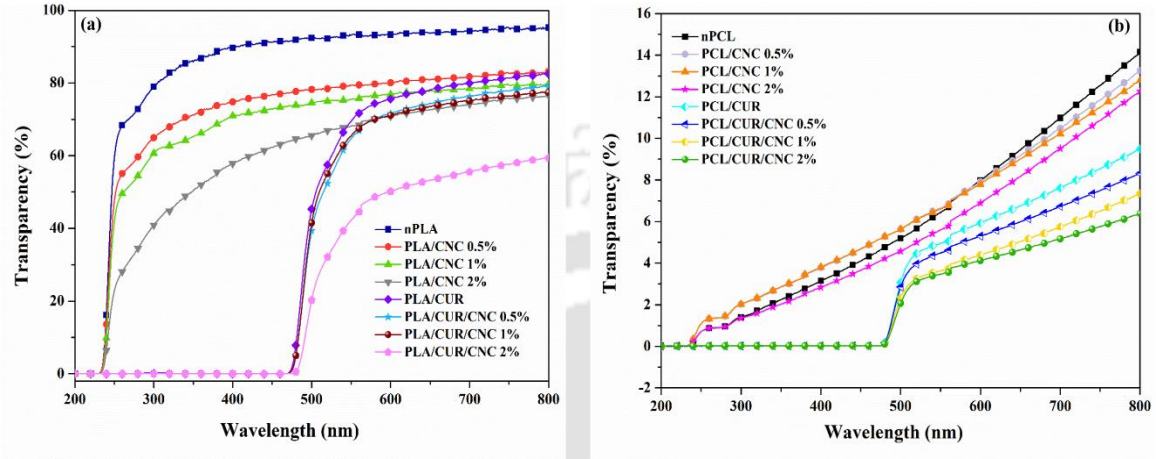

Figure 8.4: Transparency of (a) neat PLA, PLA/CNC, and PLA/CUR/CNC bio-composites, and (b) neat PCL, PCL/CNC, and PCL/CUR/CNC bio-composites.

Further, the highest reduction of around 41% was observed in PLA/CUR/CNC 2% where agglomeration of CNC particles might enhance the reduction in transparency. This analysis suggested the inclusion of CUR-administered UV-light blocking properties to the film which would protect food material from oxidation and deterioration. A similar type of observation was found for the PCL bio-composite. However, PCL film is opaque in nature, and the addition of CNC slightly reduced the transparency whereas, CUR loading blocked the UV-light passage. This observation suggested the addition of CUR would develop packaging material for UV-light sensitive food.

8.2.5 Water Vapor Transmission Rate Analysis

The WVTR of nPLA and PLA bio-composites have been ascribed in **Figure 8.5a**. The WVTR of nPLA was 72.4 g.m/m^2.s.Pa and incorporation of CNC reduced the WVTR value

in PLA/CNC bio-composites. The 0.5% loading of CNC showed the highest reduction in WVTR (56.5 g.m/m^2.s.Pa). However, increasing the CNC concentration (1% and 2%) enhanced WVTR which was not higher than nPLA film. The reduction in WVTR after the incorporation of CNC could be attributed to the high crystalline nature of CNC which acted as an efficient nucleating agent and provided impermeable region in the matrix due to the high degree of crystallinity as discussed in Chapter 7. The presence of nucleated crystals and CNCs effectively enhanced the travel path length more tortuous for the passage of water vapor, which reduced the diffusion process thereby lowering the WVTR. Conversely, higher loading of CNC enhanced WVTR which might be due to the agglomeration of particles which creates more free space available for the passage of more water vapor. Further, the addition of CUR reduced WVTR significantly in PLA/CNC film as compared to PLA film. This occurred might be related to the hydrophobic nature of CUR. The highest reduction was noticed in PLA/CUR/CNC 0.5% film with a value of 43.2 g.m/m^2.s.Pa.

The nPCL film exhibited a WVTR value of 60.3 g.m/m^2.s.Pa, which was less than the nPLA film. A similar trend was obtained in the case of PCL/CNC bio-composite, where 0.5% CNC incorporation exhibited a value of 51.3 g.m/m^2.s.Pa. The highest reduction observed in PCL/CUR/CNC 1% (46.8 g.m/m^2.s.Pa) film among all CUR-loaded films as depicted in **Figure 8.5b**. This analysis suggested the addition of CNC with lower loading and CUR reduced the WVTR value of the film which is one predominant criterion for the selection of food packaging material.

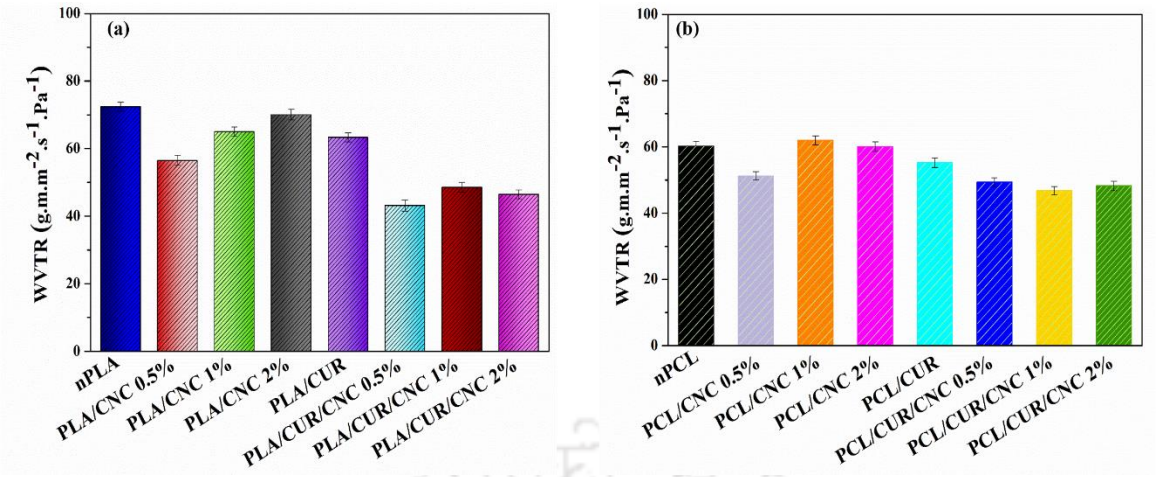

Figure 8.5: Water vapor transmission rate of (a) neat PLA, PLA/CNC, and PLA/CUR/CNC bio-composites, and (b) neat PCL, PCL/CNC, and PCL/CUR/CNC bio-composite films.

8.2.6 Water Contact Angle Analysis

The surface hydrophilicity/hydrophobicity of the developed film was studied by water contact angle (WCA) analysis. The static contact angles of the PLA-based were depicted in **Figure 8.6a**. The WCA of nPLA film was 78.6±1.8° which indicated the hydrophobic nature of the film. The addition of CNC enhanced surface hydrophobicity and the highest value obtained in PLA/CNC was 0.5% (94.9±2.9°). However, CNC loading at 1% and 2% showed 86.5±1.9°, and 82.3±1.9°, respectively, which was lesser than 0.5% CNC loading but higher than nPLA film. The observed findings were supported by the WVTR values of the PLA/CNC bio-composite film. Further, the inclusion of CUR enhanced the hydrophobicity to 105.3±2.1° in PLA/CUR film. The highest surface hydrophobicity was obtained in PLA/CUR/CNC 0.5% film with a value of 115±3.2°. The hydrophobic behavior also increased in PLA bio-composite loaded with 1% and 2% CNC to 109.9±1.1° and 106±1.8°, respectively. The hydrophobic nature of CUR and the high crystalline nature of CNC were responsible for the rise in WCA of the developed film.

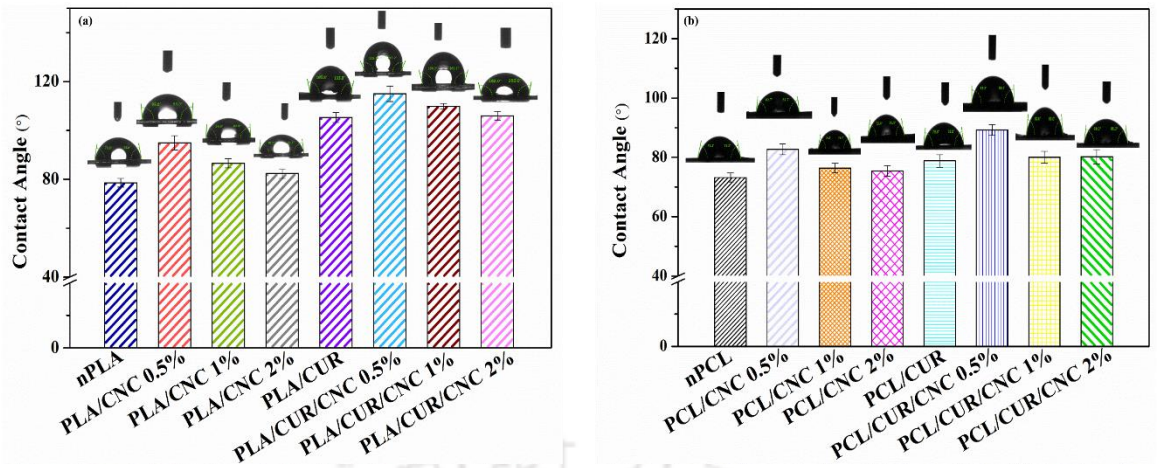

Figure 8.6: Water contact angle of (a) neat PLA, PLA/CNC, and PLA/CUR/CNC bio-composites, and (b) neat PCL, PCL/CNC, and PCL/CUR/CNC bio-composite films.

The WCA of nPCL film was 73.2±1.5°, indicating its hydrophobic nature. Further, the incorporation of CNC and CUR significantly increased the surface hydrophobicity as depicted in **Figure 8.6b**. The trend of the obtained result was similar to PLA bio-composite film.

8.2.7 XRD Analysis

The XRD diffraction pattern of the casted films is presented in **Figure 8.7**. PLA diffraction patterns revealed the intrinsic semi-crystalline nature of the polymers. The presence of a characteristic band of PLA at 16.6, and 19.03° indicated the semi-crystalline nature of nPLA film. The addition of CNC into the polymer matrix enhanced the intensity of PLA characteristics peaks. Besides, new peaks were observed at 14.8, and 22.2° in all PLA/CNC bio-composite films which could be attributed to the CNC polymorphs. The intensity of characteristic peaks increased in bio-composite films with increasing the CNC concentration as compared to nPLA film as depicted in **Figure 8.7a**. The inclusion of CUR showed improved crystallinity in PLA/CUR as higher intense peaks were observed in comparison to nPLA film. Further addition of CUR into the PLA/CNC matrix exhibited

higher intense peaks than PLA/CNC films. Similarly, the addition of CNC into PCL enhanced the peak intensity however, effective results were obtained after the addition of CUR into the PCL/CNC matrix. Contrary to PLA bio-composites, new peak was not found in PCL bio-composites. The obtained intensified peak indicated the enhancement in crystalline property in the developed bio-composite after the inclusion of CNC and CUR bio-fillers. The obtained result is in line with the WVTR data.

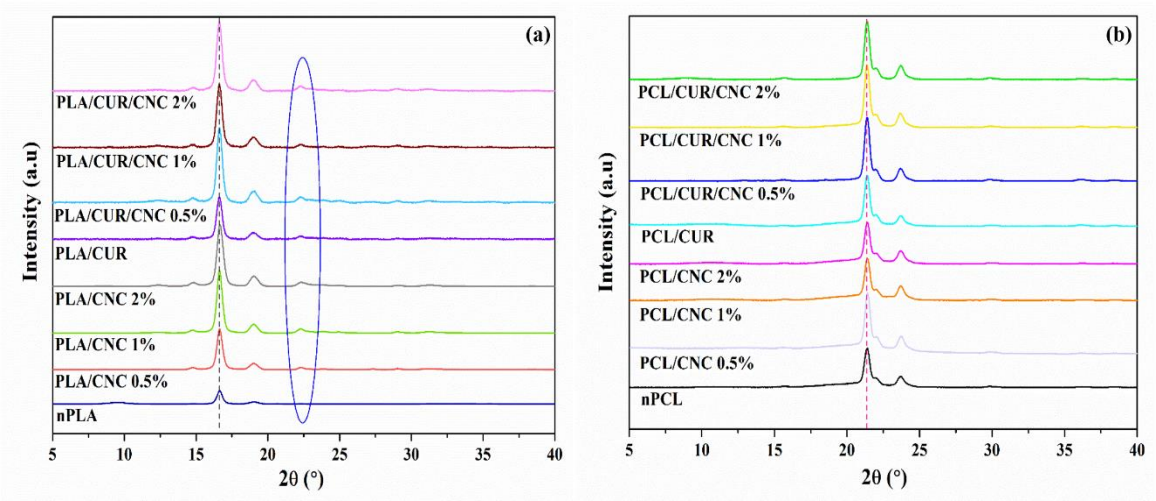

Figure 8.7: XRD analysis of (a) neat PLA, PLA/CNC, and PLA/CUR/CNC bio-composites, and (b) neat PCL, PCL/CNC, and PCL/CUR/CNC bio-composite films.

8.2.8 Migration Study

8.2.8.1 Overall Migration

Three different aqueous food simulants namely water, acetic acid (3% v/v), and ethanol (15% v/v) were used to perform the overall migration studies of PLA/CNC and PCL/CNC bio-composite films to determine the total amount of non-volatile substances that might migrate into foodstuff from developed PLA and PCL films and to understand the effect of cellulose nanocrystals (CNC) on the migration property of PLA and PCL fractions that might tend to migrate when these films brought in contact with food material. The overall migration of PLA bio-composite films was performed at 70 °C for 2 h and 25± 2 °C for 10

days for PCL bio-composite films in three types of food simulants as shown in **Figure 8.8 a,b**. The overall migration of neat PLA and PLA/CNC bio-nanocomposite films was higher in ethanol as a simulant. Next to ethanol simulant, maximum migration was observed in acetic acid and then the least migration was observed in water comparatively. The maximum migration level in ethanol was 5.5 mg dm^{-2} for PLA/CNC 2%. However, this value is much lower than the migration limits for food contact materials, 10 mg dm^{-2} or 60 mg kg^{-1} of simulant, established by the current legislation (Commission Directive, 2002/72/EC). By comparison of the total migration values for all PLA films in ethanol, there was a clear effect of the presence of CNCs that promote significantly the migration of the simulant. The PLA/CNC 0.5% and 1% had the overall migration value of 4.9 and 5.3 mg dm^{-2} as compared to the nPLA value of 4.2 mg dm^{-2} and a similar trend was followed for other simulants (water and acetic acid) and obtained values were below the migration limit. Moreover, the increment in overall migration value in CNC-incorporated film samples might be related to the higher incubation temperature that could have relaxed the chains and enhanced the diffusion of simulants which allowed migrants to move out.

Thermodynamic properties, such as polarity and solubility, play an important role in migration due to interactions between the polymer, migrants, and the food simulant. The poor solubility of a migrant in the food simulant could retain them inside the polymer matrix. However, a simultaneous effect based on the high affinity between the food simulant and the polymer matrix could be also present leading to the absorption by the polymer matrix. In addition, the sorption of certain organic solvents could cause swelling of the polymer matrix, thereby enlarging the gaps between the molecules and enhancing the additive migration [254]. In the case of the present work, migration in all types of food simulant was observed and was more in ethanol simulant, which could be due to absorption

of the solvent in the polymer matrix, leading to the release of small particles like nanocrystals and PLA degradation products.

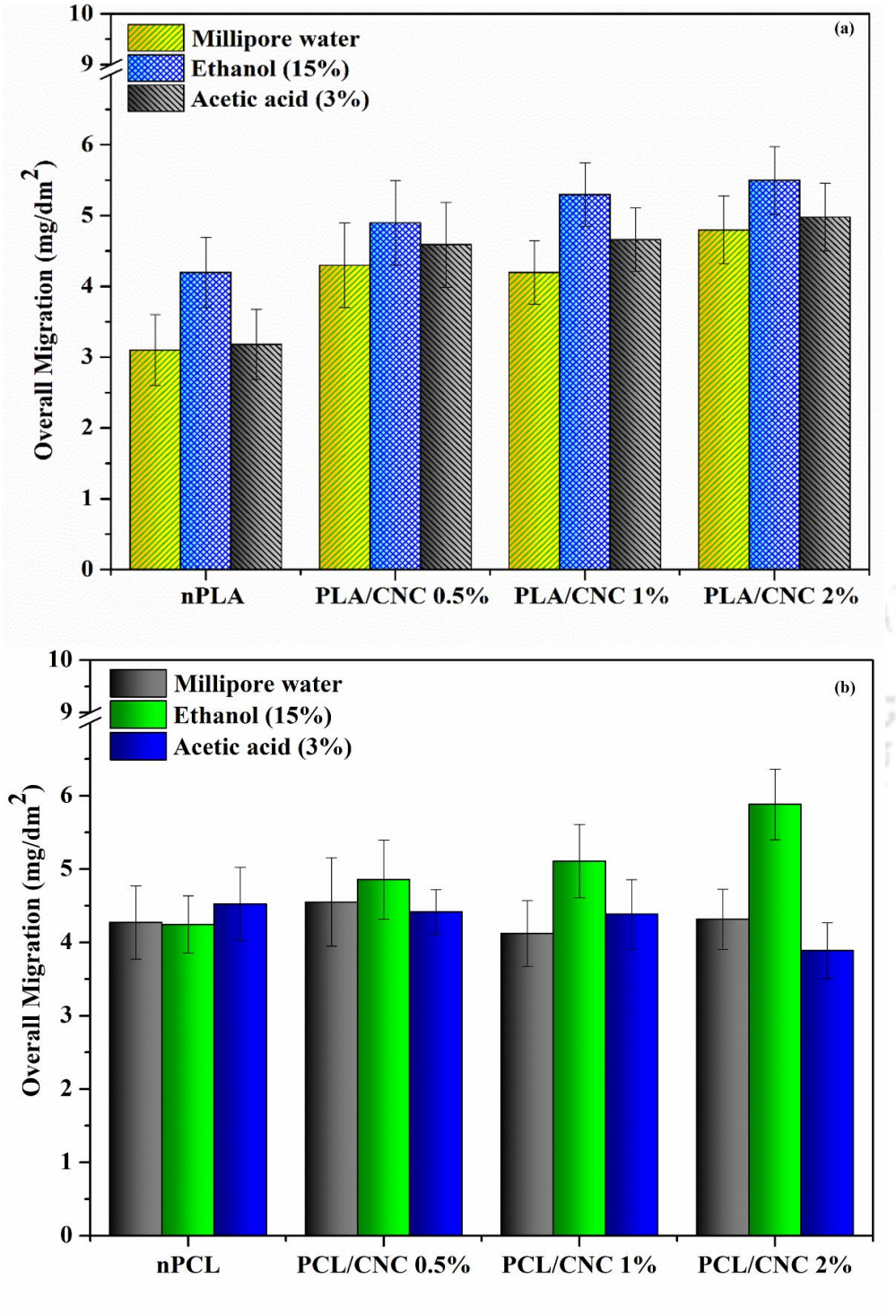

Figure 8.8: Overall migration of (a) PLA, and (b) PCL bio-composite films in three types of food simulant.

The overall migration study of PCL bio-composite film was performed with the previously mentioned three types of food simulants. A similar observation was found in the case of PCL bio-composite films and the highest migration was obtained in ethanol simulant. Besides, higher migration was observed in PCL/CNC bio-nanocomposite (5.9 mg dm^{-2}). With increasing concentration of CNC, migrant value was increased same as observed in PLA/CNC bio-nanocomposite as compared to neat PCL film. Most importantly, the overall migration value for all the PCL films did not cross the maximum specified limit (10 mg dm^{-2}). In addition, several factors such as degradation of polymer chains in the presence of food simulants, migration of low molecular weight chains into simulants, lowering of glass transition temperature (T_g), and formation of higher fractions of crystallites can lead to significant variations in overall migration values.

8.2.8.2 Specific Migration Kinetics

In recent days, active packaging has gained huge attention due to its effective preservation properties to keep food products longer times with improved quality and safety through releasing active agents/compounds enriched with antimicrobial or antioxidant activity. In the present study, curcumin (CUR) was selected as one of such bioactive compounds that were incorporated as a specific/active agent in the polymer matrix (PLA and PCL) to understand the effect of nanoparticles i.e., CNC that was added to the neat polymer to improve the physicochemical property of the developed bio-composite film, on the migration of CUR from the packaging film. Numerous scientific investigations have demonstrated during the last two decades that migration from food-contact materials into food and food simulants are predictable physical processes. Mass transfer from plastic material into foodstuffs in most cases obeys Fick's laws of diffusion. Generally, the release of substances that involve migration is the result of diffusion, dissolution, and equilibrium processes [255]. Various factors influence the migration of a substance from the packaging

material including the film fabrication method, the volatility, and polarity of the substance, the chemical interaction between the substance and polymer chains, hydrophobicity and hydrophilicity of the polymer as well as food properties and composition [246]. In general, an active substance can be migrated into a food simulant by swelling-controlled migration where three main step mechanisms are involved. Firstly, the absorption of solvent from the food simulant which leads to the swelling effect of the polymer, next the active compound molecule being dissolved or dispersed in the polymeric matrix and finally the active compound migrating to the food simulant [45].

- ***Specific Migration Kinetics of PLA Bio-composite Films***

Four types of CUR-loaded PLA bio-composite films were fabricated namely, PLA/CUR, PLA/CUR/CNC 0.5%, PLA/CUR/CNC 1%, PLA/CUR/CNC 1%, and PLA/CUR/CNC 2% to understand the migration mechanism of CUR from the film with or without the presence of nanoparticle (CNC). To make the system easily understandable, a constant amount of CUR was loaded onto each type of film where nanoparticle (CNC) concentration was varied (0.5, 1, 2 wt.%) for obtaining the concentration effect on migration of CUR. The specific migration study was performed using a 15% ethanol solution as a food simulant, which was selected based on the overall migration result as a maximum migrant was obtained from this simulant. Therefore, a specific migration study under 15% ethanol would provide the highest migration of active agents as curcumin is also well dissolved in ethanol solution. In addition, PLA and CUR both are GRAS substances, hence it is desirable to obtain the maximum release of CUR to obtain optimum quality food products with prolonged shelf-life. Therefore, some mathematical models were used to understand and visualize the effect of CNC on the migration rate of CUR. The storage condition and collection of samples at the particular interval were mentioned in Chapter 2. The migration kinetics of CUR from the bio-composite films was investigated using Zero order, First

order, Higuchi, and Korsemeyer-Peppas models. Since these models are usually useful to fit only the data up to 60% of the drug released over time, therefore the data were calculated and plotted based on 60% migration by considering it as the saturation point [256].

The zero-order kinetic model prediction of CUR-loaded bio-composite film has been depicted in **Figure 8.9**. The data were calculated after collecting the sample at a particular time interval (0, 6, 9, 12, 24, 36, 48, and 120 h) during storage at 40 °C. The data were plotted ($1-M_t/M_0$) against time up to 48h as at this point saturation was achieved. In addition, in the case of zero-order kinetics, the assumption suggested that the migration of an active agent is only a function of time and the process takes place at a constant rate independent of active agent concentration.

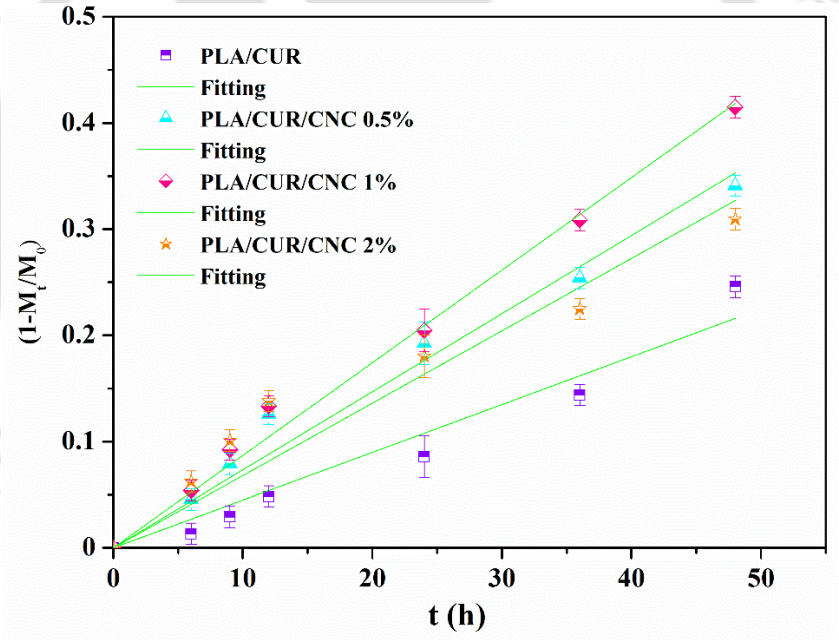

Figure 8.9: Zero-order migration profile of curcumin molecules from PLA bio-composite films.

The zero-order kinetic model suggested that the presence of CNC increased the CUR migration rate through higher diffusion as compared to PLA/CUR film. The higher rate of migration might be attributed to polymer matrix erosion and hydrolytic cleavage of the polymer chain. The zero-order migration rate constant (k_0) of PLA/CUR film was

0.0045 s^{-1}, where an increasing value of rate constant was observed in PLA/CNC/CUR film with increasing the CNC contraction such as 0.0074, 0.0087, and 0.0068 for 0.5%, 1%, and 2% CNC loading. However, a slight reduction was noticed in the case of the 2% CNC loaded sample although the value was higher than PLA/CUR film. This could be due to the agglomeration of nanoparticles hindering the path through which CUR diffused. The data point was fitted using non-linear curve fitting and R^2 is provided in **Table 8**.1.

The first-order kinetic model considers the overall diffusion process to be a single process and is used to evaluate the migration systems that were strongly controlled by the loaded quantities of the studied active agent [246]. The migration of the active/specific agent into the food simulant was initially analyzed for its fit to a first-order kinetics model and used to determine the initial migration rate. The assumption of this model are as follows: the diffusion from the polymer film into the food/food simulant is one-dimensional, and the migrant is homogenously distributed in the polymeric film at the beginning of the mass transfer. Besides, the food simulant was well mixed, no boundary resistance existed for the transfer of the migrant from the film to the food simulant, and the distribution of the migrant in the food simulant after the mass transfer was homogenous and the number of migrants not decompose or evaporated during the migration process. **Figure 8.10** represents the first-order kinetic model prediction for PLA bio-composite films. The higher value of first-order migration rate constant (k_1) in CNC-loaded PLA/CUR film as compared to only CUR-loaded film suggested higher migration of CUR from PLA/CUR/CNC film. The obtained data were plotted (ln $(1-M_t/M\infty)$ against time and fitting was performed. The k_1 and R^2 values of PLA/CUR and PLA/CUR/CNC films were provided in **Table 8.1** The increase in k_1 might be related to the diffusion and dissolution of CUR through the matrix and the presence of CNC might create voids thereby enabling the release of CUR from the film.

Table 8.1: Migration co-efficient of curcumin from developed active films to food simulant using four different mathematical model.

Sample Designation	Zero Order		First Order		Higuchi			Korsemeyer-peppas			
	k_0 (s^{-1})	R^2	k_1 (s^{-1})	R^2	k (s^{-1})	D (cm^2s^{-1})	R^2	k (s^{-1})	D (cm^2s^{-1})	n	R^2
PLA/CUR	0.0045	0.9839	0.0050	0.9766	0.9005	1.12×10^{-8}	0.9839	0.1112	1.32×10^{-9}	1.39	0.9969
PLA/CUR/CNC 0.5%	0.0074	0.9919	0.0086	0.9953	1.4714	1.60×10^{-8}	0.9919	1.3623	1.48×10^{-8}	0.83	0.9957
PLA/CUR/CNC 1%	0.0087	0.9971	0.0107	0.9959	1.7444	2.22×10^{-8}	0.9971	1.2015	1.53×10^{-8}	0.91	0.9976
PLA/CUR/CNC 2%	0.0068	0.9765	0.0079	0.9831	1.3629	2.15×10^{-8}	0.9765	2.2511	3.56×10^{-8}	0.67	0.9909

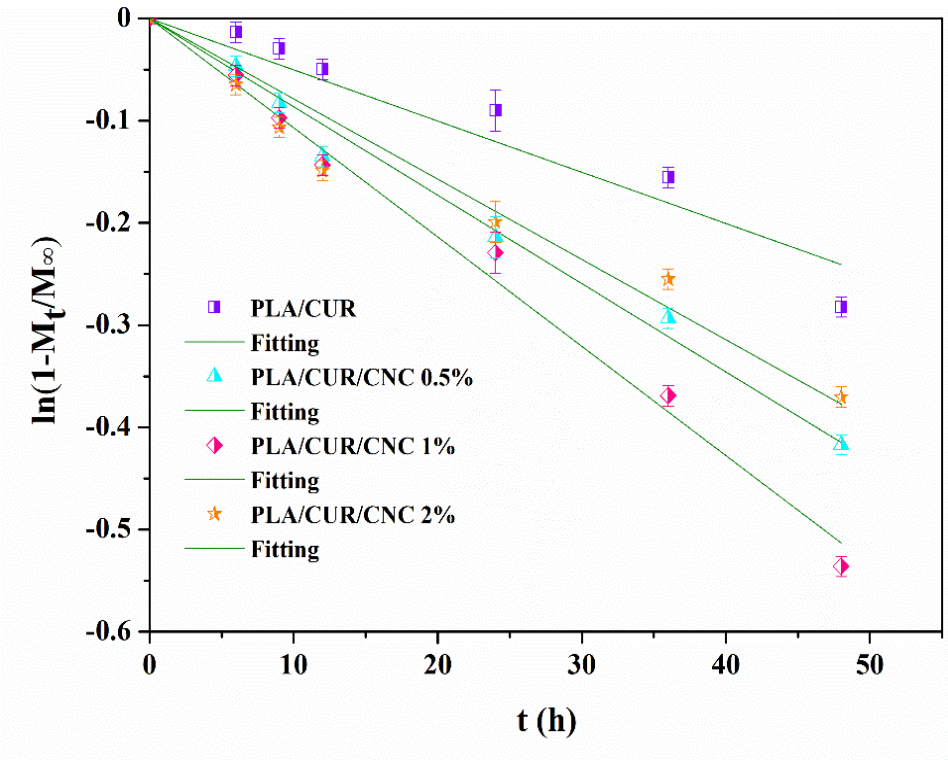

Figure 8.10: First-order migration profile of curcumin molecules from PLA bio-composite films.

The Higuchi model describes the migrant (active agent) release as a diffusion process based on Fick's law which is square root time dependent. The assumptions of this model are the matrix contains an initial specific agent concentration much higher than the solubility of a specific agent, diffusion is unidirectional, because the edge effects are negligible, the thickness of the polymeric is much larger than the size of the specific molecules, swelling or dissolution of the matrix is negligible, and diffusivity of the migrant is constant. **Figure 8.11** describes the Higuchi model (M_t/M_∞ vs $t^{1/2}$) of PLA bio-composite films. The migration rate constant (k) and diffusivity (D) was calculated using this model and the results indicated the presence of CNC in the film enhanced the diffusivity significantly as a result rate of migration was increased. The fitted value, k, and D values were inserted in **Table 8.1**.

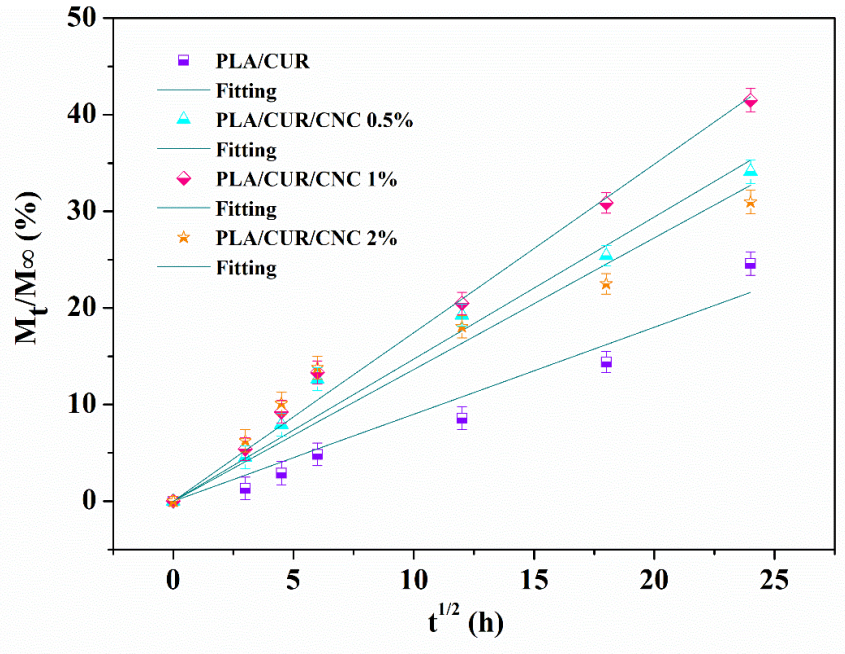

Figure 8.11: Higuchi model of migration profile of curcumin molecules from PLA bio-composite films.

Korsemeyer-Peppas model was developed specifically for the migration of a specific molecule from a polymeric matrix based on the power law model, which is useful for the study of drug release (migration of specific agents) from polymeric systems when the release mechanism is unknown or when more than one type of phenomenon of migration is involved [257, 258]. It can be seen as a generalization of the observation of the superposition of two independent mechanisms of specific agent transport, relaxation, and diffusion. This model provides information on the migration rate constant (k), diffusion coefficient (D), and diffusion exponent (n). The Korsemeyer-Peppas kinetic model data (M_t/M_∞) were plotted against time (t) and depicted in **Figure 8.12**. Depending on the value of 'n' the migration behavior of an active/specific agent in a matrix system can be predicted. The presence of CNC increased the migration rate of CUR (2.25 s^{-1}) from film significantly as compared to PLA/CUR film (0.11 s^{-1}). A higher diffusion coefficient (D) was obtained in film samples containing CNC nanoparticles. The D value was increased with the higher loading of CNC, respectively as compared to PLA/CUR film. The 'n' value of PLA/CUR

was 1.39 which is >1, indicating planner geometry of thin film which followed Super Case II transport phenomena. This phenomenon is an extreme form of transport when during the sorption process, tension and breaking of the polymer or solvent crazing occurred.

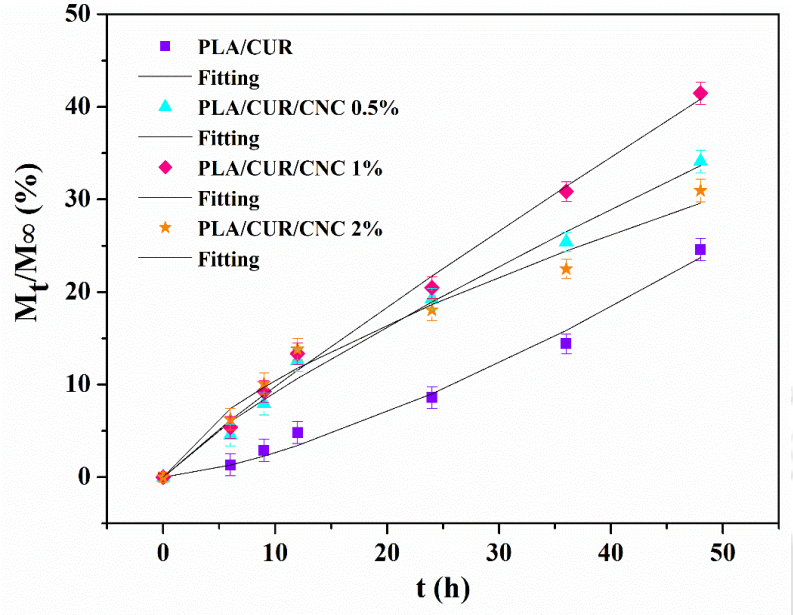

Figure 8.12: Korsemeyer-Peppas model of migration profile of curcumin molecules from PLA bio-composite films.

Further, the obtained 'n' value of PLA/CUR/CNC films with varying CNC loading of 0.5, 1, and 2 wt.% was 0.83, 0.91, and 0.67, respectively which was in the range of 0.5<n <1, indicated anomalous transport. The model is non-Fickian or anomalous transport, and the mechanism of migration is governed by diffusion and swelling. The diffusion and swelling rates are comparable. The rearrangement of polymeric chains occurring slowly and the diffusion process simultaneously cause time-dependent anomalous effects. The R^2 value of the fitting curve was inserted in **Table 8.1**.

Amongst the four kinetic models, the best-fitted model was selected based on the R^2 value as depicted in **Table 8.1**. The Korsemeyer-Peppas diffusion model was found to be the best-fitted kinetic model for CUR-loaded PLA bio-composite films.

- ***Specific Migration Kinetics of PCL Bio-composite Films***

Similar to CUR-loaded PLA bio-composite films, four types of PCL bio-composites were developed. The ethanol solution (15%) was selected as food simulant based on overall migration data and the specific migration was performed at 7 °C and samples were collected at a particular time interval (0, 6, 12, 24, 36, 48, 60, 72, 84, 96, and 108 h) during the experiment. In the case of PCL bio-composite films saturation was reached at 108 h. Four different types of kinetics models were used in this case same as mentioned in section **8.2.8.2.1.** The zero and first-order plots have been depicted in **Figure 8.13a,b,** whereas Higuchi and Korsemeyer-Peppas plots are represented in **Figure 8.14a,b**, respectively. Interestingly, a significant reduction in CUR migration rate was observed in CNC-loaded PCL film as compared to PCL/CUR film. A similar trend in reduced migration in presence of CNC was obtained from all four types of the mathematical model as tabulated in **Table 8.1**.

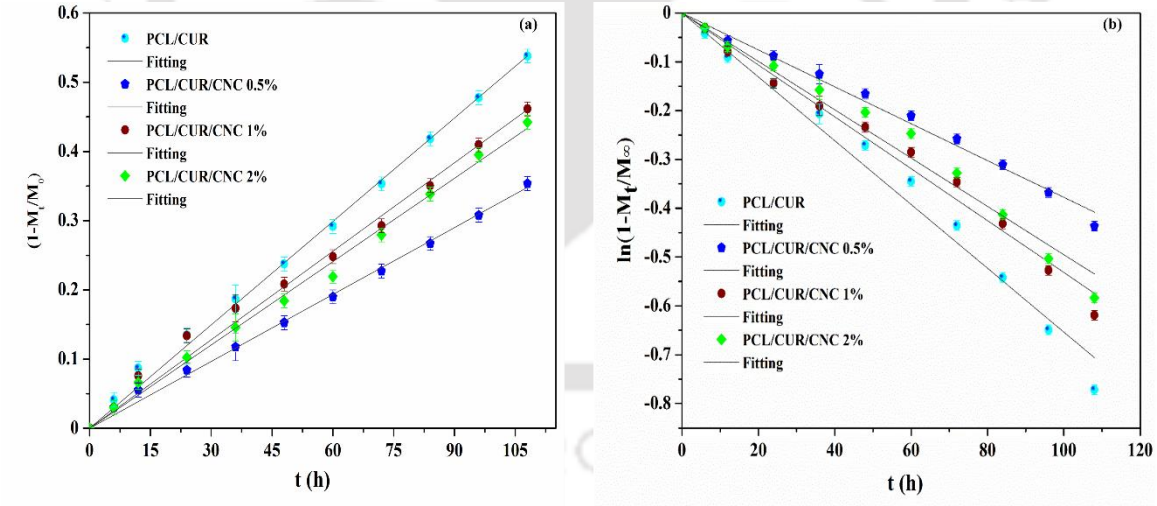

Figure 8.13: (a) Zero-order, and (b) First-order migration profile of curcumin molecules from PCL bio-composite films.

Further, a reduction in diffusion coefficient (D) was obtained from both Higuchi and Korsemeyer-Peppas mathematical models. The diffusion exponent (n) value of PCL/CUR and 0.5%, 1% CNC-loaded film were 0.94, 0.96, and 0.90, respectively, indicating

anomalous transport. However, PCL/CUR/CNC 2% film showed 'n' of 1.02, suggesting super case II transport behavior of CUR migration. The reduction in the migration rate of CUR might be attributed due to the storage of the sample at 7 °C which was above T_g and below the melting temperature (T_m) and in this condition, semicrystalline polymers such as PCL begins to soften but did not exhibit fluid behavior. At this particular temperature above T_g and below T_m the state of the polymer is in a rubbery region where the material can exhibit large elongations under relatively low load. Further, the presence of CNC in the PCL/CUR matrix reduced the migration rate of CUR effectively which could be attributed to the restriction of the movement of CUR by blocking of pathway due to the presence of nanoparticles between the passage in the rubbery state of the polymer and provide more entangled polymer which allows slow release of curcumin.

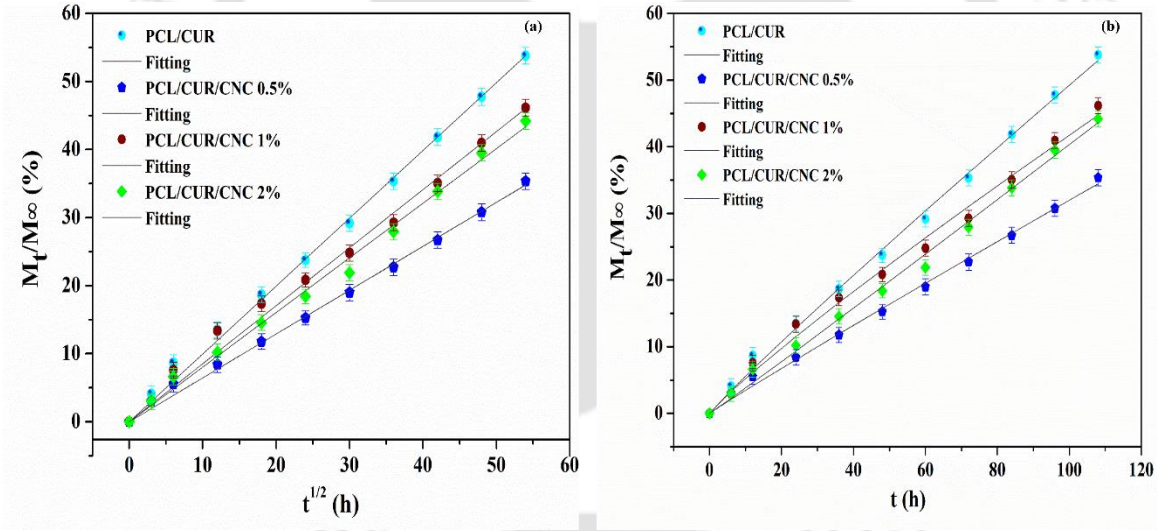

Figure 8.14: (a) Higuchi, and (b) Korsemeyer-Peppas migration profile of curcumin molecules from PCL bio-composite films.

8.2.9 Antioxidant Activity

The antioxidant activity in terms of free radical DPPH scavenging activity was determined for developed PLA and PCL bio-composite films and represented in **Figure 8.15**. The antioxidant activity prevents free radical generation which is responsible for occurring off

odor, rancidity, lipid oxidation, discoloration, and others. The antioxidant activity of nPLA film was 16.8% and the incorporation of CNC did not alter the antioxidant activity effectively in PLA/CNC bio-composites. This outcome might be due to the absence of antioxidant activity in CNC. However, the addition of a fixed amount of CUR significantly enhanced the antioxidant activity by 67%. The antioxidant activity of PLA/CUR, and PLA/CNC/CUR was 83% and 84%, respectively. However, the presence of CNC and increasing concentration of CNC did not affect the antioxidant activity.

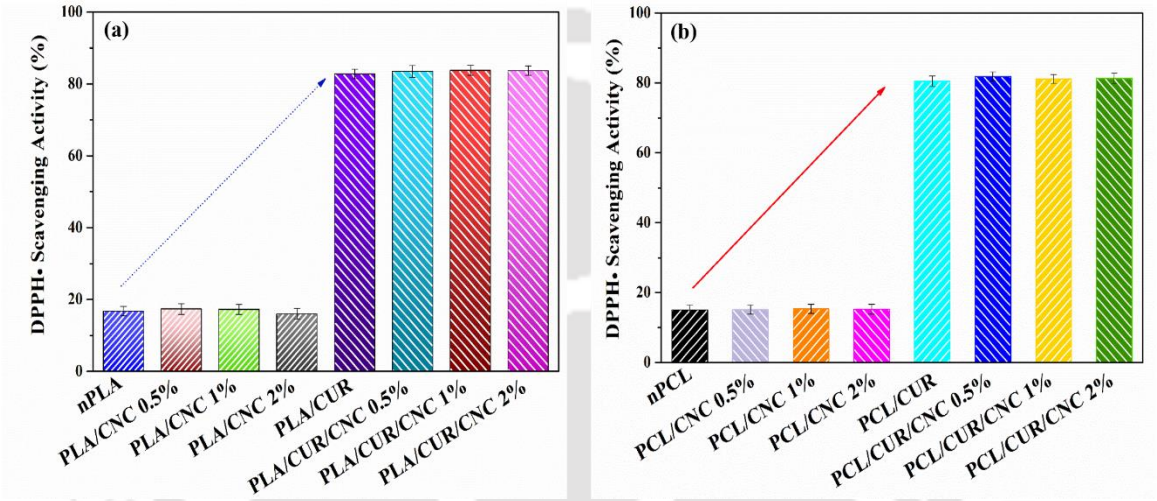

Figure 8.15: Antioxidant activity of (a) neat PLA, PLA/CNC, and PLA/CUR/CNC bio-composites, and (b) neat PCL, PCL/CNC, and PCL/CUR/CNC bio-composite films.

Similar results were obtained in the case of PCL bio-composites. Where, the addition of curcumin enhanced antioxidant activity from 15% to 81%, in the case of nPCL and PCL/CNC/CUR bio-composites, respectively. The obtained antioxidant activity in bio-composite films came from phenolic groups present in the CUR. The CUR-incorporated PLA and PCL bio-composite films with high antioxidant activity can be used as an active secondary packaging material to package foods sensitive to oxidative stress to prevent oxidative degradation and enhance shelf-life.

8.2.10 Antimicrobial Activity

The antimicrobial activity of developed PLA and PCL bio-composites as secondary active packaging material against two typical food pathogenic bacteria, *E. coli,* and *S. aureus*, was investigated using the colony counting method, as depicted in **Figures 8.16 & 8.17**. The nPLA and PLA/CNC bio-composite films when incubated with bacteria, exhibited no antimicrobial activity for both pathogens as the bulky colony was found as picturized in **Figure 8.16**. However, the addition of CUR into PLA the matrix exhibited the occurrence of the lesser colony in the plates, incubated with respective pathogens (**Figure 8.16)**. A superior antimicrobial behavior with a colony inhibition rate of around 87 and 77% for *E. coli*, and *S. aureus,* respectively were obtained.

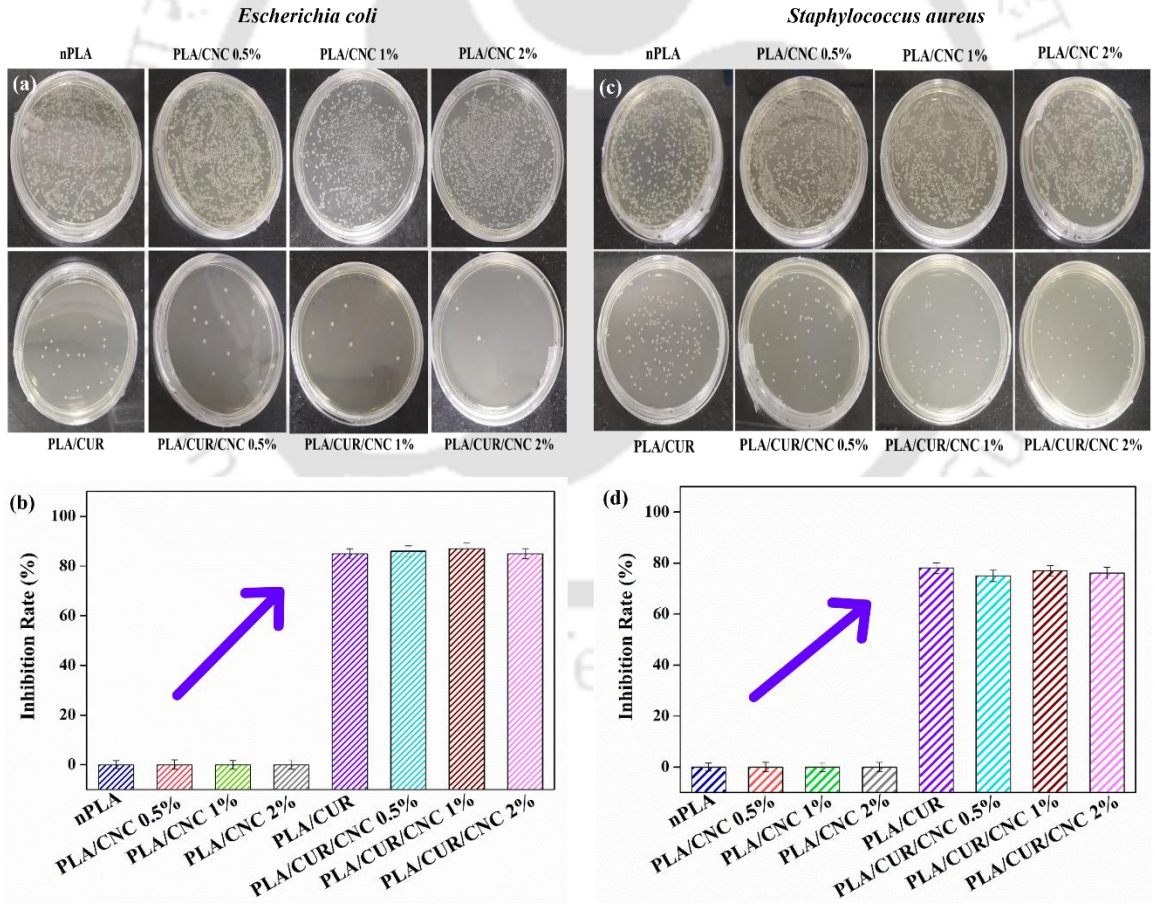

Figure 8.16: Antimicrobial activity of *E. coli* (a, b), and *S. aureus* (c, d) in developed PLA bio-composite films.

The incubated plates contain developed PCL bio-composite films with the food pathogens have been described in **Figure 8.17**. The incorporation of CUR into PCL and PCL/CNC-matrix exhibited significant antimicrobial activity with an inhibition rate of 88% and 73% for *E. coli* and *S. aureus*, respectively. Since neat PCL and CNC are devoid of antimicrobial property, therefore, no inhibition rate was found in nPCL and PCL/CNC bio-composite films, and dense colonies were exhibited in the incubated plates (**Figure 8.17**).

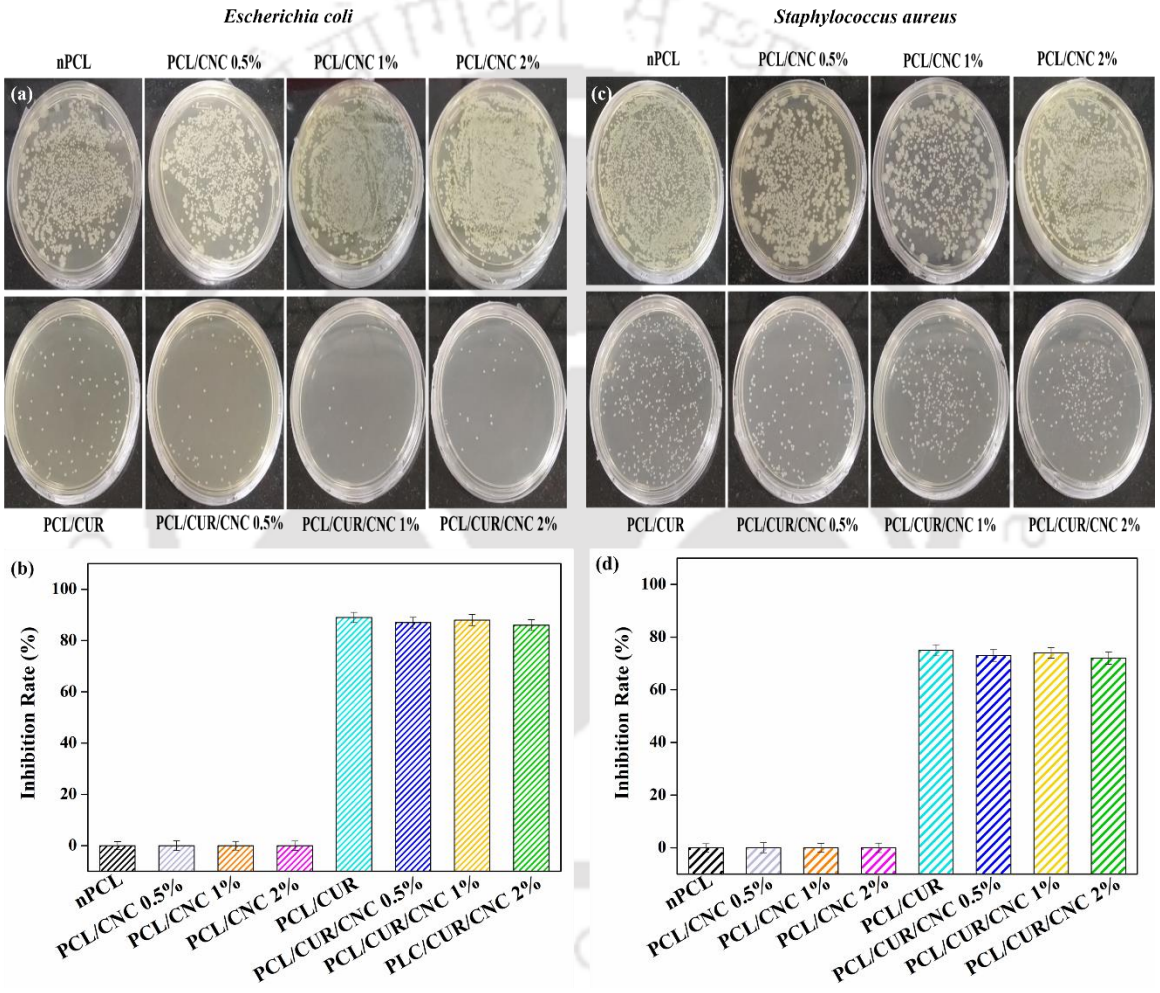

Figure 8.17: Antimicrobial activity of *E. coli* (a, b), and *S. aureus* (c, d) in developed PCL bio-composite films.

Moreover, the presence of CNC did not affect the antimicrobial activity in developed bio-composites. The results indicated higher antimicrobial activity against *E. coli* was observed in both CUR-incorporated PLA and PCL bio-composites. It was confirmed that CUR

contributed antimicrobial properties to the developed bio-composite films. In addition, CUR destroys the cell protein (FtsZ) by binding to it and restricts to form of protein assembly, thereby hindering the Z-ring formation and finally inhibiting the cell migration and growth of microorganisms as this protein is essential for microbial cell division and viability of bacteria [209]. Besides, reported literature indicated that the association of CUR with the cell membrane damage membrane activity and peptidoglycan layer of Gram-positive and Gram-negative bacteria thereby preventing microbial growth. Moreover, CUR-incorporated PLA and PCL bio-composite film can be used as active food packaging material to protect the food from food pathogens.

8.2.11 Biocompatibility Study

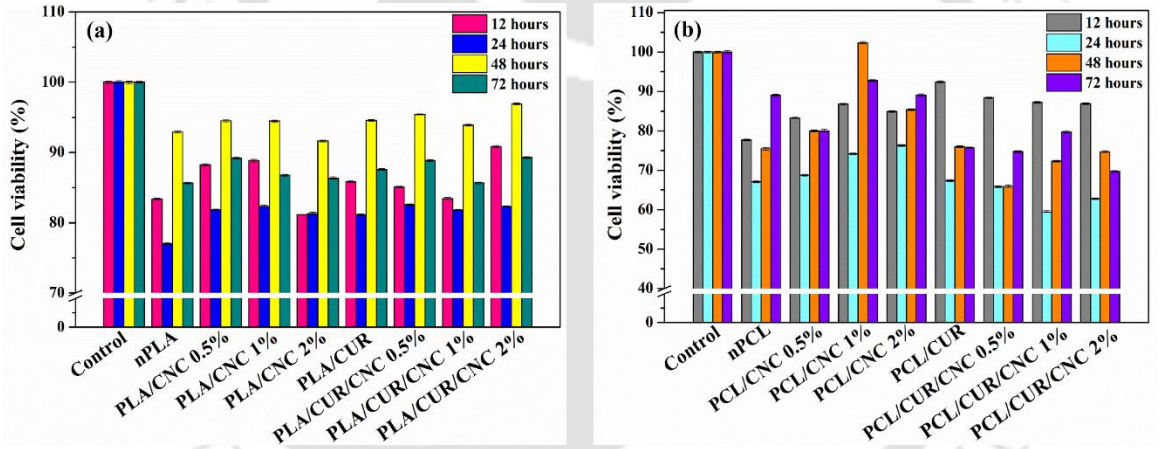

Figure 8.18: Effect of CNC and CUR on the biocompatibility of (a) PLA, and (b) PCL-based bio-composite films on BHK-21 fibroblast cells exposed for 72 h. The media along with the cell without the presence of any film sample was considered the control.

The biocompatibility of the bio-composite films was studied in vitro by incubating them with BHK-21 fibroblast cells for 72 h, and the results are shown in **Figure 8.18**. All films showed a cell viability of 80% or more in PLA bio-composites and more than 75% in PCL bio-composite after 72 h of incubation, and there was no significant difference in the cell

viability of the bio-composite film according to the amount of CNC and CUR added to the PLA bio-composite whereas slight variation was noticed in case of PCL films. The results indicated that the addition of CNC and CUR did not negatively affect the biocompatibility of the PLA and PCL-based bio-composite films. However, the control sample without the film sample showed 100% cell viability whereas, at the end of 72 h of incubation around 80% cell viability was observed in the film sample. This reduction in the percentage of cell viability in film samples might be attributed to the presence of a trace amount of trapped solvent in the polymer matrix. In this study, chloroform was used as the solvent for dissolving the polymers. However, the cell viability of all films was more than 50% indicating the non-toxic nature of the film sample hence, the developed films can be used as secondary food packaging material.

8.2.12 Application of Developed Bio-composite Films on Potato Cubes as Secondary Packaging Material

The fabricated PLA and PCL-based bio-composite films were used as secondary packaging material for the packaging of potato cubes. Small pouches were made by developed film and potato cubes were packed inside the packet and heat sealing was done to close the mouth of the pouch and stored at room temperature (25±5 °C) for 7 days. The weight loss and firmness of the potato cubes after 7 days were measured to know the physical condition of the food. It is well known that cut potatoes are prone to browning/blackening if kept under open air hence, visual observation was conducted to find out any color changes and visible mold occurrence at the end of the storage days.

- ***Weight Loss***

The percentage of weight loss was measured after seven days of storage. For this study, two types of control samples were selected one was keeping potato cubes under open air and another one was potato cubes kept inside the nPLA packet to draw the comparison.

The highest weight loss was observed in the control sample which was around 9%, and in potatoes kept inside the nPLA pouch was 7%. The addition of CNC into the polymer matrix reduced moisture evaporation and maximum weight loss was obtained at 5%. The reduction in weight loss of potato cubes might be related to improved crystallinity and enhancement of the tortuous path of the nPLA packet which restricts the water vapor passage from food through the packaging material. Further, there were no such significant changes in weight loss were noticed with increasing CNC concentration in packaging material. In addition, the CUR-incorporated PLA/CNC packet showed a minimum moisture loss of 4% which indicated the presence of CUR restricted the moisture loss due to its hydrophobic nature. A similar trend was observed in the PCL bio-composite as well.

- ***Firmness***

After the completion of storage days, the texture analysis was conducted by measuring the firmness of the potato cubes. A significant loss in firmness was observed in the control sample and compared to samples kept inside the pouch as depicted in **Figure 8.19b.** The inclusion of CUR along with CNC restricted the loss in firmness and showed optimum results. The highest firmness (5 N) was observed in samples stored inside the packet of PLA/CUR/CNC 0.5%. The synergistic effect of CNC and CUR restricted the loss of texture in stored samples which is supported by the weight loss analysis. Further, film characteristics of improved water vapor transmission rate and improved crystallinity after the addition of bio-filler CNC and CUR prevent moisture and texture loss when food samples come in contact with packaging film.

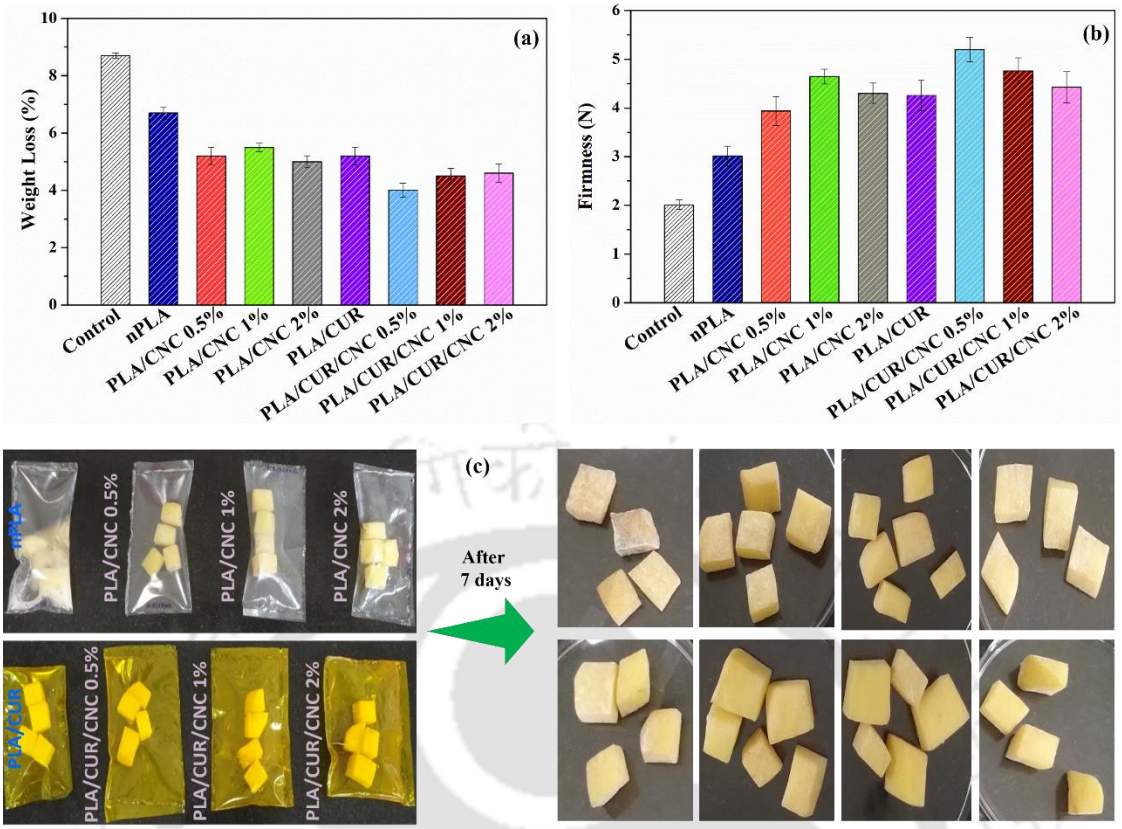

Figure 8.19: (a) Weight loss, (b) Firmness of stored potato cubes after seven days, (c) Visual appearance of the packet along with food during storage and after completion of the storage period.

- ***Visual Appearance and Mold Growth***

On completion of the storage period, surface blackening and visible mold growth were observed in the control sample stored under open air and in the nPLA packet sample. However, no blackening or browning was observed in samples stored in packets containing CUR. The obtained results were attributed to the antimicrobial nature of CUR which inhibited the growth of mold in a stored food sample. Besides, CUR might protect the food sample from deterioration due to its UV-light blocking property.

8.3 Summary

The presented work in this chapter suggests that the incorporation of curcumin into PLA/CNC and PCL/CNC bio-composite films successfully developed active packaging

films. The effect of cellulose nanocrystals in the biopolymer matrix was also investigated in terms of water vapor barrier properties, surface wettability, crystallinity, and overall and specific migration test in consideration of the intended application in food packaging. The effect of CNC on the migration of curcumin from the packaging material to the food simulant was studied. Besides, various physicochemical and biochemical studies were performed to obtain the characteristic effect of curcumin in the film. The curcumin-incorporated films showed effectively higher antioxidant and antimicrobial activity, and excellent UV-light blocking properties. All developed films were non-toxic in nature. Importantly, the incorporation of CNC enhanced the curcumin migration rate from PLA bio-composite films during storage at 40 °C. It is noteworthy to mention that, the faster rate of curcumin migration enhanced the food shelf-life by protecting the food from oxidation, light sensitivity, and microbial attack. However, a slower rate of curcumin migration was observed in presence of CNC from PCL/CNC bio-composite films than neat PCL film during storage at 7 °C. Various mathematical models were used to understand the mechanism of curcumin migration and the effect of CNC on it. Korsemeyer-Peppas model was found to best fitted model. The overall migration of PLA/CNC and PCL/CNC bio-composite films was under the specified limit. Therefore, CNC and CUR can be used as effective bio-fillers to fabricate active film for food packaging which would provide extended shelf-life with improved quality.

CHAPTER 9

CONCLUSION & FUTURE PERSPECTIVES

This chapter summarizes the key findings of the thesis work and highlights the fundamental issues and provides perspectives for future studies on algae biomass waste for sustainable food packaging applications.

9.1 Conclusion

The foremost priority of this research work is the utilization of algae biomass residue which is a bio waste and the development of sustainable primary and secondary food packaging material for shelf-life extension of fresh produce and reduction of postharvest loss. The innovations and applications of bio-fillers extracted from waste algae biomass in development of sustainable primary and secondary food packaging material in this current thesis work include: (i) green extraction and process optimization of crude algae ethanolic extract and characterization of waste algae biomass powder and its extract and algal extract incorporated chitosan-based casted edible active film as primary packaging material, (ii) application of developed chitosan and algae extract incorporated (CS/CAEE) edible coating solution on fresh produce such as tomato, chili, onion, and potato and shelf-life storage study of coated and control samples, (iii) development of algae extract and turmeric essential oil incorporated guar gum-based edible packaging, (iv) optimization of edible gum-based coating for shelf-life extension of the cut potato, (v) isolation of cellulose nanocrystals (CNC) from residual green algae biomass and development of PLA and PCL bio-composites for food packaging by incorporation of two type of bio-fillers CNC and algae waste powder (WABR) and their detailed characterization on crystallization behavior, and (vi) fabrication of curcumin and CNC loaded sustainable active secondary

packaging material and migration study of developed films. In this context, this thesis has addressed the use of bioactive compounds and nanomaterials by utilizing waste algae biomass residue and incorporating these bio-fillers to modify the inherent characteristics of sustainable biopolymers for primary (edible film and coating) and secondary food packaging applications. The developed edible coatings are effectively extended the shelf-life and quality of fresh produce. The key outcome of this thesis work are as follows: firstly, the waste algae biomass, specifically *Dunaliella tertiolecta* was utilized for first time to develop primary active edible packaging material by incorporating algae extract comprised of various bioactive compounds to arrest the post-harvest losses; secondly, the non-toxic algae extract incorporated chitosan-based edible packaging films were rich in antioxidants due to presence of bioactive compounds mainly β-carotene, which tuned the inherent physicochemical properties of biopolymer such as reduced water vapor permeability, blocked UV-Vis light transmission, improved tensile strength, and effectively extended the shelf-life of fresh produce such as tomato, potato, onion, and green chilli; thirdly, inclusion of turmeric essential oil along with algae extract provided significant synergistic effect in the developed guar gum-based edible films that tuned the physicochemical and microbial characteristics of the edible active films by imparting superior antioxidant and antimicrobial activity, UV-light blocking property, and application of guar gum-based edible coating on cut potatoes significantly reduced browning during storage at room temperature; fourthly, bio-nanostructured materials such as cellulose nanocrystals was isolated from the waste algae biomass powder and inclusion of isolated CNC into biopolymers for the development of secondary food packaging material provided bio-nanocomposite films with improved crystalline property and acted as superior nucleating agent; fifthly, the presence of CNC enhanced migration rate of specific agent i.e., curcumin from the packaging film to food simulant based on the storage condition; and sixthly, the

developed sustainable edible packaging formulation can be helpful to agricultural people to keep their produce safe after harvest using edible coating technology. The research work presented in the thesis focuses on the fabrication of sustainable primary and secondary food packaging materials by utilizing bio waste, algae biomass residue, and prolonging the shelf-life of fresh produce, using the developed sustainable packaging material. The major findings and conclusions drawn from the research work are summarized below:

- The ultrasound-assisted green extraction was followed to obtain crude algae ethanolic extract (CAEE) and optimization of the extract based on the highest DPPH antioxidant activity was achieved, using response surface methodology (RSM). The optimized extract was rich in various bioactive compounds mainly β-carotene. The CAEE-incorporated developed edible bio-composite films effectively improved UV-Vis light-blocking properties, antioxidant and antimicrobial activity, and reduced water vapor barrier permeability. The tuned properties in developed edible films would successfully help to extend the shelf-life of food with quality. The obtained extract was found as nontoxic.
- The chitosan-based algae extract incorporated novel edible coating solution effectively enhanced the shelf-life of fresh produce such as tomato, green chili, potato, and onion using a simple dip coating technique by controlling physicochemical, biochemical, and microbial properties, such as respiration, water vapor transmission, oxidation, and ripening during storage at room temperature (25± 2 ℃, 50-70 % RH). The shelf-life of above-mentioned fresh produce was extended by one month, ten days, and two months, respectively, where the coating material effectively suppressed the budding/germination in onion. The developed formulation was biocompatible in nature.

- Algae extract was found as compatible with guar gum matrix and the inclusion of turmeric essential oil exhibited synergistic effects in the developed edible film properties. The CAEE/TEO loaded guar gum film showed effective reduction in water vapor transmission rate, and significantly improved surface hydrophobicity. These edible films were superior in antioxidant and antimicrobial activity, and exhibited excellent UV-light blocking properties. Therefore, the developed edible films would be advantageous for longer storage of light-sensitive and perishable food products.
- The guar gum-based CAEE and TEO-incorporated edible coating formulations were applied on cut potato cubes as a semipermeable layer and optimization of the edible coating was performed using RSM to determine the best formulation for sliced potatoes for extending the shelf-life and stored under ambient conditions (25± 2 °C, 50-70 % RH). It is noteworthy to mention that the formulated GG/CAEE/TEO coating exhibited the best result with improving the color and surface properties, barrier properties, and other physicochemical and biochemical properties of the coated products by controlling oxygen and carbon dioxide transmission rate, and water vapor transmission rate, and by inhibiting the appearance of browning due to suppression of oxidation and mold growth by strong antimicrobial property of TEO. Therefore, this work indicated algae extract is compatible with essential oil means with other bio-fillers for fabricating different types of packaging material with improved characteristic properties.
- The isolated cellulose nanocrystals (CNC) from waste algae biomass were highly crystalline with 89% crystalline index and had a needle-like morphology with a dominant cellulose type I polymorph. Biodegradable PLA and PCL-based secondary packaging materials were fabricated and reinforced with algae biomass residue (ABR) and isolated algal cellulose nanocrystals (CNC). The nanostructured bio-filler

incorporated PLA and PCL bio-composites film provided superior crystallinity. However, ABR-incorporated bio-composite films showed improved crystallinity than neat polymer film but lower than CNC-loaded film. Therefore, ABR can also be used as a bio-filler in polymeric matrix based on the requirement, and improvement in crystallinity is one advantageous property for food packaging material also waste algae can be utilized as resource material for CNC fabrication.

- The overall migration study was conducted for CNC-incorporated developed bio-composite films and it was found that the migration value was under the standard limit after the incorporation of CNC. The curcumin-loaded bio-composite was developed as active secondary packaging. A higher rate of curcumin migration was obtained in the presence of CNC from PLA bio-nanocomposite films during storage at 40 °C, which helped to protect shorter shelf-life food. However, the slow migration of curcumin observed from PCL bio-nanocomposite film in presence of CNC during refrigerated storage would be helpful for the long-term storage of food. Moreover, the inclusion of curcumin positively improved the packaged material quality and shelf-life while tested of cut potatoes. The addition of curcumin effectively enhanced the antioxidant and antimicrobial properties of packaging films. All the developed secondary films were non-toxic in nature and therefore can be used as food packaging material.
- Based on the outcome of the research work, the waste biomass of green algae *Dunaliella tertiolecta* can be utilized as a bio-filler, a resource material for cellulose, bio-nanostructured material, and bioactive compounds. It is noteworthy to mention that waste algae biomass extract incorporated developed non-toxic edible films and coating promisingly extended the shelf-life of fresh produce with improved quality attributes during ambient storage. Specifically, the formulated edible coating could effectively reduce postharvest loss thereby would maintain the economic condition. Therefore, the

Dunaliella biomass waste can be utilized for development of food packaging material. The outcome of the research also provides alternative solution to prolong the shelf-life of perishable with farmer-friendly technology and showcasing a pathway of utilizing *Dunaliella* biomass waste.

9.2 Future perspectives of the research work

The future perspectives of the research can be as follows:

- Scaling up of the edible coating using a dipping technique to coat a higher quantity of fresh produce.
- Other than dip coating, spraying, brushing, and fluidized-bed coating techniques can be applied to coat the fresh produce.
- Application of formulated coating on other food products can be done to check the effectiveness.
- The coated fresh produce can be stored under a modified and controlled atmosphere to identify the effectiveness of the coating material.
- The shelf-life study of food products wrapped in developed edible films can be checked.
- Fabrication of algal bioactive incorporated edible hydrogel and inclusion into secondary biodegradable packaging.
- Other algae species can be utilized for the development of food packaging material.
- The extrusion technique can be adopted to develop algae biomass-incorporated packaging material for industrial viability.

Appendix

Table A1: Coded values of factors with corresponding experimental and predicted responses.

Run	Ethanol concentration (%)	Solvent to solid ratio (mL/g)	Time (min)	Frequency (kHz)	Antioxidant Activity (%)	
					Actual	Predicted
1	-1	1	1	-1	18.6558	18.54306
2	0	0	0	0	31.8411	31.93703
3	0	-2	0	0	34.0761	34.25677
4	0	0	0	2	30.7682	31.69736
5	-2	0	0	0	10.869	10.30987
6	-1	-1	1	-1	20.01432	20.78878
7	0	0	2	0	27.04121	27.34109
8	0	0	0	-2	30.01135	28.63165
9	1	1	1	-1	31.96257	33.79309
10	-1	1	-1	-1	23.28677	23.67502
11	0	0	0	0	31.407	31.93703
12	-1	1	1	1	18.5744	18.45446
13	0	0	0	0	31.407	31.93703
14	1	-1	-1	-1	32.29572	33.24384
15	1	1	-1	-1	31.45894	31.36383
16	1	-1	-1	1	36.66305	36.39815
17	1	-1	1	1	36.99102	37.43094
18	0	2	0	0	31.05996	30.42875
19	0	0	0	0	32.89618	31.93703
20	1	-1	1	-1	40.8779	39.46548
21	-1	-1	-1	1	27.93325	26.93091
22	1	1	1	1	33.32276	32.05626
23	-1	1	-1	1	27.7405	28.77528
24	0	0	-2	0	32.19069	31.44027
25	0	0	0	0	32.18094	31.93703

26	0	0	0	0	31.88997	31.93703
27	1	1	-1	1	34.76214	34.81585
28	-1	-1	-1	-1	21.2395	22.12836
29	2	0	0	0	34.91855	35.02714
30	-1	-1	1	1	20.685	20.40247

Table A2: Degradation result of nCS and developed CS/CAEE films at 5% ($T_{5\%}$) and 10% ($T_{10\%}$) weight loss with first and second maximum degradation (T_{max}).

Film Sample	**$T_{5\%}$ (°C)**	**$T_{10\%}$ (°C)**	**First Degradation (T_{max}) (°C)**	**Second Degradation (T_{max}) (°C)**
nCS	71.1±0.17	98.4±0.23	75.46±0.02	308.51±0.12
CS/CAEE 4%	86.5±0.05	124.2±0.17	113.75±0.08	298.39±0.21
CS/CAEE 8%	84.4±0.03	120.3±0.11	113.75±0.16	298.39±0.22
CS/CAEE 12%	87.2±0.25	125.9±0.12	113.75±0.17	295.12±0.05
CS/CAEE 16%	84.4±1.05	118.7±1.19	113.75±0.16	296.02±0.07
CS/CAEE 20%	77.1±1.15	107.4±1.07	76.12±0.14	293.41±0.09
CS/CAEE 24%	84.4±0.05	113.1±0.16	76.12±0.06	292.02±0.13
CS/CAEE 28%	109.7±0.17	156.8±0.07	106.81±0.07	291.36±0.17

Table A3: Sensory analysis of control and coated tomatoes during storage at ambient conditions. Each value is the average mean of three replicates and '±' indicates the standard deviation.

Sample	Storage days											
	0 day			5 day			15 day			30 day		
	Taste	Flavor	Overall Acceptability	Taste	Flavor	Overall Acceptability	Taste	Flavor	Overall Acceptability	Taste	Flavor	Overall Acceptability
Control	6.1±1.1	5.9±1.1	7±1.2	5.7±1.4	5.8±1.1	5±1.4	ND	ND	1±1.1	ND	ND	1±0.8
nCS	6.2±1.1	5.9±1.0	7±1.1	5.9±1.1	5.9±1.0	7±1.0	5.6±1.3	5.7±1.1	5±1.2	ND	3±1.2	2±1.1
CS/CAEE 2%	6.0±1.1	6.0±1.3	7±1.0	5.9±1.2	5.9±1.2	7±1.1	5.8±1.2	5.9±1.3	6.5±1.2	5.7±1.0	5±1.1	5.5±0.9
CS/CAEE 4%	6.1±1.2	5.9±1.2	7±0.8	5.9±0.9	5.9±1.1	7±1.1	5.8±1.2	5.7±1.3	6.8±1.0	5.8±1.2	5±1.0	6±0.8

Table A4: Color parameter (L*, a* & b*) of coated green chili with control during storage and '±' indicates standard deviation.

Samples	Color parameters	Zero (0^{th}) day	Final (8^{th}) day
Uncoated	L*	32.69 ± 0.12	46.69 ± 0.18
(Control)	a*	-8.77 ± 0.21	4.88 ± 0.28
	b*	18.83 ± 0.12	36.44 ± 0.23
nCS	L*	22.17 ± 0.17	31.17 ± 0.19
	a*	-10.13 ± 0.31	-3.51 ± 0.23
	b*	22.17 ± 0.17	31.17 ± 0.19
CS/CAEE 4%	L*	40.81 ± 0.23	41.35 ± 0.18
	a*	-11.10 ± 0.13	-7.36 ± 0.35
	b*	27.59 ± 0.15	28.82 ± 0.27
CS/CAEE 12%	L*	38.85 ± 0.33	42.59 ± 0.11
	a*	-10.26 ± 0.24	-8.49 ± 0.31
	b*	22.93 ± 0.11	25.19 ± 0.17
CS/CAEE 20%	L*	41.06 ± 0.25	43.79 ± 0.11
	a*	-10.23 ± 0.34	-6.67 ± 0.19
	b*	26.54 ± 0.22	27.28 ± 0.12
CS/CAEE 28%	L*	42.45 ± 0.36	40.32 ± 0.22
	a*	-7.79 ± 0.13	-6.47 ± 0.35
	b*	27.31 ± 0.15	28.542 ± 0.27

Table A5: Color parameter of developed guar gum-based edible active films and '±' indicates standard deviation.

Films	L*	a*	b*	ΔE	YI
Control	85.46±1.67	2.78±0.50	14.83±2.02	18.08±1.67	24.78±1.86
EF A	86.23±1.83	2.16±0.43	14.87±2.33	17.51±1.83	24.64±2.25
EF B	84.23±0.43	4.12±0.36	25.97±2.33	27.94±0.43	44.03±1.42
EF C	81.26±3.50	7.56±1.76	34.19±5.37	37.08±3.50	60.09±4.50
EF D	77.32±2.12	12.12±2.26	43.8±5.21	48.24±2.12	80.91±3.16
EF E	78.28±4.38	8.60±1.33	44.36±2.74	47.53±4.38	80.94±5.38

Table A6: Thermogravimetric analysis of bio-fillers ABR, WABR, extracted algal cellulose, and isolated CNC.

Sample Name	T_{onset} (°C)	T_{max1} (°C)	T_{max2} (°C)
ABR	252	322	583
WABR	255	338	517
Algal Cellulose	292	364	567
CNCs	282	311	369

Table A7: Non-isothermal differential scanning calorimetric analysis of PLA bio-composite films.

Sample Name	T_g (°C)	T_{cc} (°C)	T_{m1} (°C)	T_{m2} (°C)
Neat PLA	58.2	135.8	-	167.1
PLA/CNC0.5	58.5	119.3	166.5	-
PLA/CNC1	58.5	115.1	164.3	169.7
PLA/CNC2	59.2	111.5	163.4	169.5
PLA/WABR0.5	58.6	123.3	-	166.9
PLA/WABR1	58.5	123.8	-	166.8
PLA/WABR2	58.7	122.8	-	166.9

Table A8: Predicted isothermal crystallization parameters of PLA bio-composite samples using Avrami theorem, as determined by differential scanning calorimetry.

Sample Name	k (min^{-1})	n	$t_{0.5}$ (min)	Φ(t) (%)
Neat PLA	0.003	2.12	13.1	28
PLA/CNC0.5	0.022	2.15	4.9	53
PLA/CNC1	0.036	2.21	3.1	58
PLA/CNC2	0.058	2.67	2.5	57

PLA/WABR0.5	0.004	2.39	8.6	40
PLA/WABR1	0.016	2.15	5.8	53
PLA/WABR2	0.015	2.17	5.9	52

Table A9: The lamellar thickness and long period of neat PLA and PLA bio-composite films determined by the SAXS analysis.

Sample Name	Lamellar thickness (*l*)	Long period (D)
Neat PLA	5.4	19.0
PLA/CNC0.5	7.9	19.6
PLA/CNC1	8.1	20.3
PLA/CNC2	8.2	20.9
PLA/WABR0.5	7.6	20.3
PLA/WABR1	7.8	19.6
PLA/WABR2	8	19.6

Table A10: Non-isothermal parameters of neat PCL and its bio-composites where, T_c, T_m, and ΔH_m denotes crystallization, melting peak temperature and melting enthalpy of first cooling and second heating cycle.

Sample Name	T_c (°C)	T_m (°C)	ΔH_m (J/g)
Neat PCL	29.4	57.8	74.41
PCL/CNC/0.5	35.5	58.0	71.95
PCL/CNC/1	35.1	58.3	72.93
PCL/CNC/2	35.0	58.0	71.12
PCL/WABR/0.5	35.0	58.0	72.86
PCL/WABR/1	35.1	57.7	72.2
PCL/WABR/2	34.1	57.9	70.42

Table A11: Predicted isothermal crystallization parameters of bio-composites with n, k, $t_{0.5}$, Φ(t) denotes rate constant, Avrami exponent, half time and degree of crystallization, respectively.

Sample Name	n	k (min^{-1})	$t_{0.5}$ (min)	Φ(t)
Neat PCL	2.96	0.002	7.21	0.82
PCL/WABR /0.5	2.61	0.119	1.96	0.78
PCL/WABR/1	2.39	0.297	1.43	0.58
PCL/WABR/ 2	1.94	0.626	1.05	0.37
PCL/CNC/ 0.5	2.90	0.082	2.09	0.58
PCL/CNC/ 1	2.53	0.214	1.59	0.80
PCL/CNC/ 2	2.30	0.401	1.27	0.70

Table A12: Thermal analysis of PLA and PCL bio-composites.

Sample	T_{on} (°C)	T_{max} (°C)
nPLA	353.42	388.01
PLA/CNC 0.5%	350.28	386.95
PLA/CNC 1%	345.66	384.92
PLA/CNC 2%	346.12	384.43
PLA/CUR	341.04	379.84
PLA/CUR/CNC 0.5%	344.32	384.72
PLA/CUR/CNC 1%	341.53	385.11
PLA/CUR/CNC 2%	342.38	385.54
nPCL	396.86	436.20
PCL/CNC 0.5%	399.81	435.75
PCL/CNC 1%	393.01	435.30
PCL/CNC 2%	399.80	433.49
PCL/CUR	401.53	436.79
PCL/CUR/CNC 0.5%	400.38	435.16
PCL/CUR/CNC 1%	397.10	437.89
PCL/CUR/CNC 2%	397.33	433.79

Table A13: Color properties of PLA and PCL active films.

Film Samples	L*	a*	b*	ΔE*	YI
nPLA	87.47± 0.09	-2.53±0.02	11.96±0.12	14.49±0.14	19.53±0.08
PLA/CNC 0.5%	88.52± 0.15	-2.40±0.05	11.46±0.15	13.38±0.18	18.50±0.12
PLA/CNC 1%	87.61±0.16	-2.34±0.08	11.52±0.30	14.06±0.15	18.78±0.16
PLA/CNC 2%	87.36±0.07	-2.46±0.03	11.97±0.17	14.56±0.09	19.57±0.11
PLA/CUR	80.47±0.92	5.07±0.58	102.85±6.54	102.51±0.65	182.54±0.21
PLA/CUR/CNC 0.5%	80.98±0.66	3.3±1.80	104.04±6.03	103.52±0.51	183.52±0.34
PLA/CUR/CNC 1%	80.73±0.67	3.25±2.51	102.23±3.33	101.77±0.41	180.87±0.33
PLA/CUR/CNC 2%	81.98±0.43	2.34±0.74	93±0.99	92.44±0.31	162.02±0.81
nPCL	89.48± 0.04	-0.96±0.03	7.56±0.17	10.00±0.09	12.07±0.26
PCL/CNC 0.5%	89.34±0.12	-0.94±0.02	7.41±0.19	10.04±0.08	11.84±0.30
PCL/CNC 1%	89.46±0.17	-0.95±0.03	7.80±0.06	10.15±0.17	12.45±0.12
PCL/CNC 2%	89.26±0.05	-0.97±0.03	7.78±0.01	10.30±0.05	12.45±0.02
PCL/CUR	81.99±0.83	1.9±2.50	94.05±0.54	93.46±0.35	163.83±0.71
PCL/CUR/CNC 0.5%	83.19±0.41	-0.79±1.10	95.14±0.48	94.311±0.45	163.34±0.89
PCL/CUR/CNC 1%	83.75±0.03	-2.04±0.59	96.17±0.21	95.26±0.21	164.01±0.42
PCL/CUR/CNC 2%	83.69±0.16	-2.17±0.45	96.20±0.23	95.30±0.24	164.19±0.65

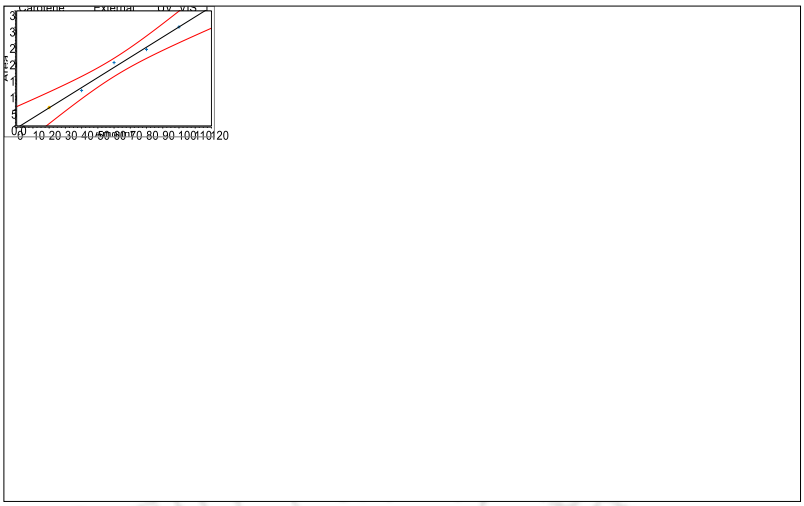

Figure A1: Standard calibration curve of β-carotene where, R^2=0.9911.

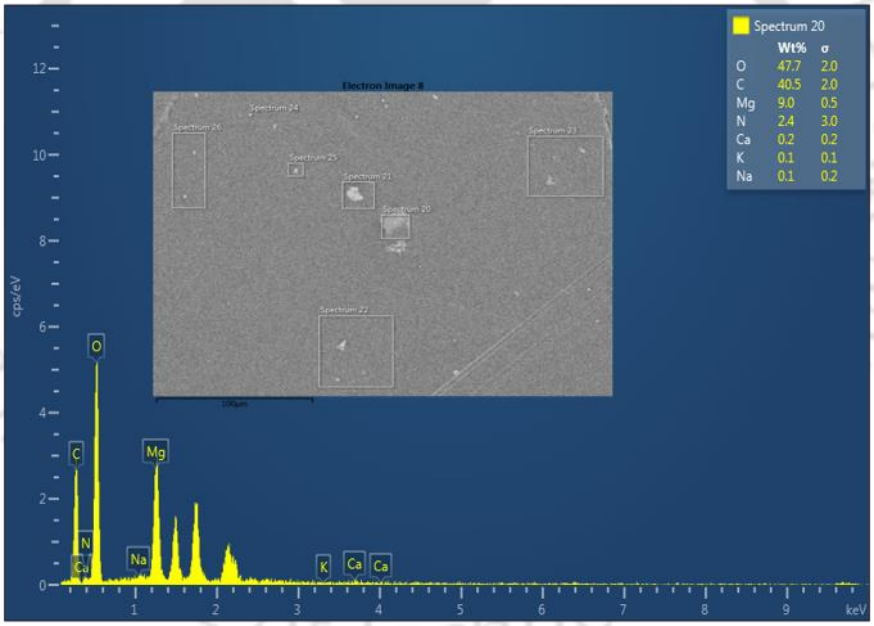

Figure A2: Energy dispersive X-ray Microscopy image of developed CS/CAEE 28% films.

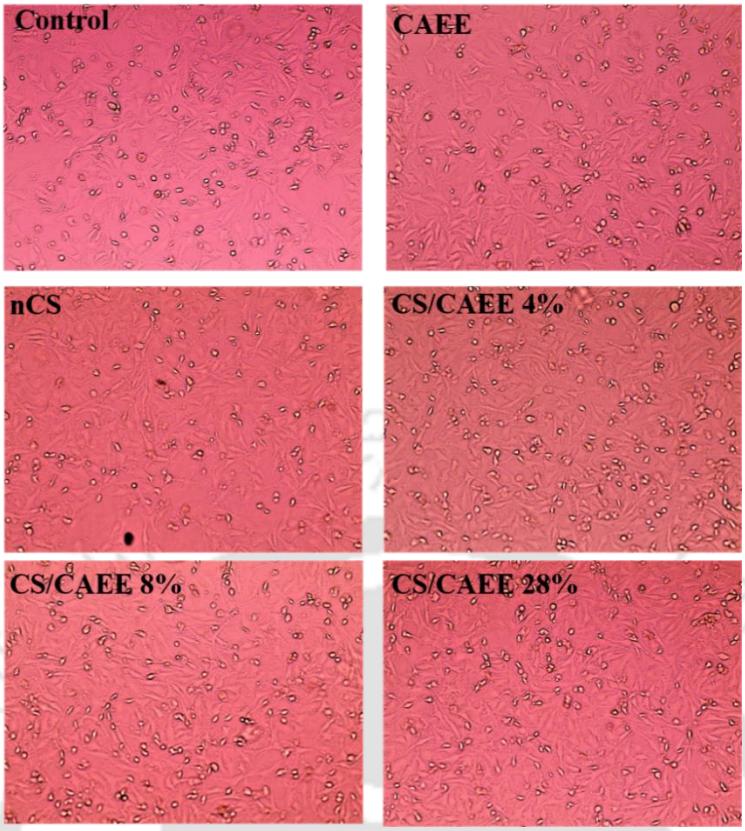

Figure A3: BHK-21 cell proliferation on control, CAEE, nCS, CS/CAEE 4%, CS/CAEE 8%, and CS/CAEE 28% after 72 h incubation.

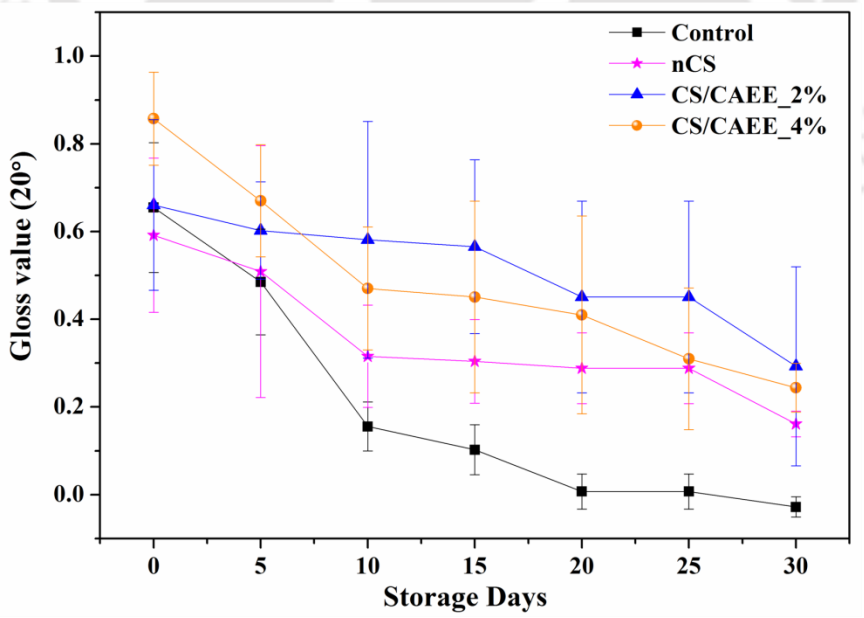

Figure A4: Gloss value measured at a lower angle of control and coated tomatoes during storage at 27-30 °C for 30 days. Each value is the average mean of three replicates, and vertical bars represent the standard deviation.

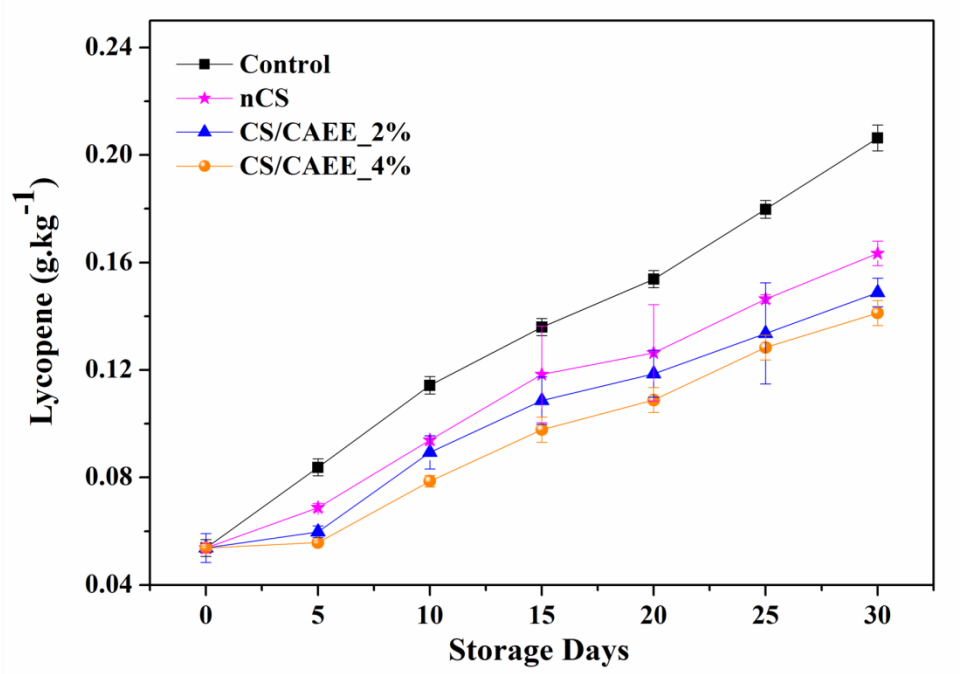

Figure A5: Lycopene contents of control and coated tomatoes measured by UV-Vis Spectrophotometer during storage at 27-30 °C for 30 days. Each value is the average mean of three replicates, and vertical bars represent the standard deviation.

Figure A6: Digital images of the developed PLA bio-composite films.

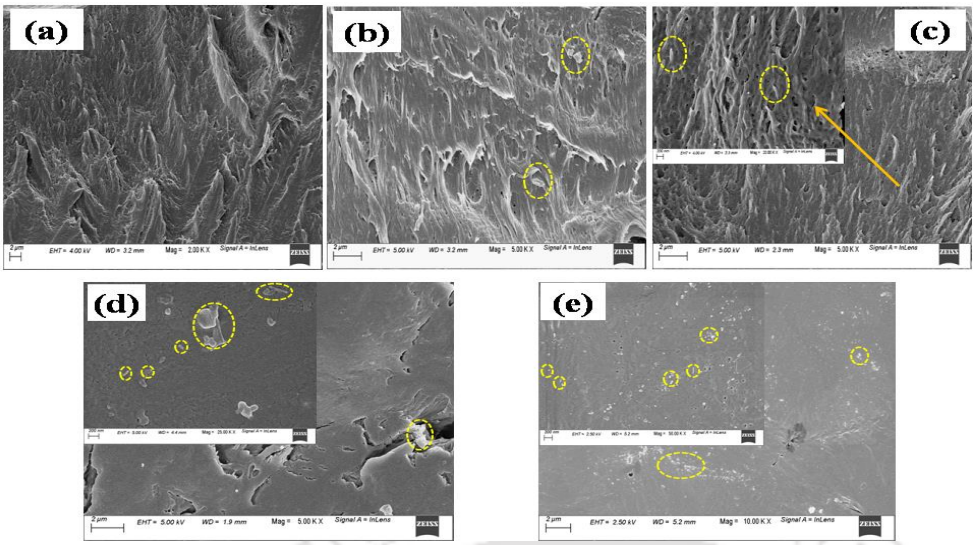

Figure A7: FESEM images of (a) Neat PLA, (b) PLA/WABR 0.5, (c) PLA/CNC 0.5, (d) PLA/CNC 1, and (e) PLA/CNC 2 films.

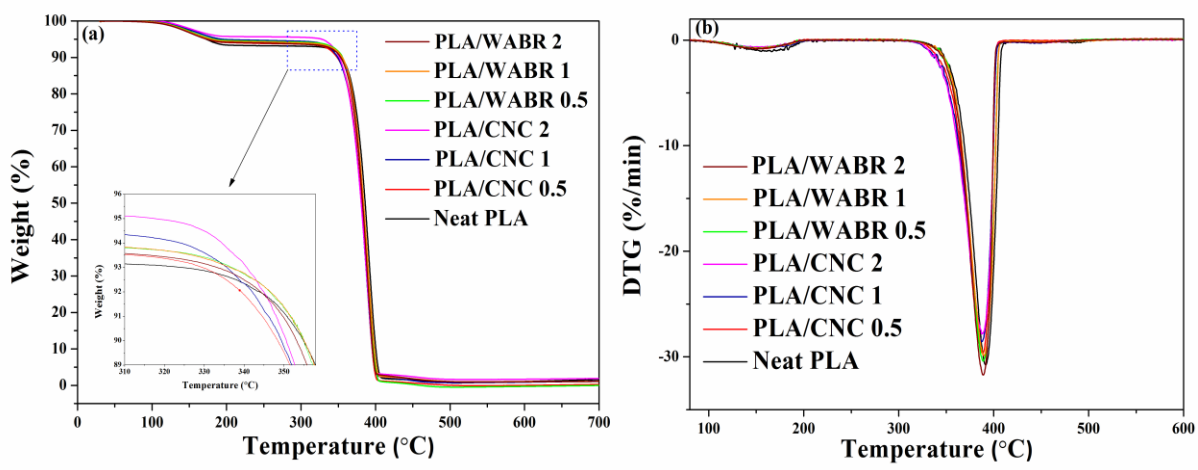

Figure A8: (a) TGA thermographs and (b) Derivative curves, of all the developed bio-composite films.

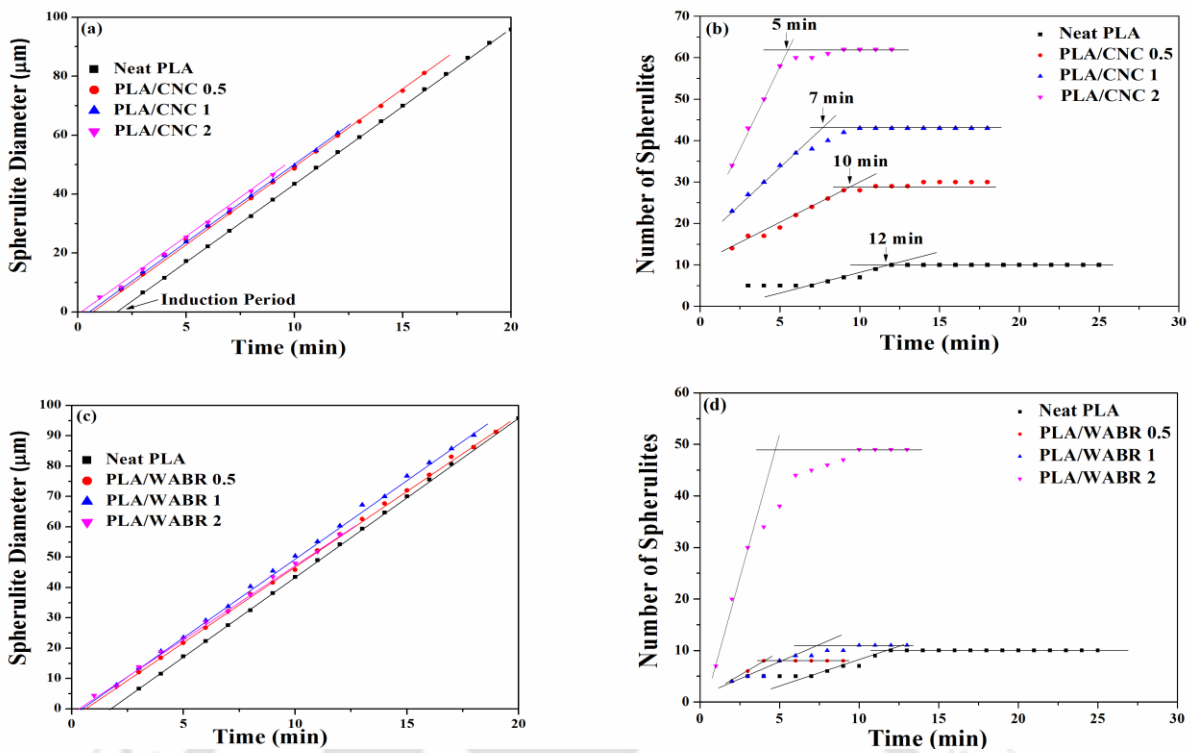

Figure A9: The POM observations of (a) Spherulite growth rate, (b) Number of spherulites, in the PLA/CNC bio-nanocomposites, and (c) Spherulite growth rate, (d) Number of spherulites, in the PLA/WABR bio-composite films, concerning time interval at an isothermally crystallized temperature of 125 °C.

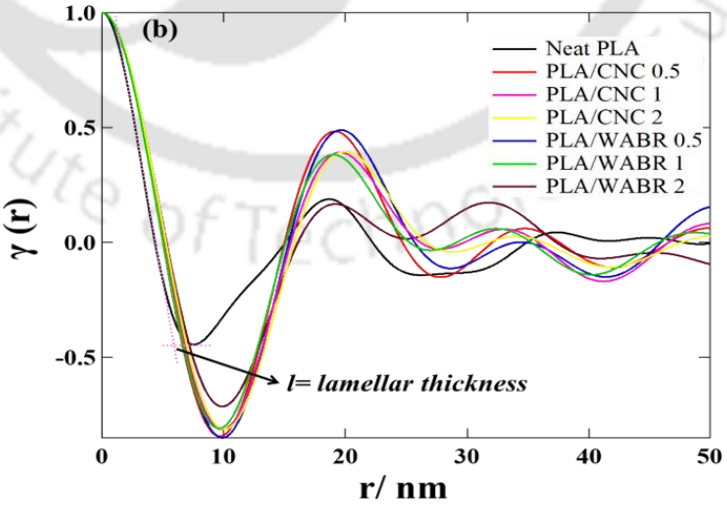

Figure A10: Comparison of lamellar thickness between the developed PLA bio-composites and neat PLA.

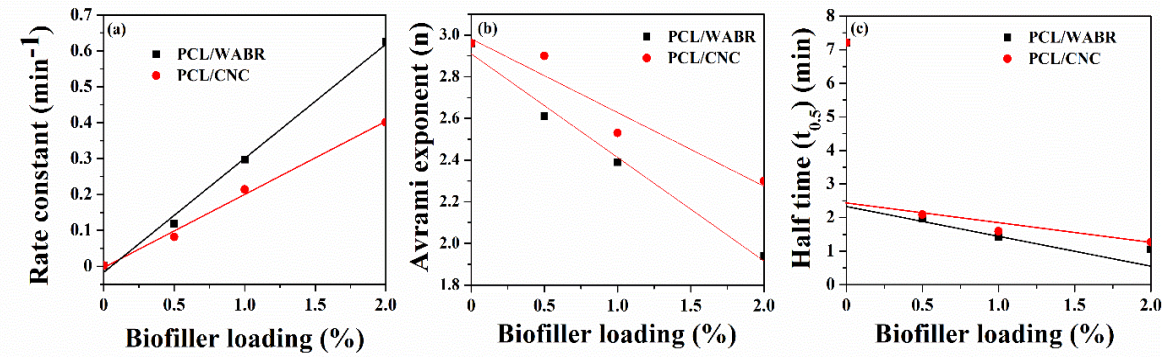

Figure A11: Comparison of (a) rate constant 'k', (b) Avrami exponent 'n', and (c) half time ($t_{0.5}$) of the PCL/WABR bio-composites and PCL/CNC bio-nanocomposite films at varying bio-filler loading.

Research Outcome

Patent:

1. Katiyar V, & **Mondal K**, A chitosan-based de-oiled green algae extract additive edible packaging formulation**,** Indian Patent No. 42019.

Research Articles:

1. **Mondal K**, Sakurai S, Okahisa Y, Goud V. V, & Katiyar V. (2021). "Effect of cellulose nanocrystals derived from Dunaliella tertiolecta marine green algae residue on the crystallization behavior of poly(lactic acid)". **Carbohydrate polymers**, IF:10.723, 261, 117881.
2. **Mondal K**, Sakurai S, Goud V. V, & Katiyar V. (2021). "Utilization of microalgae residue and isolated cellulose nanocrystals: A study on crystallization kinetics of poly(ε-caprolactone) bio-composites". **International Journal of Biological Macromolecules**, IF:8.025, 5191, 521-530.
3. **Mondal K**, Bhattacharjee S, Mudenur C, Ghosh T, Goud V. V, & Katiyar V. (2022). "The development of antioxidant-rich edible active films and coatings incorporated with de-oiled ethanolic green algae extract is a candidate for prolonging the shelf life of fresh produce". **RSC advances**, IF:4.036, 12(21), 13295-13313.
4. **Mondal K**, Goud V. V, & Katiyar V. (2022). "Effect of Waste Green Algal Biomass Extract Incorporated Chitosan-Based Edible Coating on the Shelf Life and Quality Attributes of Tomato". **ACS Food Science & Technology**, IF:1.718, 2(7), 1151-1165.

Research Article Communicated:

1. **Mondal K,** Bhattacharjee S, Goud V. V, & Katiyar V. (2023). "Development of guar gum-based active films integrated with green algae biomass extract and turmeric essential oil: physicochemical, barrier, rheological, antioxidant, and antimicrobial properties". **Food Hydrocolloids**, (Under Review)

Research Articles under Preparation:

1. **Mondal K,** Goud V. V, & Katiyar V. Optimization of guar gum-based anti-browning coating for shelf-life extension of the cut potato (under preparation)
2. **Mondal K,** Goud V. V, & Katiyar V. Studies on migration properties of algal CNC and curcumin incorporated PLA and PCL bio-composites (under preparation)

Contribution in Research Articles during PhD Tenure in Similar Areas:

1. Bhasney S. M, **Mondal K**, Kumar A, & Katiyar V. (2020). "Effect of microcrystalline cellulose [MCC] on morphological and crystalline behavior of high-density polyethylene [HDPE]/polylactic acid [PLA] blends"**. Composite Science and Technology,** IF: 9.879, 107941.
2. Ghosh T, **Mondal K**, Giri B. S, & Katiyar, V. (2021). "Silk nanodisc-based edible chitosan nanocomposite coating for fresh produces A candidate with superior thermal, hydrophobic, optical, mechanical, and food properties". **Food Chemistry**, IF: 9.231, 360, 130048.

Book Chapters:

1. **Mondal, K**., Ghosh, T., Bhagabati, P., & Katiyar, V. 'Sustainable Nanostructured Materials in Food Packaging', In book: Dynamics of Advanced Sustainable Nanomaterials and Their Related Nanocomposites at the Bio-Nano Interface, (2019). Elsevier, (pp. 171-213).
2. **Mondal, K**., Mulchandani, N., Mondal, S., & Katiyar, V. 'Synthesis of Biomass Derived Cellulose Nanocrystals and its Composites', In book: 'Advances in Sustainable Polymers: Fabrication and Characterization (2019). (pp. 237-269) Springer, Singapore.
3. **Mondal, K**., Ghosh, T., & Katiyar, V. 'Nanotechnology in Antimicrobial Edible Packaging: A Candidate for Prolong shelf life of Food Commodities' In book: Nanotechnology in Edible Food Packaging: Food Preservation Practices for a Sustainable Future (2021), 978-981-336-169-0.
4. **Mondal, K**., Ghosh, T., & Katiyar, V. 'Edible Food Packaging in Targeted Food Preservation' In book: Nanotechnology in Edible Food Packaging: Food Preservation Practices for a Sustainable Future (2021), 978-981-336-169-0.
5. Mudenur, C., **Mondal, K**., Singh, U., & Katiyar, V. 'Production of Polyhydroxyalkanoates and Its Potential Applications', In book: 'Advances in Sustainable Polymers: Processing and Application' (2019). (pp. 131-164). Springer, Singapore.
6. Ghosh, T., **Mondal, K.,** & Katiyar, V. 'Current Prospects of Bio-based Nanostructured Materials in Food Safety and Preservation, In book: Food Product Optimization for Quality and Safety Control: Process, Monitoring, and Standards' (2020). Apple Academic Press.

7. Ghosh, T., **Mondal, K.,** & Katiyar, V. 'Encapsulation: A Customized Practice for Minimization of Food Waste', In book: Food loss and waste reduction: Technical solutions and control (2020). Apple Academic Press (CRC Press).
8. Ghosh, T., **Mondal, K.,** & Katiyar, V. 'Lipid Nanoparticles for Edible Food Packaging' In book: Nanotechnology in Edible Food Packaging: Food Preservation Practices for a Sustainable Future (2021), 978-981-336-169-0.
9. Ghosh, T., **Mondal, K.,** & Katiyar, V. 'Chitosan based Nanostructured Materials in Edible Food Packaging' In book: Nanotechnology in Edible Food Packaging: Food Preservation Practices for a Sustainable Future (2021), 978-981-336-169-0.

Conference Proceedings:

1. **Mondal, K**, Shinichi S, Bhagabati P, Goud V. V., and Katiyar V. (2019). Fabrication of nano cellulose from marine green algae residue and their effects as filler in developing biodegradable polymer composite." In Proceedings of the international symposium on a new era in food science and technology, Japan, vol.28.

Oral & Poster Presentations:

1. **K. Mondal**, V. V. Goud, and V. Katiyar. (Oral), Fabrication and characterization of algae extract incorporated chitosan-based edible active packaging material for shelf-life extension of fresh produces. North-East Research Conclave (NERC-2022), 20^{th}-22^{th} May 2022 at Indian Institute of Technology Guwahati, Guwahati, India.
2. **K. Mondal,** V. V. Goud, and V. Katiyar. (Oral), Development of antioxidant-rich edible active films & coatings incorporated with de-oiled green algae extract. Annual Session of Indian Institute of Chemical Engineers (CHEMCON-2021), 26^{th} - 30^{th} December 2021 at CSIR - Institute of Minerals and Materials Technology, Bhubaneswar, India.
3. **K. Mondal**, S. Sakurai, P. Bhagabati, V. V. Goud, and V. Katiyar. (Poster), Fabrication of nano cellulose from marine green algae residue and their effects as filler in developing biodegradable polymer composite. International Symposium on a New Era in Food Science and Technology 2019 UGSAS-GU & BWEL Joint Poster Session on Agricultural and Basin Water Environmental Sciences, Gifu University, Japan.
4. **K. Mondal**, V. V. Goud, and V. Katiyar. (Poster), Utilization of Marine Green Algae Waste to Nano Cellulose and Their Effects as an effective filler for Developing Biodegradable Composites for Food Packaging' 27th Indian Convention of Food Scientists and Technologists: Raising Agro-processing & integrating Novel

technologies for boosting organic wellness (RAINBOW), January-February, 30th -1st, 2020, Tezpur University, Assam, India.

News Articles:

1. https://indianexpress.com/article/technology/science/iit-guwahati-researcher-fruits-and-vegetables-coating-shelf-life-8124514/
2. https://theprint.in/science/iit-guwahati-researchers-create-edible-coating-to-boost-shelf-life-of-fruits-vegetables/1109375/
3. https://www.deccanherald.com/national/iit-guwahati-researchers-develop-edible-coating-to-keep-fruits-vegetables-fresh-up-to-2-months-1140439.html
4. https://www.foodingredientsfirst.com/news/indian-scientists-develop-biodegradable-edible-coating-for-fresh-produce-to-boost-shelf-life.html
5. eastmojo.com/assam/2022/09/26/iit-guwahati-develops-strategy-to-deliver-chemo-drugs-to-cancer-cells/
6. https://www.bhaskar.com/happylife/news/iit-guwahati-developed-an-edible-coating-that-makes-food-stay-fresh-130260930.html
7. https://www.youtube.com/watch?v=Fz-4mfpIuT0
8. https://www.sentinelassam.com/guwahati-city/iit-g-scientists-develop-biodegradable-edible-coatings-to-extend-shelf-life-of-fruits-vegetables-610023
9. https://theshillongtimes.com/2022/08/29/iit-g-develops-edible-coating-to-extend-shelf-life-of-fruits-vegetables/
10. https://www.youtube.com/watch?v=lHcdq0sQwUI
11. https://algaeplanet.com/iit-guwahati-researchers-develop-edible-coating-for-produce/
12. https://www.youtube.com/watch?v=cShsr6Go6Iw
13. https://www.youtube.com/watch?v=8FBSy1Rh3UY
14. https://www.newscrab.com/lifestyle/Edible-coating-made-by-IIT-Guwahati-tomato-will-last-a/cid8469019.htm

References

1. Silvestre, C., Duraccio, D., & Cimmino, S. (2011). Food packaging based on polymer nanomaterials. Progress in polymer science, 36(12), 1766-1782.
2. Lithner, D., Larsson, Å., & Dave, G. (2011). Environmental and health hazard ranking and assessment of plastic polymers based on chemical composition. Science of the total environment, 409(18), 3309-3324.
3. Thakur, S., Verma, A., Sharma, B., Chaudhary, J., Tamulevicius, S., & Thakur, V. K. (2018). Recent developments in the recycling of polystyrene-based plastics. Current Opinion in Green and Sustainable Chemistry, 13, 32-38.
4. Moreira, D., Gullón, B., Gullón, P., Gomes, A., & Tavaria, F. (2016). Bioactive packaging uses antioxidant extracts for the prevention of microbial food spoilage. Food & function, 7(7), 3273-3282.
5. Deshmukh, A. R., Aloui, H., Khomlaem, C., Negi, A., Yun, J. H., Kim, H. S., & Kim, B. S. (2021). Biodegradable films based on chitosan and defatted Chlorella biomass: Functional and physical characterization. Food Chemistry, 337, 127777.
6. Remya, S., Mohan, C. O., Bindu, J., Sivaraman, G. K., Venkateshwarlu, G., & Ravishankar, C. N. (2016). Effect of chitosan-based active packaging film on the keeping quality of chilled stored barracuda fish. Journal of Food Science and Technology, 53(1), 685-693.
7. Siripatrawan, U., & Harte, B. R. (2010). Physical properties and antioxidant activity of an active film from chitosan incorporated with green tea extract. Food hydrocolloids, 24(8), 770-775.
8. Mondal, K., Ghosh, T., Bhagabati, P., & Katiyar, V. (2019). Sustainable nanostructured materials in food packaging. In Dynamics of advanced sustainable nanomaterials and their related nanocomposites at the bio-nano interface (pp. 171-213). Elsevier.
9. Carocho, M., Morales, P., & Ferreira, I. C. (2015). Natural food additives: Quo vadis?. Trends in Food Science & Technology, 45(2), 284-295.
10. Narayanan, M., Loganathan, S., Valapa, R. B., Thomas, S., & Varghese, T. O. (2017). UV protective poly (lactic acid)/rosin films for sustainable packaging. International journal of biological macromolecules, 99, 37-45.
11. Ribeiro-Santos, R., Andrade, M., de Melo, N. R., &Sanches-Silva, A. (2017). Use of essential oils in active food packaging: Recent advances and future trends. Trends in food science & technology, 61, 132-140.

12. Molina-Besch, K., Wikström, F., & Williams, H. (2019). The environmental impact of packaging in food supply chains does the life cycle assessment of food provide the full picture?. The International Journal of Life Cycle Assessment, *24*(1), 37-50.
13. Borgaonkar, N. K., Bhargava, C., & Kushwaha, A. (2022). Fidelity of NGOs toward zero waste in India: A conceptual framework for sustainability. In Emerging Trends to Approaching Zero Waste (pp. 153-173). Elsevier.
14. https://timesofindia.indiatimes.com/india/the-amount-of-indias-post-harvest-agricultural-produce-that-goes-waste/articleshow/53806764.cms
15. Dainelli, D., Gontard, N., Spyropoulos, D., Zondervan-van den Beuken, E., &Tobback, P. (2008). Active and intelligent food packaging: legal aspects and safety concerns. Trends in Food Science & Technology, 19, S103-S112.
16. Tajik, S., Maghsoudlou, Y., Khodaiyan, F., Jafari, S.M., Ghasemlou, M. and Aalami, M., 2013. Soluble soybean polysaccharide: A new carbohydrate to make a biodegradable film for sustainable green packaging. Carbohydrate polymers, 97(2), pp.817-824.
17. de Moura, M.R., Aouada, F.A., Avena-Bustillos, R.J., McHugh, T.H., Krochta, J.M. and Mattoso, L.H., 2009. Improved barrier and mechanical properties of novel hydroxypropyl methylcellulose edible films with chitosan/tripolyphosphate nanoparticles. Journal of Food Engineering, 92(4), pp.448-453.
18. Dash, M., Chiellini, F., Ottenbrite, R. M., & Chiellini, E. (2011). Chitosan—A versatile semi-synthetic polymer in biomedical applications. Progress in polymer science, 36(8), 981-1014.
19. Kong, M., Chen, X.G., Xing, K. and Park, H.J., 2010. Antimicrobial properties of chitosan and mode of action: a state of the art review. International journal of food microbiology, 144(1), pp.51-63.
20. Choi, C., Nam, J. P., & Nah, J. W. (2016). Application of chitosan and chitosan derivatives as biomaterials. Journal of Industrial and Engineering Chemistry, 33, 1-10.
21. Kong, M., Chen, X.G., Xue, Y.P., Liu, C.S., Yu, L.J., Ji, Q.X., Cha, D.S. and Park, H.J., 2008. Preparation and antibacterial activity of chitosan microshperes in a solid dispersing system. Frontiers of Materials Science in China, 2(2), pp.214-220.
22. Elsabee, M. Z., & Abdou, E. S. (2013). Chitosan based edible films and coatings: A review. Materials Science and Engineering: C, 33(4), 1819-1841.
23. van den Broek, L. A., Knoop, R. J., Kappen, F. H., & Boeriu, C. G. (2015). Chitosan films and blends for packaging material. Carbohydrate polymers, 116, 237-242.

24. Gupta, S., & Variyar, P. S. (2018). Guar gum: a versatile polymer for the food industry. In Biopolymers for food design (pp. 383-407). Academic Press.
25. Tahir, H. E., Xiaobo, Z., Mahunu, G. K., Arslan, M., Abdalhai, M., & Zhihua, L. (2019). Recent developments in gum edible coating applications for fruits and vegetables preservation: A review. Carbohydrate polymers, 224, 115141.
26. Banegas, R. S., Zornio, C. F., Borges, A. D. M., Porto, L. C., & Soldi, V. (2013). Preparation, characterization, and properties of films obtained from cross-linked guar gum. Polímeros, 23, 182-188.
27. Kurek, M., Garofulić, I. E., Bakić, M. T., Ščetar, M., & Uzelac, V. D. (2018). Development and evaluation of a novel antioxidant and pH indicator film based on chitosan and food waste sources of antioxidants. Food Hydrocolloids, 84, 238-246.
28. Venkatachalam, K., & Lekjing, S. (2020). A chitosan-based edible film with clove essential oil and nisin for improving the quality and shelf life of pork patties in cold storage. RSC advances, 10(30), 17777-17786.
29. Balti, R., Mansour, M. B., Sayari, N., Yacoubi, L., Rabaoui, L., Brodu, N., & Massé, A. (2017). Development and characterization of bioactive edible films from spider crab (Maja crispata) chitosan incorporated with Spirulina extract. International journal of biological macromolecules, 105, 1464-1472.
30. Kumar, N., Ojha, A., Upadhyay, A., Singh, R., & Kumar, S. (2021). Effect of active chitosan-pullulan composite edible coating enrich with pomegranate peel extract on the storage quality of green bell pepper. LWT, 138, 110435.
31. Quintana, S. E., Llalla, O., García-Risco, M. R., & Fornari, T. (2021). Comparison between essential oils and supercritical extracts into chitosan-based edible coatings on strawberry quality during cold storage. The Journal of Supercritical Fluids, 171, 105198.
32. Won, J. S., Lee, S. J., Park, H. H., Song, K. B., & Min, S. C. (2018). Edible coating using a chitosan-based colloid incorporating grapefruit seed extract for cherry tomato safety and preservation. Journal of food science, 83(1), 138-146.
33. Mannozzi, C., Tylewicz, U., Chinnici, F., Siroli, L., Rocculi, P., Dalla Rosa, M., & Romani, S. (2018). Effects of chitosan based coatings enriched with procyanidin by-product on quality of fresh blueberries during storage. Food Chemistry, 251, 18-24.
34. Aydogdu, A., Radke, C. J., Bezci, S., & Kirtil, E. (2020). Characterization of curcumin incorporated guar gum/orange oil antimicrobial emulsion films. International journal of biological macromolecules, 148, 110-120.

35. Kirtil, E., Aydogdu, A., Svitova, T., & Radke, C. J. (2021). Assessment of the performance of several novel approaches to improve physical properties of guar gum based biopolymer films. Food Packaging and Shelf Life, 29, 100687.
36. Arfat, Y. A., Ejaz, M., Jacob, H., & Ahmed, J. (2017). Deciphering the potential of guar gum/Ag-Cu nanocomposite films as an active food packaging material. Carbohydrate Polymers, 157, 65-71.
37. Saurabh, C. K., Gupta, S., & Variyar, P. S. (2022). Development of grape pomace extract based edible coating for shelf life extension of pomegranate arils. Journal of Food Measurement and Characterization, 16(1), 590-597.
38. Ruelas-Chacon, X., Contreras-Esquivel, J. C., Montañez, J., Aguilera-Carbo, A. F., Reyes-Vega, M. L., Peralta-Rodriguez, R. D., & Sanchéz-Brambila, G. (2017). Guar gum as an edible coating for enhancing shelf-life and improving postharvest quality of roma tomato (Solanum lycopersicum L.). Journal of Food Quality, 2017.
39. Das, D., Ara, T., Dutta, S., & Mukherjee, A. (2011). New water resistant biomaterial biocide film based on guar gum. Bioresource Technology, 102(10), 5878-5883.
40. Saurabh, C. K., Gupta, S., Bahadur, J., Mazumder, S., Variyar, P. S., & Sharma, A. (2015). Mechanical and barrier properties of guar gum based nano-composite films. Carbohydrate polymers, 124, 77-84.
41. BeMiller, J. N. (2019). 9-Guar, locust bean, Tara, and Cassia gums. Carbohydrate chemistry for food scientists, 241-252.
42. Lim, L. T. (2008). Auras R. Rubino M. Prog. Polym. Sci, 33(8), 820-852.
43. Datta, R., Tsai, S. P., Bonsignore, P., Moon, S. H., & Frank, J. R. (1995). Technological and economic potential of poly (lactic acid) and lactic acid derivatives. FEMS microbiology reviews, 16(2-3), 221-231.
44. Garlotta, D., 2001. A literature review of poly (lactic acid). Journal of Polymers and the Environment, 9(2), pp.63-84.
45. Del Nobile, M.A., Conte, A., Buonocore, G.G., Incoronato, A.L., Massaro, A. and Panza, O., 2009. Active packaging by extrusion processing of recyclable and biodegradable polymers. Journal of Food Engineering, 93(1), pp.1-6.
46. Kamal, M.R. and Khoshkava, V., 2015. Effect of cellulose nanocrystals (CNC) on rheological and mechanical properties and crystallization behavior of PLA/CNC nanocomposites. Carbohydrate polymers, 123, pp.105-114.

47. Barsanti, L., Coltelli, P., Evangelista, V., Frassanito, A. M., Passarelli, V., Vesentini, N., &Gualtieri, P. (2008). Oddities and curiosities in the algal world. In Algal toxins: nature, occurrence, effect and detection (pp. 353-391). Springer, Dordrecht.
48. Das, P., Aziz, S. S., &Obbard, J. P. (2011). Two phase microalgae growth in the open system for enhanced lipid productivity. Renewable Energy, 36(9), 2524-2528.
49. Spolaore, P., Joannis-Cassan, C., Duran, E., & Isambert, A. (2006). Commercial applications of microalgae. Journal of bioscience and bioengineering, 101(2), 87-96.
50. Brennan, L., &Owende, P. (2010). Biofuels from microalgae—a review of technologies for production, processing, and extractions of biofuels and co-products. Renewable and sustainable energy reviews, 14(2), 557-577.
51. Kumar, R., Bansal, V., Tiwari, A. K., Sharma, M., Puri, S. K., Patel, M. B., &Sarpal, A. S. (2011). Estimation of glycerides and free fatty acid in oils extracted from various seeds from the Indian region by NMR spectroscopy. Journal of the American Oil Chemists' Society, 88(11), 1675-1685.
52. Ścieszka, S., & Klewicka, E. (2019). Algae in food: A general review. Critical reviews in food science and nutrition, 59(21), 3538-3547.
53. Becker, E. W. (2013). Microalgae for human and animal nutrition. Handbook of microalgal culture: applied phycology and biotechnology, 461-503.
54. Tamiya, H. (1957). Mass culture of algae. Annual Review of Plant Physiology, 8(1), 309-334.
55. Pulz, O., & Gross, W. (2004). Valuable products from biotechnology of microalgae. Applied microbiology and biotechnology, 65(6), 635-648.
56. Liang, S., Liu, X., Chen, F., & Chen, Z. (2004). Current microalgal health food R & D activities in China. In Asian pacific phycology in the 21st century: Prospects and challenges (pp. 45-48). Springer, Dordrecht.
57. Soletto, D., Binaghi, L., Lodi, A., Carvalho, J. C. M., & Converti, A. (2005). Batch and fed-batch cultivations of Spirulina platensis using ammonium sulphate and urea as nitrogen sources. Aquaculture, 243(1-4), 217-224.
58. Lafarga, T. (2019). Effect of microalgal biomass incorporation into foods: Nutritional and sensorial attributes of the end products. Algal Research, 41, 101566.
59. Torres, S., Navia, R., Campbell Murdy, R., Cooke, P., Misra, M., &Mohanty, A. K. (2015). Green composites from residual microalgae biomass and poly (butylene adipate-co-terephthalate): processing and plasticization. ACS Sustainable Chemistry & Engineering, 3(4), 614-624.

60. Toro, C., Reddy, M. M., Navia, R., Rivas, M., Misra, M., &Mohanty, A. K. (2013). Characterization and application in biocomposites of residual microalgal biomass generated in third generation biodiesel. Journal of Polymers and the Environment, 21(4), 944-951.
61. Tran, D. T., Lee, H. R., Jung, S., Park, M. S., & Yang, J. W. (2016). Lipid-extracted algal biomass based biocomposites fabrication with poly (vinyl alcohol). Algal research.
62. Arrieta, M. P., de Dicastillo, C. L., Garrido, L., Roa, K., & Galotto, M. J. (2018). Electrospun PVA fibers loaded with antioxidant fillers extracted from Durvillaea antarctica algae and their effect on plasticized PLA bionanocomposites. European Polymer Journal, 103, 145-157.
63. Fabra, M. J., Falcó, I., Randazzo, W., Sánchez, G., & López-Rubio, A. (2018). Antiviral and antioxidant properties of active alginate edible films containing phenolic extracts. Food Hydrocolloids, 81, 96-103.
64. Iannace, S., Nocilla, G., & Nicolais, L. (1999). Biocomposites based on sea algae fibers and biodegradable thermoplastic matrices. Journal of Applied Polymer Science, 73(4), 583-592.
65. Garrido, T., Penalba, M., de la Caba, K., & Guerrero, P. (2016). Injection-manufactured biocomposites from extruded soy protein with algae waste as a filler. Composites Part B: Engineering, 86, 197-202.
66. Carissimi, M., Flôres, S. H., &Rech, R. (2018). Effect of microalgae addition on active biodegradable starch film. Algal research, 32, 201-209.
67. Bulota, M., & Budtova, T. (2016). Valorisation of macroalgae industrial by-product as filler in thermoplastic polymer composites. Composites Part A: Applied Science and Manufacturing, 90, 271-277.
68. Mishra RK, Ha SK, Verma K, Tiwari SK (2018) Recent progress in selected bio-nanomaterials and their engineering applications: An overview. J Sci Adv Mater Devices 3:263–288 . doi: 10.1016/j.jsamd.2018.05.003
69. Owusu PA, Asumadu-Sarkodie S (2016) A review of renewable energy sources, sustainability issues and climate change mitigation. Cogent Eng 3:1167990 . doi: 10.1080/23311916.2016.1167990
70. Figueiredo, J. A., Ismael, M. I., Anjo, C. M. S., & Duarte, A. P. (2010). Cellulose and derivatives from wood and fibers as renewable sources of raw-materials. Carbohydrates in Sustainable Development I, 117-128.

71. Nickerson, R. F., & Habrle, J. A. (1947). Cellulose intercrystalline structure. Industrial & Engineering Chemistry, 39(11), 1507-1512.
72. Rånby BG (1951) Fibrous macromolecular systems. Cellulose and muscle. The colloidal properties of cellulose micelles. Discuss Faraday Soc 11:158–164 . doi: 10.1039/DF9511100158
73. Habibi, Y., Lucia, L. A., & Rojas, O. J. (2010). Cellulose nanocrystals: chemistry, self-assembly, and applications. Chemical reviews, 110(6), 3479-3500.
74. Katiyar, V., Bhardwaj, U., & Dhar, P. (2013, April). PHB/Cellulose whiskers based bionanocomposites: Fabrication and properties evaluation for food packaging applications. In abstracts of papers of the American Chemical Society (Vol. 245). 1155 16th ST, NW, Washington, DC 20036 USA: Amer. Chemical Soc.
75. Arvanitoyannis, I. S., & Bosnea, L. (2004). Migration of substances from food packaging materials to foods. Critical reviews in food science and nutrition, 44(2), 63-76.
76. Welle, F., Mauer, A., & Franz, R. (2002). Migration and sensory changes of packaging materials caused by ionising radiation. Radiation Physics and Chemistry, 63(3-6), 841-844.
77. Fortunati, E., Peltzer, M., Armentano, I., Torre, L., Jiménez, A., & Kenny, J. M. (2012). Effects of modified cellulose nanocrystals on the barrier and migration properties of PLA nano-biocomposites. Carbohydrate polymers, 90(2), 948-956.
78. Rodríguez-Martínez, A. V., Sendón, R., Abad, M. J., González-Rodríguez, M. V., Barros-Velázquez, J., Aubourg, S. P., ... & de Quirós, A. R. B. (2016). Migration kinetics of sorbic acid from polylactic acid and seaweed based films into food simulants. LWT-Food Science and Technology, 65, 630-636.
79. Jafarzadeh, S., Nafchi, A. M., Salehabadi, A., Oladzad-Abbasabadi, N., & Jafari, S. M. (2021). Application of bio-nanocomposite films and edible coatings for extending the shelf life of fresh fruits and vegetables. Advances in Colloid and Interface Science, 291, 102405.
80. Nair, M. S., Tomar, M., Punia, S., Kukula-Koch, W., & Kumar, M. (2020). Enhancing the functionality of chitosan-and alginate-based active edible coatings/films for the preservation of fruits and vegetables: A review. International Journal of Biological Macromolecules, 164, 304-320.
81. Kaya, M., Ravikumar, P., Ilk, S., Mujtaba, M., Akyuz, L., Labidi, J., ... & Erkul, S. K. (2018). Production and characterization of chitosan based edible films from Berberis crataegina's fruit extract and seed oil. Innovative Food Science & Emerging Technologies, 45, 287-297.

82. Breda, C. A., Morgado, D. L., de Assis, O. B. G., & Duarte, M. C. T. (2017). Effect of chitosan coating enriched with pequi (Caryocar brasiliense Camb.) peel extract on quality and safety of tomatoes (Lycopersicon esculentum Mill.) during storage. Journal of Food Processing and Preservation, 41(6), e13268.
83. Dhumal, C. V., Ahmed, J., Bandara, N., & Sarkar, P. (2019). Improvement of antimicrobial activity of sago starch/guar gum bi-phasic edible films by incorporating carvacrol and citral. Food Packaging and Shelf Life, 21, 100380.
84. Ebrahimi, F., & Rastegar, S. (2020). Preservation of mango fruit with guar-based edible coatings enriched with Spirulina platensis and Aloe vera extract during storage at ambient temperature. Scientia Horticulturae, 265, 109258.
85. Huang, Q., Qian, X., Jiang, T., & Zheng, X. (2019). Effect of chitosan and guar gum based composite edible coating on quality of mushroom (Lentinus edodes) during postharvest storage. Scientia Horticulturae, 253, 382-389.
86. Dong, F., & Wang, X. (2018). Guar gum and ginseng extract coatings maintain the quality of sweet cherry. LWT, 89, 117-122.
87. Naeem, A., Abbas, T., Ali, T. M., & Hasnain, A. (2018). Effect of guar gum coatings containing essential oils on shelf life and nutritional quality of green-unripe mangoes during low temperature storage. International journal of biological macromolecules, 113, 403-410.
88. Kim HM, Wi SG, Jung S, Song Y, Bae H-J (2015) Efficient approach for bioethanol production from red seaweed Gelidium amansii. Bioresour Technol 175:128–134. doi: 10.1016/j.biortech.2014.10.050
89. Mihranyan A (2011) Cellulose from cladophorales green algae: From environmental problem to high-tech composite materials. J Appl Polym Sci 119:2449–2460. doi: 10.1002/app.32959
90. George J, Sabapathi S (2015) Cellulose nanocrystals: synthesis, functional properties, and applications. Nanotechnol Sci Appl 8:45–54. doi: 10.2147/NSA.S64386
91. Fortunati, E., Luzi, F., Puglia, D., Petrucci, R., Kenny, J. M., & Torre, L. (2015). Processing of PLA nanocomposites with cellulose nanocrystals extracted from Posidonia oceanica waste: Innovative reuse of coastal plant. Industrial Crops and Products, 67, 439-447.
92. El Achaby, M., Kassab, Z., Aboulkas, A., Gaillard, C., & Barakat, A. (2018). Reuse of red algae waste for the production of cellulose nanocrystals and its application in polymer nanocomposites. International Journal of Biological Macromolecules, 106, 681–691.

93. Dhar, P., Tarafder, D., Kumar, A., & Katiyar, V. (2015). Effect of cellulose anocrystal polymorphs on mechanical, barrier and thermal properties of poly(lactic acid) based bionanocomposites. RSC Advances, 5, 60426–60440.

94. Commission Regulation. (2011). Commission Regulation (EU) No 10/2011 on plastic materials and articles intended to come into contact with food. Official Journal of European Communities

95. Loader, N. J., Robertson, I., Barker, A. C., Switsur, V. R., & Waterhouse, J. S. (1997). An improved technique for the batch processing of small wholewood samples to α-cellulose. Chemical Geology, 136, 313–317.

96. Van Wychen, S., & Laurens, L. M. (2016). Determination of total carbohydrates in algal biomass: laboratory analytical procedure (LAP) (No. NREL/TP-5100-60957). National Renewable Energy Lab.(NREL), Golden, CO (United States).

97. Godlewska, K., Michalak, I., Tuhy, Ł., & Chojnacka, K. (2017). The influence of pH of extracting water on the composition of seaweed extracts and their beneficial properties on Lepidium sativum. BioMed research international, 2017.

98. Das, A. B.; Goud, V. V.; Das, C. Extraction of phenolic compounds and anthocyanin from black and purple rice bran (Oryza sativa L.) using ultrasound: A comparative analysis and phytochemical profiling. Ind. Crops Prod. 2017, 95, 332−341.

99. Dudonne, S., Poupard, P., Coutiere, P., Woillez, M., Richard, T., Merillon, J. M., & Vitrac, X. (2011). Phenolic composition and antioxidant properties of poplar bud (Populus nigra) extract: individual antioxidant contribution of phenolics and transcriptional effect on skin aging. Journal of agricultural and food chemistry, 59(9), 4527-4536.

100. Pandey, A.K., Katiyar, V., Sasaki, S., & Sakurai, S. (2019). Accelerated crystallization of poly(l -lactic acid) by silk fibroin nanodisc. Polymer Journal, 51, 1173–1180.

101. Anglès, M. N.; Dufresne, A. (2000) Plasticized Starch/Tunicin Whiskers Nanocomposites. 1. Structural Analysis. Macromolecules, 33 (22), 8344–8353.

102. Bajić, M., Ročnik, T., Oberlintner, A., Scognamiglio, F., Novak, U., & Likozar, B. (2019). Natural plant extracts as active components in chitosan-based films: A comparative study. Food packaging and shelf life, 21, 100365.

103. Song, Y., Zhang, H., Huang, H., Zhang, Y., Wang, H., Li, Y., & Wang, C. (2022). Allicin-Loaded Electrospun PVP/PVB Nanofibrous Films with Superior Water Absorption and Water Stability for Antimicrobial Food Packaging. ACS Food Science & Technology.

104. Khatri, D., & Chhetri, S. B. B. (2020). Reducing sugar, total phenolic content, and antioxidant potential of nepalese plants. BioMed Research International, 2020.
105. Javanmardi, J., & Kubota, C. (2006). Variation of lycopene, antioxidant activity, total soluble solids and weight loss of tomato during postharvest storage. Postharvest biology and technology, 41(2), 151-155.
106. Barros, L., Ferreira, M. J., Queiros, B., Ferreira, I. C., & Baptista, P. (2007). Total phenols, ascorbic acid, β-carotene and lycopene in Portuguese wild edible mushrooms and their antioxidant activities. Food chemistry, 103(2), 413-419.
107. Kim, J. H., & Min, S. C. (2017). Microwave-powered cold plasma treatment for improving microbiological safety of cherry tomato against Salmonella. Postharvest Biology and Technology, 127, 21-26.
108. Devlieghere, F., Vermeulen, A., & Debevere, J. (2004). Chitosan: antimicrobial activity, interactions with food components and applicability as a coating on fruit and vegetables. Food Microbiol. 21, 703−714.
109. Rojas-Graü, M. A., Tapia, M. S., & Martín-Belloso, O. (2008). Using polysaccharide-based edible coatings to maintain quality of fresh-cut Fuji apples. LWT–Food Sci. Technol. 41, 139−147.
110. Alam, M. A., Alam, M., Hakim, M., Huq, A. O., Moktadir, S. G. (2014). Development of fiber enriched herbal biscuits: a preliminary study on sensory evaluation and chemical composition. Int. J. Nutr. Food Sci. 3, 246-250.
111. Remya, S., Mohan, C. O., Bindu, J., Sivaraman, G. K., Venkateshwarlu, G., & Ravishankar, C. N. (2016). Effect of chitosan based active packaging film on the keeping quality of chilled stored barracuda fish. Journal of Food Science and Technology, 53(1), 685-693.
112. Siripatrawan, U., & Harte, B. R. (2010). Physical properties and antioxidant activity of an active film from chitosan incorporated with green tea extract. Food hydrocolloids, 24(8), 770-775.
113. Moreira, D., Gullón, B., Gullón, P., Gomes, A., & Tavaria, F. (2016). Bioactive packaging using antioxidant extracts for the prevention of microbial food-spoilage. Food & function, 7(7), 3273-3282.
114. Deng, J., Zhu, E. Q., Xu, G. F., Naik, N., Murugadoss, V., Ma, M. G., ... & Shi, Z. J. (2022). Overview of renewable polysaccharide-based composites for biodegradable food packaging applications. Green Chemistry, 24(2), 480-492.

115. Nair, M. S., Saxena, A., & Kaur, C. (2018). Characterization and antifungal activity of pomegranate peel extract and its use in polysaccharide-based edible coatings to extend the shelf-life of capsicum (Capsicum annuum L.). Food and bioprocess technology, 11(7), 1317-1327.

116. Dutta, P. K., Tripathi, S., Mehrotra, G. K., & Dutta, J. (2009). Perspectives for chitosan based antimicrobial films in food applications. Food Chemistry.№ 114. P. 1173-1182.

117. Bertolo, M. R., Martins, V. C., Horn, M. M., Brenelli, L. B., & Plepis, A. M. (2020). Rheological and antioxidant properties of chitosan/gelatin-based materials functionalized by pomegranate peel extract. Carbohydrate polymers, 228, 115386.

118. Ghosh, T., Teramoto, Y., & Katiyar, V. (2019). Influence of nontoxic magnetic cellulose nanofibers on chitosan based edible nanocoating: a candidate for improved mechanical, thermal, optical, and texture properties. Journal of agricultural and food chemistry, 67(15), 4289-4299.

119. Ojagh, S. M., Rezaei, M., Razavi, S. H., & Hosseini, S. M. H. (2010). Development and evaluation of a novel biodegradable film made from chitosan and cinnamon essential oil with low affinity toward water. Food Chemistry, 122(1), 161-166.

120. Nowzari, F., Shábanpour, B., & Ojagh, S. M. (2013). Comparison of chitosan–gelatin composite and bilayer coating and film effect on the quality of refrigerated rainbow trout. Food chemistry, 141(3), 1667-1672.

121. Dos Santos, T. C., Rescignano, N., Boff, L., Reginatto, F. H., Simões, C. M. O., de Campos, A. M., & Mijangos, C. U. (2017). Manufacture and characterization of chitosan/PLGA nanoparticles nanocomposite buccal films. Carbohydrate polymers, 173, 638-644.

122. Ferreira, C. O., Nunes, C. A., Delgadillo, I., & Lopes-da-Silva, J. A. (2009). Characterization of chitosan–whey protein films at acid pH. Food research international, 42(7), 807-813.

123. Kalita, N. K., Nagar, M. K., Mudenur, C., Kalamdhad, A., & Katiyar, V. (2019). Biodegradation of modified Poly (lactic acid) based biocomposite films under thermophilic composting conditions. Polymer Testing, 76, 522-536.

124. Lan, W., Wang, S., Chen, M., Sameen, D. E., Lee, K., & Liu, Y. (2020). Developing poly (vinyl alcohol)/chitosan films incorporate with d-limonene: Study of structural, antibacterial, and fruit preservation properties. International journal of biological macromolecules, 145, 722-732.

125. Bhardwaj, U., Dhar, P., Kumar, A., & Katiyar, V. (2014). Polyhydroxyalkanoates (PHA)-cellulose based nanobiocomposites for food packaging applications. In Food additives and packaging (pp. 275-314). American Chemical Society.
126. Akretche, H., Pierre, G., Moussaoui, R., Michaud, P., & Delattre, C. (2019). Valorization of olive mill wastewater for the development of biobased polymer films with antioxidant properties using eco-friendly processes. Green Chemistry, 21(11), 3065-3073.
127. Zhang, W., Li, X., & Jiang, W. (2020). Development of antioxidant chitosan film with banana peels extract and its application as coating in maintaining the storage quality of apple. International Journal of Biological Macromolecules, 154, 1205-1214.
128. Silva-Weiss, A., Bifani, V., Ihl, M., Sobral, P. J. A., & Gómez-Guillén, M. C. (2013). Structural properties of films and rheology of film-forming solutions based on chitosan and chitosan-starch blend enriched with murta leaf extract. Food hydrocolloids, 31(2), 458-466.
129. Zhang, X., Lian, H., Shi, J., Meng, W., & Peng, Y. (2020). Plant extracts such as pine nut shell, peanut shell and jujube leaf improved the antioxidant ability and gas permeability of chitosan films. International journal of biological macromolecules, 148, 1242-1250.
130. Liu, T., Liu, L., Gong, X., Chi, F., & Ma, Z. (2021). Fabrication and comparison of active films from chitosan incorporating different spice extracts for shelf life extension of refrigerated pork. Lwt, 135, 110181.
131. Gómez, B., Barba, F. J., Domínguez, R., Putnik, P., Kovačević, D. B., Pateiro, M., ... & Lorenzo, J. M. (2018). Microencapsulation of antioxidant compounds through innovative technologies and its specific application in meat processing. Trends in Food Science & Technology, 82, 135-147.
132. Zou, S., Wu, Y., Yang, M., Li, C., & Tong, J. (2009). Thermochemical catalytic liquefaction of the marine microalgae Dunaliella tertiolecta and characterization of bio-oils. Energy & Fuels, 23(7), 3753-3758.
133. Lafarga, T. (2019). Effect of microalgal biomass incorporation into foods: Nutritional and sensorial attributes of the end products. *Algal Research*, *41*, 101566.
134. Bisht, B., Kumar, V., Gururani, P., Tomar, M. S., Nanda, M., Vlaskin, M. S., ... & Kurbatova, A. (2021). The potential of nuclear magnetic resonance (NMR) in metabolomics and lipidomics of microalgae-a review. Archives of Biochemistry and Biophysics, 710, 108987.
135. Foley, P. M., Beach, E. S., & Zimmerman, J. B. (2011). Algae as a source of renewable chemicals: opportunities and challenges. Green Chemistry, 13(6), 1399-1405.

136. Mondal, K., Sakurai, S., Okahisa, Y., Goud, V. V., & Katiyar, V. (2021). Effect of cellulose nanocrystals derived from Dunaliella tertiolecta marine green algae residue on crystallization behaviour of poly (lactic acid). Carbohydrate Polymers, 261, 117881.

137. Mondal, K., Bhagabati, P., Goud, V. V., Sakurai, S., & Katiyar, V. (2021). Utilization of microalgae residue and isolated cellulose nanocrystals: A study on crystallization kinetics of poly (ε-caprolactone) bio-composites. International Journal of Biological Macromolecules, 191, 521-530.

138. Mihranyan, A.(2011). Cellulose from cladophorales green algae:From environmental problem to high-tech composite materials. Journal of Applied Polymer Science, 119, 2449-2460.

139. Juneja, A., Ceballos, R.M., & Murthy, G.S.(2013). Effects of Environmental Factors and Nutrient Availability on the Biochemical Composition of Algae for Biofuels Production: A Review. Energies, 6, 4607–4638.

140. Bulota, M., & Budtova, T.(2015). PLA/algae composites: Morphology and mechanical properties. Composites Part A: Applied Science and Manufacturing,73, 109–115.

141. Elfassy, T., Yi, S., Eisenhower, D., Lederer, A., Curtis, C.J. (2015). Use of Sodium Information on the Nutrition Facts Label in New York City Adults with Hypertension. Journal of the Academy of Nutrition and Dietetics, 115, 278–283.

142. Bergman, C., Gray-Scott, D., Chen, J.-J., Meacham, S.(2009). What is Next for the Dietary Reference Intakes for Bone Metabolism Related Nutrients Beyond Calcium: Phosphorus, Magnesium, Vitamin D, and Fluoride? Critical Reviews in Food Science and Nutrition, 49, 136–144.

143. Chadwick, D.J., Whelan, J.(2008). Aluminium in Biology and Medicine. John Wiley & Sons.

144. Winkler, H.C., Suter, M., Naegeli, H. (2016). Critical review of the safety assessment of nano-structured silica additives in food. Journal of Nanobiotechnology, 14, 44.

145. Zhong, Z., Li, G., Zhu, B., Luo, Z., Huang, L., Wu, X. (2012). A rapid distillation method coupled with ion chromatography for the determination of total sulphur dioxide in foods. Food Chemistry, 131, 1044–1050.

146. Deyhim, F., Teeter, R.G. (1991). Research Note: Sodium and Potassium Chloride Drinking Water Supplementation Effects on Acid-Base Balance and Plasma Corticosterone in Broilers Reared in Thermoneutral and Heat-Distressed Environments. Poultry Science, 70, 2551–2553.

147. Arena, G., Copat, C., Dimartino, A., Grasso, A., Fallico, R., Sciacca, S., Fiore, M., Ferrante, M. (2015). Determination of total vanadium and vanadium(V) in groundwater from Mt. Etna and estimate of daily intake of vanadium(V) through drinking water. Journal of Water and Health, 13, 522–530.

148. Samuelson, G., Bratteby, L.-E., Berggren, K., Elverby, J.-E., Kempe, B. (1996). Dietary iron intake and iron status in adolescents. Acta Paediatrica, 85, 1033–1038.

149. Watts, P., Howe, P., Organization, W.H. (2010). Strontium and Strontium Compounds. World Health Organization

150. Liu, C. T., Wu, C. Y., Weng, Y. M., & Tseng, C. Y. (2005). Ultrasound-assisted extraction methodology as a tool to improve the antioxidant properties of herbal drug Xiao-chia-hu-tang. *Journal of ethnopharmacology*, *99*(2), 293-300.

151. Lucarini, M., & Pedulli, G. F. (2010). Free radical intermediates in the inhibition of the autoxidation reaction. *Chemical Society Reviews*, *39*(6), 2106-2119.

152. Cheung, Y. C., Siu, K. C., Liu, Y. S., & Wu, J. Y. (2012). Molecular properties and antioxidant activities of polysaccharide–protein complexes from selected mushrooms by ultrasound-assisted extraction. *Process Biochemistry*, *47*(5), 892-895.

153. Hosikian, A., Lim, S., Halim, R., & Danquah, M. K. (2010). Chlorophyll extraction from microalgae: a review on the process engineering aspects. *International journal of chemical engineering*, *2010*.

154. Iglesias, M. J., Soengas, R., Probert, I., Guilloud, E., Gourvil, P., Mehiri, M., ... & Ortiz, F. L. (2019). NMR characterization and evaluation of antibacterial and antiobiofilm activity of organic extracts from stationary phase batch cultures of five marine microalgae (Dunaliella sp., D. salina, Chaetoceros calcitrans, C. gracilis and Tisochrysis lutea). Phytochemistry, 164, 192-205.

155. Nicolau, R., Leloup, M., Lachassagne, D., Pinault, E., & Feuillade-Cathalifaud, G. (2015). Matrix-assisted laser desorption/ionization time-of-flight mass spectrometry (MALDI–TOF–MS) coupled to XAD fractionation: Method to algal organic matter characterization. Talanta, 136, 102-107.

156. Fraser, P. D., Enfissi, E. M., Goodfellow, M., Eguchi, T., & Bramley, P. M. (2007). Metabolite profiling of plant carotenoids using the matrix-assisted laser desorption ionization time-of-flight mass spectrometry. The Plant Journal, 49(3), 552-564.

157. Mishra, A., Kavita, K., & Jha, B. (2011). Characterization of extracellular polymeric substances produced by micro-algae Dunaliella salina. Carbohydrate Polymers, 83(2), 852-857.

158. A. S.Sarpal, C. M.Teixeira, S.Mesquita, I. C.Costa, and R. M. S.Paulo,Adv MicrobiolBiotechnol, 2018,11, 555812.

159. TSUKIDA, K., SAIKI, K., & SUGIURA, M. (1981). Structural elucidation of the main cis-β-carotenes. Journal of nutritional science and vitaminology, 27(6), 551-561.

160. Wang, L., Dong, Y., Men, H., Tong, J., & Zhou, J. (2013). Preparation and characterization of active films based on chitosan incorporated tea polyphenols. Food hydrocolloids, 32(1), 35-41.

161. Zhang, X., Liu, Y., Yong, H., Qin, Y., Liu, J., & Liu, J. (2019). Development of multifunctional food packaging films based on chitosan, TiO2 nanoparticles and anthocyanin-rich black plum peel extract. Food Hydrocolloids, 94, 80-92.

162. Yong, H., Wang, X., Bai, R., Miao, Z., Zhang, X., & Liu, J. (2019). Development of antioxidant and intelligent pH-sensing packaging films by incorporating purple-fleshed sweet potato extract into chitosan matrix. Food Hydrocolloids, 90, 216-224.

163. Deshmukh, A. R., Jeong, J. W., Lee, S. J., Park, G. U., & Kim, B. S. (2019). Ultrasound-assisted facile green synthesis of hexagonal boron nitride nanosheets and their applications. ACS Sustainable Chemistry & Engineering, 7(20), 17114-17125.

164. Deshmukh, A. R., Aloui, H., & Kim, B. S. (2020). In situ growth of gold and silver nanoparticles onto phyto-functionalized boron nitride nanosheets: Catalytic, peroxidase mimicking, and antimicrobial activity. Journal of Cleaner Production, 270, 122339.

165. S. U.Kadam, S. K.Pankaj, B. K.Tiwari, P. J.Cullen, and C. P.O'Donnell, Food Packaging and Shelf Life, 2015,6, 68-74.

166. Hernández-Muñoz, P., López-Rubio, A., Lagarón, J. M., & Gavara, R. (2004). Formaldehyde cross-linking of gliadin films: effects on mechanical and water barrier properties. Biomacromolecules, 5(2), 415-421.

167. Gupta, A., Pal, A. K., Woo, E. M., & Katiyar, V. (2018). Effects of amphiphilic chitosan on stereocomplexation and properties of poly (lactic acid) nano-biocomposite. Scientific reports, 8(1), 1-13.

168. Chiellini, E., Cinelli, P., Ilieva, V. I., & Martera, M. (2008). Biodegradable thermoplastic composites based on polyvinyl alcohol and algae. Biomacromolecules, 9(3), 1007-1013.

169. M.Romanelli Vicente Bertolo, V.da Conceicao Amaro Martins, A. M.de GuzziPlepis, and SBogusz Junior,Journal of Applied Polymer Science, 2021,138, 50052.

170. M. Á. V.Rodrigues, M. R. V.Bertolo, C. A.Marangon, V. D. C. A.Martins, and A. M.de GuzziPlepis, International Journal of Biological Macromolecules, 2020,160, 769-779.

171. Silva-Weiss, A., Bifani, V., Ihl, M., Sobral, P. J. D. A., & Gómez-Guillén, M. C. (2014). Polyphenol-rich extract from murta leaves on rheological properties of film-forming solutions based on different hydrocolloid blends. Journal of Food Engineering, 140, 28-38.
172. Du, W. X., Olsen, C. W., Avena-Bustillos, R. J., Friedman, M., & McHugh, T. H. (2011). Physical and antibacterial properties of edible films formulated with apple skin polyphenols. Journal of Food Science, 76(2), M149-M155.
173. Peng, Y., Wang, Q., Shi, J., Chen, Y., & Zhang, X. (2019). Optimization and release evaluation for tea polyphenols and chitosan composite films with regulation of glycerol and Tween. Food Science and Technology, 40, 162-170.
174. Priyadarsini, K. I., Maity, D. K., Naik, G. H., Kumar, M. S., Unnikrishnan, M. K., Satav, J. G., & Mohan, H. (2003). Role of phenolic OH and methylene hydrogen on the free radical reactions and antioxidant activity of curcumin. Free Radical Biology and Medicine, 35(5), 475-484.
175. Talón, E., Trifkovic, K. T., Nedovic, V. A., Bugarski, B. M., Vargas, M., Chiralt, A., & González-Martínez, C. (2017). Antioxidant edible films based on chitosan and starch containing polyphenols from thyme extracts. Carbohydrate polymers, 157, 1153-1161.
176. Jouki, M., Yazdi, F. T., Mortazavi, S. A., & Koocheki, A. (2014). Quince seed mucilage films incorporated with oregano essential oil: Physical, thermal, barrier, antioxidant and antibacterial properties. Food Hydrocolloids, 36, 9-19.
177. Min, D., Li, Z., Ai, W., Li, J., Zhou, J., Zhang, X., ... & Guo, Y. (2020). The co-regulation of ethylene biosynthesis and ascorbate–glutathione cycle by methy jasmonate contributes to aroma formation of tomato fruit during postharvest ripening. Journal of Agricultural and Food Chemistry, 68(39), 10822-10832.
178. Maqbool, M., Ali, A., Alderson, P. G., Zahid, N., & Siddiqui, Y. (2011). Effect of a novel edible composite coating based on gum arabic and chitosan on biochemical and physiological responses of banana fruits during cold storage. Journal of agricultural and food chemistry, 59(10), 5474-5482.
179. Priyadarshi, R., Ezati, P., & Rhim, J. W. (2021). Recent advances in intelligent food packaging applications using natural food colorants. ACS Food Science & Technology, 1(2), 124-138.
180. Mahalik, N. P., & Nambiar, A. N. (2010). Trends in food packaging and manufacturing systems and technology. Trends in food science & technology, 21(3), 117-128.
181. Wang, H., Qian, J., & Ding, F. (2018). Emerging chitosan-based films for food packaging applications. Journal of agricultural and food chemistry, 66(2), 395-413.

182. Duan, C., Meng, X., Meng, J., Khan, M. I. H., Dai, L., Khan, A., ... & Ni, Y. (2019). Chitosan as a preservative for fruits and vegetables: a review on chemistry and antimicrobial properties. Journal of Bioresources and Bioproducts, 4(1), 11-21.

183. Mohammed Fayaz, A., Balaji, K., Girilal, M., Kalaichelvan, P. T., & Venkatesan, R. (2009). Mycobased synthesis of silver nanoparticles and their incorporation into sodium alginate films for vegetable and fruit preservation. Journal of agricultural and food chemistry, 57(14), 6246-6252.

184. Meena, M., Pilania, S., Pal, A., Mandhania, S., Bhushan, B., Kumar, S., ... & Saharan, V. (2020). Cu-chitosan nano-net improves keeping quality of tomato by modulating physio-biochemical responses. Scientific reports, 10(1), 1-11.

185. Pinzon, M. I., Sanchez, L. T., Garcia, O. R., Gutierrez, R., Luna, J. C., & Villa, C. C. (2020). Increasing shelf life of strawberries (Fragaria ssp) by using a banana starch-chitosan-Aloe vera gel composite edible coating. International Journal of Food Science & Technology, 55(1), 92-98.

186. Ali, A., Maqbool, M., Alderson, P. G., & Zahid, N. (2013). Effect of gum arabic as an edible coating on antioxidant capacity of tomato (Solanum lycopersicum L.) fruit during storage. Postharvest Biology and Technology, 76, 119-124.

187. Mondal, K., Bhattacharjee, S. K., Mudenur, C., Ghosh, T., Goud, V. V., & Katiyar, V. (2022). Development of antioxidant-rich edible active films and coatings incorporated with de-oiled ethanolic green algae extract: a candidate for prolonging the shelf life of fresh produce. RSC advances, 12(21), 13295-13313.

188. Story, E. N., Kopec, R. E., Schwartz, S. J., & Harris, G. K. (2010). An update on the health effects of tomato lycopene. Annual review of food science and technology, 1, 189-210.

189. Sganzerla, W. G., Ribeiro, C. P. P., Uliana, N. R., Rodrigues, M. B. C., da Rosa, C. G., Ferrareze, J. P., ... & Nunes, M. R. (2021). Bioactive and pH-sensitive films based on carboxymethyl cellulose and blackberry (Morus nigra L.) anthocyanin-rich extract: A perspective coating material to improve the shelf life of cherry tomato (Solanum lycopersicum L. var. cerasiforme). Biocatalysis and Agricultural Biotechnology, 33, 101989.

190. Wu, M., & Kubota, C. (2008). Effects of high electrical conductivity of nutrient solution and its application timing on lycopene, chlorophyll and sugar concentrations of hydroponic tomatoes during ripening. Scientia Horticulturae, 116(2), 122-129.

191. Araújo, J. M. S., de Siqueira, A. C. P., Blank, A. F., Narain, N., & de Aquino Santana, L. C. L. (2018). A cassava starch–chitosan edible coating enriched with Lippia sidoides Cham. essential oil and pomegranate peel extract for preservation of Italian tomatoes (Lycopersicon esculentum Mill.) stored at room temperature. Food and Bioprocess Technology, 11(9), 1750-1760.

192. Arias, R., Lee, T. C., Logendra, L., & Janes, H. (2000). Correlation of lycopene measured by HPLC with the L*, a*, b* color readings of a hydroponic tomato and the relationship of maturity with color and lycopene content. Journal of Agricultural and Food Chemistry, 48(5), 1697-1702.

193. Soto-Muñoz, L., Palou, L., Argente-Sanchis, M., Ramos-López, M. A., & Pérez-Gago, M. B. (2021). Optimization of antifungal edible pregelatinized potato starch-based coating formulations by response surface methodology to extend postharvest life of 'Orri'mandarins. Scientia Horticulturae, 288, 110394.

194. Meena, M., Pilania, S., Pal, A., Mandhania, S., Bhushan, B., Kumar, S., ... & Saharan, V. (2020). Cu-chitosan nano-net improves keeping quality of tomato by modulating physio-biochemical responses. Scientific reports, 10(1), 1-11.

195. Mustapha, A. T., Zhou, C., Wahia, H., Amanor-Atiemoh, R., Otu, P., Qudus, A., ... & Ma, H. (2020). Sonozonation: Enhancing the antimicrobial efficiency of aqueous ozone washing techniques on cherry tomato. Ultrasonics Sonochemistry, 64, 105059.

196. Chaturvedi, K., Sharma, N., & Yadav, S. K. (2019). Composite edible coatings from commercial pectin, corn flour and beetroot powder minimize post-harvest decay, reduces ripening and improves sensory liking of tomatoes. International journal of biological macromolecules, 133, 284-293.

197. Maringgal, B., Hashim, N., Tawakkal, I. S. M. A., & Mohamed, M. T. M. (2020). Recent advance in edible coating and its effect on fresh/fresh-cut fruits quality. Trends in Food Science & Technology, 96, 253-267.

198. Kumar, P., Sethi, S., Sharma, R. R., Srivastav, M., & Varghese, E. (2017). Effect of chitosan coating on postharvest life and quality of plum during storage at low temperature. Scientia Horticulturae, 226, 104-109.

199. JiangA., Arul, J., Ponnampalam, R., & Boulet, M. (1991). Use of chitosan coating to reduce water loss and maintain quality of cucumber and bell pepper fruits. Journal of food processing and preservation, 15(5), 359-368.

200. Tsaniklidis, G., Delis, C., Nikoloudakis, N., Katinakis, P., & Aivalakis, G. (2014). Low temperature storage affects the ascorbic acid metabolism of cherry tomato fruits. Plant Physiology and Biochemistry, 84, 149-157.

201. Lee, S. K., & Kader, A. A. (2000). Preharvest and postharvest factors influencing vitamin C content of horticultural crops. Postharvest biology and technology, 20(3), 207-220.

202. El Ghaouth, A., Arul, J., Ponnampalam, R., & Boulet, M. (1991). Use of chitosan coating to reduce water loss and maintain quality of cucumber and bell pepper fruits. Journal of food processing and preservation, 15(5), 359-368

203. Xing, Y., Li, X., Xu, Q., Jiang, Y., Yun, J., & Li, W. (2010). Effects of chitosan-based coating and modified atmosphere packaging (MAP) on browning and shelf life of fresh-cut lotus root (Nelumbo nucifera Gaerth). Innovative food science & emerging technologies, 11(4), 684-689.

204. Siddiqui, M. Z., Chowdhury, A. R., & Prasad, N. (2016). Evaluation of phytochemicals, physico-chemical properties and antioxidant activity in gum exudates of Buchanania lanzan. Proceedings of the National Academy of Sciences, India Section B: Biological Sciences, 86(4), 817-822.

205. Tripathi, J., Ambolikar, R., Gupta, S., & Variyar, P. S. (2022). Preparation and characterization of methylated guar gum based nano-composite films. Food Hydrocolloids, 124, 107312.

206. Saurabh, C. K., Gupta, S., Variyar, P. S., & Sharma, A. (2016). Effect of addition of nanoclay, beeswax, tween-80 and glycerol on physicochemical properties of guar gum films. Industrial Crops and Products, 89, 109-118.

207. Singh, S., Sankar, B., Rajesh, S., Sahoo, K., Subudhi, E., & Nayak, S. (2011). Chemical composition of turmeric oil (Curcuma longa L. cv. Roma) and its antimicrobial activity against eye infecting pathogens. Journal of Essential Oil Research, 23(6), 11-18.

208. Musso, Y. S., Salgado, P. R., & Mauri, A. N. (2017). Smart edible films based on gelatin and curcumin. Food hydrocolloids, 66, 8-15.

209. Roy, S., & Rhim, J. W. (2020). Preparation of carbohydrate-based functional composite films incorporated with curcumin. Food Hydrocolloids, 98, 105302.

210. Singh, T. P., Chatli, M. K., & Sahoo, J. (2015). Development of chitosan based edible films: process optimization using response surface methodology. Journal of Food Science and Technology, 52(5), 2530-2543.

211. Ahmed, J., Hiremath, N., & Jacob, H. (2016). Antimicrobial, rheological, and thermal properties of plasticized polylactide films incorporated with essential oils to inhibit

Staphylococcus aureus and Campylobacter jejuni. Journal of food science, 81(2), E419-E429.

212. Fabra, M. J., Talens, P., & Chiralt, A. (2008). Effect of alginate and λ-carrageenan on tensile properties and water vapour permeability of sodium caseinate–lipid based films. Carbohydrate Polymers, 74(3), 419-426.

213. Wang, B., Zhang, W., Bai, X., Li, C., & Xiang, D. (2020). Rheological and physicochemical properties of polysaccharides extracted from stems of Dendrobium officinale. Food Hydrocolloids, 103, 105706.

214. Emragi, E., Kalita, D., & Jayanty, S. S. (2022). Effect of edible coating on physical and chemical properties of potato tubers under different storage conditions. LWT, 153, 112580.

215. Kalita, D., & Jayanty, S. S. (2014). Comparison of polyphenol content and antioxidant capacity of colored potato tubers, pomegranate and blueberries. J. Food Process. Technol, 5(8), 1-7.

216. Hellmann, H., Goyer, A., & Navarre, D. A. (2021). Antioxidants in potatoes: A functional view on one of the major food crops worldwide. Molecules, 26(9), 2446.

217. Abd-Elsalam, K. A., & Khokhlov, A. R. (2015). Eugenol oil nanoemulsion: antifungal activity against Fusarium oxysporum f. sp. vasinfectum and phytotoxicity on cottonseeds. Applied Nanoscience, 5(2), 255-265.

218. Murmu, S. B., & Mishra, H. N. (2017). Optimization of the arabic gum based edible coating formulations with sodium caseinate and tulsi extract for guava. LWT, 80, 271-279.

219. Hashemi, S. M. B., & Khaneghah, A. M. (2017). Characterization of novel basil-seed gum active edible films and coatings containing oregano essential oil. Progress in Organic Coatings, 110, 35-41.

220. Reyes-Chaparro, P., Gutierrez-Mendez, N., Salas-Muñoz, E., Ayala-Soto, J. G., Chavez-Flores, D., & Hernández-Ochoa, L. (2015). Effect of the addition of essential oils and functional extracts of clove on physicochemical properties of chitosan-based films. International Journal of Polymer Science, 2015.

221. Losic, D., Mitchell, J. G., & Voelcker, N. H. (2009). Diatomaceous lessons in nanotechnology and advanced materials. Advanced Materials, 21(29), 2947-2958.

222. Chen, L., Liu, T., Zhang, W., Chen, X., & Wang, J. (2012). Biodiesel production from algae oil high in free fatty acids by two-step catalytic conversion. Bioresource Technology, 111, 208-214.

223. Sucaldito, M. R., & Camacho, D. H. (2017). Characteristics of unique HBr-hydrolyzed cellulose nanocrystals from freshwater green algae (Cladophora rupestris) and its reinforcement in starch-based film. Carbohydrate Polymers, 169, 315-323.

224. Chen, Y. W., Lee, H. V., Juan, J. C., & Phang, S. M. (2016). Production of new cellulose nanomaterial from red algae marine biomass Gelidium elegans. Carbohydrate polymers, 151, 1210-1219.

225. Ko, S. W., Soriano, J. P. E., Unnithan, A. R., Lee, J. Y., Park, C. H., & Kim, C. S. (2018). Development of bioactive cellulose nanocrystals derived from dominant cellulose polymorphs I and II from Capsosiphon Fulvescens for biomedical applications. International journal of biological macromolecules, 110, 531-539.

226. Dean, K. M., Petinakis, E., Meure, S., Yu, L., & Chryss, A. (2012). Melt strength and rheological properties of biodegradable poly (lactic aacid) modified via alkyl radical-based reactive extrusion processes. Journal of Polymers and the Environment, 20(3), 741-747.

227. Jiang, H., Srichuwong, S., Campbell, M., & Jane, J. L. (2010). Characterization of maize amylose-extender (ae) mutant starches. Part III: Structures and properties of the Naegeli dextrins. Carbohydrate polymers, 81(4), 885-891.

228. Cameron, M. C., Ross, A. G., & Percival, E. G. V. (1948). Methods for the routine estimation of mannitol, alginic acid, and combined fucose in seaweeds. Journal of the Society of Chemical Industry, 67(4), 161-164.

229. Weemaes, C. A., Ooms, V., Van Loey, A. M., & Hendrickx, M. E. (1999). Kinetics of chlorophyll degradation and color loss in heated broccoli juice. Journal of Agricultural and Food Chemistry, 47(6), 2404-2409.

230. Mukarakate, C., Mittal, A., Ciesielski, P. N., Budhi, S., Thompson, L., Iisa, K., ... & Donohoe, B. S. (2016). Influence of crystal allomorph and crystallinity on the products and behavior of cellulose during fast pyrolysis. ACS Sustainable Chemistry & Engineering, 4(9), 4662-4674.

231. Doh, H., Lee, M. H., & Whiteside, W. S. (2020). Physicochemical characteristics of cellulose nanocrystals isolated from seaweed biomass. Food hydrocolloids, 102, 105542.

232. Gong, J., Li, J., Xu, J., Xiang, Z., & Mo, L. (2017). Research on cellulose nanocrystals produced from cellulose sources with various polymorphs. RSC advances, 7(53), 33486-33493.

233. Battegazzore, D., Bocchini, S., & Frache, A. (2011). Crystallization kinetics of poly (lactic acid)-talc composites. Express Polym. Lett, 5(10), 849-858.

234. Lorenzo, A. T., Arnal, M. L., Albuerne, J., & Müller, A. J. (2007). DSC isothermal polymer crystallization kinetics measurements and the use of the Avrami equation to fit the data: Guidelines to avoid common problems. Polymer testing, 26(2), 222-231.

235. Gazzotti, S., Farina, H., Lesma, G., Rampazzo, R., Piergiovanni, L., Ortenzi, M. A., & Silvani, A. (2017). Polylactide/cellulose nanocrystals: The in situ polymerization approach to improved nanocomposites. European Polymer Journal, 94, 173-184.

236. Gårdebjer, S., Bergstrand, A., Idström, A., Börstell, C., Naana, S., Nordstierna, L., & Larsson, A. (2015). Solid-state NMR to quantify surface coverage and chain length of lactic acid modified cellulose nanocrystals, used as fillers in biodegradable composites. Composites Science and Technology, 107, 1-9.

237. Cser, F. (2001). About the Lorentz correction used in the interpretation of small angle X-ray scattering data of semicrystalline polymers. Journal of applied polymer science, 80(12), 2300-2308.

238. Habibi, Y., & Dufresne, A. (2008). Highly filled bionanocomposites from functionalized polysaccharide nanocrystals. Biomacromolecules, 9(7), 1974-1980.

239. Mi, H. Y., Jing, X., Peng, J., Salick, M. R., Peng, X. F., & Turng, L. S. (2014). Poly (ε-caprolactone)(PCL)/cellulose nano-crystal (CNC) nanocomposites and foams. Cellulose, 21(4), 2727-2741.

240. Marcovich, N. E., Auad, M. L., Bellesi, N. E., Nutt, S. R., & Aranguren, M. I. (2006). Cellulose micro/nanocrystals reinforced polyurethane. Journal of materials research, 21(4), 870-881.

241. Hivechi, A., Bahrami, S. H., & Siegel, R. A. (2019). Drug release and biodegradability of electrospun cellulose nanocrystal reinforced polycaprolactone. Materials Science and Engineering: C, 94, 929-937.

242. Barghini, A., Ivanova, V. I., Imam, S. H., & Chiellini, E. (2010). Poly-(ε-caprolactone)(PCL) and poly (hydroxy-butyrate)(PHB) blends containing seaweed fibers: Morphology and thermal-mechanical properties. Journal of Polymer Science Part A: Polymer Chemistry, 48(23), 5282-5288.

243. Liu, H., Huang, Y., Yuan, L., He, P., Cai, Z., Shen, Y., ... & Xiong, H. (2010). Isothermal crystallization kinetics of modified bamboo cellulose/PCL composites. Carbohydrate Polymers, 79(3), 513-519.

244. Dhanvijay, P. U., & Shertukde, V. V. (2011). Crystallization of biodegradable polymers. Polymer-Plastics Technology and Engineering, 50(13), 1289-1304.

245. Gumede, T. P., Luyt, A. S., Tercjak, A., & Müller, A. J. (2019). Isothermal crystallization kinetics and morphology of double crystalline PCL/PBS blends mixed with a polycarbonate/MWCNTs masterbatch. Polymers, 11(4), 682.

245. Tawakkal, I. S., Cran, M. J., & Bigger, S. W. (2016). Release of thymol from poly (lactic acid)-based antimicrobial films containing kenaf fibres as a natural filler. LWT-Food Science and Technology, 66, 629-637.

247. Fortunati, E., Armentano, I., Iannoni, A., Barbale, M., Zaccheo, S., Scavone, M., ... & Kenny, J. M. (2012). New multifunctional poly (lactide acid) composites: Mechanical, antibacterial, and degradation properties. Journal of Applied Polymer Science, 124(1), 87-98.

248. Martino, V. P., Jimenez, A., Ruseckaite, R. A., & Averous, L. (2011). Structure and properties of clay nano-biocomposites based on poly (lactic acid) plasticized with polyadipates. Polymers for Advanced Technologies, 22(12), 2206-2213.

249. Azizi Samir, M. A. S., Alloin, F., & Dufresne, A. (2005). Review of recent research into cellulosic whiskers, their properties, and their application in the nanocomposite field. Biomacromolecules, 6(2), 612-626.

250. Subbuvel, M., & Kavan, P. (2022). Preparation and characterization of polylactic acid/fenugreek essential oil/curcumin composite films for food packaging applications. International Journal of Biological Macromolecules, 194, 470-483.

251. Roy, S., & Rhim, J. W. (2020). Preparation of antimicrobial and antioxidant gelatin/curcumin composite films for active food packaging application. Colloids and Surfaces B: Biointerfaces, 188, 110761.

252. Salmieri, S., Islam, F., Khan, R. A., Hossain, F. M., Ibrahim, H. M., Miao, C., ... & Lacroix, M. (2014). Antimicrobial nanocomposite films made of poly (lactic acid)–cellulose nanocrystals (PLA–CNC) in food applications—part B: effect of oregano essential oil release on the inactivation of Listeria monocytogenes in mixed vegetables. Cellulose, 21(6), 4271-4285.

253. Bagheri, M., & Mahmoodzadeh, A. (2020). Polycaprolactone/graphene nanocomposites: synthesis, characterization and mechanical properties of electrospun nanofibers. Journal of Inorganic and Organometallic Polymers and Materials, 30(5), 1566-1577.

254. Zygoura, P. D., Paleologos, E. K., & Kontominas, M. G. (2011). Changes in the specific migration characteristics of packaging–food simulant combinations caused by ionizing radiation: Effect of food simulant. Radiation Physics and Chemistry, 80(8), 902-910.

255. Crank, J., & Crowley, A. B. (1979). On an implicit scheme for the isotherm migration method along orthogonal flow lines in two dimensions. International Journal of Heat and Mass Transfer, 22(10), 1331-1337.

256. Cid, A. G., Sonvico, F., Bettini, R., Colombo, P., Gonzo, E., Jimenez-Kairuz, A. F., & Bermúdez, J. M. (2020). Evaluation of the drug release kinetics in assembled modular systems based on the Dome Matrix technology. Journal of Pharmaceutical Sciences, 109(9), 2819-2826.

257. Peppas, N. A., & Narasimhan, B. (2014). Mathematical models in drug delivery: How modeling has shaped the way we design new drug delivery systems. Journal of Controlled Release, 190, 75-81.

258. Peppas, N. A., & Buri, P. A. (1985). Surface, interfacial and molecular aspects of polymer bioadhesion on soft tissues. Journal of Controlled Release, 2, 257-275.